"Inference and Study of Immune Network Biology in a Complex Stress-mediated Illness"

by

Saurabh Vashishtha

A thesis submitted in partial fulfillment of the requirements for

the degree of

DOCTOR OF PHILOSOPHY

in

Experimental Medicine

Department of Medicine
University of Alberta

© Saurabh Vashishtha, 2019

Abstract

Gulf War Illness (GWI) is a complex debilitating condition presenting with a diverse array of symptoms that include fatigue, memory and cognitive difficulties, headaches, sleep disturbances, gastrointestinal problems, skin rashes, as well as musculoskeletal/joint pain. It affects up to one third of the US veterans returning from the 1991 Persian Gulf conflict (Operation Desert Storm). The overarching objective of this study is to integrate clinical understanding of the disease with basic research in molecular medicine using a systems biology approach to pinpoint underlying mechanisms of disease and inform treatment more effectively.

In the first part of this thesis, we survey several popular reverse engineering methods for inferring directed networks from time course data and assess their suitability to the narrow range of conditions and low sampling frequencies typical of human clinical studies. Based on this assessment we develop a novel variant of such methods that leverages simulations of biologically realistic artificial networks to optimize the recovery of actual biological networks from data in a problem-specific manner. Using this simulation-based tuning approach we identify and extract candidate immune signaling patterns, which are then filtered by projecting onto a literature-informed mechanistic model of immune regulation. This literature-informed data mining identified characteristically active feed-forward mechanisms connecting IL-23 and IL-17 through IL-6 and IL-10 as distinguishing control elements in GWI. Furthermore, simulations of an IL-6 receptor antagonist applied in combination with either a Th1 (IL-2, IFNγ, TNFα) or IL-23 receptor antagonist predicted a partial rescue of immune response circuitry in GWI.

To support the *in vivo* testing of these in silico predictions, the last part of this thesis is directed at establishing the mechanistic similarity of the human GWI condition

with a stress-potentiated response to neurotoxic exposure in mouse. In support of this, undirected networks were constructed linking 12 cytokines measured in peripheral blood in mice challenged with Lipopolysaccheride (LPS) after exposure to the sarin surrogate DFP (Diisopropyl fluorophosphates) under conditions of simulated stress induced by corticosterone (CORT) doping of their drinking water. An evolutionarily conserved GWI-specific motif linking IL-6, IL-8, IL1β, TNF-α, IL-5 and IFN-γ was identified supporting the alignment of mouse and human cytokine co-expression networks. Collectively this thesis proposes a network identification methodology which is robust to the limitations of human data, testable hypotheses supporting the partial recovery of immune signaling networks in GWI-affected veterans and the network informed validation of an animal model in which such hypotheses might be explored *in vivo*.

Preface

This thesis is an original work by Saurabh Vashishtha. The major part of the research conducted under this thesis forms part of a multi-year study funded by the US Department of Defense entitled “Understanding Gulf War Illness: An Integrative Modeling Approach”. This study was led by an international research consortium, consisting of a clinical core led by Dr. Nancy Klimas at Nova Southeastern University, Fort Lauderdale, MI, USA, an animal model core led by Dr. James O’ Callaghan at the Centers for Disease Control and Prevention (CDC) - National Inst. for Occupational Safety and Health (NIOSH) and a computational core led by Adjunct Associate Professor Dr. Gordon Broderick at the University of Alberta where the current thesis work was performed.

The current work consists of three core components making up chapters 2, 3 and 4 of this thesis. Chapter 2 of this thesis describing the analytical framework has been published as Vashishtha S, Broderick G, Craddock TJA, Fletcher MA, Klimas NG (2015) “*Inferring Broad Regulatory Biology from Time Course Data: Have We Reached an Upper Bound under Constraints Typical of In Vivo Studies?”* PLoS ONE 10(5): e0127364. The quantitative analysis and simulation experiments described in Chapter 2 were my original work. Dr. Gordon Broderick was the principal academic supervisor, corresponding author and oversaw study design, concept formulations and manuscript composition.

Chapter 3 of this thesis consists of an application of this framework to human subject data and is being submitted for publication as Vashishtha S, Broderick G, Craddock TJA, Barnes ZM, Collado F, Fletcher MA, Klimas NG *“Leveraging Prior Knowledge to Recover Characteristic Immune Regulatory Motifs in Gulf War Illness”* in Frontiers in Physiology. The clinical assessment and human subject selection were

performed under the direction of Dr. Nancy Klimas with all omics experimental measurements conducted under the direction of Dr. Mary Ann Fletcher. All human subject work was conducted under protocols approved by the IRB at Nova Southeastern University, the Miami Veterans Affairs Medical Center and the University of Alberta (Pro 00005853). The statistical analysis and inference and analysis of directed networks described in Chapter 3 were my original work.

In Chapter 4 of this thesis, we assess the relevance of a mouse exposure model to the human illness condition. All animal procedures were performed under the direction of Dr. James P. O'Callaghan at CDC-NIOSH according to protocols approved by the latter's Institutional Animal Care and Use Committee and the U.S. Army Medical Research and Materiel Command Animal Care and Use Review Office. The CDC-NIOSH animal facility is certified by the Association for Assessment and Accreditation of Laboratory Animal Care International (AAALAC International). I was involved in all the steps of the quantitative analysis of experimental data as well as the inference of undirected networks and their novel analysis using the principles of network theory under the supervision of Dr. Gordon Broderick.

Dedicated to
my late mother & my father

Acknowledgements

This work would not have been possible without the help and support of many people. First and foremost, I would like to thank my thesis advisor, Dr. Gordon Broderick. I am thankful for his unwavering support, and for providing a healthy balance of guidance and freedom throughout my graduate years. Additionally, I thank my co-supervisor Dr. Ross Tsuyuki and thesis committee member, Dr. Sol Efroni for their continuous support and guidance throughout the program. I am grateful to all the current and past members of Broderick clinical systems biology group specially, Hooman Sedghamiz, Matt Morris and Mark Rice for their encouragement and support throughout the program.

I have a deep sense of gratitude and regard for all the people who voluntarily donated the blood, due to which it became possible to pursue some of the research directions. For collaboration outside of the Broderick lab, I thank Drs. Nancy Klimas, Mary Ann Fletcher, James O' Callaghan and members of their lab. No modeling and inference efforts would be complete without accompanying data, I would like to thank Zachary Barnes from Klimas Lab, who generously shared hard-won data with me, as well as stimulating discussions to understand the data better. I would like to specially thank Dr. Lindsay Michalovicz and Dr. Travis Craddock for reading through my work and guiding me in the right direction.

Finally, I thank my friends and family for providing encouragement, adventure, and distraction for helping to maintain my life outside of the research. Specially, My wife Noopur, who supported me in my stubborn and at times bewildering pursuit of science, and I am thankful for her encouragement and love.

Table of Contents

List of Tables

List of Figures

List of Abbreviation

GWI	Gulf War Illness
CFS/ME	Chronic Fatigue Syndrome/Myalgic Encephalomyelitis
FM	Fibromyalgia
HC	Healthy Control
HPA axis	hypothalamic-pituitary-adrenal axis
DC	Dendritic Cells
NK cells	Natural Killer cells
NPY	Neuropeptide Y
IL	Interleukins
TNF	Tumor Necrosis factor
IFNγ	Interferon-gamma
CD	Cluster of differentiation
Th	T-helper
PBMC	Peripheral Blood Mononuclear cells
CMI	Chronic Multi-symptom Illness
AChE	Acetyl cholinesterase
DFP	diisopropyl fluorophosphate
PB	Pyridostigmine Bromide
CPF	Chlorpyrifos
CPO	Chlorpyrifos Oxon
PER	Permethrin
DEET	N,N-diethyl-meta-toluamide
PHA	Phytohemagglutinin
NF-κB	Nuclear Factor Kappa-B
MK	MonoKine
CK	Lymphokine
ATP	Adenosine Tri Phosphate
ACTH	Adreno Corticotropin hormone
PTSD	Post-traumatic stress disorder
RA	rheumatoid arthritis
IBD	Inflammatory Bowel Diseases
UC	Ulcerative Colitis
AIDS	Acquired immune deficiency syndrome
MDD	Major depression disorder
ALS	Amyotrophic lateral sclerosis
MS	Multiple sclerosis
PD	Parkinson's disease
fMRI	functional magnetic resonance imaging
MRI	Magnetic resonance imaging
MRS	Magnetic resonance spectroscopy
SPECT	Single-photon emission computed tomography
BDNF	Brain-Derived Neurotrophic Factor
TrkB	Tropomyosin-related kinase B
CamKII	Calcium/calmodulin-protein kinase II alpha
BBB	Blood Brain Barrier
CNS	Central Nervous System

DG	Dentate Gyrus
mtDNAcn	mitochondrial DNA copy numbers
ELISAs	enzyme-linked immunosorbent assays
ODE	Ordinary differential equation
DBN	Dynamic Bayesian Networks
BN	Boolean network
PBN	Probabilistic Boolean networks
DREAM	Dialogue on Reverse Engineering Assessment and Methods
BNFINDER	Bayes Net Finder
GlobalMIT	Global Mutual Information Test
BANJO	Bayesian Network Inference with Java Objects
DREM	Dynamic regulatory events Miner
TIGRESS	Trustful Inference of Gene REgulation using Stability Selection
CLR	Context likelihood of relatedness
TD- ARACNE	Time Delay ARACNE
NIR	Network Identification by multiple regressions
TDSS	Time Delay S-system
NeRDS	Network Reconstruction via Dynamic Systems
ARACNE	Algorithm for the Reconstruction of Accurate Cellular Networks
MNI	Mode-of-action by Network Identification
TSNI	Time Series Network Identification
lasso	least absolute shrinkage and selection operator
SMETS	Semi Metric Ensemble Time Series
IRMA	*In vivo* Reverse-engineering and Modeling Assessment
STRING	Search Tool for the Retrieval of Interacting Genes
NLP	natural language processing
SVD	Singular Value Decomposition
PCA	Principal Component Analysis
PPV	Positive predictive Value
NPV	Negative predictive Value
GED	Graph Edit Distance
FFL	Feed-Forward Loop
ANOVA	Analysis of Variance
CV	coefficient of variability
ROC	Receiver-operating curve
GXT	Graded eXercise Test
BMI	Body Mass Index
PEM	Post-Exertional Malaise
MFI	Multidimensional Fatigue Inventory
SF-36	Short form-36 survey
RNA	Ribonucleic acid

Chapter 1: Introduction & Background

1.1 Introduction

1.1.1 Gulf War Illness: Background

An alarming number of the veterans returned from 1990-91 Persian Gulf War theatre reported a complex constellation of symptoms including debilitating fatigue, musculoskeletal discomfort, skin rashes, and cognitive dysfunction [1, 2]. Studies have shown that these numerous chronic nonspecific symptoms are reported by Gulf War veterans more often than their non-deployed peers [2]. The term Gulf War Illness (GWI) has now been used to describe these chronic inexplicable symptoms, which is estimated to affect approximately 25 - 32% of the 7,00,000 Gulf War veterans returning from the Operation Desert Storm [2]. The etiology of this complex multi-symptom illness that affects multiple systems including immune, endocrine and nervous systems remains unknown.

1.1.2 Case definition

Several case definitions have been used to define the GWI symptoms including chronic multi-symptom illness (CMI) [2], the Kansas GWI definition [3], the Haley syndrome criteria [4] and adaptations of these frameworks. Of these, Fukuda/CMI and the Steele/ Kansas definitions are the most commonly used definitions to define GWI. According to CMI, A GWI veteran must report one or more symptoms present for 6 months or longer from at least two of the following three categories [2]: (i) Fatigue, (ii) Mood and cognition (symptoms of feeling depressed, difficulty in remembering or concentrating, feeling moody, feeling anxious, trouble finding words, or difficulty sleeping), and (iii) Musculoskeletal (symptoms of joint pain, joint stiffness, or muscle pain). In comparison, the Kansas case definition of GWI requires veterans to have multiple moderate to severe chronic symptoms in at least three of the following six defined symptom domains: Fatigue / sleep problems, Somatic pain, Neurologic / cognitive / mood symptoms,

Gastrointestinal symptoms, Respiratory symptoms and Skin abnormalities. Veterans who have severe psychiatric disorders or other medical conditions that might predict similar symptoms are excluded in the Kansas criteria [3]. The Fukuda/CMI criterion is broader and generally served as the initial base for screening veterans for the Steele/Kansas GWI definition. The CMI case definition was recommended for clinical use and the Kansas definition was recommended for research use by 2014 Institute of Medicine (IOM) panel [5].

1.1.3 Potential causes of GWI

Several conditions, events and exposures encountered by servicemen including infectious agents, medical prophylactic treatment with reversible and irreversible acetylcholinesterase (AChE) inhibitors such as pyridostigmine bromide (PB) and pesticides containing organophosphates such as chlorpyrifos (CPF), chlorpyrifos oxon (CPO), permethrin (PER) and dichlorvos, the insect repellent, N,N-diethyl-meta-toluamide (DEET), depleted uranium, oil fires and burn pit exposures, chemical and biological warfare agents such as exposure to nerve agent, sarin gas as well as physiological and psychological combat stress have been proposed as potential instigators to the development of GWI [2, 6]. Several epidemiological studies have been performed to uncover the actual cause of the GWI. Some studies have linked all of the exposures such as PB, organophosphate pesticides, and nerve agents as well as environmental and physical challenges to GWI [7-9], whereas others pointed towards only a limited number of significant risk factors for GWI [10, 11]. These huge differences in the findings of epidemiological studies suggest enormous inconsistency in the prior information (data) used to reach the conclusions and may lead to errors in evaluating associations between GWI and Gulf War exposures [12]. Indeed, there is scarce information about the exposures since limited official records of specific exposures in

specific veteran groups were kept. Therefore, veterans were asked to self-report the details of exposures. Despite this heterogeneity, the use of organophosphate pesticides and PB during the Gulf War were consistently identified as the most significant risk factors for GWI across all studies and populations on the considerations of confounding effects of concurrent exposures [13]. In parallel with epidemiological studies, several animal models of GWI have been developed and used to study the individual as well as synergistic effects of different exposures in the Gulf war theatre. These studies also suggest that individual/synergistic effects of several organophosphates such as PB, CPF, CPO, DEET and/or nerve gas Sarin exposure in the presence/absence of physiological stress may lead to the symptoms as seen in GWI.

1.1.4 Debilitating pathophysiology

Our understanding of the pathophysiology of GWI generally remains incomplete despite evidence pointing to the involvement of the basic stress response. As a result, we still do not have a characteristic biomarker for this illness. Interestingly, symptoms of GWI including, long-term and severe fatigue that is not relieved by rest, gastrointestinal disorders, and neurological impairments, clinically resemble that of another stress-mediated illness: Chronic Fatigue Syndrome/Myalgic Encephalomyelitis (CFS/ME) [14-16] to such an extent that GWI has been addressed as a different subset of CFS/ME. Furthermore, immune and neuroendocrine irregularities such as impaired NK cell cytotoxicity as well as dysfunction of the hypothalamic-pituitary-adrenal (HPA) stress response axis have been reported in both CFS/ME [17-19] and GWI [20-22]. Reduction in NK cell cytotoxicity has been associated with reduced levels of perforin in CFS/ME [23]. Similarly levels of intracellular perforin have also been observed in CD3−/CD56+ NK and CD3+/CD8+ cytotoxic T cells in GW veterans [24]. However, mechanistic details behind these similarities remain uncharacterized.

Conversely, several studies have highlighted significant differences between CFS/ME and GWI. First and foremost, unlike CFS/ME, multiple factors including environmental exposures, toxins, vaccines, and unknown infectious agents have been associated as potential triggers for GWI [2]. Furthermore, an evaluation of the presence of fibromyalgia (FM), multiple chemical sensitivity and psychiatric comorbidity in male veterans and male civilians with CFS/ME suggested that CFS/ME may have different underlying cause in veterans versus civilian populations [25]. Moreover, early studies of cytokine transcripts were able to differentiate the Gulf war veterans diagnosed with CFS/ME from healthy controls. Gulf war veterans with CFS had significantly higher levels of IL-2, IL-10, IFN-γ and TNF-α transcripts than healthy veterans returned from the Gulf war theatre. However, non-veterans suffering from CFS/ME were not significantly different from their respective controls [26]. In addition, our group has more recently observed differences in the immune signatures in GWI as well as CFS/ME in gender specific manner [27]. A linear classification model was constructed using stepwise variable selection to differentiate male and female, GWI and CFS/ME subjects from controls and each other. In this study, a decreased Th2 polarity was reported in female subjects with CFS/ME as compared to GWI and differences in IL-23/Th17/IL-17 axis were suggested to delineate GWI and CFS/ME. In particular, this study was able to differentiate female GWI and female CFS/ME subjects almost perfectly on the basis of IL-1b and IL-5 levels alone, albeit in a small pilot cohort (n = 10). However, male GWI could not be distinguished easily from their CFS/ME counterparts on the basis of minimally overlapping cytokine markers as these typically trended in the same direction compared to control. However, male GWI subjects were successfully differentiated from their CFS/ME counterparts in another recent study from our group where a 3-way multivariate projection model based on 12 markers of endocrine and immune function measured at three time points before during and after maximal exercise was used to

differentiate GWI subjects from healthy as well as CFS/ME subjects [28]. More recently, Khaiboulina and colleagues surveyed 77 serum cytokines and used Random Forest algorithm to identify a group of five cytokines namely, IL-7, IL-4, TNF-α, IL-13 and IL-17F to distinguish GWI and CFS/ME groups [29]. Their results suggested the involvement of Th1 and Th17 cytokines in GWI while Th1 and Th2 cytokines as well as a more diverse group of inflammatory cytokines and mononuclear chemo-attractant cytokines were suggested to characterize CFS/ME [29]. These observations, taken together, suggest different pathophysiology for both the illnesses namely, GWI and CFS/ME despite their overlapping clinical presentation. Nonetheless, pathophysiology of ME/CFS and GWI still remain elusive and more research is needed to characterize the underlying mechanisms and address the similarities as well as the differences between these illnesses.

1.2 Multiple system dysfunction in GW veterans

1.2.1 Immune dysregulation

The immune system is a remarkably complex system of the body that protects the host from both external (such as bacteria and viruses) and internal threats (such as malignant transformation). In general, the immune system is separated into two branches namely, 'the innate immune system' and 'the adaptive immune system'. The innate immune system comprises primarily, white blood cells (leukocytes) such as Natural Killer (NK) cells, mast cells, eosinophils, basophils and phagocytic cells such as macrophages, neutrophils and dendritic cells to identify and eliminate the pathogens whereas the adaptive immune system consists of lymphocytes such as T cells and B cells [30]. The innate immune system responds rapidly to common pathogens but has a lack of specificity, whereas the adaptive immune system responds precisely, but takes several days or weeks to develop the response. However, subsequent exposure leads to a more vigorous and rapid adaptive memory response [31]. Multiple studies have reported

alterations in the immune cells of Gulf war veterans. For example, CD19+ B cell population along with the concentration of autoantibodies directed against myelin basic protein (MBP) in striated as well as smooth muscles were significantly elevated in GW veterans [20]. Moreover, significantly decreased cytotoxic activity of NK cells was reported in Gulf war veterans in comparison to controls [20, 26]. Similar impairment of NK cell activity was also reported in the ME/CFS patients [19].

1.2.1.1 Cytokines and their dysregulation in GWI

Immune cells communicate extensively with each other in mounting a response. This networked communication between immune cells is facilitated by small (~5-20 kDa) multifunctional immunomodulating glycoproteins called 'cytokines' that play important role in cell signaling. Over 300 cytokines have been identified so far including a host of chemokines, lymphokines, interferons (IFNs) and growth factors. In general, all major cytokines can be grouped into six families namely, Interleukins, Interferons (IFNs), Tumor Necrosis Factors (TNF) family, chemokines, growth factors and colony stimulating factors (CSF) (Table 1.1). Several other classification schemes have been utilized to group cytokines on the basis of their function (pro-inflammatory and anti-inflammatory), three-dimensional structure (Type-1 and Type-2 cytokines) and the structural homology of their receptors. A prominent feature of cytokines is that they allow the integration of immune cell behaviour in time across locations as immune responses are generated and may act in autocrine (on the cells that secrete them), paracrine (nearby cells), or in some instances in endocrine manner (on distant cells). Generally, cytokines are pleiotropic in nature i.e. a cytokine can have multiple functions. For example, interleukin-4 (IL-4) promotes the differentiation of the naive T cell, activates B-cells to produce immunoglobulin E, and inhibits macrophage activation [32].

Table 1.1: Cytokine families with their representative cytokines and their actions

Cytokine family	Representative cytokines	Actions
Interferon family	IFN-α, IFN-β, IFN-γ	Antiviral proteins
Tumor Necrosis Factor Family	TNF-α, TNF-β	Regulate inflammatory and immune responses
Interleukin family	All subfamilies from IL-1 to IL-20	Various actions depending on the interleukin and source cell
Chemokine family	IL-8, MCP-1, MIP-1α, MIP-1β, RANTES	Direct cell migration, adhesion and activation
Haematopoietins or colony stimulating factors	IL-3, G-CSF (granulocyte colony stimulating factor), GM-CSF (Granulocyte-macrophage-CSF), M-CSF (Macrophage-CSF)	Promote cell proliferation and differentiation
Growth factors	TGF-α (Transforming growth factor α), TGF-β (Transforming growth factor-β), Epidermal growth factors, Fibroblast growth factors, Platelet-derived growth factors 1& 2	Regulation of immune cells

In addition, cytokines can also be redundant in their actions i.e., many cytokines can have similar functions, for example, IL-2, IL-4, and IL-5 all stimulate proliferation of B cells [32]. This already complex cytokine action is further complicated by the fact that cytokines can act synergistically as well as antagonistically. Moreover, cytokines are often produced in a cascade as one cytokine binds to a receptor of target cell and evokes it to synthesize additional cytokines in response to a challenge. Cytokines play important roles in cellular activation, relocation and differentiation and in maintaining tissue homeostasis [33]. Circulating immune cells and tissue-specific cells secrete cytokines in response to trauma, inflammation and infection to send signals to other

cells. As a result of this, certain specific cytokine levels may be up or down regulated to provide the proper cues to target cells. Accordingly, these specific cytokines along with the cells they recruit determine the nature of immune response at a given location and given time. For example, IL-12 alone generates a Th1 pro-inflammatory response as a ligand to macrophages in JAK-STAT pathway, but this response is down regulated in the presence of IL-10 [34]. Depending on the cues, the target cells may activate, proliferate, or move to the site of infection or immune attack in response to the signals received from the cytokines. Anomalies in this communication may cause certain chronic conditions.

Since, immune cells and cytokines work in concert to formulate an effective immune response to an antigen or immune challenge, it was not totally unexpected to observe anomalies in the expression of cytokines in the GW veteran population. Several early studies of immune dysfunction in GW veterans confirmed altered cytokine levels in GWI though some early findings were contradictory. For example, Rook and Zumla initially proposed a shift towards type-2 (Th2) response as a characteristic immune signature in this population [35]. However, this was not observed in the several other veteran cohorts. In 1999, Zhang and coworkers found evidence of a type-1 (Th1) response with significant up regulation of RNA transcript for IL-2 and IFNγ, but neither IL-4 nor IL-6 in a population of gulf war veterans with CFS [26]. Similarly, the findings of Skowera and colleagues [36] suggested primarily an ongoing Th1-type immune activation in symptomatic GW veterans with elevated levels of IL-2, and IFN-γ producing CD4+ cells in the absence of *in vitro* stimulation and an expansion of IL-10 producing memory CD4+ cells in the presence of *in vitro* stimulation [36]. Conversely, regression and factor analytic methods were used in Brimacombe et al. (2002) to conclude a relationship of Th1 markers with the diagnosis of CFS and Th2 markers with the cognitive abilities in GW veterans [37]. Not surprisingly, Peakman and coworkers in 2006 conducted a broad survey of literature and found no evidence to support

dominant polarization towards Th2 immune status alone in symptomatic GW veterans [38]. An exploration of vaccination effects found a mix of Th1 (IFNγ and IL-2) and Th2 (predominantly IL-13) recall response to anthrax vaccine, whereas response to plague was polarized toward Th1 in male GW veterans [39]. Our preliminary works in small cohorts of GW veterans are also consistent with a mixed Th1: Th2 immune status [28, 40]. Our group has found higher TNFα response to Phytohemagglutinin (PHA) stimulation in GWI subjects at rest as well as IL-5 and IFNγ response during the course of a maximal exercise challenge [28]. Similarly, several other investigators have either observed or proposed the dysfunction of immune system in GW veterans [41-44].

Among these studies of immune system alterations, some specific studies [40, 45] from our group are of note, namely our investigation of immune signaling networks across several levels of biology using the mathematical foundations of graph theory. In a pilot study, we observed differences in the topology of immune signaling networks in healthy and GW veterans [40]. Graph theoretical analysis suggested the differences in the connectivity of NPY, IL-1α, TNF-α and CD2+/CD26+ nodes in healthy and GWI networks at rest. Physiological stress of Graded exercise caused significant restructuring around nodes for CD19+ B cell population, IL-5, IL-6 and soluble CD26 concentrations that was subsided post-exercise. More detailed analysis suggested that these restructured B and T cell motifs were in strong influence of IL-1α and CD2+/CD26+ nodes that potentially boosted lymphocyte and HPA axis stimulation in the context of mixed Th1:Th2 immune signature [40]. More recently, our group used gene expression profiles of peripheral blood mononuclear cells (PBMC) to numerically estimate the activity of 500 documented pathways in GW veterans and compared them with that of healthy veteran subjects. Our results suggested significant increases in the activity of pathways related to neuroendocrine-immune signalling and inflammatory activity in GWI, and significant decrease in the pathways related to apoptotic signalling [45].

Furthermore, multilayered networks linking these pathways with symptom severity via changes in immune cell abundance, function and signaling were constructed. Uninterrupted links of pathway clusters supporting “neuronal development and migration” as well as “androgen mediated activation of NF-kB” with GWI symptoms via nodes representing the changes in the plasma levels of IL-10 and numbers of CD2+ suggested an over-expression of known exercise response mechanisms as well as illness-specific changes that may involve an overlapping stress-potentiated neuro-inflammatory response [45]. Taken together, these observations provide additional evidence of immune dysfunction in GW veterans.

1.2.2 Neuro-endocrine dysfunction

There is mounting evidence suggesting neuroendocrine and immunological dysfunction in Gulf war veterans that may be potentiated by response to stress whether psychological, physiological, chemical or other. In a series of studies, Golier and colleagues investigated the possible link of the dysregulation of the hypothalamus-pituitary-adrenal (HPA) axis with the pathophysiology of GWI [21, 22, 46, 47]. The HPA-axis is a well-integrated neuroendocrine circuit that connects immune and endocrine systems with the central nervous system (CNS). Dysregulation in the HPA axis might significantly impact the function and status of the immune system as well as supporting neuroinflammation. Golier and colleagues in 2006 exposed symptomatic Gulf war veterans without any psychiatric illness, veterans with Post-traumatic stress disorder (PTSD) alone as well as non-deployed veterans to a synthetic glucocorticoid such as dexamethasone (DEX) and compared the levels of adreno corticotropin hormone (ACTH) in each group. They found that the suppression of the secretion of ACTH by the synthetic glucocorticoid was significantly aggravated in symptomatic Gulf War veterans without psychiatric illness, as well as in veterans with Post traumatic stress disorder

(PTSD) alone in comparison to the non-deployed veterans [21], suggesting altered feedback regulation of the HPA axis. In addition, the suppression of in situ cortisol by exposure to DEX was also found to be significantly greater in Gulf War veterans without psychiatric illness and Gulf War veterans with PTSD only than non-deployed veterans and Gulf War veterans with both PTSD and Major depression disorder (MDD) [22]. The main finding of this study was that Gulf War deployment was associated with significantly greater cortisol suppression by DEX on controlling for weight, smoking status, PTSD, and MDD. PTSD was not associated with response to DEX. Further, these same investigators observed substantial reductions in both basal and metyrapone-stimulated levels of ACTH compared to healthy non-deployed veterans, suggesting that this might be due to a significantly attenuated ACTH response by the pituitary in veterans with GWI without PTSD [46, 47]. However, the mechanisms behind this reduced drive to the HPA axis for the excess responsiveness to neuroendocrine challenge have yet to be characterized. Other associated pathophysiology may include hypersensitivity of normal cytokine feedback to the HPA axis [48] as well as the expected stress-induced release of neuropeptides such as NPY and its mediation of innate immune response and cortisol levels [49].

1.2.3 Neurological dysfunction

As mentioned earlier, GW veterans were potentially exposed to several neurotoxic agents in the war theater such as pesticides, chemical warfare and PB, etc... Accordingly, increased rate of several neurological conditions such as Amyotrophic lateral sclerosis (ALS), brain cancers, migraine/headaches, seizures, neuritis and neuralgia, multiple sclerosis (MS) and Parkinson's disease (PD) have been reported in GW veterans [13]. However, there has been a lack of consistency in the reports of occurrence of these neurological conditions. For instance, several studies have reported

higher rate of ALS in GW veterans until Horner and colleagues in 2008, suggested it as a time-dependent outbreak that disappeared after 10 years of deployment [50]. In accordance, epidemiological studies performed afterwards support the findings of Horner et al. (2008) [50] and did not find mortalities from ALS in deployed GW veterans in excess of controls [51]. Similarly, no significant differences were found in mortality due to brain cancer, Parkinson's Disease (PD) and Multiple Sclerosis (MS) overall in GW veterans and controls [51]. Similarly, there were no significant differences in the occurrence of MS in GW veterans in comparison to non-veterans [52]. Nonetheless, another study reported 64% of the GW veterans with CFS/ME as well as non-veterans with CFS/ME were diagnosed with chronic migraines/headaches, which is significantly higher rate than that seen in healthy controls [53]. Moreover, veterans exposed to the highest levels of contaminants from oil well fires were reported to have increased rates of brain cancer deaths [51]. Results such as this support the existence of possible subgroups in GWI [13].

In keeping with this, the results of neuroimaging studies have also supported the existence of subgroups in the GWI population. In 2003, Rayhan and colleagues [54] performed repeated 2-back working memory test with functional magnetic resonance imaging (fMRI) before and after bicycle exercise stress test and assessed the levels of lactate metabolite in the prefrontal cortex prior to and after an exercise challenge in ill GW veterans. Some veterans had decreased 2-back score but significantly elevated prefrontal lactate levels whereas some veterans had increased 2-back score compared to no change in 2-back score in healthy controls. Receiver-operating curve (ROC) assessment of classification on the basis of prefrontal lactate levels prior to exercise demonstrated the possible existence of two diametrically opposed subgroups in GWI [54]. Similarly, Weiner (2005) performed magnetic resonance imaging (MRI) and

spectroscopy (MRS) to initially identify brain metabolic abnormalities in choline/creatine ratios in GW veterans meeting Haley Syndrome 2 (Confusion-ataxia) criteria for GWI [55] but failed to confirm these findings in another study with a separate group where N -acetylaspartate (NAA), creatine and choline levels did not differ significantly in symptomatic versus asymptomatic GW veterans [56].

Reduced white and grey matter volumes in cortical regions, reduced signalling in the thalamus, caudate, hippocampus, globus pallidus and putamen have been consistently reported in several imaging studies [57-59]. Specifically, fatigue, pain and hyperalgesia in this population were associated with the diminished white matter integrity in GW veterans with CFS/ME or CMI in a group of fMRI studies [53, 54, 57]. Other imaging studies used physostigmine infusions to challenge the cholinergic system [58, 60] and reported abnormal cerebral blood flow through the hippocampus before the physostigmine challenge, and after the challenge in an fMRI study [58]. Veterans satisfying the criteria of Haley syndromes 2 (Confusion-ataxia) and 3 (Neuropathic pain) showed significantly abnormal increases in regional cerebral blood flow in the hippocampus of both hemispheres [58]. Another study using single-photon emission computed tomography (SPECT) reported similarly elevated cerebral blood flow after a physostigmine challenge [60] collectively suggesting the exposure to chemicals in War Theater that can act on the cholinergic system. Collectively, all these findings suggest abnormalities in the central nervous system of this population.

1.2.4 Dysfunction of other systems

As, mentioned earlier, several lines of research have suggested dysfunction in immune, endocrine and central nervous signaling in GWI. Other abnormalities have also been reported in this population in recent years. For example, In 2014, Georgopoulos and coworkers [44] reported a significant reduction in the six alleles of a protective human

leukocyte antigen. In a follow up study by the same group in 2016, Authors [61] demonstrated the presence of HLA- and non-HLA-related neural influences on Neurological-Cognitive-Mood (NCM), Pain and Fatigue symptom severity in GWI, suggesting an involvement of genetic vulnerability to disruption of neuro-immune function. In another line of research, mitochondrial dysfunction has been linked to GWI with a hypothesis that chemical exposures related to the Gulf War can be toxic to mitochondria and can cause the symptoms related to GWI such as fatigue and dysfunction of brain, muscle, gastro-intestine, sleep and autonomic nervous system [13]. Recently, It has been observed that post-exercise recovery rate of phosphocreatine was significantly slower in GW veterans in comparison to controls matched for the age, sex and ethnicity [62]. Phosphocreatine is a back-up energy source for muscles that is depleted during exercise, and the speed of recovery is dependent on the rate of mitochondrial ATP synthesis. Delayed recovery of phosphocreatine has been confirmed as a robust measure of mitochondrial defects *in vivo* [63]. More recently, significantly elevated mitochondrial DNA lesion frequencies and mitochondrial DNA copy numbers (mtDNAcn) were found in the peripheral blood mononuclear cells (PBMC) of GW veterans than controls, indicating the mitochondrial dysfunction in this population, albeit in a pilot cohort [64].

The findings of these human studies provide strong evidence of the broad insult to multiple affected systems. However, there are no widely accepted broadly applicable clinical markers of GWI known at this time. There are many reasons that might have affected the progression towards definitive clinical markers. For example, early studies of GWI were hampered by a still evolving case definition and studies are still challenged by the highly heterogeneous nature of this illness group. Moreover, there are no specific details of exposures that could explain who exposed to what chemicals. Importantly to

this work, conventional approaches still focused narrowly on small sets of markers without casting these in the context of a coordinated network of interacting cellular and molecular components. It is our belief that connectivity offers a highly complementary perspective, one that supports a higher contextual resolution that more faithfully represents mechanisms of illness. Focus on these mechanisms rather than expression of markers promises among other things to facilitate the translational integration of human and animal studies targeting different systems of the body thereby helping fill the remaining gaps in our understanding.

1.3 Animal models of GWI

Faced with a scarcity of data rigorously linking specific groups of Gulf war veterans to their different exposures, various animal models were tested across a range of possible exposures. For example, veterans were widely exposed to carbamates (in prophylactic medicines), organophosphates (in pesticides and nerve agents) that act as reversible or irreversible inhibitor of AChE enzyme activity respectively. Therefore, chronic inhibition of AChE enzyme activity by organophosphates and/or carbamates is widely hypothesized as a key mechanism underlying the persistent sickness behaviour that manifests in GWI veterans. Acetylcholine (ACh) is a neurotransmitter that binds to its receptors present on postsynaptic membrane for transmitting signals to and from innervated muscles. AChE enzyme is an enzyme capable of hydrolyzing the ACh and as a result, it helps in maintaining the low level of ACh on the postsynaptic membrane, required for uninterrupted neurotransmission [65]. The inhibition of AChE enzyme inhibits the hydrolysis of ACh leading to increase in concentration at the postsynaptic membrane. This eventually causes disrupted neurotransmission and the hyper-stimulation of nicotinic and muscarinic receptors [65]. Various animal models including rat, mouse, insects and bovine have been used to study the adverse effects of a number

of chemical exposures in Gulf war such as pesticides, PB, insect repellants, nerve agents and stress either alone or in combination as well as underlying mechanisms including AChE inhibition [13].

Of all the exposures, PB, a carbamate medication that also acts as reversible inhibitor of the AChE enzyme activity was perhaps the most widely studied as a causative agent of GWI. This hypothesis was further supported by the fact that the 1991 Gulf war was the only conflict in which PB was widely used by military personnel as a prophylactic measure to protect against effects of possible nerve gas attacks [66]. Indeed, the findings of the early studies established the adverse effects of PB on nerve and immune function [67, 68], along with its effects on cardiovascular structure [69], muscular [70] and gastrointestinal systems [71]. More recently, the administration of PB prior to a stressor was linked to long-term learning and social behavioural changes such as implulsiveness and aggressiveness in a rat model of GWI [72]. In an extension of this study, the expression of genes associated with stress response, learning and memory were surveyed in the hippocampus and hypothalamus of rats. Their results suggested that exposure to PB prior to stress applied daily for 10 days increased the expression of three genes in the hippocampal region implicated in memory development, namely brain-derived neurotrophic factor (BDNF), tropomyosin-related kinase B (TrkB) and calcium/calmodulin-protein kinase II alpha (CamKII) [73]. However, these changes in gene expression in the central nervous system (CNS) were not linked to a disruption of Blood Brain Barrier (BBB) integrity [74].

In addition to PB, veterans were exposed to several other irreversible and reversible AChE inhibiting organophosphates, such as pyrehtroid-based pesticide Permethrin (PER), Chloropyrifos (CPF), Chlorpyrifos Oxon (CPO), the insect repellant N, N-diethyl-m-toluamide (DEET) and possibly low levels of the nerve gas Sarin. In recent

years, the effects of these potential organophosphate exposures have also been investigated in various animal models of GWI with or without PB. For example, exposure to acute levels of PB and PER for 10 days in a mouse model of GWI leads to an increase in the anxiety-like behaviour, psychomotor problems and delayed cognitive impairment in exposed animals [75]. In addition, an increased astrogliosis was observed in exposed mice after 150 days (chronic post-exposure) [75]. The elevated levels of precursors of phosphocholine that are required for the endogenous synthesis of ACh enzyme namely, phosphatidylcholine (PC) and sphingomyelin (SM) further supported this mouse model of GWI [76]. In another mouse model of GWI, 6 month-old mice exposed to the CPF alone as well as in combination with PB and PER (CPF + PB + PER) showed significantly reduced levels of the synaptophysin in the hippocampus and number of doublecortin positive cells in dentate gyrus (DG) [77]. This significant reduction in synaptophysin and doublecortin indicate compromised synaptic integrity and altered neuronal differentiation. In addition, a significant increase in brain acetylcholine (ACh) levels was also observed in mice exposed to CPF with or without PB and PER [77]. In addition, the effects of combined exposure to PB, DEET and PER with or without physiological stress for 4 weeks were investigated in adult mice [78]. Mice exposed to the combination of PB + DEET + PER exhibited depressive and anxiety-like behaviour with spatial learning and memory dysfunction. Mild stress exacerbated these behavioural impairments in spatial learning and memory. Indeed, the mice exposed to PB, DEET and PER exhibited reduced neurogenesis, partial neuron loss, and mild inflammation in the hippocampus even 2 months after exposure [78]. Consistent with this, mice exposed to PB+DEET for a period of 2 weeks followed by a sarin gas surrogate, diisopropyl fluorophosphate (DFP), exhibited alterations in dopamine and glutamatergic neurotransmission. As with combined exposure to PB + DEET + DFP, exposure to CPF as well as DFP alone for a week, caused similar effects in these mice

[79]. In a separate study in 2011, Middlemore-Risher and colleagues observed a concentration-dependent increase in mitochondrial length, a decrease in mitochondrial number (indicative of increased fusion events), and a decrease in mitochondrial movement in axons of rats after 1 or 24 h exposure to CPF and its active metabolite CPO [80]. Interestingly enough, these changes occurred at concentrations of CPF and CPO that did not inhibit acetyl cholinesterase activity, again suggesting the involvement of some mechanism other than cholinergic transmission [80]. Likewise, mice exposed to CPF for 5-days at subclinical level showed an early (2-7 days) increase in synaptic transmission in the CA3-CA1 region of the hippocampus after CPF injection. Conversely, a decrease in the CA1 spine density as well as synaptic transmission was observed in these mice as long as 3 months later [81]. Moreover, signs of cholinergic toxicity were absent in these mice again suggesting a mechanism other than AChE inhibition for these adverse effects [81]. Similar to CPF exposure, a low dose exposure to DFP for 5 days caused chronic depression, anxiety and memory problems even after 3 months of the exposure in a rat model of GWI [82]. Moreover, chronic low dose of DFP exposure was able to damage the neurons in these rats [82]. Indeed, exposure to DFP alone was able to cause neuroinflammation throughout the brain of mice as well as rats [83, 84]. However, prior exposure to corticosterone equivalent to levels induced by physiological stress potentiated the neuroinflammation caused by DFP alone in both rat and mouse models of GWI [83, 84]. In contrast, a chronic 2-week exposure to PB/DEET in the absence of stress hormone neither produced neuroinflammation alone nor was able to raise the level of neuroinflammation caused by DFP in this model of GWI [83].

Indeed, animal models provide critical insights into the effects of exposure to agents used in the GW theatre and results strongly support a neuro-immune basis for this illness. However, similar cytokine or phospholipid surveys are not easily obtained from human brains. Also, animal models until now have largely focused indirectly on the

effects of exposure and have not attempted to directly mimic neuro-immune signaling in the brains of affected veterans. Despite the collective body of evidence from the animal studies mentioned above, the picture of the GWI pathobiology in humans is still blurred. Nonetheless, findings from animal and human studies alike suggest that the synergistic or individual adverse effects of organophosphates present in theatre in prophylactic medicines, pesticides and nerve agents along with physiological or psychological stress might have altered neuro-immune signaling in genetically susceptible GW veterans. Considering the extensive cross-talk between the brain and the periphery we propose that the evaluation of easily accessible clinical markers with far reaching inflammatory effects such as cytokines offers a promising opportunity for identifying biomarkers as well as therapeutic solutions for GWI.

1.4 Cytokines: Potential biomarkers of cell signalling in GWI

As mentioned earlier, the involvement of complex patterns of cytokine signaling in most of the aspects of immune response has gained in appreciation in the last two decades and cytokine surveys have been widely used as reliable indicators of inflammation, disease state, or response to therapy in a wide variety of pathologies. Measurement of peripheral cytokine levels remain an attractive avenue to evaluate the state and severity of inflammation in different diseases where diagnostic tests are currently either too invasive or not available at all. For example, altered cytokine profiles have been observed in several complex chronic illnesses including, Gulf War Illness (GWI) [26, 27, 29], rheumatoid arthritis (RA) [85], Chronic Fatigue Syndrome (CFS) [86, 87], Multiple Sclerosis (MS) [88, 89], Inflammatory Bowel Diseases (IBDs) such as Ulcerative Colitis (UC) [90, 91] and Crohn's Disease [91, 92] as well as several types of cancers including colorectal carcinoma [93], ovarian cancer [94] and pancreatic cancer [95]. Accordingly, cytokine panels are increasingly used as clinical markers of pathogenesis in a range of

diseases [34]. Moreover, cytokine therapies are also among the most promising avenues of treatment in several infectious, autoimmune and immunosuppressive illnesses [96]. Indeed, the therapeutic administration of cytokines, modulation of cytokine action, or at times immune gene therapy is being used for a wide range of infectious and autoimmune diseases, in immuno-compromised patients with AIDS, and in neoplasia [96].

As mentioned earlier, human as well as animal studies of GWI have confirmed the alterations in the expression levels of inflammatory cytokines in the periphery and brain respectively, suggesting an inflammatory response to stress and neurotoxins [26, 27, 83]. Indeed, inflammation is a major part of GWI and can affect multiple behaviours including sleep, pain, appetite and cognition (learning and memory) that could fit into the definition of 'sickness behaviour'. Interestingly, it is already known that cytokines can interact with neurons [97] and in turn give rise to a 'sickness behaviour' [98]. Therefore, a basic understanding of the complex inner-workings of the immune system moves us one step closer to integrating sickness behaviour symptoms with what we know about physiology.

Despite these observations, it is still challenging to use cytokines as a diagnostic tool due to their complex pleiotropy. The levels of individual cytokines vary greatly from person to person due to several factors such as physiological environment including stress, fitness level and feeding state of individual, their location, signals received by the releasing cells and the type of target cells [99]. Therefore, it is challenging for traditional univariate approaches that study one element at a time to decode their behaviour as a part of an integrated ecosystem. Historically, experimental techniques such as enzyme-linked immune sorbent assays (ELISAs) were restricted to measuring a small number of cytokines in each sample. However, commercially available multiplex assays have now enabled the quantitative measurements of fifty or more cytokines simultaneously and are

allowing investigators to address the contextual complexity of immune responses [99]. With the advent of these new broad-spectrum assays it is now possible to observe and map the community-wide immune dialogues supported by cytokine signaling and deploy new data analytical techniques of these patterns towards the study of chronic complex illnesses such as GWI.

1.5 Systems Biology: Background

Although the reductionist approach of studying individual elements of biological systems has served us well in the past and continues to provide insights into the workings of these entities, it is increasingly clear that these diverse, pleiotropic units exist in the context of a larger and well-integrated community and interact dynamically to produce a coherent behaviour directed at efficiently accomplishing their biological function [100]. Our current understanding of networked biological systems is that they are robust to random perturbations and external attacks across different scales of biology. Indeed, robust networks ensure the maintenance of specific functionalities against perturbations or challenges by applying alternative modes of action through adequate control of structural and functional components [101]. In biological systems specifically, the maintenance of functionality is determined by the individual biological constituents involved and underlying communication patterns among them [100]. A perturbation such as an immune challenge or environmental condition might force a biological system to move out of its normal stable steady state i.e. resting homeostasis. If conditions are such that the system remains within a prescribed operating range (basin of attraction), then it will return back to its original resting state upon removal of the challenge. Notwithstanding, if a significant challenge persists and results in conditions outside the normal response envelope the system may adopt an alternative response to the perturbation by recruiting failsafe mechanisms not normally used. The existence of

functionally redundant constituents for example, duplicate genes, parallel pathways that might complement the function of other genes/ pathways through alternative mechanisms in case of failure have been reported in several biological systems [102-104]. Such an adaptive response to external stimuli would manifest as an observable restructuring of interaction patterns among the active constituents of that biological system.

The properties that emerge from the collective behaviour of this kind of complex interaction between entities are challenging to explain by traditional piecewise approaches. In the last two decades, the rise of “omics” research (genomics, proteomics, metabolomics etc.) and the emergence of high throughput technologies such as next-generation sequencing, gene expression profiling, mass spectrometry, and multiplex assays as well as flow cytometry and other technologies offering single-cell resolution have provided breadth of coverage to capture the comprehensive snapshots of biological processes in a cellular environment by their extended capability of measuring multiple genes, proteins, metabolites, cells and/or cytokines [105]. Indeed, enormous amounts of data are generated today through these next-gen technologies. However, the data generated is similar to the list of parts of any engineered system such as radio, television, or a car’s electric system without any wiring diagram or manual [106]. It is impossible to fix or recreate a complex system without the wiring diagram. By the same token, it is necessary to understand the underlying wiring patterns of the complex human physiological systems if we are to formulate and test clinical hypotheses in any but the simplest of pathologies, otherwise this enormous amount of data may eventually leave us data rich and knowledge poor [105]. A holistic systems biological approach provides a framework that bridges experiments with mathematical and computational concepts to infer the complex interactions of interdependent cellular components (cells, genes, proteins, metabolites etc.) within a biological system, the evolution of these system-wide

relationships with time and the emergent behaviours they support in response to external perturbations at various levels of biological complexity [105].

1.5.1 Inference of regulatory interactions

One of the key challenges in studying biological systems is to unravel the underlying complex interactions that determine the function and behaviour of a biological system. This complexity is such that much of this underlying circuitry is still unknown after decades of efforts, especially as it applies to higher organisms such as humans. As a consequence of this inherent interactivity in biological systems, changes in the expression levels of active biological markers reflect the underlying recruitment and instantiation of an active regulatory mechanisms and this can be represented as changes in network structure. Therefore, a better understanding of the structure of these co-expression networks has the potential to enhance our diagnostic potential [107]. Social and behavioural networks are widely studied using the principles of classical statistics and graph theory. Application of these principles can be directly extended to another level of biology. For example, gene co-expression networks are widely studied using Pearson or Spearman's correlation coefficients as measure of association. More sophisticated measures such as mutual information have also been deployed in tools such as ARACNE (Algorithm for the Reconstruction of Accurate Cellular Networks) [108]. ARACNE has been used to map nonlinear associations among transcription factors and their target genes in several diseases including brain tumors [109], oncogenesis [110] and Schizophrenia [111]. Though informative, the inferred undirected networks represent static snapshots of the underlying interactions, typically at rest. Indeed such association networks fail to elucidate the direction of flow of regulatory information and as such are devoid of cause and effect information.

Most biological systems are dynamic in nature and therefore the expression/abundance of genes/proteins or other biomolecules changes with time and in response to different perturbations and so their interaction patterns. Static regulatory networks are unable to capture the evolution of regulatory networks. Approaches such as Dynamic Bayesian networks [112], regression based approaches such as TIGRESS [113], GENIE3 [114] and others have been developed to infer the structure of directed graphs active in the data. The added knowledge about the direction and mode of information flow could be very helpful to identify the underlying regulatory principles. For example, enrichment of specific feed-forward motifs was identified in a microRNA-transcription factor regulatory network of Schizophrenia documented in the databases [115]. In principle, one should know the structure of regulatory interactions *a priori* to identify such specific principles of regulation. However, a major challenge for the systems/network biology is that a significant part of regulatory circuitry still remains to be discovered. In such cases, the temporal patterns of expression/abundance must be used as proxy to infer causality. The inference of underlying wiring of complex biological systems with the help of computational and mathematical methods may help us to predict the missing circuitry that can be further verified experimentally. Several methods were developed for the inference of directed networks from time course data using different mathematical foundations. These methods range from simple and effective methodologies such as rate equation models [116] to more complex model forms such as formal Hill kinetics [117].

1.5.2 Wiring of biological systems is not random

In general, any complex system with interacting constituents can generally be represented as graphs/networks where individual constituents represented as nodes/vertices and the interactions among them represented as edges/links. Depending

on the type of data available, these edges can further illustrate the direction of regulation as well as the mode of action i.e., activator or inhibitor in the regulatory network to further facilitate the simulation of complex system behaviours. Real world networks were initially considered random in structure and studied using the model proposed by Erdos-Renyi [118]. In the late 90s, two simultaneous studies observed that real world networks connectivity is not randomly distributed but arranged according to certain principles. In particular, Watts and Strogatz (1998) [119] observed that any node in a real world network could be reached from any other node by following only a few links. In other words, the average path length between two nodes or the diameter of a real-world network is relatively shorter than that of random networks. Structures such as these were said to have a small-world architecture [119]. In addition, small-world networks exhibit a high degree of clustering meaning essentially that any two nodes having a same third node as a shared neighbour have a higher probability of being neighbours to one another and can be described as having a high clustering coefficient. Simultaneously, Barabási and Albert (1999) [120] observed that the degree distribution in real world networks including biological networks do not follow a Poisson distribution rather approximates the power law distribution:

$$\rho(k) \sim k^{-\gamma} \quad (1.1),$$

where, γ is the degree component. They termed this structure as 'scale-free'. Power law distribution implies that most nodes in a real-world network have a few connections with increasingly small number of highly connected 'hubs'. Several biological networks such as metabolic networks, neuronal network in *Caenorhabditis elegans*, and protein-protein interaction networks have been reported with the characteristics of both scale-free as well as small-world networks [119, 121]. These observations in biological networks have revolutionized the application of graph/network theory to the systematic analysis of

design principles in complex biological networks and have given rise to a new field called ‘Network Biology’. Several of the classical graph theoretical measures of topology namely, degree distribution, clustering coefficient, shortest path length etc. have been widely used to study the global topological properties of biological networks. As per our current understanding, the global structural features of biological networks ensure robustness against random attacks and exposures. For example, higher clustering coefficients imply the existence of topological modules or a community structure in a biological network. These modules define the tightly connected sets of genes, proteins or cells that accomplish a certain function together and confer robustness to the system from random environmental perturbations or bacterial and viral attacks by virtue of their usually weak connections to more remote outer nodes/modules [122]. Many studies supported the existence of modules or community structure in biological networks for example, metabolic networks [123], gene regulatory networks and protein-protein interaction networks [124]. Moreover, alterations in topological modules have been reported in several diseases such as Inflammatory bowel disease (IBD) [125], Alzheimer’s [126] and Parkinson’s disease [127].

In addition, several other local specialized patterns of interaction such as ‘hubs’, ‘motifs’, and ‘bottlenecks’ are reported in biological networks and have been shown to play important roles in maintaining the robust function of a biological system. For example, highly connected ‘hubs’ in otherwise sparsely connected biological networks create inhomogeneity in network structure that eventually provides robustness against frequently occurring random errors [128]. However, this is traded off with the lethality caused by the removal of ‘hub’ nodes from the network. Hub proteins tend to be encoded by essential genes and the removal of highly connected ‘hubs’ proteins from the protein-protein interaction networks confirmed to be lethal at least in the model organisms [129]. Similarly, ‘motifs’ that are specific patterns of interactions among small

subset of 3-4 nodes are significantly overrepresented in complex biological networks compared to random networks [130] and have been shown to play important roles in ensuring the robustness of biological systems [131]. For example, positive and negative feedback loops are used in a wide range of regulatory networks, including the cell cycle, the circadian clock and chemotaxis [100, 132]. Similarly, so-called 'bottlenecks' are the genes/proteins with high network betweenness centralities; these have an even higher tendency than a hub gene/ protein of being essential to network function [133]. Findings such as these underscore the importance of changes in local topological properties such as betweenness centrality, degree centrality (hub nodes) or activation of an alternative motif as such, can lead to the significant alterations in the overall function of a biological network. Several other graph theoretical measures such as closeness centrality, eigenvector centrality as well as hub and authority scores are available to further quantify local changes in network connectivity and provide details into the importance of a node in the context of the greater network.

1.6 Hypothesis and current study

As described in several of the sections above, GWI is a debilitating illness with complex constellation of symptoms that affect several systems of the body including immune, endocrine and nervous system. Although, several animal and human studies link GWI to the stress response, there is still no clear idea of its pathophysiology. One of the important reasons behind this ambiguity may be that most of the animal and human studies were limited to the survey of a handful of genes/cytokines/phospholipids and did not study them as part of a complex system of interacting components. It is now increasingly clear that biological systems are robust and try to maintain their core functionalities against attacks and challenges by using alternative mechanisms supported through specific topological structures of molecular and cellular networks. In

doing so, the system can move back and forth from its stable steady state to alternative response states within the variety of basins. In certain cases such as in response to an illness, the human physiological system might move out of range of its central basin or resting state to an alternative homeostatic region in an effort to adapt and under certain conditions it might not come back to its original state [101]. In this study, we hypothesize that GWI is a condition where the regulation of principal physiological systems have been displaced from their original homeostasis to a less efficient but persistent alternative regulatory regime. In this thesis, we focus on immune function and the cytokine signaling networks that oversee this as it applies to Gulf war veterans. Since cytokines work in close collaboration with each other, therefore we further hypothesize that the cytokine communication patterns would be altered in response to a challenge in veterans affected with GWI in a way that differs significantly from their healthy counterparts. In principle, these regulatory networks can be used to identify alternative steady states by considering the biochemical kinetics of the system. Such stable regulatory modes each support alternative patterns of interaction and will manifest as structurally different biomarker association networks. In this thesis, we focus on exploring this further by studying changes in immune networks manifested in experimental; data collected in different subject groups by using formal graph theoretical methods. We posit that characteristic network signatures exist for chronic illness conditions and that these may eventually determine important drug targets. Specifically, they may support the network-informed design of treatments able to overcome the biochemical energy barrier separating stable healthy immune regulation from the persistent dysregulated GWI homeostatic regime (Figure 1.1). The hypothesis being that the illness-specific appearance of subsets of associations and the disappearance of others may indirectly point to the characteristic activation and inactivation of signaling mechanisms involved in perpetuating illness. This focus on normalizing associations

differs significantly from the conventional clinical use of observational data, which remains rooted in the normalization of individual marker expression. Interventions directed at restoring abhorrent association patterns instead of normalizing marker expression would in essence be targeting root-cause illness mechanisms. Indeed this work presents metrics for describing a departure from desired regulatory patterns of marker co-expression that can be used as quantitative measures of illness severity and conversely measures of success of an intervention.

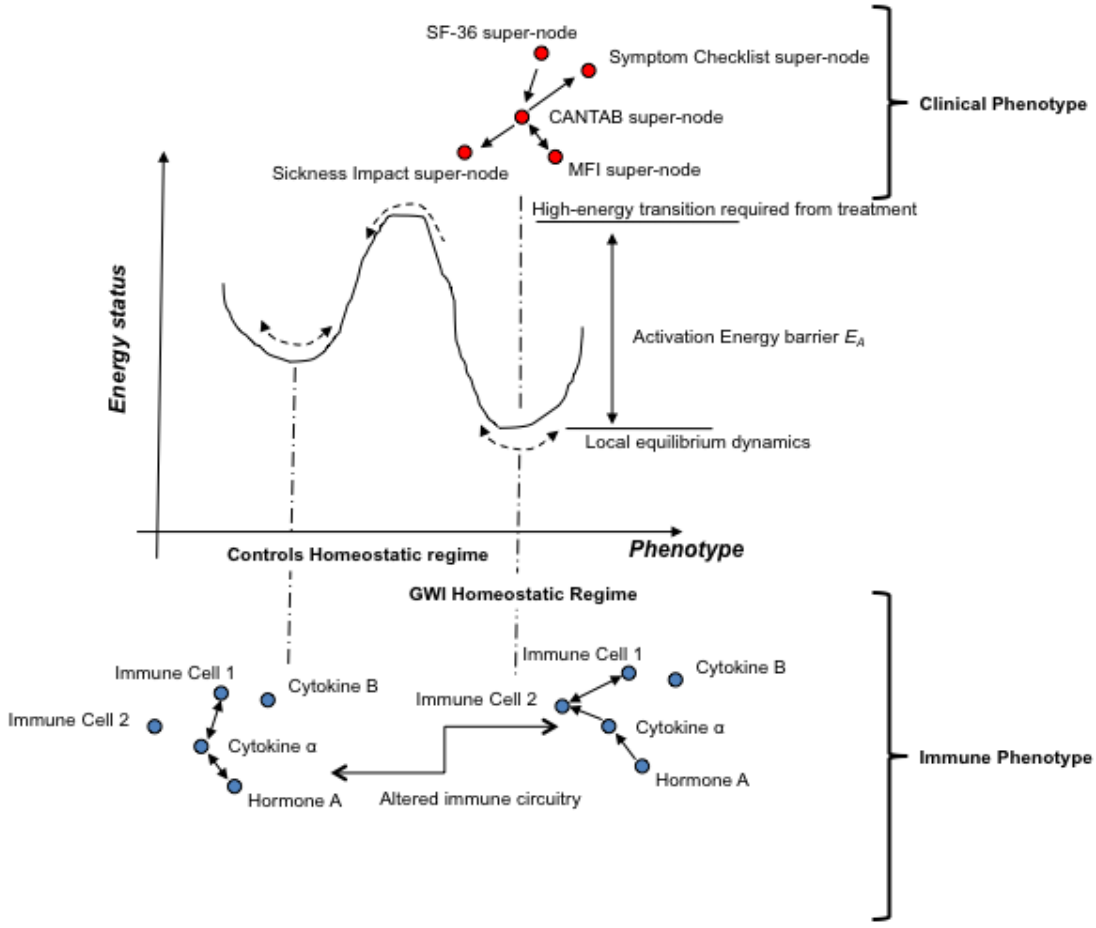

Figure 1.1: Conceptual framework of the hypothesis: GWI homeostatic regime is different from the homestatic regime in healthy controls and require to cross an energy barrier to move to the healthy regime. Studying the alterations in the underlying molecular patterns may help to plan the treatment to identify the drug targets in the circuitry to make the circuitry more like healthy controls and cross the energy barrier.

Several systems-directed studies conducted by our group have compared the topological architecture in immune signaling networks constructed from *a priori* defined clinical groups of GWI and healthy controls with the aim of identifying illness-specific network features. Indeed, this research has successfully identified individual elements and local sub-assemblies that drive the symptom-mediated shifts in the topology of these networks across several levels of biological complexity [40, 45]. However, these studies consisted of early analyses in static snapshot data and as such did not support direct consideration of the subsequent dynamical modes supporting the emergence and exacerbation of symptoms [134,135].

In this thesis, we move towards the inference of directed networks from time course data in an effort to gain additional insight into altered immune regulatory principles that might support the persistence of GWI. As mentioned earlier, several methods with different mathematical backgrounds have been proposed for the identification of underlying directed regulatory networks. However, there remain several unanswered questions regarding the identifiability of directed networks under experimental constraints typical of *in vivo* studies such as, suitability and performance of methods, data requirements, and other important aspects such as optimization of parameters for improving the performance of these methods. In Chapter 2, we explore the issues mentioned above in detail. In Chapter 3, we define functional sets in a multiplex panel of 16-cytokines and use the insights and methods developed in Chapter 2 along with prior knowledge of cytokine signaling to infer the interaction networks among these functional sets. A theoretical comparison of the immune network structure across subject groups identified significant feed-forward mediation of IL-23 and IL-17 by IL-6 and IL-10 as distinguishing control elements that were characteristically active in GWI versus healthy veterans. Furthermore, simulated restructuring of the regulatory circuitry in GWI that would result by applying an IL-6 receptor antagonist in combination

with either a Th1 (IL-2, IFNγ, TNFα) or IL-23 receptor antagonist predicted a partial rescue of immune response elements previously associated with illness severity.

In Chapter 4, we extended the systems biological approach to study the cytokine communication patterns in a mouse model of GWI and constructed the undirected co-expression patterns among 12-cytokines in response to the neurotoxin relevant to GWI namely, Diisopropyl fluorophosphates (DFP), a sarin gas surrogate with and without prior physiological stress. Although, the effects of DFP were subdued in the conventional comparison of immune marker levels. Clear topological differences due to the inclusion of DFP in the exposure regimen were evident in the comparison of immune association networks in response to CORT LPS and CORT DFP LPS exposures. Our results also confirm the role of CORT in the exacerbation and consistency of inflammatory response in the periphery. Further, we attempted to align these immune response networks to DFP in mice with prior exposure to CORT equivalent to physiological stress with the immune signaling network observed in human subjects affected with GWI. To our surprise, we identified an evolutionarily conserved characteristic active motif that was shared between the mouse and high trauma GWI. The detailed studies are described in chapters ahead.

1.7 References

1. Haley, R. W. (1997) Is Gulf War Syndrome Due to Stress? The Evidence Reexamined, *Am J Epidemiol.* **146**, 695-703.

2. Fukuda, K., Nisenbaum, R., Stewart, G. Thompson, W. W., Robin, L., Washko, R. M., Noah, D. L., Barrett, D. H., Randall, B., Herwaldt, B. L., Mawle, A. C., Reeves, W. C., (1998) Chronic multisymptom illness affecting air force veterans of the gulf war, *JAMA.* **280**, 981-988.

3. Steele, L. (2000) Prevalence and Patterns of Gulf War Illness in Kansas Veterans: Association of Symptoms with Characteristics of Person, Place, and Time of Military Service, *Am J Epidemiol.* **152**, 992-1002.

4. Haley, R. W., Kurt, T. L. & Hom, J. (1997) Is there a gulf war syndrome? Searching for syndromes by factor analysis of symptoms, *JAMA.* **277**, 215-222.

5. Institute of, Medicine (2014) Chronic Multisymptom Illness in Gulf War Veterans: Case Definitions Reexamined, The National Academies Press, Washington, DC.

6. Gronseth, G. S. (2005) Gulf War Syndrome: A Toxic Exposure? A Systematic Review, *Neurol Clin.* **23**, 523-540.

7. Golomb, B. A. (2008) Acetylcholinesterase inhibitors and Gulf War illnesses, *Proc Natl Acad Sci.* **105**, 4295-4300.

8. Kerr Kathleen, J. (2015) Gulf War illness: an overview of events, most prevalent health outcomes, exposures, and clues as to pathogenesis in *Rev Environ Health* 273-286.

9. Cherry, N., Creed, F., Silman, A., Dunn, G., Baxter, D., Smedley, J., Taylor, S. & Macfarlane, G. (2001) Health and exposures of United Kingdom Gulf war veterans. Part II: The relation of health to exposure, *Occup Environ Med.* **58**, 299-306.

10. Nisenbaum, R., Barrett, D. H., Reyes, M. & Reeves, W. C. (2000) Deployment Stressors and a Chronic Multisymptom Illness among Gulf War Veterans, *J Nerv Ment Dis.* **188**, 259-266.

11. Wolfe, J., Proctor, S. P., Erickson, D. J. & Hu, H. (2002) Risk Factors for Multisymptom Illness in US Army Veterans of the Gulf War, *J Occup Environ Med.* **44**, 271-281.

12. Steele, L., Sastre, A., Gerkovich, M. M. & Cook, M. R. (2012) Complex Factors in the Etiology of Gulf War Illness: Wartime Exposures and Risk Factors in Veteran Subgroups, *Environ Health Perspect.* **120**, 112-118.

13. White, R. F., Steele, L., O'Callaghan, J. P., Sullivan, K., Binns, J. H., Golomb, B. A., Bloom, F. E., Bunker, J. A., Crawford, F., Graves, J. C., Hardie, A., Klimas, N., Knox, M., Meggs, W. J., Melling, J., Philbert, M. A. & Grashow, R. (2016) Recent research on Gulf War illness and other health problems in veterans of the 1991 Gulf War: Effects of toxicant exposures during deployment, *Cortex.* **74**, 449-475.

14. Kang, H. K., Natelson, B. H., Mahan, C. M., Lee, K. Y. & Murphy, F. M. (2003) Post-traumatic stress disorder and chronic fatigue syndrome-like illness among Gulf War veterans: a population-based survey of 30,000 veterans, *Am J Epidemiol.* **157**, 141-148.

15. Eisen, S. A., Kang, H. K., Murphy, F. M., Blanchard, M. S., Reda, D. J., Henderson, W. G., Toomey, R., Jackson, L. W., Alpern, R., Parks, B. J., Klimas, N., Hall, C., Pak, H. S., Hunter, J., Karlinsky, J., Battistone, M. J., Lyons, M. J. & Investigators, G. W. S. P. (2005) Gulf war veterans' health: Medical evaluation of a U.S. cohort, *Ann Intern Med.* **142**, 881-890.

16. Nicolson, G. L. & Nicolson, N. L. (1998) Gulf War illnesses: Complex medical, scientific and political paradox, *Med Confl Surviv.* **14**, 156-165.

17. Crofford, L. J., Young, E. A., Engleberg, N. C., Korszun, A., Brucksch, C. B., McClure, L. A., Brown, M. B. & Demitrack, M. A. (2004) Basal circadian and pulsatile ACTH and cortisol secretion in patients with fibromyalgia and/or chronic fatigue syndrome, *Brain Behav Immun.* **18**, 314-325.

18. Demitrack, M. A., Dale, J. K., Straus, S. E., Laue, L., Listwak, S. J., Kruesi, M. J. P., Chrousos, G. P. & Gold, P. W. (1991) Evidence for Impaired Activation of the Hypothalamic-Pituitary-Adrenal Axis in Patients with Chronic Fatigue Syndrome, *J Clin Endocrinol Metab.* **73**, 1224-1234.

19. Fletcher, M. A., Maher, K. J. & Klimas, N. G. (2002) Natural killer cell function in chronic fatigue syndrome, *Clin Appl Immunol Rev.* **2**, 129-139.

20. Vojdani, A. & Thrasher, J. D. (2004) Cellular and humoral immune abnormalities in Gulf War veterans, *Environ Health Perspect.* **112**, 840-846.

21. Golier, J. A., Legge, J. & Yehuda, R. (2006) The ACTH Response to Dexamethasone in Persian Gulf War Veterans, *Ann N Y Acad Sci.* **1071**, 448-453.

22. Golier, J. A., Schmeidler, J., Legge, J. & Yehuda, R. (2006) Enhanced cortisol suppression to dexamethasone associated with Gulf War deployment, *Psychoneuroendocrinology.* **31**, 1181-1189.

23. Maher, K. J., Klimas, N. G. & Fletcher, M. A. (2005) Chronic fatigue syndrome is associated with diminished intracellular perforin, *Clin Exp Immunol.* **142**, 505-511.

24. Whistler, T., Fletcher, M. A., Lonergan, W., Zeng, X.-R., Lin, J.-M., LaPerriere, A., Vernon, S. D. & Klimas, N. G. (2009) Impaired immune function in Gulf War Illness, *BMC Med Genomics.* **2**, 12.

25. Ciccone, D. S., Weissman, L. & Natelson, B. H. (2008) Chronic Fatigue Syndrome in Male Gulf War Veterans and Civilians, *J Health Psychol.* **13**, 529-536.

26. Zhang, Q., Zhou, X.-D., Denny, T., Ottenweller, J. E., Lange, G., LaManca, J. J., Lavietes, M. H., Pollet, C., Gause, W. C. & Natelson, B. H. (1999) Changes in Immune Parameters Seen in Gulf War Veterans but Not in Civilians with Chronic Fatigue Syndrome, *Clin Diagn Lab Immunol.* **6**, 6-13.

27. Smylie, A. L., Broderick, G., Fernandes, H., Razdan, S., Barnes, Z., Collado, F., Sol, C., Fletcher, M. A. & Klimas, N. (2013) A comparison of sex-specific immune signatures in Gulf War illness and chronic fatigue syndrome, *BMC Immunology.* **14**, 29.

28. Broderick, G., Fletcher, M. A., Gallagher, M., Barnes, Z., Vernon, S. D. & Klimas, N. G. (2012) Exploring the Diagnostic Potential of Immune Biomarker Coexpression in Gulf War Illness in *Psychoneuroimmunology Methods Mol Biol (Methods and Protocols)* (Yan, Q., ed) pp. 145-164, Humana Press, Totowa, NJ.

29. Khaiboullina, S. F., DeMeirleir, K. L., Rawat, S., Berk, G. S., Gaynor-Berk, R. S., Mijatovic, T., Blatt, N., Rizvanov, A. A., Young, S. G. & Lombardi, V. C. (2015) Cytokine expression provides clues to the pathophysiology of Gulf War illness and myalgic encephalomyelitis, *Cytokine.* **72**, 1-8.

30. Janeway, C., Travers, P., Walport, M. & Shlomchik, M. (2001) *Immunobiology*, Fifth edn, New York and London: Garland Science.

31. Parkin, J. & Cohen, B. (2001) An overview of the immune system, *The Lancet.* **357**, 1777-1789.

32. Mack, C. L. (2007) Serum cytokines as biomarkers of disease and clues to pathogenesis, *Hepatology.* **46**, 6-8.

33. Dembic, Z. (2015) Chapter 1 - Introduction—Common Features About Cytokines in *The Cytokines of the Immune System* pp. 1-16, Academic Press, Amsterdam.

34. Monastero, R. N. & Pentyala, S. (2017) Cytokines as Biomarkers and Their Respective Clinical Cutoff Levels, *Int J Inflam.* **2017**, 1-12.

35. Rook, G. A. W. & Zumla, A. Gulf War syndrome: is it due to a systemic shift in cytokine balance towards a Th2 profile?, *The Lancet.* **349**, 1831-1833.

36. Skowera, A., Hotopf, M., Sawicka, E., Varela-Calvino, R., Unwin, C., Nikolaou, V., Hull, L., Ismail, K., David, A. S., Wessely, S. C. & Peakman, M. (2004) Cellular Immune Activation in Gulf War Veterans, *J Clin Immunol.* **24**, 66-73.

37. Brimacombe, M., Zhang, Q., Lange, G. & Natelson, B. H. (2002) Immunological Variables Mediate Cognitive Dysfunction in Gulf War Veterans but Not Civilians with Chronic Fatigue Syndrome, *Neuroimmunomodulation.* **10**, 93-100.

38. Peakman, M., Skowera, A. & Hotopf, M. (2006) Immunological dysfunction, vaccination and Gulf War illness, *Phil Trans R Soc B: Biol Sci.* **361**, 681-687.

39. Allen, J. S., Skowera, A., Rubin, G. J., Wessely, S. & Peakman, M. (2006) Long-Lasting T Cell Responses to Biological Warfare Vaccines in Human Vaccinees, *Clin Infect Dis.* **43**, 1-7.

40. Broderick, G., Kreitz, A., Fuite, J., Fletcher, M. A., Vernon, S. D. & Klimas, N. (2011) A pilot study of immune network remodeling under challenge in Gulf War Illness, *Brain Behav Immun.* **25**, 302-313.

41. Israeli, E. (2012) Gulf War Syndrome as a part of the autoimmune (autoinflammatory) syndrome induced by adjuvant (ASIA), *Lupus.* **21**, 190-194.

42. Moss, J. I. (2013) Gulf War illnesses are autoimmune illnesses caused by increased activity of the p38/MAPK pathway in CD4+ immune system cells, which was caused by nerve agent prophylaxis and adrenergic load, *Med Hypotheses.* **81**, 1002-1003.

43. Parkitny, L., Middleton, S., Baker, K. & Younger, J. (2015) Evidence for abnormal cytokine expression in Gulf War Illness: A preliminary analysis of daily immune monitoring data, *BMC Immunol.* **16**, 57.

44. Georgopoulos, A. P., James, L. M., Mahan, M. Y., Joseph, J., Georgopoulos, A. & Engdahl, B. E. (2015) Reduced Human Leukocyte Antigen (HLA) Protection in Gulf War Illness (GWI), *EBioMedicine.* **3**, 79-85.

45. Broderick, G., Ben-Hamo, R., Vashishtha, S., Efroni, S., Nathanson, L., Barnes, Z., Fletcher, M. A. & Klimas, N. (2013) Altered immune pathway activity under exercise challenge in Gulf War Illness: An exploratory analysis, *Brain Behav Immun.* **28**, 159-169.

46. Golier, J. A., Schmeidler, J., Legge, J. & Yehuda, R. (2007) Twenty-four Hour Plasma Cortisol and Adrenocorticotropic Hormone in Gulf War Veterans: Relationships to Posttraumatic Stress Disorder and Health Symptoms, *Biol Psychiatry.* **62**, 1175-1178.

47. Golier, J. A., Schmeidler, J. & Yehuda, R. (2009) Pituitary response to metyrapone in Gulf War veterans: Relationship to deployment, PTSD and unexplained health symptoms, *Psychoneuroendocrinology.* **34**, 1338-1345.

48. Johnson, J. D., O'Connor, K. A., Watkins, L. R. & Maier, S. F. (2004) The role of IL-1β in stress-induced sensitization of proinflammatory cytokine and corticosterone responses, *Neuroscience.* **127**, 569-577.

49. Morgan III, C. A., Rasmusson, A. M., Wang, S., Hoyt, G., Hauger, R. L. & Hazlett, G. (2002) Neuropeptide-Y, cortisol, and subjective distress in humans exposed to acute stress: replication and extension of previous report, *Biol Psychiatry.* **52**, 136-142.

50. Horner, R. D., Grambow, S. C., Coffman, C. J., Lindquist, J. H., Oddone, E. Z., Allen, K. D. & Kasarskis, E. J. (2008) Amyotrophic Lateral Sclerosis among 1991 Gulf War Veterans: Evidence for a Time-Limited Outbreak, *Neuroepidemiology.* **31**, 28-32.

51. Barth, S. K., Kang, H. K., Bullman, T. A. & Wallin, M. T. (2009) Neurological mortality among U.S. veterans of the Persian Gulf War: 13-year follow-up, *Am J Ind Med.* **52**, 663-670.

52. Wallin, M. T., Kurtzke, J. F., Culpepper, W. J., Coffman, P., Maloni, H., Haselkorn, J. K. & Mahan, C. M. (2014) Multiple Sclerosis in Gulf War Era Veterans. 2. Military Deployment and Risk of Multiple Sclerosis in the First Gulf War, *Neuroepidemiology.* **42**, 226-234.

53. Rayhan, R., Ravindran, M. & Baraniuk, J. (2013) Migraine in gulf war illness and chronic fatigue syndrome: prevalence, potential mechanisms, and evaluation, *Front Physiol.* **4**, 181.

54. Rayhan, R. U., Raksit, M. P., Timbol, C. R., Adewuyi, O., VanMeter, J. W. & Baraniuk, J. N. (2013) Prefrontal lactate predicts exercise-induced cognitive dysfunction in Gulf War Illness, *Am J Trans Res.* **5**, 212-223.

55. Weiner, M. W. (2005) Magnetic resonance and spectroscopy of the human brain in Gulf War illness in *Fort Detrick, MD: US Army Medical Research and Materiel Command*

56. Weiner, M. W., Meyerhoff, D. J., Neylan, T. C., Hlavin, J., Ramage, E. R., McCoy, D., Studholme, C., Cardenas, V., Marmar, C., Truran, D., Chu, P. W., Kornak, J., Furlong, C. E. & McCarthy, C. (2011) The Relationship Between Gulf War Illness, Brain N-acetylaspartate, and Post-Traumatic Stress Disorder, *Military Med.* **176**, 896-902.

57. Rayhan, R. U., Stevens, B. W., Timbol, C. R., Adewuyi, O., Walitt, B., VanMeter, J. W. & Baraniuk, J. N. (2013) Increased Brain White Matter Axial Diffusivity Associated with Fatigue, Pain and Hyperalgesia in Gulf War Illness, *PLOS ONE.* **8**, e58493.

58. Li, X., Spence, J. S., Buhner, D. M., Hart, J., Cullum, C. M., Biggs, M. M., Hester, A. L., Odegard, T. N., Carmack, P. S., Briggs, R. W. & Haley, R. W. (2011) Hippocampal Dysfunction in Gulf War Veterans: Investigation with ASL Perfusion MR Imaging and Physostigmine Challenge, *Radiology.* **261**, 218-225.

59. Chao, L. L., Abadjian, L., Hlavin, J., Meyerhoff, D. J. & Weiner, M. W. (2011) Effects of low-level sarin and cyclosarin exposure and Gulf War Illness on Brain Structure and Function: A study at 4T, *Neurotoxicology.* **32**, 814-822.

60. Haley, R. W., Spence, J. S., Carmack, P. S., Gunst, R. F., Schucany, W. R., Petty, F., Devous, M. D., Bonte, F. J. & Trivedi, M. H. (2009) Abnormal brain response to cholinergic challenge in chronic encephalopathy from the 1991 Gulf War, *Psychiatry Res.* **171**, 207-220.

61. James, L. M., Engdahl, B. E., Leuthold, A. C. & Georgopoulos, A. P. (2016) Brain Correlates of Human Leukocyte Antigen (HLA) Protection in Gulf War Illness (GWI), *EBioMedicine.* **13**, 72-79.

62. Koslik, H. J., Hamilton, G. & Golomb, B. A. (2014) Mitochondrial Dysfunction in Gulf War Illness Revealed by 31Phosphorus Magnetic Resonance Spectroscopy: A Case-Control Study, *PLOS ONE.* **9**, e92887.

63. Thompson, C. H., Kemp, G. J., Sanderson, A. L. & Radda, G. K. (1995) Skeletal muscle mitochondrial function studied by kinetic analysis of postexercise phosphocreatine resynthesis, *J Appl Physiol.* **78**, 2131-2139.

64. Chen, Y., Meyer, J. N., Hill, H. Z., Lange, G., Condon, M. R., Klein, J. C., Ndirangu, D. & Falvo, M. J. (2017) Role of mitochondrial DNA damage and dysfunction in veterans with Gulf War Illness, *PLOS ONE.* **12**, e0184832.

65. Čolović, M. B., Krstić, D. Z., Lazarević-Pašti, T. D., Bondžić, A. M. & Vasić, V. M. (2013) Acetylcholinesterase Inhibitors: Pharmacology and Toxicology, *Curr Neuropharmacol.* **11**, 315-335.

66. Golomb, B. A. & Anthony., C. R. (1999) A Review of the Scientific Literature as It Pertains to Gulf War Illnesses: Pyridostigmine Bromide. in Santa Monica, CA: RAND Corporation, .

67. Drake-Baumann, R. & Seil, F. J. (1999) Effects of exposure to low-dose pyridostigmine on neuromuscular junctions *in vitro* in *Muscle Nerve* pp. 696-703

68. Peden-Adams, M. M., Dudley, A. C., EuDaly, J. G., Allen, C. T., Gilkeson, G. S. & Keil, D. E. (2004) Pyridostigmine Bromide (PYR) Alters Immune Function in B6C3F1 Mice, *Immunopharmacol Immunotoxicol.* **26**, 1-15.

69. Bernatova, I., Babal P Fau - Grubbs, R. D., Grubbs Rd Fau - Morris, M. & Morris, M. (2006) Acetylcholinesterase inhibition affects cardiovascular structure in mice, *Physiol Res.* **55**, Suppl1:S89-97.

70. Adler, M., Deshpande, S. S., Foster, R. E., Maxwell, D. M. & Albuquerque, E. X. (1992) Effects of subacute pyridostigmine administration on mammalian skeletal muscle function, *J Appl Toxicol.* **12**, 25-33.

71. Kluwe, W. M., Page, J. G., Toft, J. D., Ridder, W. E. & Chung, H. (1990) Pharmacological and Toxicological Evaluation of Orally Administered Pyridostigmine in Dogs, *Toxicological Sci.* **14**, 40-53.

72. Lamproglou, I., Barbier, L., Diserbo, M., Fauvelle, F., Fauquette, W. & Amourette, C. (2009) Repeated stress in combination with pyridostigmine: Part I: Long-term behavioural consequences, *Behav Brain Res.* **197**, 301-310.

73. Barbier, L., Diserbo, M., Lamproglou, I., Amourette, C., Peinnequin, A. & Fauquette, W. (2009) Repeated stress in combination with pyridostigmine: Part II: Changes in cerebral gene expression, *Behav Brain Res.* **197**, 292-300.

74. Amourette, C., Lamproglou, I., Barbier, L., Fauquette, W., Zoppe, A., Viret, R. & Diserbo, M. (2009) Gulf War illness: Effects of repeated stress and pyridostigmine treatment on blood–brain barrier permeability and cholinesterase activity in rat brain, *Behav Brain Res.* **203**, 207-214.

75. Abdullah, L., Crynen, G., Reed, J., Bishop, A., Phillips, J., Ferguson, S., Mouzon, B., Mullan, M., Mathura, V., Mullan, M., Ait-Ghezala, G. & Crawford, F. (2011) Proteomic CNS Profile of Delayed Cognitive Impairment in Mice Exposed to Gulf War Agents, *NeuromolMed.* **13**, 275-288.

76. Abdullah, L., Evans, J. E., Montague, H., Reed, J. M., Moser, A., Crynen, G., Gonzalez, A., Zakirova, Z., Ross, I., Mullan, C., Mullan, M., Ait-Ghezala, G. & Crawford, F. (2013) Chronic elevation of phosphocholine containing lipids in mice exposed to Gulf War agents pyridostigmine bromide and permethrin, *Neurotoxicol Teratol.* **40**, 74-84.

77. Ojo, J. O., Abdullah, L., Evans, J., Reed, J. M., Montague, H., Mullan, M. J. & Crawford, F. C. (2014) Exposure to an organophosphate pesticide, individually or in combination with other Gulf War agents, impairs synaptic integrity and neuronal differentiation, and is accompanied by subtle microvascular injury in a mouse model of Gulf War agent exposure, *Neuropathology.* **34**, 109-127.

78. Parihar, V. K., Hattiangady, B., Shuai, B. & Shetty, A. K. (2013) Mood and Memory Deficits in a Model of Gulf War Illness Are Linked with Reduced Neurogenesis, Partial Neuron Loss, and Mild Inflammation in the Hippocampus, *Neuropsychopharmacology.* **38**, 2348-2362.

79. Torres-Altoro, M. I., Mathur, B. N., Drerup, J. M., Thomas, R., Lovinger, D. M., O'Callaghan, J. P. & Bibb, J. A. (2011) Organophosphates dysregulate dopamine signaling, glutamatergic neurotransmission, and induce neuronal injury markers in striatum, *J Neurochem.* **119**, 303-313.

80. Middlemore-Risher, M.-L., Adam, B.-L., Lambert, N. A. & Terry, A. V. (2011) Effects of Chlorpyrifos and Chlorpyrifos-Oxon on the Dynamics and Movement of Mitochondria in Rat Cortical Neurons, *J Pharmacol Exp Ther.* **339**, 341-349.

81. Speed, H. E., Blaiss, C. A., Kim, A., Haws, M. E., Melvin, N. R., Jennings, M., Eisch, A. J. & Powell, C. M. (2012) Delayed Reduction of Hippocampal Synaptic Transmission and Spines Following Exposure to Repeated Subclinical Doses of Organophosphorus Pesticide in Adult Mice, *Toxicoll Sci.* **125**, 196-208.

82. Phillips, K. F. & Deshpande, L. S. (2016) Repeated low-dose organophosphate DFP exposure leads to the development of depression and cognitive impairment in a rat model of Gulf War Illness, *Neurotoxicology.* **52**, 127-133.

83. O'Callaghan, J. P., Kelly, K. A., Locker, A. R., Miller, D. B. & Lasley, S. M. (2015) Corticosterone primes the neuroinflammatory response to DFP in mice: potential animal model of Gulf War Illness, *J Neurochem.* **133**, 708-721.

84. Koo, B.-B., Michalovicz, L. T., Calderazzo, S., Kelly, K. A., Sullivan, K., Killiany, R. J. & O'Callaghan, J. P. (2018) Corticosterone potentiates DFP-induced neuroinflammation and affects high-order diffusion imaging in a rat model of Gulf War Illness, *Brain Behav Immun.* **67**, 42-46.

85. Wright, H. L., Bucknall, R. C., Moots, R. J. & Edwards, S. W. (2012) Analysis of SF and plasma cytokines provides insights into the mechanisms of inflammatory arthritis and may predict response to therapy, *Rheumatology.* **51**, 451-459.

86. Wong, N., Nguyen, T., Brenu, E. W., Broadley, S., Staines, D. & Marshall-Gradisnik, S. (2015) A Comparison of Cytokine Profiles of Chronic Fatigue Syndrome/Myalgic Encephalomyelitis and Multiple Sclerosis Patients, *Int J Clin Med.* **06**, 769-783.

87. Montoya, J. G., Holmes, T. H., Anderson, J. N., Maecker, H. T., Rosenberg-Hasson, Y., Valencia, I. J., Chu, L., Younger, J. W., Tato, C. M. & Davis, M. M. (2017) Cytokine signature associated with disease severity in chronic fatigue syndrome patients, *Proc Natl Acad Sci.* **114**, E7150-E7158.

88. Oreja-Guevara, C., Ramos-Cejudo, J., Aroeira, L. S., Chamorro, B. & Diez-Tejedor, E. (2012) TH1/TH2 Cytokine profile in relapsing-remitting multiple sclerosis patients treated with Glatiramer acetate or Natalizumab, *BMC Neurol.* **12**, 95.

89. Kallaur, A. P., Oliveira, S. R., Simão, A. N. C., Alfieri, D. F., Flauzino, T., Lopes, J., de Carvalho Jennings Pereira, W. L., de Meleck Proença, C., Borelli, S. D., Kaimen-Maciel, D. R., Maes, M. & Reiche, E. M. V. (2017) Cytokine Profile in Patients with Progressive Multiple Sclerosis and Its Association with Disease Progression and Disability, *Mol Neurobiol.* **54**, 2950-2960.

90. Rodríguez-Perlvárez, M. L., García-Sánchez, V., Villar-Pastor, C. M., González, R., Iglesias-Flores, E., Muntane, J. & Gómez-Camacho, F. (2012) Role of serum cytokine profile in ulcerative colitis assessment, *Inflamm Bowel Dis.* **18**, 1864-1871.

91. Műzes, G., Molnár, B., Tulassay, Z. & Sipos, F. (2012) Changes of the cytokine profile in inflammatory bowel diseases, *World J Gastroenterol.* **18**, 5848-5861.

92. Zorzi, F., Monteleone, I., Sarra, M., Calabrese, E., Marafini, I., Cretella, M., Sedda, S., Biancone, L., Pallone, F. & Monteleone, G. (2013) Distinct Profiles of Effector Cytokines Mark the Different Phases of Crohn's Disease, *PLOS ONE.* **8**, e54562.

93. Kantola, T., Klintrup, K., Väyrynen, J. P., Vornanen, J., Bloigu, R., Karhu, T., Herzig, K. H., Näpänkangas, J., Mäkelä, J., Karttunen, T. J., Tuomisto, A. & Mäkinen, M. J. (2012) Stage-dependent alterations of the serum cytokine pattern in colorectal carcinoma, *Br J Cancer.* **107**, 1729-1736.

94. Matte, I., Lane, D., Laplante, C., Rancourt, C. & Piché, A. (2012) Profiling of cytokines in human epithelial ovarian cancer ascites, *Am J Cancer Res.* **2**, 566-580.

95. Roshani, R., McCarthy, F. & Hagemann, T. (2014) Inflammatory cytokines in human pancreatic cancer, *Cancer Lett.* **345**, 157-163.

96. Cutler, A. & Brombacher, F. (2005) Cytokine Therapy, *Ann N Y Acad Sci.* **1056**, 16-29.

97. Dustin, M. L. (2012) Signaling at neuro/immune synapses, *J Clin Invest.* **122**, 1149-1155.

98. Tracey, K. J. (2010) Understanding immunity requires more than immunology, *Nat Immunol.* **11**, 561-564.

99. Zhou, X., Fragala, M. S., McElhaney, J. E. & Kuchel, G. A. (2010) Conceptual and methodological issues relevant to cytokine and inflammatory marker measurements in clinical research, *Curr Opin Clin Nutr Metab Care.* **13**, 541-547.

100. Kitano, H. (2002) Computational systems biology, *Nature.* **420**, 206-210.

101. Kitano, H. (2004) Biological robustness, *Nat Rev Genet.* **5**, 826-837.

102. Li, J., Yuan, Z. & Zhang, Z. (2010) The Cellular Robustness by Genetic Redundancy in Budding Yeast, *PLOS Genet.* **6**, e1001187.

103. Gu, Z., Steinmetz, L. M., Gu, X., Scharfe, C., Davis, R. W. & Li, W.-H. (2003) Role of duplicate genes in genetic robustness against null mutations, *Nature.* **421**, 63-66.

104. Kelley, R. & Ideker, T. (2005) Systematic interpretation of genetic interactions using protein networks, *Nature Biotech.* **23**, 561-566.

105. Broderick, G. & Craddock, T. J. A. (2013) Systems biology of complex symptom profiles: Capturing interactivity across behaviour, brain and immune regulation, *Brain Behav Immun.* **29**, 1-8.

106. Barabasi, A.-L., Gulbahce, N. & Loscalzo, J. (2011) Network medicine: a network-based approach to human disease, *Nat Rev Genet.* **12**, 56-68.

107. de la Fuente, A. (2010) From 'differential expression' to 'differential networking' – identification of dysfunctional regulatory networks in diseases, *Trends Genet.* **26**, 326-333.

108. Margolin, A. A., Nemenman, I., Basso, K., Wiggins, C., Stolovitzky, G., Favera, R. D. & Califano, A. (2006) ARACNE: An Algorithm for the Reconstruction of Gene Regulatory Networks in a Mammalian Cellular Context, *BMC Bioinformatics.* **7**, S7.

109. Carro, M. S., Lim, W. K., Alvarez, M. J., Bollo, R. J., Zhao, X., Snyder, E. Y., Sulman, E. P., Anne, S. L., Doetsch, F., Colman, H., Lasorella, A., Aldape, K., Califano, A. & Iavarone, A. (2009) The transcriptional network for mesenchymal transformation of brain tumours, *Nature.* **463**, 318-325.

110. Sumazin, P., Yang, X., Chiu, H.-S., Chung, W.-J., Iyer, A., Llobet-Navas, D., Rajbhandari, P., Bansal, M., Guarnieri, P., Silva, J. & Califano, A. (2011) An Extensive MicroRNA-Mediated Network of RNA-RNA Interactions Regulates Established Oncogenic Pathways in Glioblastoma, *Cell.* **147**, 370-381.

111. Torkamani, A., Dean, B., Schork, N. J. & Thomas, E. A. (2010) Coexpression network analysis of neural tissue reveals perturbations in developmental processes in schizophrenia, *Genome Res.* **20**, 403-412.

112. Yu, J., Smith, V. A., Wang, P. P., Hartemink, A. J. & Jarvis, E. D. (2004) Advances to Bayesian network inference for generating causal networks from observational biological data, *Bioinformatics.* **20**, 3594-3603.

113. Haury, A.-C., Mordelet, F., Vera-Licona, P. & Vert, J.-P. (2012) TIGRESS: Trustful Inference of Gene REgulation using Stability Selection, *BMC Syst Biol.* **6**, 145.

114. Huynh-Thu, V. A., Irrthum, A., Wehenkel, L. & Geurts, P. (2010) Inferring Regulatory Networks from Expression Data Using Tree-Based Methods, *PLOS ONE.* **5**, e12776.

115. Guo, A.-Y., Sun, J., Jia, P. & Zhao, Z. (2010) A Novel microRNA and transcription factor mediated regulatory network in schizophrenia, *BMC Syst Biol.* **4**, 10.

116. Yeung, M. K. S., Tegner, J. & Collins, J. J. (2002) Reverse engineering gene networks using singular value decomposition and robust regression, *Proc Natl Acad Sci USA.* **99**, 6163-6168.

117. Schmidt, M. D., Vallabhajosyula, R. R., Jenkins, J. W., Hood, J. E., Soni, A. S., Wikswo, J. P. & Lipson, H. (2011) Automated refinement and inference of analytical models for metabolic networks., *Phys Biol* **8**, 055011.

118. Erdös, P. & Rényi, A. (1959) On random graphs, I, *Publ Math (Debrecen).* **6**, 290-297.

119. Watts, D. J. & Strogatz, S. H. (1998) Collective dynamics of 'small-world' networks, *Nature.* **393**, 440-442.

120. Barabási, A.-L. & Albert, R. (1999) Emergence of Scaling in Random Networks, *Science.* **286**, 509-512.

121. Fell, D. A. & Wagner, A. (2000) The small world of metabolism, *Nature Biotech.* **18**, 1121-1122.

122. Newman, M. (2003) The Structure and Function of Complex Networks, *SIAM Rev.* **45**, 167-256.

123. Ravasz, E., Somera, A. L., Mongru, D. A., Oltvai, Z. N. & Barabási, A. L. (2002) Hierarchical Organization of Modularity in Metabolic Networks, *Science.* **297**, 1551-1555.

124. Han, J.-D. J., Bertin, N., Hao, T., Goldberg, D. S., Berriz, G. F., Zhang, L. V., Dupuy, D., Walhout, A. J. M., Cusick, M. E., Roth, F. P. & Vidal, M. (2004) Evidence for dynamically organized modularity in the yeast protein–protein interaction network, *Nature.* **430**, 88-93.

125. Baldassano, S. N. & Bassett, D. S. (2016) Topological distortion and reorganized modular structure of gut microbial co-occurrence networks in inflammatory bowel disease, *Sci Rep.* **6**, 26087.

126. Palesi, F., Castellazzi, G., Casiraghi, L., Sinforiani, E., Vitali, P., Gandini Wheeler-Kingshott, C. A. M. & D'Angelo, E. (2016) Exploring Patterns of Alteration in Alzheimer's Disease Brain Networks: A Combined Structural and Functional Connectomics Analysis, *Front Neurosci.* **10**, 380.

127. Sang, L., Zhang, J., Wang, L., Zhang, J., Zhang, Y., Li, P., Wang, J. & Qiu, M. (2015) Alteration of Brain Functional Networks in Early-Stage Parkinson's Disease: A Resting-State fMRI Study, *PLOS ONE.* **10**, e0141815.

128. Albert, R., Jeong, H. & Barabási, A.-L. (2000) Error and attack tolerance of complex networks, *Nature.* **406**, 378-382.

129. Jeong, H., Mason, S. P., Barabási, A. L. & Oltvai, Z. N. (2001) Lethality and centrality in protein networks, *Nature.* **411**, 41-42.

130. Milo, R., Shen-Orr, S., Itzkovitz, S., Kashtan, N., Chklovskii, D. & Alon, U. (2002) Network Motifs: Simple Building Blocks of Complex Networks, *Science.* **298**, 824-827.

131. Prill, R. J., Iglesias, P. A. & Levchenko, A. (2005) Dynamic Properties of Network Motifs Contribute to Biological Network Organization, *PLOS Biol.* **3**, e343.

132. Alon, U., Surette, M. G., Barkai, N. & Leibler, S. (1999) Robustness in bacterial chemotaxis, *Nature.* **397**, 168-171.

133. Yu, H., Kim, P. M., Sprecher, E., Trifonov, V. & Gerstein, M. (2007) The Importance of Bottlenecks in Protein Networks: Correlation with Gene Essentiality and Expression Dynamics, *PLOS Comp Biol.* **3**, e59.

134. Vergelli, M., Mazzanti, B., Traggiai, E., Biagioli, T., Ballerini, C., Parigi, A., Konse, A., Pellicanò, G. & Massacesi, L. (2001) Short-term evolution of autoreactive T cell repertoire in multiple sclerosis, *J Neurosci Res.* **66**, 517-524.

135. Aschbacher, K., Adam, E. K., Crofford, L. J., Kemeny, M. E., Demitrack, M. A. & Ben-Zvi, A. (2012) Linking disease symptoms and subtypes with personalized systems-based phenotypes: A proof of concept study, *Brain Behav Immun.* **26**, 1047-1056.

2 Chapter 2: Inferring regulatory biology from time course data under Constraints Typical of *In Vivo* studies

A version of this chapter has been published as:

Vashishtha, S., Broderick, G., Craddock, T. J. A., Fletcher, M. A., Klimas, N.G. (2015) Inferring Broad Regulatory Biology from Time Course Data: Have We Reached an Upper Bound under Constraints Typical of *In Vivo* Studies? PLoS ONE 10(5): e0127364.

2.1 Introduction

Before the emergence of high throughput techniques, biology was deeply entrenched in a reductionist study of one component gene or protein at a time. Though now often depreciated, such studies have provided a wealth of information about the various roles of individual molecular entities. With the advent of high throughput techniques such as microarray, mass spectrometry, RNA-seq, chip-seq and multi-channel flow cytometry, it is now possible to simultaneously survey many cellular components including mRNA, proteins, and metabolites. There is now a growing appreciation that almost all biological morphologies and functions emerge as a result of complex interactions between constituent molecules or entities [1]. These interactions drive fundamental processes within various intra-cellular compartments, ultimately determining the behaviour of a cell as well as the extent and nature of signaling with neighbouring cells [2] in both health and disease. As such, understanding these interactions can ultimately lead to more effective clinical treatments. Specifically, an integrative systems approach to biology has the potential to provide new insights into complex illnesses by leveraging broad molecular and cellular surveys [3] to cast various disease-associated genes and related pathways [4] in the proper mechanistic context. However, two major challenges exist: (i) the accurate identification of biological regulatory networks, also called reverse engineering and, (ii) the quantitative study of regulatory network structure and function, as it applies to clinical medicine.

In the past two decades, the reverse engineering of causal gene regulatory networks from time course expression profiles has received special attention with a number of methods and mathematical formulations being proposed for network inference. In Appendix 2.1, we present a summary of the principal methods grouped into several broad classes, namely: Logic-based models such as Boolean networks (BN) [4-

9], probability based methods such as dynamic Bayesian networks (DBN) [10-17] information theoretic approaches [18, 19], and Ordinary Differential Equations (Linear and Non-linear) based methods [20-28]. In addition, model free approaches with roots in machine learning/data mining [29-31] and hybrid methods [18, 32-35] have also become popular avenues for the inference of directed biological regulatory networks from time course data. A number of excellent reviews exist that describe the underlying principles, advantages and limitations of various inference methods [36-45]. However, with the exception of the DREAM (Dialogue on Reverse Engineering Assessment and Methods) community-wide challenge [46-50], very few initiatives have sought to compare the relative performance of these methods directly [51-54] and in quantitative terms. They do agree nonetheless that the availability of suitable data constitutes one of the primary obstacles to the more complete and accurate inference of directed biological networks [49]. This is only exacerbated with *in vivo* human or animal studies where blood can only be sampled at low frequency (10– 15 time points) across a relatively short time horizon (24 hours or less). Moreover, for budgetary reasons such detailed studies are typically limited to relatively small subject groups (often less than 20 subjects) examined under a select number of response conditions (often only 1) [55].

It is very important to keep such experimental limitations in mind if in addition to recovering connectivity one is also attempting to infer directed networks for the purpose of designing candidate treatment courses that might be directly predictive of clinical trial outcomes in human subjects. If this is the objective then the method must also allow the user to simulate the dosage and timing of specific network perturbations. While several important inference algorithms have been proposed (Appendix 2.1), many require a quantity and type (e.g., knockout) of data that is more consistent with *in vitro* experimentation in cell cultures than with *in vivo* experimentation in human or animal subjects. For example, Boolean network (BN) models allow the user to draw on a

broader body of *a priori* knowledge and represent response dynamics as discrete on off transitions with a simple delay. However, BN algorithms such as REVEAL [6] remain computationally expensive and sensitive to experimental noise [56]. Moreover, discrete on-off behaviour remains a coarse-grained approximation with a resolution that is typically unsuitable for treatment design beyond the initial exploratory phases. These issues are partially addressed by computationally faster and noise-tolerant probabilistic Boolean networks (PBN) [8, 9] where relationships between variables are captured as joint probability distributions. Dynamic Bayesian networks (DBN) offer further improvements in the analysis of experimental time course data [57] and several algorithms have been proposed including BANJO [10] BNFINDER [14, 15], GlobalMIT [13], and DREM [16, 17]. While DBNs can infer feedback loops they continue to require data exceeding that of typical *in vivo* animal studies despite efforts to control computational complexity with alternative scoring methods such as GlobalMIT [13] and BNFINDER 2 [15]. Similar to DBNs, information theoretic algorithms such as Dynamic CLR [18] and TD-ARACNE [19], have become available to infer regulatory networks from time course data. In general, information theoretic approaches use a generalization of the pair-wise correlation coefficient called mutual information (MI) [58]. As with the basic Bayesian model, MI is a non-parametric measure, making no assumption regarding the distribution of the data. Although such methods typically require substantial amounts of data, improvements in performance reported for TD-ARACNE are such that we have retained the latter as a candidate method in the current comparative analysis.

Making simplifying assumptions about the distribution of the data allows one to move towards more conventional regression-based models. Perhaps the simplest of these are time delay forecasting models that are based on Granger causality. With roots in machine learning and data mining these methods are often called model-free since

they do not assume any regulatory model structure *a priori*. However, their general applicability is accompanied by a substantial data requirement that matches or even exceeds that of DBNs [59] despite the recent introduction of LASSO penalties [31, 60]. The discrete time equivalent of an ODE, a classical difference equation, can be obtained by restricting this type of forecast model to a single time step lag in the response variable and no lag in the regressor variables. Indeed this is the basic model underlying the TSNI integral method [20] evaluated in this work. Classical continuous ODE models have long been used to describe biochemical reaction kinetics. The data requirements of ODE based methods, at least in their basic linear form, can be quite succinct and this form can readily capture the direction and type of regulation. These models can also be used directly to simulate treatment perturbations making them well suited to support the computational design of clinical interventions. Of the popular ODE-based methods surveyed in Appendix 2.1, some like NIR [22], and the Inferelator [25] require additional prior information, for example the use of gene knockout data, making them less suitable for human in-vivo studies. Moving beyond a linear ODE formulation several variants of the nonlinear ODE S-system model have been proposed such as TDSS [27] and NeRDS [28]. However, increases in the number of model parameters leads to a corresponding increase in the data requirements [28]. Moreover, this does not necessarily lead to an increase in fidelity as some of the results presented here will show. Hybrid methods combine the strengths of different methodologies. For example, the algorithm proposed in [18] combines the scalability of information theoretic method CLR and causal inference capability of ODE based method, the Inferelator. However, with few exceptions [34], these methods require the expression time course be supplemented with different types of data such as knockout and knockdown data that are not frequently available for human subjects [18, 32, 33].

In the present study, we focus on the inference of local directed regulatory

networks from time course data with properties similar to those that might be obtained from animal or human subjects under *in vivo* conditions. In keeping with this, we have attempted to assess algorithms whose data requirements (data type and quantity) are in line with that typically available from *in vivo* time course studies and that also support the resolution required to simulate treatment kinetics. Based on our survey of methods, we found ODE-based algorithms like TSNI [24], TSNI integral [20] and the one proposed in Yeung et al. (2002) [21], most suitable. The algorithm proposed in [21] and TSNI use similar techniques of Singular Value Decomposition (SVD) and Principal Component Analysis (PCA) for dimensionality reduction. In contrast, TSNI integral uses a forward stepwise regression technique to infer sparse directed networks. Furthermore the conventional gradient formulation of the rate equation is re-written as finite difference equations in TSNI integral to improve performance on noisy experimental data [20]. The architecture of these methods, like most, is based on generic core components that include feature selection and parameter estimation steps. To further explore how performance might be affected by design choices in these component parts we constructed and re-assembled these simple generic building blocks de novo, applying two popular classes of feature selection to a conventional linear ODE model namely the truncation of candidate terms or their projection onto composite constructs. Finally, we also assessed the performance of TD-ARACNE [19] since the latter is reported to have circumvented the typically large data requirements associated with conventional information theoretic methods. Because there are no widely agreed upon benchmark circuits in humans where the true circuit structure is known we used simulated data generated by a gene network simulator NetSim [61] to provide an equitable benchmark. This also made it possible to alter the underlying network size as well as sampling rate and the number of time courses in each data set. To our knowledge this type of standardized comparison focused on methods that are robust to the constraints of *in*

vivo human studies and that also offer sufficient temporal resolution for simulation-based treatment design has not been conducted previously, especially not at the level of the component parts.

We found that all methods performed similarly on noise-free simulated data, with the exception of the information theoretic method TD-ARACNE, which typically exhibited a lower median performance. In selecting ODE model terms, truncation was less tolerant of experimental noise than projection-based approaches. Irrespective of noise levels, we found that all methods were extremely affected by the reduction in network edge density obtained in larger networks. In smaller simulated networks consisting of 5– 10 nodes with edge densities similar to typical biological networks (10– 30%), values in excess of 0.40 were obtained for the F-score, an aggregate measure summarizing precision and recall. To explore the broader applicability of these results, we assessed the leading ODE-based methods in recovering the DREAM 3 in silico 10-node networks [48], the 5-node Yeast synthetic IRMA network [62] as well as a 9-node human HeLa cell cycle network [30, 63]. Results were comparable to those obtained on NetSim simulated networks of similar size and edge density. All methods were found to be more sensitive to the number of time courses than to sample frequency. Based on the results of this simulation study, at least 10 time course experiments, sampled at 10 time points, would be required to infer a 10 node network with a median recall and median F score of 53%(±3%) and 0.39 (±0.04) respectively. In aggregating multiple experiments the most significant improvement in performance was obtained by using the broken stick projection method on groups of 10 or more time course profiles.

It would appear that inference of directed regulatory networks still faces challenges and that less intrusive sampling techniques, i.e. higher frequency, and safer perturbation protocols may be required if we are to infer regulatory networks that fully exploit the breadth of current multiplex surveys. It should be noted that the basic

inference models examined in this work are not novel, nor were they intended to be. Instead the analysis conducted here focused specifically on how standard methods might be deployed under conditions typical of *in vivo* studies in human or animal subjects. Our results emphasize the value of aggregating networks identified from individual time courses and the stratification of subjects into groups. This work also highlighted the importance of tuning the algorithm parameters using *a priori* simulation of artificial biological networks comparable in size and complexity. Indeed, default parameter values do not perform well across a broad range of conditions and even a simple reverse engineering model if tuned correctly has the potential to perform as well as more sophisticated methods. For the moment at least, both the data and the methods appear better suited to the study of individual transcription factor sub networks, as well as cytokine signaling and flow cytometric studies in groups of experimental subjects.

2.2 Materials and Methods

2.2.1 Ethical approval

This study received ethics approval by the University of Alberta Health Research Ethics Board (MS4_Pro00018859) and the Miami Veterans Affairs Medical Center Research and Development Committee (file 4987.76).

2.2.2 Simulated experimental data

To reliably assess the performance of the selected methods we used simulated data such that the true structure of the underlying regulatory network was known, and we could alter network parameters in a controlled manner (network size, time points, noise levels, etc.). All reference networks were created and their behaviour simulated using a gene network simulator known as NetSim [61]. NetSim enforces some of the known topological properties of biological regulatory networks such as sparseness, scale-free

distribution of connectivity, and clustering granularity independent of the number of nodes. Un-weighted directed networks were produced where the sign of the edge (positive or negative) described the type of regulatory action (+1 for promotion or -1 for inhibition). These network interactions were then translated into fuzzy logic statements by NetSim. The target transition state for a given node at time t+1 is determined by resolving the fuzzy logic statement describing the regulation of that node. A sigmoidal activation function is then used by NetSim to modulate the incremental transition from the node' s current state in the direction of its target state. This incremental change in state is weighted by a time constant capturing both synthesis and degradation dynamics. In all simulations the parameters describing node dynamics were sampled from Gaussian distributions with mean and standard deviation as recommended by the authors. Similarly the initial states were assigned randomly for all nodes at the beginning of each simulation run. Consistent with the current literature [19], we computed all performance metrics based on the direction (source to target) but not the type of interaction (promotion or inhibition). Reverse engineering algorithms are commonly evaluated based on the recovery of regulatory networks using very similar or even identical models as those used in the generation of simulation data. In this work we made concerted efforts to avoid this; using standard ODE and probabilistic models to recover networks from data that was generated by logic-based simulation instead. We consider this to be a more challenging task.

2.2.3 Selected network identification methods

2.2.3.1 Rate equation models

A standard rate equation model is a popular formulation used as the foundation for a broad group of contemporary network identification methods [21-24], including that of one proposed by Yeung and colleagues [21], Network Identification by multiple

Regression (NIR) [22], Mode-of-action by Network Identification (MNI) [64], Time Series Network Identification (TSNI) [24], TSNI integral [20] and others. According to this model, the rate of change in concentration of one gene/transcript/protein can be described through a linear system of ordinary differential equations (ODEs) as a function of the current concentration of other genes/ transcripts/proteins as described in Eq 1, where $a_{i,j}$ is the parameter describing interaction between node *i* and *j* . More precisely, it represents the influence of node j on the rate of change of expression of node *i*. A positive value of $a_{i,j}$ represents activation of node *i* by node *j*, negative value represents inhibition and zero value represents no interaction between node *j* and *i* .

$$\frac{\partial x_i}{\partial t} = a_{i,1}x_1 + a_{i,2}x_2 + \cdots + a_{i,n}x_n \quad (2.1),$$

Eq (2.1) can be rewritten in the matrix form (Eq 2.2). Here, X is an n x1 vector and A is an n x n matrix containing the weight of all the edges of the network. This matrix has also been called the adjacency matrix.

$$\dot{X}(t) = A \cdot X(t) \quad (2.2),$$

Many methods including the popular time-series network identification (TSNI) method proposed in [24] accommodate external perturbations u(t) to the system. For example, dose response experiments provide a strong basis for the identification of system dynamics. In accounting for external perturbations, Eq 2.2 will become,

$$\dot{X}(t) = A \cdot X(t) + B \cdot u(t) \quad (2.3),$$

Here, B is similar in size to A and u (t) represents the external perturbation at time t.

While most ODE-based methods use the instantaneous derivative at time t, a recent extension called TSNI integral [20] uses an equivalent model integrated and rewritten as a finite difference equation (Eq 2.4) as a means of improving robustness in the presence of experimental noise.

$$\int_0^{t_f} \dot{X}(t)\partial t = A\int_0^{t_f} X(t)\partial t + B\int_0^{t_f} U(t)\partial t, \qquad f = 1,2,K,M \tag{2.4}$$

Whether based on the conventional differential equation or the equivalent finite difference equation, the final form is that of a linear regression model where estimates for the values of the unknown parameter sets A and B (Eq 2.3) are recovered from the experimental data.

In biological systems, the regressor terms in these equations are not expressed independently of one another but rather follow coordinated patterns. Traditional ordinary least squares estimation will generally perform poorly when correlated or collinear terms are used together as these leading to an increase in the uncertainty in parameter estimation referred to as variance inflation [65]. This is typically resolved by one of the two basic approaches namely truncation and projection. The first of these consists in selecting subsets of the original regressors that are minimally redundant. In this work we used a stepwise variable selection [66] method whereby terms were evaluated sequentially based on their respective partial-F test values. Model terms with a p (partial F) < 0.05 were selected for recruitment into the ODE regression model while those currently in the model but showing a revised p (partial F) > 0.10 were pruned.

The second approach consists of projecting the original regressor variables onto a new set of aggregate constructs that are mutually independent. These constructs or latent vectors consist of weighted linear combinations of the original variables and are typically estimated using a diagonal covariance matrix estimate produced by singular value decomposition (SVD) or principal component analysis (PCA) [67]. The most significant of these latent vectors (LV) then serve as a basis for least square regression and the identification of the parameter set A. While there exist as many LV as original variables, the bulk of the shared signal is typically recovered in the first few features. In this work we used an extension of standard PCA called partial least squares (PLS)

regression [68, 69] to identify the structure of the LVs. We then evaluated two methods for selecting the number of these features that should be retained, namely the so-called broken stick method, a variant of Horn' s technique [70] for determining significant decrease in the importance of the leading eigenvalues [71], and the Bartlett' s method [72] which evaluates the trailing eigenvalues for equality. These and other methods are reviewed in Jackson (1991b) [73] and more recently Peres-Neto et al., (2005) [74]. Finally, consistent with the compatible literature, we also applied pre-processing of the data that included log transformation and z-score normalization. We also applied a first order hold interpolation model for inferring values between sample points.

2.2.3.1.1 Parameter tuning of ODE-based models

Both stepwise sequential selection and PLS projection methods were evaluated for identification of the conventional ODE model. The finite difference formulation was evaluated as implemented in the TSNI integral method. The latter uses stepwise feature selection in its estimation of the parameter set A. In addition, for this method we used the final prediction error (TSNIF) with the default parameters values with the exception of the parameter ' restk' which we tuned to obtain the maximum F score, a combined measure of positive predictive value (PPV) and recall. The 'restk' parameter imposes sparseness to the inferred network and therefore affects the F score directly. For more details on TSNI integral, we refer readers to [20]. TSNI integral is freely available at the URL: http://dibernardo.tigem.it/softwares/time-series-network-identification-tsni integral.

In order to assess permutations of the basic algorithmic components associated with the conventional ODE formulation, we implemented these separately rather than use the specific combinations encoded into existing packages. In these implementations we again tuned the algorithm parameters to each problem scenario in an attempt to provide best achievable F score. For example, in the case of stepwise variable selection

the null probability threshold values for inclusion and removal into the model (p_{enter} and $p_{removel}$) were tuned. To mimic this in the case of projection methods the variable influence on projection (VIP) [68] was used. Based on this metric PLS regression terms were ranked according to the weight of their contribution to the latent vectors capturing the most overall variability in the data. Typically a VIP> 1.0 is considered significant; this threshold was optimized here for each scenario. Finally, in order to retain only the most important edges the resulting networks were pruned on the basis of the quantile rank of the edge weight. Here again the quantile threshold applied to the edge weight was tuned for each scenario. This was done using a global optimization method, namely a constrained simulated annealing, to balance computational cost and thoroughness. All algorithms were encoded in MatLab using the functions available in the Statistics Toolbox and the Global Optimization Toolbox (The MathWorks, Inc., Natick, MA).

2.2.3.2 Information theoretic Time-Delay ARACNE (TD-ARACNE)

TD-ARACNE [19] is an extended version of the popular information-theoretic algorithm ARACNe (Algorithm for the Reconstruction of Accurate Cellular Networks) [75] that also retrieves the statistical time dependency between sequential gene expression profiles. Similar to ARACNe, the information theoretic measure of Mutual Information (MI) is used to capture the dependency between two molecular species or network nodes, with statistically independent nodes having a MI value of 0. The MI value between two nodes *i* and *j* can be represented as described in Eq 2.5.

$$MI_{i,j} = H_i + H_j - H_{i,j} \quad (2.5),$$

where H_i and H_j are the entropies of nodes *i* and *j* respectively. Entropy H is defined as follows where $p(x_i)$ is the probability that node *i* will assume state *i=1:n*:

$$H(X) = \sum_{i=1}^{n} \rho(x_i)\, log\big(\rho(x_i)\big) \quad (2.6)$$

TD-ARACNE infers directed networks in three steps: 1) detection of the time

point corresponding to the initial change in expression for all individual nodes e.g genes, 2) network construction based on pair-wise MI and 3) network pruning. The first step is meant to identify possible regulator nodes or genes based on the sequence of activation. The initial change of expression (IcE) in a sequence of expression values for gene g_a; $g_a^0, g_a^1, \ldots g_a^t$ can be defined as follows (Eq 2.7) where τ_{up} and τ_{down} are two fold-change thresholds defining relative increase or decrease in expression.

$$IcE\left(g_a\right) = \arg_j \min\left[g_a^0 / g_a^j \geq \tau_{up} \text{ or } g_a^j / g_a^0 \leq \tau_{down}\right] \quad (2.7)$$

In the second step, TD-ARACNE uses bootstrapping to identify significant statistical dependencies between the activation of gene a at time t and gene b at time $t+\Delta t$. This is subject to the constraint of temporal precedence whereby gene 'a' may only influence gene 'b' if IcE(g_a) ≤ IcE (g_b). In the last step TD-ARACNE uses an additional information theoretic measure Data Processing Inequality (DPI) [76] to identify and remove indirect associations, first among synchronously expressed nodes and in a second step across time points. TD-ARACNE is freely available as part of the Bioconductor package and can be downloaded from http://www.bioconductor.org/packages/2.12/bioc/html/TDARACNE.html or from http://bioinformatics.biogem.it. For further details about TD-ARACNE, we refer readers to Zoppoli et al. (2009) [19]. In our assessment, all user-adjustable parameters were set to the optimal values recommended by the authors for a network of equivalent node degree.

2.2.4 Assessing network recovery

We assessed the performance of each selected method on the different sizes of networks, noise levels and time points. We use standard statistical measures such as positive predictive value (PPV), recall and F1 score to report the performance for each method. PPV describes the number of correctly identified connections as a fraction of all

connections inferred, both correctly (true positive, TP) and incorrectly identified (false positive, FP) (Eq 2.8). Recall is calculated as the number of connections that were correctly recovered by the algorithm expressed as a fraction of all connections present in the true simulated network, namely those that were recovered (true positive, TP) as well as those that were missed (false negative, FN) (Eq 2.9).

$$PPV = \frac{\text{Truly inferred connections}}{\text{Total inferred connections}} = \frac{TP}{TP + FP} \tag{2.8}$$

$$\text{Recall} = \frac{\text{Truly inferred connections}}{\text{Total no. of connections in true network}} = \frac{TP}{TP + FN} \tag{2.9}$$

F1 score (F) is an aggregate measure combining PPV and recall. It is akin to the geometric mean of PPV and recall and can be represented as follows:

$$F = \frac{2(PPV \times recall)}{PPV + recall} \tag{2.10}$$

2.3 Results

2.3.1 Personalized networks

Personalized medicine is directed at the identification of illness and intervention at the level of a specific individual. While this is an attractive goal, several questions arise. For example, if we wanted to recover a network from a single experiment for a given individual, how well would we do on average in a diverse population? Moreover, how would the result change for the same person from one day to the next?

2.3.1.1 Mapping individuals with a single time course experiment

To explore the effects of person-to-person variability on network recovery we used NetSim to generate 20 sparse modular networks randomly, composed of 10 nodes each and with similar topological characteristics. Each simulated 10-node network consisted of 10–20 interactions that translated into median edge density of 15.6%. Edge density for a directed network of E edges and N nodes can be calculated as E/N(N-1). This

number of nodes and edge density is consistent with the scale found in synthetic biological networks that have been studied *in vitro*. For example, E.coli SOS response network that is often used in the evaluation of reverse engineering methods consists 8–9 nodes [19, 24] and the edge density of cortico-cortical fiber tract of the mammalian brain ranges between 10–30% [77]. We used each simulated network to generate a single time course that was sampled at 10, 25 and 50 time points. Expression profiles were generated both with and without 20% Gaussian noise allowing us to assess the effect of sampling frequency and experimental noise respectively on the performance of selected methods (Figure 2.1). For noise-free data all methods performed over a narrow range of median F scores (0.2–0.26) (Appendix 2.2a).

Nonetheless, results of a two-way analysis of variance (ANOVA) presented in Table 2.1 show that F score is significantly affected by the choice of method irrespective of noise ($p <= 0.001$). Though sampling frequency did not affect F scores significantly in the presence of 20% Gaussian noise ($p = 0.69$) over this initial range of values, this factor did trend towards significance in the absence of noise ($p = 0.07$).

Table 2.1. Impact of sample size, experimental noise and algorithm selection on network recovery: Results of a two-way ANOVA for the F score obtained by applying the 5 reverse engineering methods to single time course simulations of 20 different sparse and modular 10-node biological networks sampled at 10, 25 and 50 time points, both with and without 20% experimental noise (Figure 2.1).

Effect	Sum Sq.	d.f.	Median Sq.	F	Null p
0% Noise					
Time points	0.0224	2	0.0112	2.66	0.07
Method	0.0772	4	0.0193	4.57	0.0014
Method x Time points	0.0313	8	0.0039	0.93	0.49
20% Noise					
Time points	0.0046	2	0.0023	0.377	0.69
Method	0.1986	4	0.0497	8.055	0
Method x Time points	0.0494	8	0.0062	1.001	0.44

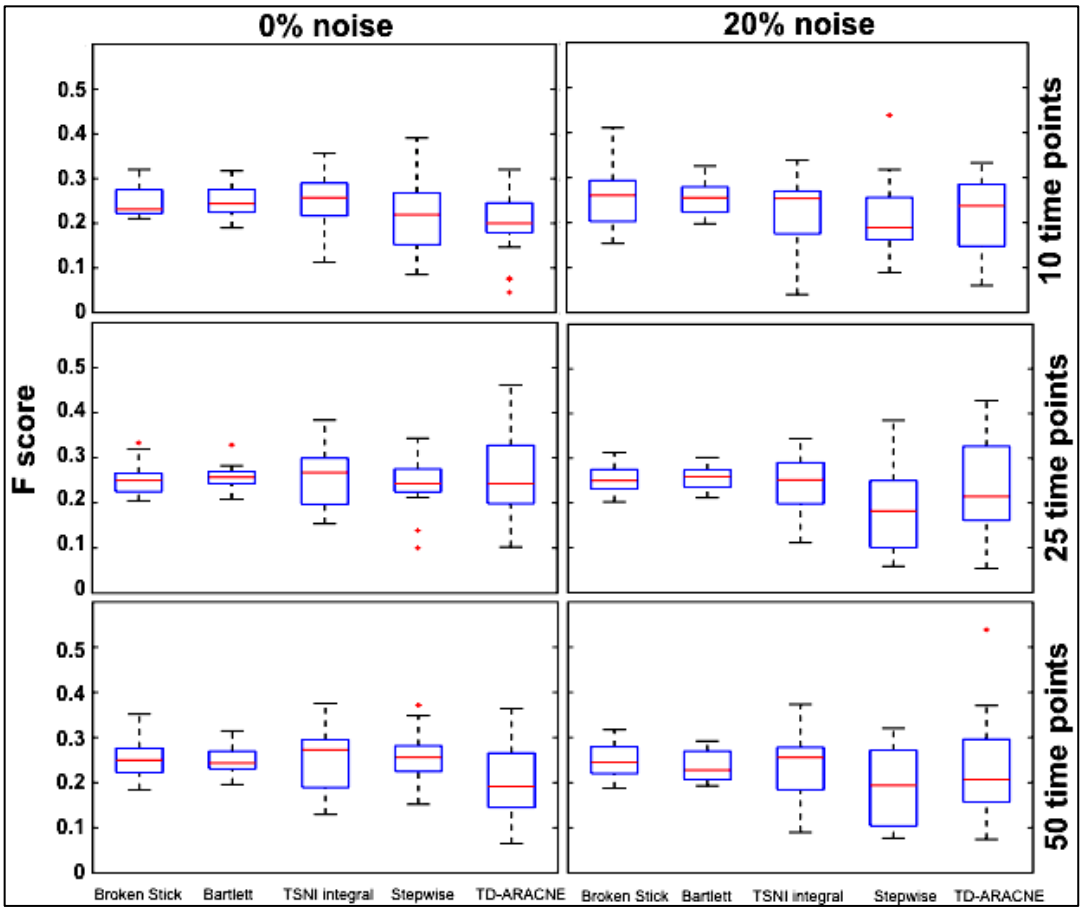

Figure 2.1: Median performance of selected methods across a range of networks: 20 different simulated networks of 10 nodes each were used to generate a single time course profile sampled at 10, 25 and 50 time points. Box plots show the median and inter-quartile range of F scores for selected methods namely, Broken stick, Bartlett, TSNI integral, stepwise and TD-ARACNe (left to right), on the datasets in the absence of noise (Box plots on the left) and on the datasets with 20% random noise added (Box plots on the right).

Indeed while the majority of methods appear relatively robust (Figure 2.1 and Appendix 2.2a,b) the inclusion of noise produced a noticeable decrease in network recall and corresponding significant decrease in the median F score in the case of the stepwise fit method. Both Bartlett's and broken stick methods for the selection of latent features in the ODE projection model produced comparable results in terms of PPV, recall and F score values. On average, both of these methods could infer 70–95% of the true network (median recall). However, this required that 5–7 connections be inferred for

every true connection recovered, leading to low median PPV. Slightly better PPV values were obtained with the stepwise fit to the conventional ODE however in the presence of noise this method could only infer 15–30% of the true network leading to lower F scores. The finite equation based TSNI integral provided equivalent or slightly better median PPV but with a loss of approximately 5–30% in coverage of the true network (median recall) resulting median F scores comparable to those obtained with the projection techniques. The information theoretic method TD-ARACNE produced the sparsest estimates of all selected methods. TD-ARACNE was able to infer one true connection out of every 4–6 inferred connections i.e. 18–25% PPV. However, this improvement in PPV cost most of the reference network unrecovered (Figure 2.1). Also, only minimal effects of noise were observed on PPV, recall and F score at any of the three sampling frequencies for this method.

2.3.1.2 Variations in time course from the same individual

In addition to person-to-person variability we may also expect a slightly different response from the same person on any given day. To explore the consistency of recovery for a specific network from any single experiment we randomly generated a reference network of 10 nodes consisting of 19 interactions (i.e. 21% edge density) with modular topology using NetSim. We then used this fixed reference network to simulate 20 different expression time courses each initiated at random conditions. These were once again sampled at 10, 25 or 50 time points respectively in the presence and absence of 20% noise. Similar trends in performance were observed when using the different methods for the recovery of a single reference network as was observed across the different networks (data not shown). Improved F scores were observed at higher edge density but these remained below 0.40 even in the absence of noise.

2.3.1.3 Scaling to larger networks

Most of the proposed network inference methods have been found to work better on small sub-networks of 5–10 nodes whether they be rate equation based such as TSNI integral or information theoretic like TD-ARACNE [19, 20]. However, Vinh and colleagues in 2012 [78], questioned how representative the recovery statistics might be on such small networks. To explore this further, we used the above-mentioned methods to recover networks including those composed of a larger number of nodes than that found in the synthetic networks typically reported. We constructed random reference networks composed of 5,10,15, 20, 30 and 50 nodes and with decreasing order of edge densities of 40, 21, 11, 8, 5 and 3% respectively, all with the same properties of sparseness and modularity. Each network was used to generate 20 simulated time course experiments, sampled at 50 time points, where 20% Gaussian noise was added to mimic experimental noise (Appendix 2.3). Overall a significant drop in median F-score was observed with increasing number of nodes or decreasing edge density for all the methods (Table 2.2, $p<0.01$). Rate equation models, both ODE from projection-based regression and difference equation formulations (i.e. TSNI integral) performed better than TD-ARACNE and step-wise truncation on sparse networks constructed with up to 15 nodes i.e. with 11–40% edge densities. However, for networks with edge densities of less than 10% or more than 15 nodes, no noticeable difference in performance was observed among methods (Figure 2.2). All methods delivered an F score below 0.10 in their recovery of a 50-node sparse modular network with 3% edge density. In the case of rate equation models identified with projection methods (i.e. ODE-Bartlett and ODE-broken stick) and TSNI integral, the loss in performance was driven mainly by a loss in PPV. This was not the case for the remaining methods, stepwise regression and TD-ARACNe, where both PPV and recall were adversely affected by increasing node degree and decreasing edge density (Appendix 2.3).

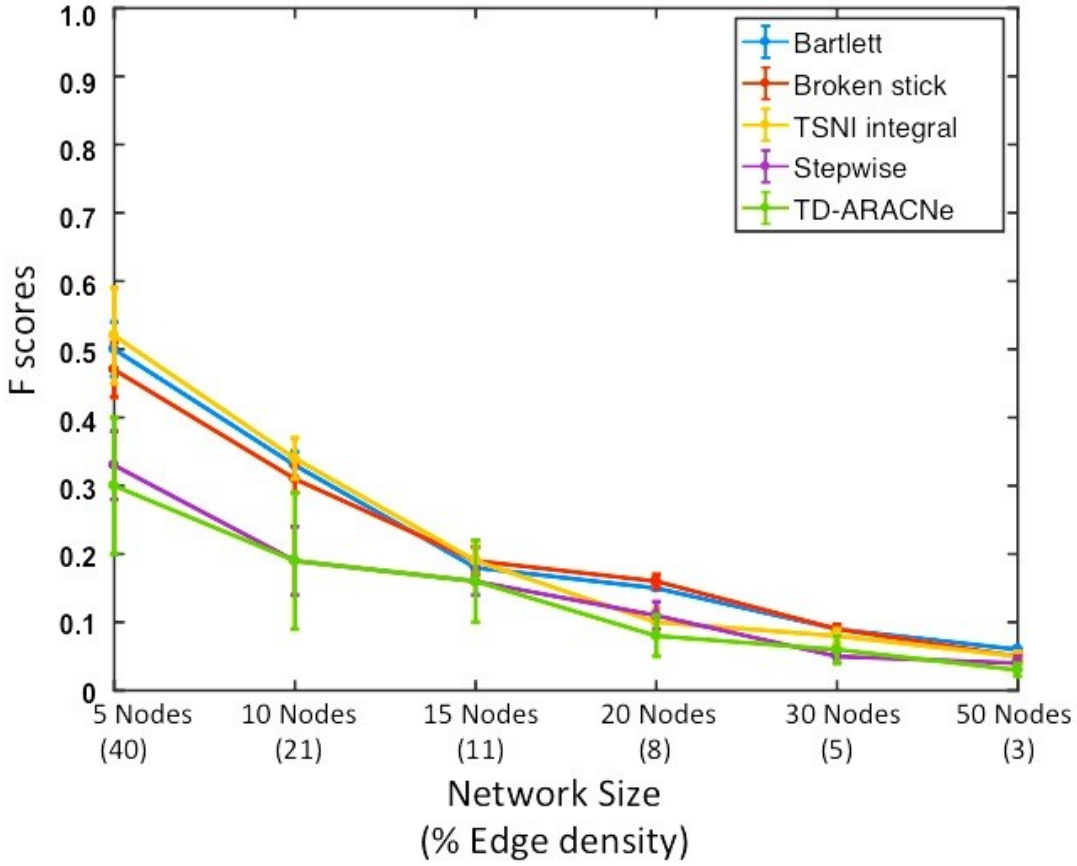

Figure 2.2: Effect of network scale and edge density on the performance of different methods. For each network scale of node degree between 5 and 50 nodes, a single reference network was created. From each network 20 simulated time courses were obtained using different initial conditions and sampled at 50 time points. All time courses included 20% Gaussian noise. F scores were obtained based on the network recovered from each simulated time course and median values plotted against node scale and with respective edge density.

Table 2.2 Two-way ANOVA of F score values corresponding to the recovery of random reference networks composed of 5,10,15, 20, 30 and 50 nodes with 40,21,11,8,5,and 3% edge densities respectively, all with the same properties of sparseness and modularity. Each network was used to generate 20 simulated time course experiments, sampled at 50 time points, where 20% Gaussian noise was added to mimic experimental noise (Figure 2.2, Appendix 2.3)

Effect	Sum Sq.	d.f.	Median Sq.	F	Null p
Method	0.662	4	0.165	61.14	***0.00***
Node degree/Edge density	9.312	5	1.862	688.44	***0.00***
Method x Node degree	0.598	20	0.029	11.06	***0.00***

2.3.2 Using repeated time course experiments

As experimental subjects are typically stratified into more homogenous phenotypic groups for study, it may be more relevant to the current realm of clinical research to examine the effects of noise when aggregating several time course experiments in some way. Instead of considering the median performance in recovering the same underlying network at the level of individual time courses we next considered how combining these separate experiments might allow us to make a stronger statement about the group. This could be compared to the difference between narrow patient sub-typing and personalized medicine.

2.3.2.1 Combining networks from the same individual

First, we explored how repeating a challenge multiple times on the same subject might bring us closer to our eventual goal of delivering personalized medicine. We constructed a 10-node reference network with 19 interactions i.e. with 21% edge density and used it to generate 20 time course experiments, each sampled with 50 time points. Next, we added 20% Gaussian noise similar to the previous cases discussed above. We then applied a simple voting scheme to aggregate the networks inferred from each individual time course. A quorum rule was applied to each element across the 20-adjacency arrays. A specific element was conserved in the final consensus array if it was identified as significant in certain minimum number of time course experiments. For example, if an edge was present more frequently than a certain threshold, say 12 times across the 20 adjacency matrices, then that edge would be considered as present in the underlying network shared by the grouped experiments. The threshold frequency of occurrence for the selection of edges was determined by optimization on the basis of maximum F score achievable. Typically, a threshold of greater than 50% occurrence was sufficient to deliver stable solutions in inferring a given edge. Because of its higher sensitivity to

noise we omitted the stepwise truncation-based approach from this analysis. TD-ARACNE was included despite achieving a poor median recall on single time course experiments to provide a basis for comparison with an information theoretic approach.

In order to examine the effect of group size we repeated our analysis with each selected method on groups of 5, 10, 15 and 20 time course experiments respectively, each sampled at 50 time points (Table 2.3). As might be expected, the performance of these methods improved when inferring the networks from a group of time courses. Though TSNI integral (Table 2.3) was the least responsive when increasing the number of time courses from 1 to 20 trajectories, projection-based approaches overall produced noticeably better F-scores than did TD-ARACNE. With the latter the optimal threshold values for inclusion were so low that the aggregated consensus network approximated the set union of all individually inferred networks. In other words an edge was accepted into the aggregate network if it was present in any one of individual networks. Interestingly, TD-ARACNE continued to show an increasing trend in F-score while the other methods achieved a peak performance at group sizes of 10 or 20 trajectories. F-score is a composite measure and the improvement brought about by aggregation can be better visualized using an example network. In Figure 2.3 we present a simulated 10-node network with 19 connections (21% edge density). A group of 15 time course experiments with 50 time points each were simulated using NetSim.

Figure 2.3A and 2.3C show one of the 15 inferred networks resembling the median performance of TD-ARACNE and broken stick respectively whereas, Figure 2.3B and 2.3D show the consensus networks obtained after the aggregation of 15 inferred networks. In the case of TD-ARACNE, aggregation of networks increases the number of predicted edges whereas this same operation reduced the number of edges predicted in consensus by the broken stick method. At the level of the individual network in Figure 2.3A, TD-ARACNE predicted very sparse network of 12 connections and predicted 3 out

of 19 true connections resulting in median PPV, recall and F score values of 25%, 16% and 0.19 respectively. This performance improved on aggregation of 15 inferred networks where 9 of the 19 true connections were inferred correctly; increasing recall from 16% to 47% (Figure 2.3B). PPV also increased from 25 to 29%, yielding an aggregate network F score of 0.32.

Table 2.3: Impact of grouping single time courses: Improvement in performance of selected methods by inferring a consensus network for a group of time series experimental data. The reference network consists 10 nodes with 19 edges i.e. (21% edge density). Each experimental time series have 50 time points. A consensus threshold to achieve best possible F score value was used to infer consensus network.

Method	Group size	PPV	Recall	F score	% increase F score
Bartlett's	20	0.41	0.37	0.39	3-30% increase
	15	0.36	0.53	0.43	
	10	0.24	0.63	0.35	
	5	0.24	0.58	0.34	
	1*	0.21	0.76	0.33	
Broken stick	20	0.47	0.42	0.44	22-41% increase
	15	0.57	0.42	0.48	
	10	0.31	0.79	0.44	
	5	0.24	0.84	0.38	
	1*	0.19	0.84	0.31	
TSNI integral	20	0.31	0.58	0.4	12-24% increase
	15	0.3	0.68	0.41	
	10	0.32	0.63	0.42	
	5	0.3	0.53	0.38	
	1*	0.25	0.53	0.34	
TD-ARACNE	20	0.31	0.47	0.38	63-100% increase
	15	0.29	0.47	0.36	
	10	0.21	0.58	0.31	
	5	0.24	0.53	0.33	
	1*	0.25	0.16	0.19	

* The PPV, recall and F score values reported are equal to the median values obtained from the 20 time courses of above-mentioned network.

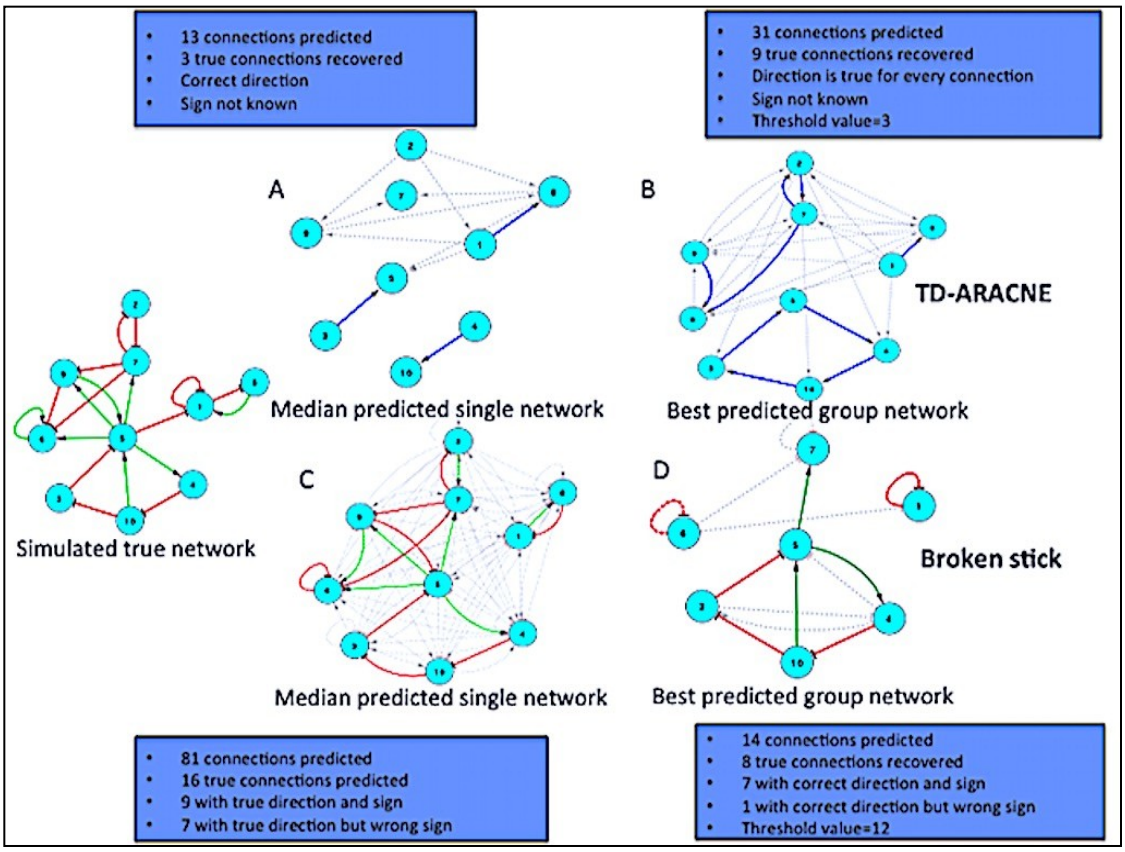

Figure 2.3: Recovery of an example 10-node network: (A) Median inference by TD-ARACNE using single time course, (B) best possible inference by TD-ARACNE using a group of 15 simulated time courses for the same network, (C) Median inference by broken stick method using single time course and (D) best possible inference by broken stick using a group of 15 simulated time courses for the same network.

However, the threshold occurrence for the inclusion of an edge in the consensus network was very low i.e. 3 events. In other words, selected edges in the aggregated network were the ones that were inferred in 3 or more networks out of 15 inferred networks. In comparison inference with broken stick achieved median recall of 84% on individual networks i.e. on average 16 out of the 19 true connections could be inferred from a single time course experiment with 50 time points (Figure 2.3C). Unfortunately in order to predict these 16 true connections (recall = 84%) 65 false positive connections were inferred (grey colored), leading to a PPV of 20%. When aggregating across a group of 15 experiments, the broken stick method inferred a consensus network of 14 connections, 8 of which were present in the true network (Figure 2.3D). This important

reduction in false positive predictions translated into a PPV of 57%. Though some loss in recall (42%) was incurred, the result was nonetheless a net gain in median F score (F = 0.48 vs 0.32). In assessing these performance metrics it is important to remember that we considered only direction of the edges, as is the norm in current literature.

2.3.2.2 Describing illness sub-group by aggregating networks across individuals

To verify how robust these results might be across different networks of the same size we simulated groups of 1, 5,10,15 and 20 time courses, sampled at 50 time points from10 different networks each comprised of 10 nodes with edge densities ranging from 0.10–0.20. These simulated time courses were then analyzed using both projection methods and TSNI integral (Figure 2.4). Despite being reasonably robust to noise, TD-ARACNE typically lagged projection based methods and TSNI integral in performance (Table 2.3 and Figure 2.3). For this reason, we omitted TD-ARACNE from further analysis. Median PPV, recall and F score for each group were calculated along with the standard error. As expected, the greater the number of time courses in a group of diverse individuals, better the performance of the method. However these improvements once again begin to taper off beyond 10–15 time courses. The F score could be improved by a factor of ~1.5 over that of a single time course by using 10 experiments with the broken stick model and 15 experiments for Bartlett's model and TSNI integral. This improvement in F score for the broken stick method was driven by an initial increase in median PPV at the expense of recall. Similar but less dramatic trends were found for TSNI integral. In contrast, recall values for the Bartlett method recovered and trended positively for group sizes above 10 time courses (Figure 2.4). Once again while the median performance of TSNI integral was slightly better on single time course experiments, the broken stick projection method delivered equivalent or slightly better performance at all other group sizes (5–20) when sampling 50 time points (Figure 2.4). A

two-way ANOVA of F-score values from grouped data confirmed the significance of this difference in performance between methods ($p = 0.008$) (Table 2.4). While the choice of group size also produced a significant affect on F score ($p = 0.000$), the combined effect of method and group size did not (Table 2.4). Further analysis revealed that the benefit of increasing group size dissipated quickly and that there was no significant effect ($p = 0.40$) on F score values for groups of 10 and more time courses. However even at these larger group sizes the choice of method ($p = 0.03$) continued to be a significant factor (not shown).

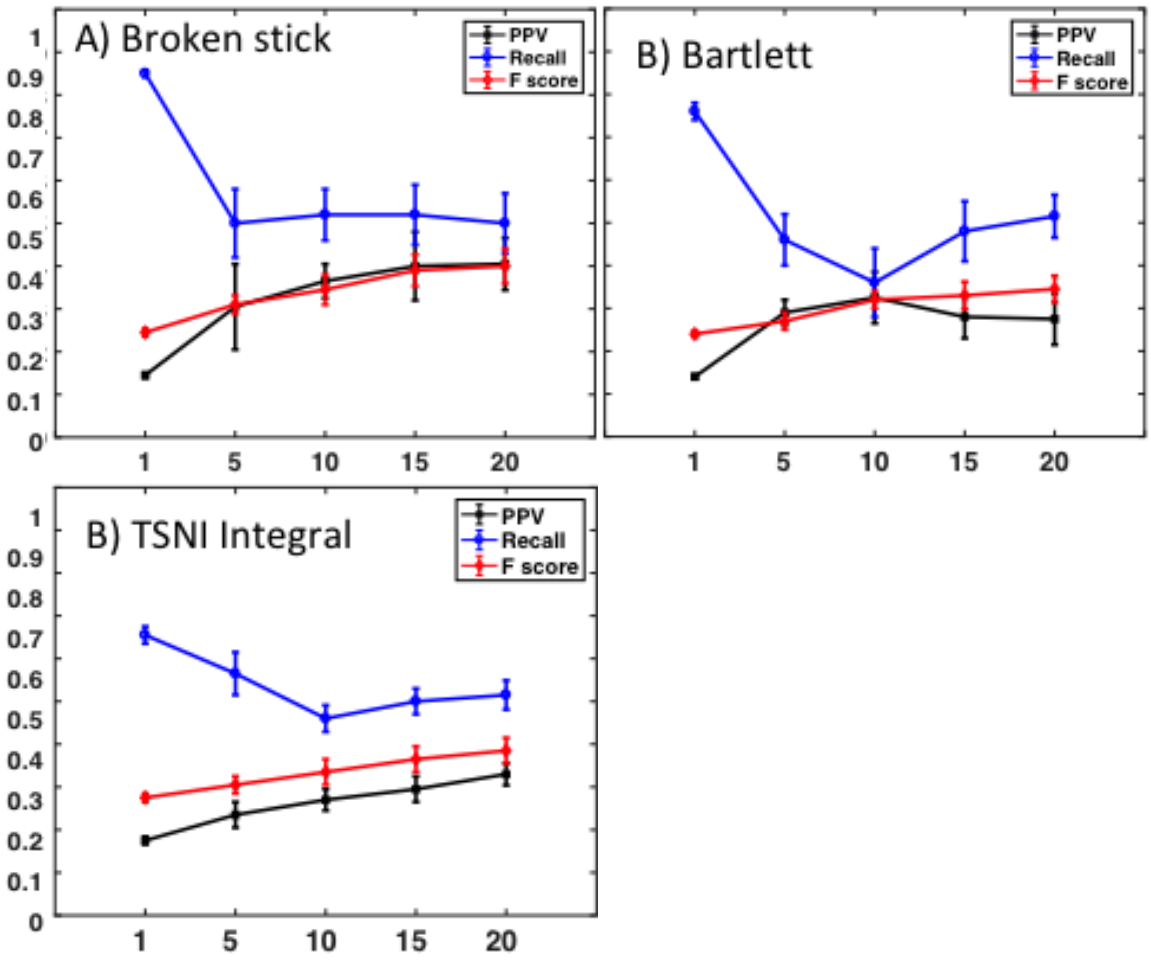

Figure 2.4: Effect of grouping time courses: Median performance calculated across subsets from 10 different 10-node simulated networks recovered using (A) Broken stick (B) Bartlett's and (C) TSNI integral methods applied to groups of time courses. Each network was used to generate groups of 1, 5, 10, 15 and 20 simulated time courses each sampled at 50 time points. All simulations included 20% experimental noise.

Table 2.4: Impact of time course aggregation into subject groups. Two way ANOVA of F score values corresponding to the recovery of 10 different networks of 10 nodes with similar properties of sparseness and modularity and with edge densities similar to those of biological networks (10–20%) using groups of 1, 5, 10, 15 and 20 time courses. Each time coursewas simulated at 50 time points and 20% Gaussian noise was added to mimic experimental noise

Effect	Sum Sq.	d.f.	Median Sq.	F	Null p
Method	0.0726	2	0.0363	4.96	0.0083
Group size	0.3306	4	0.083	11.3	0
Method x Group size	0.0245	8	0.003	0.42	0.91

2.3.2.3 Sampling for group inference

Network recovery in the previous sections was based on the availability of 50 time points. However, in actual *in vivo* studies the collection of samples at multiple time points is a significant challenge from the perspective of subject well being and cost. To explore the minimum number of time points that might be required by each method, we simulated groups of 1,5,10,15 and 20 time courses sampled at 5, 10 and 50 time points. We found that the broken stick model was less sensitive to the number of time points than the Bartlett and TSNI models. While the former produced the highest F scores when 10 and 50 samples were drawn, this improvement was only noticeable when a group of more than 10 time courses was used (Fig 2.5). In contrast, drawing 50 samples was uniformly better when using the Bartlett method almost regardless of group size. In the case of TSNI integral, the use of 10 samples was sufficient to produce comparable results, 5 samples being inadequate for all group sizes. These preliminary results suggest that while similarly affected by group size, the broken stick and TSNI integral methods may be fairly tolerant of lower sample frequency. The Bartlett method on the other hand would require the largest number of samples.

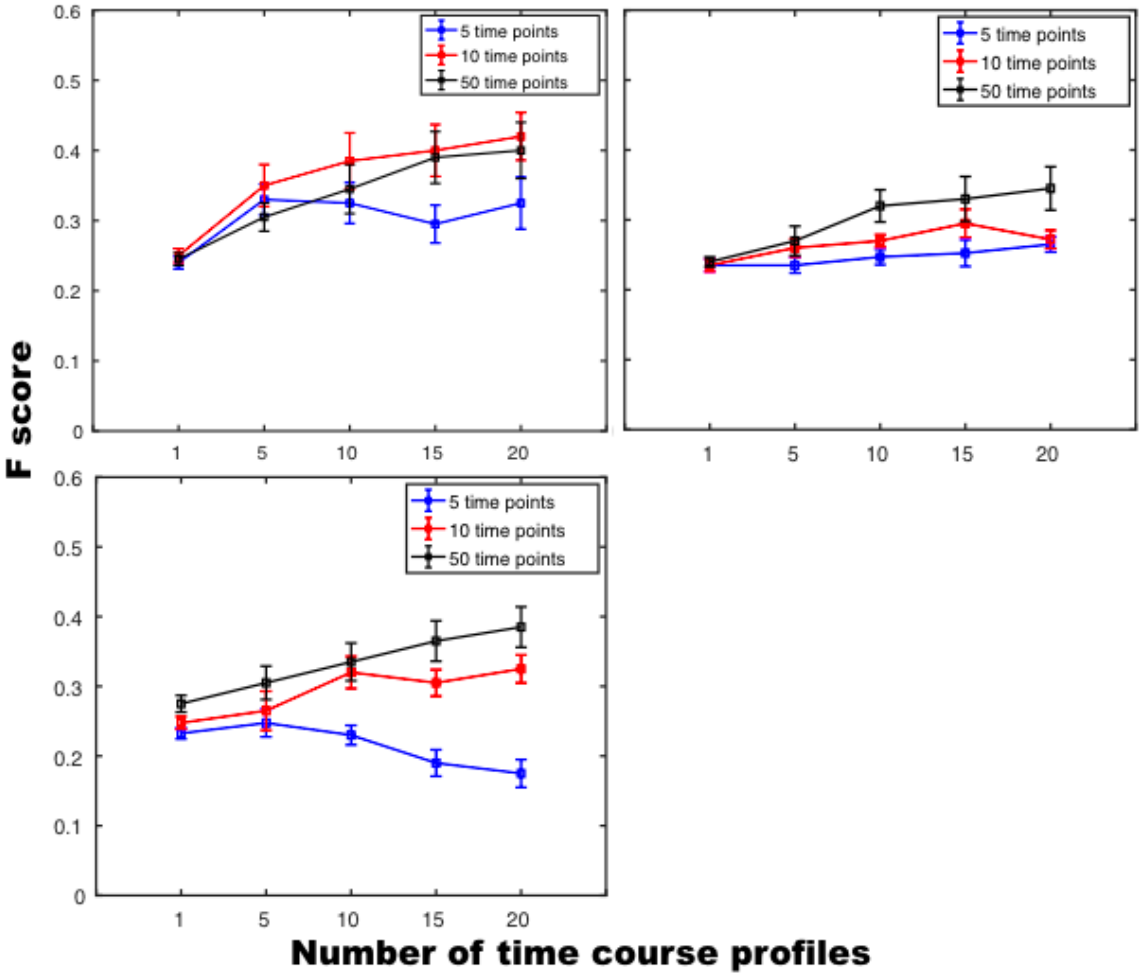

Figure 2.5: Minimum Sampling for grouping: Median F scores calculated on 10 different simulated 10-node networks recovered using (A) Broken stick (B) Bartlett's and (C) TSNI integral methods on group of expression profiles. Each network was used to generate groups of 1, 5, 10, 15 and 20 simulated time courses each sampled at 5 (blue), 10 (red) and 50 (black) time points. All simulations included 20% experimental noise.

2.3.3 General applicability of the results

2.3.3.1 Generalization of findings to the DREAM challenge

In order to facilitate a broader comparison of these findings we applied this same methodology to the in silico benchmark dataset provided under the DREAM3 sub-challenge for a set of 10-node networks. This dataset was generated using an open source Java tool, GeneNetWeaver [79], and consisted overall of 5 simulated network structures with corresponding steady state and time series data. A modular topology was

produced based on patterns of tightly connected gene clusters extracted from experimentally validated regulatory networks. More precisely, 2 out of 5 network structures were based on gene modules extracted from *in vivo* networks of E.coli [80] and the other 3 on modules from the S.cerevisiae *in vivo* network [12]. A thermodynamic quantitative model of gene regulation that includes both transcription and translation [81] was applied to these network structures to generate dynamic and static simulated experimental data [79].

In keeping with the focus of our current analysis, we used only the dynamic perturbation data. Specifically, we applied both projection-based feature selection techniques along with TSNI integral on the 4 time series provided in DREAM3 for the E.coli2 network of 15 interactions and compared their performance with the median performance obtained using NetSim data for networks with a comparable number of interactions (median interactions = 14). We found that all the selected methods performed similarly in terms of PPV, recall and F score on networks of comparable topology simulated with either NetSim or GeneNetWeaver (Appendix 2.4) suggesting that both simulators are designed to capture the similar network properties.

Further, we compared the performance of these methods with that of reported in Yip et al. (2010) [26], the winning team in the DREAM3 challenge. The latter inferred the underlying networks by combining the inferences obtained from a null hypothesis noise model applied to static knockout/ knock down data, as well as linear and nonlinear ODE models applied to perturbation time course data. Seven different batches were formed consisting of a consensus of different model inferences. We focused first on the results reported by Yip and coworkers [26] using only the time course data to support the consensus of a similar linear ODE model with a more sophisticated nonlinear model (Batch 1 Table 6 of Yip et al., 2010). We then compared the results of assessed ODE models identified from time course perturbation data with that reported in Yip et al.

(2010) [26] for the null hypothesis noise model identified from static knockout/ knockdown data (Batch 1 Table 3 of Yip et al., 2010). When applied to the DREAM3 perturbation time series data, the basic feature selection techniques assessed here based on a simple linear ODE model (br--oken stick, Bartlett' s and TSNI integral) perfo-

Table 2.5: Recovering a 10-node network from a DREAM-3 data set. Comparison of the performance obtained in inferring a 10-node network using the generic methods presented here versus the best performing methods in the DREAM 3 sub-challenge, namely the basic noise model and the combined linear/ nonlinear model.

E.coli 1 (11 interactions)					
Method	**Predicted**	**Correct**	**PPV**	**Recall**	**F score**
Yip et. al. Noise model	11	7	0.64	0.64	0.64
Yip et al. linear/nonlinear model	6	1	0.16	0.09	0.12
Broken stick	70	9	0.13	0.82	0.22
Bartlett's method	77	10	0.13	0.91	0.23
TSNI integral	10	2	0.15	0.14	0.29
E.coli 2 (15 interactions)					
Yip et. al. Noise model	16	12	0.75	0.8	0.77
Yip et al. linear/nonlinear model	5	1	0.2	0.07	0.1
Broken stick	73	12	0.16	0.8	0.27
Bartlett's method	82	14	0.17	0.9	0.28
TSNI integral	28	6	0.21	0.4	0.27
Yeast 1(10 interactions)					
Yip et. al. Noise model	11	9	0.82	0.9	0.86
Yip et al. linear/nonlinear model	5	0	0	0	0
Broken stick	72	8	0.11	0.8	0.19
Bartlett's method	83	10	0.12	1	0.22
TSNI integral	27	2	0.07	0.2	0.11
Yeast 2(25 interactions)					
Yip et. al. Noise model	13	9	0.69	0.36	0.47
Yip et al. linear/nonlinear model	5	1	0.2	0.04	0.07
Broken stick	71	19	0.26	0.74	0.38
Bartlett's method	83	23	0.28	0.9	0.42
TSNI integral	31	9	0.29	0.36	0.32
Yeast 3(22 interactions)					
Yip et. al. Noise model	12	8	0.67	0.36	0.47
Yip et al. linear/nonlinear model	5	4	0.8	0.18	0.29
Broken stick	70	14	0.2	0.61	0.3
Bartlett's method	80	18	0.22	0.8	0.34
TSNI integral	31	9	0.29	0.41	0.34

-rmed better than the combination of linear and nonlinear ODE models used in Yip et al. (2010) [26] for all networks (Table 2.5). This being said all ODE models, including those studied in this work, were outpaced by identification based exclusively on homozygous deletion data when inferring sparse networks i.e. networks with 10-15 interactions. However, Bartlett's and broken stick method of feature selection from time course data approached the performance of the noise model on slightly denser but still sparse networks i.e. Yeast 2 (25 interactions) and Yeast 3 (22 interactions) respectively (Table 2.5). F scores for the inference of the networks with 10, 15, 22 and 25 interactions were improved with increasing edge density for Bartlett' s (0.22, 0.28, 0.34 and 0.42) and broken stick method (0.19, 0.27, 0.3 and 0.38) respectively whereas that of the noise model fell (Table 2.5).

In 2010, Marbach and colleagues [49] further confirmed that the homozygous deletion data was the most informative of all types of data used in DREAM 3 challenge. However, knockdown/knockout data is not easily accessible in human subjects. In further agreement to the findings of [26] and [49], we also found that complex nonlinear models and/ or complex adjustments to linear models did not add significant value to the inference of regulatory interactions and that much simpler more computationally efficient models performed as well when feature selection parameters were optimized based on *a priori* simulations.

2.3.4 Recovery of Yeast synthetic gene network

As an additional verification of the applicability of the simulated networks used here, we again applied our simple model to data obtained from a synthetic biological network. In 2009, Cantone and coworkers [62] constructed a synthetic network of five genes in the simple eukaryotic organism Saccharomyces cerevisiae for *in vivo* Reverse-engineering

and Modeling Assessment (IRMA). This synthetic network includes a variety of regulatory interactions, thus capturing the behaviour of larger eukaryotic gene networks on a smaller scale. The network was also designed to be negligibly affected by endogenous genes, and to respond to galactose, which activates transcription of its genes.

We used the switch ‘ on’ and switch ‘ off’ time series data generated for the IRMA network and inferred the underlying regulatory interactions using projection-based feature selection and TSNI integral. Since the underlying structure of the IRMA network was known *a priori* we tuned the parameters accordingly for the algorithms in question to optimize network identification based on data averaged across of 5 time courses. All three methods performed comparably in terms of the F-score on both datasets, with the Bartlett’ s method being best performer on the switch ‘on’ and switch ‘off’ time series data respectively (Table 2.6). With the exception of TSNI integral on switch off data, all methods were found to achieve better PPV than a random reconstruction on this synthetic network. Although ODE-based TSNI, the predecessor of TSNI integral along with NIR method was reported to achieve better performance on switch ‘on’ time series (F score = 0.80) by Cantone and colleagues [62]. However Bartlett’ s method (0.67) outperformed these methods (0.60) on switch ‘off’ time series [62].

Table 2.6: Reconstruction of 5-node synthetic Yeast IRMA network. Broken stick, Bartlett’s and TSNI integral were evaluated on the dynamic data of Yeast 5 node synthetic IRMA network against performance of TSNI and NIR reported in Cantone et al. (2009) [62]. Values in parentheses show the performance when self-regulation is not considered in the inference as in DREAM 3 challenge.

	Switch on data			Switch off data		
Method	PPV	Recall	F score	PPV	Recall	F score
Broken stick	0.4(0.5)	0.67(0.67)	0.5(0.57)	0.67(0.67)	0.33(0.33)	0.44(0.44)
Bartlet	0.6(0.75)	0.5(0.5)	0.55(0.6)	0.56(0.56)	0.83(0.83)	0.67(0.67)
TSNI integral	0.4(0.63)	0.83(0.83)	0.53(0.71)	0.29(0.44)	0.67(0.67)	0.40(0.53)
Cantone et al.	1	0.67	0.8	0.75	0.5	0.6

Note that the performance of these methods in recovering the 5-node IRMA network appears better than that obtained in the case of 5-node NetSim networks with similar edge density. This is due to different optimization objectives. In the case of the NetSim networks, the tuning parameters were optimized to produce maximal median F score on a group of 20 time course profiles whereas the parameter values used in recovering the IRMA network were identified by maximizing F score on a single target time course profile.

2.3.5 Recovery of Human gene network in HeLa Cell culture

In addition to the DREAM3 and yeast IRMA data, we also used microarray time course data sampled to characterize periodically expressed transcripts during cell division in human HeLa cell line cultures [82]. This data is available at http://genome-www.stanford.edu/Human-CellCycle/HeLa. In 2008, Sambo and colleagues extracted the expression of 9 genes with known and documented interactions in the BIOGRID database (www.thebiogrid.org) sampled at 47 time points from this dataset in their assessment of the reverse engineering method CNET [63]. This same time course dataset has since been used for the assessment of several inference methods [30, 31]. It is important to note that the BIOGRID database is updated as new biological knowledge of these interactions becomes available. For example, the network obtained from BIOGRID in [30] is an updated version from the one used in [63] incorporating new interactions. We assessed projection-based feature selection techniques and TSNI integral on the BIOGRID networks used in [63] and [30] respectively. Interestingly, assessment on this network provided an opportunity to compare the performance of projection-based methods with other methods by only using perturbation data without any additional data types. Although this data provides an opportunity to further assess

our simulation results in reconstructing a human gene regulatory network it is important to remember that this remains data sampled from an *in vitro* cell culture system and hence may be sampled at a much higher rate than typically available under *in vivo* studies of human subjects. In our assessment, both projection-based techniques namely, broken stick (F scores = 0.40 and 0.56) and Bartlett' s method (0.47 and 0.60) not only outperform TSNI integral (0.17 and 0.26) in the reconstruction of 9-gene HeLa cell cycle network but also match the performance of methods used in [63] and [30] respectively (Fig 2.6; Table 2.7). These results re-affirm that even simple models tuned with *a priori* simulated data, can potentially perform as well as complex methods.

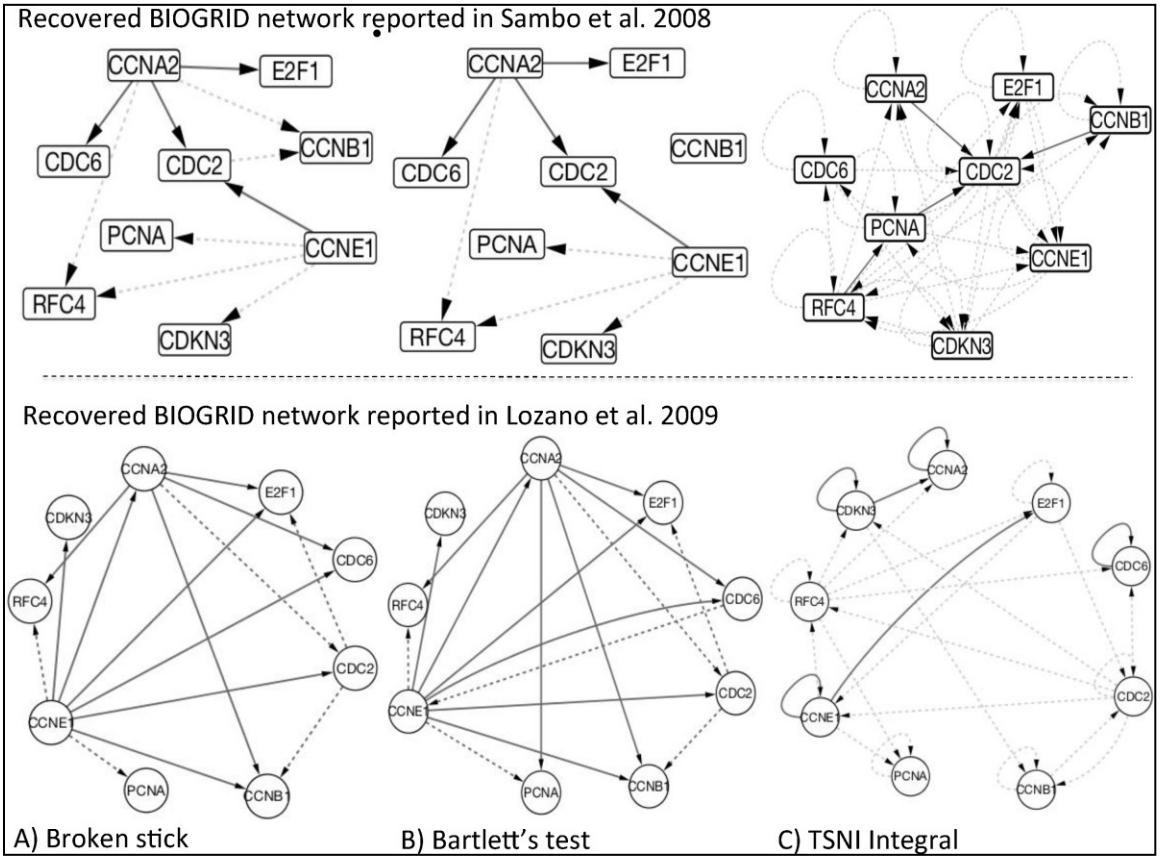

Figure 2.6: Reconstruction of human HeLa cell cycle network. Directed graphs recovered using (i) Broken stick (ii) Bartlett's feature selection and (iii) TSNI integral methods applied to the BIOGRID reference network reported in Sambo et al. (2008) and Lozano et al. (2009) (A and B). Solid lines represent correctly inferred interactions (true positives) where as dash lines represent incorrectly inferred connections (False positives).

Table 2.7: Reconstruction of 9-gene BIOGRID network related to Human HeLa cell cycle. Recovery of 9-gene BIOGRID network involved in human HeLa cell cycle by applying broken stick and Bartlett's feature selection methods compared to TSNI integral. These two versions of BIOGRID network were used to assess proposed methods in Sambo et al. (2008) and Lozano et al. (2009) respectively. Reported performance of these methods is also included.

Network	PPV	Recall	F score
BioGrid network in Sambo et al. 2008			
Sambo et al. 2008	0.36	0.44	0.40
Broken stick method	0.36	0.44	0.40
Bartlett's method	0.50	0.44	0.47
TSNI Integral	0.10	0.44	0.17
BioGrid network in Lozano et al. 2008			
Lozano et al. 2009	0.50	0.72	0.59
Broken stick method	0.63	0.50	0.56
Bartlett's method	0.65	0.55	0.60
TSNI Integral	0.22	0.30	0.26

2.4 Discussion

The main purpose of this study was to examine the core design features of some of the basic classes of methods currently available for the reverse engineering of biological networks. In particular, we attempted to gauge their applicability to data collected under experimental constraints typical of *in vivo* studies where the range of allowable perturbations (e.g., virtual absence of knockout data), the sample frequency and the number of subjects are all significantly limited. Using the two alternative types of parameter estimation commonly applied in the identification of ODE models we assessed the recovery of known networks from simulated perturbation time course data produced by the NetSim platform. Importantly, this was done under a range of sampling frequencies and group sample sizes, key parameters in the design of such experiments. The conventional gradient-based ODE form was also compared to the equivalent time-

lagged difference equation (TSNI integral). In addition, the performance of TD-ARACNE, a recently reported information theoretic method adapted for use with time course experiments was also assessed. Finally, the general applicability of our simulation results was explored by reconstructing in silico networks using data from the DREAM3 challenge, from the synthetic IRMA network as well as from 9-gene HeLa cell cycle network. In our analysis, none of the methods evaluated performed to the standards of their reported average performance on single simulated time courses created using the logic-based NetSim. It is important to note that in many cases the edge count of the simulated networks was not reported. In addition many of these methods were typically assessed under the more ideal condition where simulated time course data was generated using models similar to those encoded in the reverse engineering algorithm. For example, in evaluating the probabilistic method TD-ARACNe, a random network was used to define a set of statistical dependencies then translated these into stochastic differential equations to simulate the actual time course data [19].

Likewise, the authors of TSNI integral used very similar differential equation models to generate both the test data and to perform the reverse engineering [20]. Though this is an important departure from real-world conditions, it nonetheless offers a possible upper bound for the performance achievable under near ideal conditions. Despite such favourable conditions these reverse engineering methods barely achieve an F score of 0.4 in recovering a 10-node network from 50 time points sampled with 10% noise (based on Table 1 in [20] and Table 2 in [19]). Based on this body of literature, an F score of 0.40 might be considered a near ideal performance for these methods in recovering networks with small to moderate node degree using single time course data alone.

Here we purposely generated data using a simulation method based on a fuzzy logic framework that differed significantly from the ODE model structure used for reverse

engineering. Though still artificial, we consider this situation more realistic. Understandably under these conditions the recovery performance based on single time courses consisted in a median F score of 0.30 or less. Rather than focus on the recovery of networks in individual subjects, we used the commonly accepted practice in human studies of stratifying the cohorts into groups of subjects. In our analysis, projection methods applied to the standard ODE as well as the difference equation model (TSNI integral) were successful in recovering typical biological networks having edge densities of 10– 30%, producing a median F score of 0.40 or more when used on groups of time courses. This translated into a predictive precision (PPV) in the range of ~30– 40% with recall values between ~50– 60% for simulated data from sparsely connected artificial networks designed to exhibit key topological properties similar to those expected in real biological networks. Interestingly, this is consistent with values obtained from *in vivo* regulatory sub-networks surveyed in human immune cells. In recent work, MINDy, an extension of the information theoretic method ARACNe, was applied to the genome wide identification of modulators of the MYC transcription factor using 254 gene expression sets previously generated for several studies of normal and tumor-related B-cell phenotypes [83]. A literature-based assessment using the Ingenuity software (Ingenuity Systems) revealed that of the 83 reported direct and indirect modulators of MYC expressed in B cells and present on the array, 29 had been recovered correctly, a recall of 35%. Furthermore, 17 of the 35 transcription factors inferred as MYC modulators were either literature-validated (6 or 17%) or had enriched binding sites, leading to an overall upper bound on precision of 48%. It is important to remember that in contrast to these local regulatory modules we intentionally focused in this work on the recovery of networks exhibiting the same edge densities as those observed in broader biological networks, namely 10 – 30% [77]. We considered this a more challenging task than the recovery of more densely connected sub-networks that are typically used for

benchmarking.

Indeed, our results show that edge density and performance of the selected network recovery methods are directly proportional with higher values of edge density leading to better performance. The recovery of sparse networks is also highly relevant. Several noteworthy biological networks are known to have low edge density, for example this can be as low as 3.85% between neurons in C. elegans, and global protein-protein interaction networks in human show edge densities of ~0.4%. Our results suggest that in such sparse networks one might expect reasonable recovery only in the better-connected component sub-networks where edge density is maintained above 10%. Examples of such networks include cytokine signaling between immune cells (60% edge density), cytokine signaling with tissue (40%) and neural networks of cat brain (30% edge density) [84].

For the sparser networks studied here, we found that ODE-based methods generally performed better than TD-ARACNE under conditions that approximated *in vivo* time-course studies, namely when data collection was restricted to smaller subject groups and infrequent sampling. Among the ODE based methods, stepwise feature selection was less tolerant of experimental noise. Projection-based methods typically faired better as they aggregate terms into composite features, creating an averaging effect that attenuates noise. Unfortunately as we report in this work, projection methods tend to produce far less parsimonious models and a high rate of false positive calls. This is only compounded further in real biological networks where indirect associations may be introduced by unobserved moderators [85, 86]. Inferring networks from a set of expression time course profiles improved the performance of all selected methods. Accordingly, the recovery of personalized networks would require the use of multiple time-course experiments applied to the same subject. This is a less than desirable protocol for several reasons. A much more attainable goal consists of grouping patients

suffering from the same variant and/or stage of a disease and that share other clinical parameters, such as age, BMI, sex, ethnicity etc. Our analysis suggests that at least 10 time courses would be required for the inference of a representative network for a group of such individuals. Sample frequency is another important design consideration. We found the more parsimonious of the projection approaches i.e., broken stick and TSNI performed consistently when at least 10 time points were used. Our results also suggested that inclusion of additional time course experiments could not correct for insufficient longitudinal sampling.

Nor was there much to be gained on this type of perturbation data by increasing the complexity of the model. Marbach and colleagues [49] conducted a comparative analysis of results from all DREAM3 participating teams, some of which used sophisticated non-linear and computationally intensive methods. Though accuracies in excess of 0.60 were produced on small networks (10 nodes) they found that these results were heavily dependent on the type of data available. Indeed, the top five teams all integrated steady-state knockout and knock down data with time-series perturbation data, leveraging the complementary nature of these data sources. In fact, even though both linear and non-linear differential equations were used by the winning team [26], the best performance was based on a simple statistical noise model applied solely to steady-state homozygous knockout data. The use of more complex nonlinear ODE forms contributed little if anything towards improving the identification of the underlying networks [49]. Indeed, in single networks of 10 nodes we obtained comparable or better results using a linear ODE model alone on time course perturbation data. Though clearly a very important contributor to the accurate recovery of biological networks, the availability of large-scale deletion libraries in higher mammalian species is currently limited though ongoing efforts focused on the mouse genome are making inroads [87]. Even if such libraries were available for Homo sapiens, their analysis supports the broad

identification of direct regulatory structure but does not support the identification of co-regulatory motifs nor does it support the identification of regulatory kinetics supporting pharmacokinetic studies. The latter will require kinetic experiments over a range of frequencies as well as dose response methodology [88, 89].

Though preliminary and rooted in a set of basic assumptions regarding the properties of the data, these findings offer an approximate set of guidelines for the design of pilot studies directed at the inference of *in vivo* network regulatory kinetics as well as some approximate bounds on what we may realistically expect from simple *in vivo* perturbation studies. Our results and those of others suggest that even in the favorable case of more densely connected sub-networks such as those surrounding transcription factors, the reverse engineering algorithms and the current generation of confirmatory assays may have reached an upper bound in terms of their ability to recover the underlying regulatory network from experimental time course data. This points to the larger issue of information content in the data collected, which is limited by the breadth of experimental conditions that can be safely deployed in human subjects. Despite advances in the reverse engineering algorithms, more informative data sets will be required if we are to realize the potential of personalized network medicine. Algorithms continue to be developed that design new incremental sets of experiments in order to iteratively refine the recovery of the network model [90]. However the data requirements and the extent of the perturbations involved make these more suitable to *in vitro* studies for the moment. The translation of such methods to human studies will rely on the development of less invasive sampling techniques as well as the development of perturbation techniques that interrogate the physiological system at amplitudes comparable to that of background noise i.e., at scales that are biochemically relevant but not physiologically disruptive [91, 92]. These are typically based on methods adapted from the basic control theory of closed loop identification and are still in their infancy in

biology and medicine. In the end, the ultimate bottleneck at the present time may well be our limited ability to generate informative data rather than the design of any particular reverse engineering algorithm.

2.5 References

1. Barabasi, A.-L. & Oltvai, Z. N. (2004) Network Biology: Understanding the cell's functional organization, *Nat Rev Genet.* **5**, 101-113.

2. Barabasi, A.-L., Gulbahce, N. & Loscalzo, J. (2011) Network medicine: a network-based approach to human disease, *Nat Rev Genet.* **12**, 56-68.

3. Sauer, U., Heinemann, M. & Zamboni, N. (2007) Getting Closer to the Whole Picture, *Science.* **316**, 550-551.

4. Akutsu, T., Miyano, S. & Kuhara, S. (1999) Identification of genetic networks from a small number of gene expression patterns under the Boolean network model, *Pac Symp Biocomput*, 17-28.

5. Akutsu, T., Miyano, S. & Kuhara, S. (2000) Inferring qualitative relations in genetic networks and metabolic pathways, *Bioinformatics.* **16**, 727-734.

6. Liang, S., Fuhrman, S. & Somogyi, R. (1998) Reveal, a general reverse engineering algorithm for inference of genetic network architectures. in *Pac Symp Biocomput* pp. 18-29

7. Shmulevich, I., Dougherty, E. R., Kim, S. & Zhang, W. (2002) Probabilistic Boolean networks: a rule-based uncertainty model for gene regulatory networks, *Bioinformatics.* **18**, 261-274.

8. Martin, S., Zhang, Z., Martino, A. & Faulon, J.-L. (2007) Boolean dynamics of genetic regulatory networks inferred from microarray time series data, *Bioinformatics.* **23**, 866-874.

9. Kim, H., Lee, J. & Park, T. (2007) Boolean networks using the chi-square test for inferring large-scale gene regulatory networks, *BMC Bioinformatics.* **8**, 37.

10. Yu, J., Smith, V. A., Wang, P. P., Hartemink, A. J. & Jarvis, E. D. (2004) Advances to Bayesian network inference for generating causal networks from observational biological data, *Bioinformatics.* **20**, 3594-3603.

11. Zou, M. & Conzen, S. D. (2005) A new dynamic Bayesian network (DBN) approach for identifying gene regulatory networks from time course microarray data, *Bioinformatics.* **21**, 71-79.

12. Kim, S. Y., Imoto, S. & Miyano, S. (2003) Inferring gene networks from time series microarray data using dynamic Bayesian networks, *Brief Bioinform.* **4**, 228-235.

13. Vinh, N. X., Chetty, M., Coppel, R. & Wangikar, P. P. (2011) GlobalMIT: learning globally optimal dynamic bayesian network with the mutual information test criterion, *Bioinformatics.* **27**, 2765-2766.

14. Wilczyński, B. & Dojer, N. (2009) BNFinder: exact and efficient method for learning Bayesian networks, *Bioinformatics.* **25**, 286-287.

15. Dojer, N., Bednarz, P., Podsiadło, A. & Wilczyński, B. (2013) BNFinder2: Faster Bayesian network learning and Bayesian classification, *Bioinformatics.* **29**, 2068-2070.

16. Ernst, J., Vainas, O., Harbison, C. T., Simon, I. & Bar-Joseph, Z. (2007) Reconstructing dynamic regulatory maps, *Mol Syst Biol.* **3**, 74-74.

17. Schulz, M., Devanny, W., Gitter, A., Zhong, S., Ernst, J. & Bar-Joseph, Z. (2012) DREM 2.0: Improved reconstruction of dynamic regulatory networks from time-series expression data, *BMC Syst Biol.* **6**, 104.

18. Madar, A., Greenfield, A., Vanden-Eijnden, E. & Bonneau, R. (2010) DREAM3: Network Inference Using Dynamic Context Likelihood of Relatedness and the Inferelator, *PLoS ONE.* **5**, e9803.

19. Zoppoli, P., Morganella, S. & Ceccarelli, M. (2010) TimeDelay-ARACNE: Reverse engineering of gene networks from time-course data by an information theoretic approach, *BMC Bioinform.* **11**, 154.

20. Bansal, M. & di Bernardo, D. (2007) Inference of gene networks from temporal gene expression profiles, *IET Syst Biol.* **1**, 306-312.

21. Yeung, M. K. S., Tegner, J. & Collins, J. J. (2002) Reverse engineering gene networks using singular value decomposition and robust regression, *Proc Natl Acad Sci USA.* **99**, 6163-6168.

22. Gardner, T. S., di Bernardo, D., Lorenz, D. & Collins, J. J. (2003) Inferring Genetic Networks and Identifying Compound Mode of Action via Expression Profiling, *Science.* **301**, 102-105.

23. Tegner, J., Yeung, M. K. S., Hasty, J. & Collins, J. J. (2003) Reverse engineering gene networks: Integrating genetic perturbations with dynamical modeling, *Proc Natl Acad Sci.* **100**, 5944-5949.

24. Bansal, M., Gatta, G. D. & di Bernardo, D. (2006) Inference of gene regulatory networks and compound mode of action from time course gene expression profiles, *Bioinformatics.* **22**, 815-822.

25. Bonneau, R., Reiss, D., Shannon, P., Facciotti, M., Hood, L., Baliga, N. & Thorsson, V. (2006) The Inferelator: an algorithm for learning parsimonious regulatory networks from systems-biology data sets de novo, *Genome Biology.* **7**, R36.

26. Yip, K. Y., Alexander, R. P., Yan, K.-K. & Gerstein, M. (2010) Improved Reconstruction of In Silico Gene Regulatory Networks by Integrating Knockout and Perturbation Data, *PLoS ONE.* **5**, e8121.

27. Chowdhury, A., Chetty, M. & Vinh, N. (2013) Incorporating time-delays in S-System model for reverse engineering genetic networks, *BMC Bioinformatics.* **14**, 196.

28. Henderson, J. & Michailidis, G. (2014) Network Reconstruction Using Nonparametric Additive ODE Models, *PLoS ONE.* **9**, e94003.

29. Li, X., Rao, S., Jiang, W., Li, C., Xiao, Y., Guo, Z., Zhang, Q., Wang, L., Du, L., Li, J., Li, L., Zhang, T. & Wang, Q. K. (2006) Discovery of time-delayed gene regulatory networks based on temporal gene expression profiling, *BMC Bioinformatics.* **7**, 26.

30. Lozano, A. C., Abe, N., Liu, Y. & Rosset, S. (2009) Grouped graphical Granger modeling for gene expression regulatory networks discovery, *Bioinformatics.* **25**, 110-118.

31. ElBakry, O., Ahmad, M. O. & Swamy, M. N. S. (2013) Inference of Gene Regulatory Networks with Variable Time Delay from Time-Series Microarray Data, *IEEE/ACM Trans Comp Biol Bioinform* **10**, 671-687.

32. Greenfield, A., Madar, A., Ostrer, H. & Bonneau, R. (2010) DREAM4: Combining Genetic and Dynamic Information to Identify Biological Networks and Dynamical Models, *PLoS ONE.* **5**, e13397.

33. Greenfield, A., Hafemeister, C. & Bonneau, R. (2013) Robust data-driven incorporation of prior knowledge into the inference of dynamic regulatory networks, *Bioinformatics.* **29**, 1060-1067.

34. Li, Z., Li, P., Krishnan, A. & Liu, J. (2011) Large-scale dynamic gene regulatory network inference combining differential equation models with local dynamic Bayesian network analysis, *Bioinformatics.* **27**, 2686-2691.

35. Huynh-Thu, V. A. & Sanguinetti, G. (2015) Combining tree-based and dynamical systems for the inference of gene regulatory networks, *Bioinformatics*. **31**, 1614-1622.

36. He, F., Balling, R. & Zeng, A.-P. (2009) Reverse engineering and verification of gene networks: Principles, assumptions, and limitations of present methods and future perspectives, *J Biotech.* **144**, 190-203.

37. Karlebach, G. & Shamir, R. (2008) Modelling and analysis of gene regulatory networks, *Nat Rev Mol Cell Biol.* **9**, 770-780.

38. Cho, K.-H., Choo, S.-M., Jung, S. H., Kim, J.-R., Choi, H.-S. & Kim, J. (2007) Reverse engineering of gene regulatory networks, *IET Syst Biol.* **1**, 149-163.

39. Markowetz, F. & Spang, R. (2007) Inferring cellular networks - a review, *BMC Bioinform.* **8**, S5.

40. Jong, H. d. (2002) Modeling and simulation of genetic regulatory systems: A literature review, *J Comp Biol.* **9**, 67-103.

41. Gardner, T. S. & Faith, J. J. (2005) Reverse-engineering transcription control networks, *Phys Life Rev.* **2**, 65-88.

42. Hecker, M., Lambeck, S., Toepfer, S., van Someren, E. & Guthke, R. (2009) Gene regulatory network inference: Data integration in dynamic models, A review, *Biosystems.* **96**, 86-103.

43. Chai, L. E., Loh, S. K., Low, S. T., Mohamad, M. S., Deris, S. & Zakaria, Z. (2014) A review on the computational approaches for gene regulatory network construction, *Comput Biol Med.* **48**, 55-65.

44. Villaverde, A. F. & Banga, J. R. (2013) Reverse engineering and identification in systems biology: strategies, perspectives and challenges, *J R Soc Interface.* **11**, 0505.

45. Kim, Y., Han, S., Choi, S. & Hwang, D. (2013) Inference of dynamic networks using time-course data, *Brief Bioinform*. **15**, 212-228.

46. Stolovitzky, G., Monroe, D. O. N. & Califano, A. (2007) Dialogue on Reverse-Engineering Assessment and Methods, *Ann N Y Acad Sci.* **1115**, 1-22.

47. Stolovitzky, G., Prill, R. J. & Califano, A. (2009) Lessons from the DREAM2 Challenges, *Ann N Y Acad Sci.* **1158**, 159-195.

48. Prill, R. J., Marbach, D., Saez-Rodriguez, J., Sorger, P. K., Alexopoulos, L. G., Xue, X., Clarke, N. D., Altan-Bonnet, G. & Stolovitzky, G. (2010) Towards a Rigorous Assessment of Systems Biology Models: The DREAM3 Challenges, *PLoS ONE.* **5**, e9202.

49. Marbach, D., Prill, R. J., Schaffter, T., Mattiussi, C., Floreano, D. & Stolovitzky, G. (2010) Revealing strengths and weaknesses of methods for gene network inference, *Proc Natl Acad Sci USA*. **107**, 6286-6291.

50. Marbach, D., Costello, J. C., Kuffner, R., Vega, N. M., Prill, R. J., Camacho, D. M., Allison, K. R., Kellis, M., Collins, J. J. & Stolovitzky, G. (2012) Wisdom of crowds for robust gene network inference, *Nat Meth.* **9**, 796-804.

51. Bansal, M., Belcastro, V., Ambesi-Impiombato, A. & di Bernardo, D. (2007) How to infer gene networks from expression profiles, *Mol Syst Biol.* **3**, 78.

52. Camacho, D., Vera Licona, P., Mendes, P. & Laubenbacher, R. (2007) Comparison of Reverse-Engineering Methods Using an in Silico Network, *Ann N Y Acad Sci.* **1115**, 73-89.

53. Penfold, C. A. & Wild, D. L. (2011) How to infer gene networks from expression profiles, revisited, *Interface Focus*.

54. Hendrickx, D. M., Hendriks, M. M. W. B., Eilers, P. H. C., Smilde, A. K. & Hoefsloot, H. C. J. (2011) Reverse engineering of metabolic networks, a critical assessment, *Mol BioSyst.* **7**, 511-520.

55. Zhu J, C. Y., Leonardson AS, Wang K, Lamb JR, Emilsson V, Schadt EE (2010) Characterizing Dynamic Changes in the Human Blood Transcriptional Network, *PLoS Comput Biol.* **6(2)**, e1000671.

56. Hickman, G. J. & Hodgman, T. C. (2009) INFERENCE OF GENE REGULATORY NETWORKS USING BOOLEAN-NETWORK INFERENCE METHODS, *J Bioinform Comput Biol.* **07**, 1013-1029.

57. Li, P., Zhang, C., Perkins, E., Gong, P. & Deng, Y. (2007) Comparison of probabilistic Boolean network and dynamic Bayesian network approaches for inferring gene regulatory networks, *BMC Bioinformatics.* **8**, S13.

58. Steuer, R., Kurths, J., Daub, C. O., Weise, J. & Selbig, J. (2002) The mutual information: Detecting and evaluating dependencies between variables, *Bioinformatics.* **18**, S231-S240.

59. Zou, C. & Feng, J. (2009) Granger causality vs. dynamic Bayesian network inference: a comparative study, *BMC Bioinformatics.* **10**, 122.

60. Shojaie, A. & Michailidis, G. (2010) Discovering graphical Granger causality using the truncating lasso penalty, *Bioinformatics.* **26**, i517-i523.

61. Di Camillo, B., Toffolo, G. & Cobelli, C. (2009) A Gene Network Simulator to Assess Reverse Engineering Algorithms, *Annals New York Acad Sci.* **1158**, 125-142.

62. Cantone, I., Marucci, L., Iorio, F., Ricci, M. A., Belcastro, V., Bansal, M., Santini, S., di Bernardo, M., di Bernardo, D. & Cosma, M. P. (2009) A Yeast Synthetic Network for *In Vivo* Assessment of Reverse-Engineering and Modeling Approaches, *Cell.* **137**, 172-181.

63. Sambo, F., camillo, B. D. & Toffolo, G. (2008) CNET: an algorithm for reverse engineering of causalgene networks in *8th Workshop on Network Tools and Applications in Biology NETTAB 2008* pp. 134-136National Research Council, Milan, Italy.

64. di Bernardo, D., Thompson, M. J., Gardner, T. S., Chobot, S. E., Eastwood, E. L., Wojtovich, A. P., Elliott, S. J., Schaus, S. E. & Collins, J. J. (2005) Chemogenomic profiling on a genome-wide scale using reverse-engineered gene networks, *Nat Biotech.* **23**, 377-383.

65. Rawlings, J. O. (1988) Collinearity Diagnostics in *Applied Regression Analysis* (Barndorff-Nielsen, O., Bickel, PJ., Cleveland, WS., Dudley, RM., ed) pp. 273-281, Pacific Grove: Wadsworth and Brooks.

66. Draper, N. & Smith, H. (1998) Stepwise Regression in *Applied Regression Analysis* pp. 307-312, Wiley-Interscience, Hoboken, NJ.

67. Jackson, J. E. (1991) Singular Value Decomposition: Multidimensional Scaling I in *A User's Guide to Principal Components* pp. 189-232, John Wiley & Sons, Inc.

68. Wold, S., Sjöström, M. & Eriksson, L. (2001) PLS-regression: a basic tool of chemometrics, *Chemom Intell Lab Syst.* **58**, 109-130.

69. Wold, S., Trygg, J., Berglund, A. & Antti, H. (2001) Some recent developments in PLS modeling, *Chemom Intell Lab Syst.* **58**, 131-149.

70. Horn, J. L. (1965) A rationale and test for the number of factors in factor analysis, *Psychometrika.* **30**, 179-185.

71. Frontier, S. (1976) Étude de la décroissance des valeurs propres dans une analyse en composantes principales: comparaison avec le modèle de bâton brisé, *J Exp Marine Biol Ecol.* **25**, 67-75.

72. Bartlett, M. S. (1950) Tests of significance in factor analysis, *Br J Psych Stat Sec.* **3**, 77-85.

73. Jackson, J. E. (1991) PCA with more than Two Variables in *A User's Guide to Principal Components* (Shewhart, W. A., Wilks, S. S., ed) pp. 26-62, Wiley-Interscience, Hoboken, NJ.

74. Peres-Neto, P. R., Jackson, D. A. & Somers, K. M. (2005) How many principal components? Stopping rules for determining the number of non-trivial axes revisited., *Comp Stat Data An.* **49**, 974-997.

75. Margolin, A., Nemenman, I., Basso, K., Wiggins, C., Stolovitzky, G., Favera, R. & Califano, A. (2006) ARACNE: An Algorithm for the Reconstruction of Gene Regulatory Networks in a Mammalian Cellular Context, *BMC Bioinform.* **7**, S7.

76. Cover, T. M. & Thomas, J. A. (2006) *Elements of Information Theory*, John Wiley & Sons, New York.

77. Kaiser, M. (2011) A tutorial in connectome analysis: Topological and spatial features of brain networks, *NeuroImage.* **57**, 892-907.

78. Vinh, N. X., Chetty, M., Coppel, R. & Wangikar, P. P. (2012) Issues impacting genetic network reverse engineering algorithm validation using small networks, *Biochim Biophys Acta.* **1824**, 1434-1441.

79. Schaffter, T., Marbach, D. & Floreano, D. (2011) GeneNetWeaver: in silico benchmark generation and performance profiling of network inference methods, *Bioinformatics.* **27**, 2263-2270.

80. Gama-Castro, S., Salgado, H., Peralta-Gil, M., Santos-Zavaleta, A., Muñiz-Rascado, L., Solano-Lira, H., Jimenez-Jacinto, V., Weiss, V., García-Sotelo, J. S., López-Fuentes, A., Porrón-Sotelo, L., Alquicira-Hernández, S., Medina-Rivera, A., Martínez-Flores, I., Alquicira-Hernández, K., Martínez-Adame, R., Bonavides-Martínez, C., Miranda-Ríos, J., Huerta, A. M., Mendoza-Vargas, A., Collado-Torres, L., Taboada, B., Vega-Alvarado, L., Olvera, M., Olvera, L., Grande, R., Morett, E. & Collado-Vides, J. (2011) RegulonDB version 7.0: transcriptional regulation of Escherichia coli K-12 integrated within genetic sensory response units (Gensor Units), *Nucleic Acids Research.* **39**, D98-D105.

81. Ackers, G. K., Johnson, A. D. & Shea, M. A. (1982) Quantitative model for gene regulation by lambda phage repressor, *Proc Natl Acad Sci USA.* **79**, 1129-1133.

82. Whitfield, M. L., Sherlock, G., Saldanha, A. J., Murray, J. I., Ball, C. A., Alexander, K. E., Matese, J. C., Perou, C. M., Hurt, M. M., Brown, P. O. & Botstein, D. (2002) Identification of Genes Periodically Expressed in the Human Cell Cycle and Their Expression in Tumors, *Mol Biol Cell.* **13**, 1977-2000.

83. Wang, K., Saito, M., Bisikirska, B. C., Alvarez, M. J., Lim, W. K., Rajbhandari, P., Shen, Q., Nemenman, I., Basso, K., Margolin, A. A., Klein, U., Dalla-Favera, R. & Califano, A. (2009) Genome-wide identification of post-translational modulators of transcription factor activity in human B cells, *Nat Biotechnol.* **27**, 829-839.

84. Frankenstein, Z., Alon, U. & Cohen, I. (2006) The immune-body cytokine network defines a social architecture of cell interactions, *Biol Dir.* **1**, 32.

85. Margolin, A. A. & Califano, A. (2007) Theory and Limitations of Genetic Network Inference from Microarray Data, *Ann N Y Acad Sci.* **1115**, 51-72.

86. Margolin, A. A., Wang, K., Califano, A. & Nemenman, I. (2010) Multivariate dependence and genetic networks inference, *IET Syst Biol.* **4**, 428-440.

87. Guan, C., Ye, C., Yang, X. & Gao, J. (2010) A review of current large-scale mouse knockout efforts, *genesis.* **48**, 73-85.

88. Gollee, H., Mamma, A., Loram, I. & Gawthrop, P. (2012) Frequency-domain identification of the human controller, *Biol Cybern.* **106**, 359-372.

89. Kawada, T., Sato, T., Inagaki, M., Shishido, T., Tatewaki, T., Yanagiya, Y., Zheng, C., Sugimachi, M. & Sunagawa, K. (2000) Closed-Loop Identification of Carotid Sinus Baroreflex Transfer Characteristics Using Electrical Stimulation, *Jpn J Physiol.* **50**, 371-380.

90. Schmidt, M. D., Vallabhajosyula, R. R., Jenkins, J. W., Hood, J. E., Soni, A. S., Wikswo, J. P. & Lipson, H. (2011) Automated refinement and inference of analytical models for metabolic networks., *Phys Biol* **8**, 055011.

91. Dong, C.-Y., Yoon, T.-W., Bates, D. & Cho, K.-H. (2010) Identification of feedback loops embedded in cellular circuits by investigating non-causal impulse response components, *J Math Biol.* **60**, 285-312.

92. Dong, C.-Y., Shin, D., Joo, S., Nam, Y. & Cho, K.-H. (2012) Identification of feedback loops in neural networks based on multi-step Granger causality, *Bioinformatics.* **28**, 2146-2153.

3 Chapter 3: Leveraging Prior Knowledge to Recover Characteristic Immune Regulatory Motifs in Gulf War Illness.

3.1 Introduction

Gulf War Illness (GWI) is a complex multi-symptom illness [1] associated with deployment to the Persian Gulf between 1990-91 and presenting with symptoms that manifest across several of the body's principal regulatory systems [2-4]. Among these, our work and the work of others suggest alterations to the hypothalamic-pituitary-adrenal (HPA) response to challenge [5, 6] and that such alterations may become persistent and stable dysregulations [7]. Exercise has been used as a minimally invasive means of interrogating HPA axis response [8], one that is especially appropriate given that a chief presenting symptom of GWI is debilitating fatigue. Though data suggest that peak exercise capacity is comparable [9], these individuals report higher fatigue [10] and differ significantly from healthy control subjects in their ability to recover from these challenges. More recently in 2013, Rayhan and colleagues [11] have shown that these differences in recovery from exercise may support the identification of GWI subgroups with significant differences in autonomic response and distinct cognitive vs physical constructs of Chalder fatigue profile [12]. Exercise induced exacerbation of symptoms or post-exertional malaise (PEM) [13] has also emerged as a distinguishing feature in a sister illness myalgic encephalomyelitis/ chronic fatigue syndrome (ME/ CFS) [14] with these individuals achieving significantly lower values for oxygen consumption and workload at peak exercise and at the anaerobic threshold 24 hours after an initial maximal exercise challenge.

Our own pilot work has shown that this altered capacity for recovery from exercise also manifests as distinct trajectories in immune marker co-expression [15] and that these illness-specific alterations differ between men and women [16]. Signaling patterns that emerge in response to exercise were structurally different in GWI with the latter drawing on a larger network of alternate signaling paths in an effort to respond

adequately to challenge [17]. Moreover, these differences were linked to changes in symptom severity, extending through multiple layers of biology to altered patterns of gene expression [18] along select signaling pathways [19]. Not unexpectedly, more recent work has shown this also extends to altered cell metabolism [20], an experimental observation further validated with in silico simulations of mitochondrial function [21].

While this earlier work supported the association of symptom clusters with characteristic patterns of immune marker co-expression, it was based on samples collected prior to exercise, at peak effort and at 4 hours post-exercise. As a result, the experimental sampling frequency was insufficient to support the identification of classical rate equations models [22] that in turn might provide additional insight into the causal mechanisms driving an altered immune signaling in GWI. The objective of this work is to discover such causal mechanisms that might become characteristically activated during exercise in GWI as well as elements of immune regulation that might be conspicuously absent. Towards this we have extended sampling to include 8 blood draws collected prior to, during and up to 4 hours after peak exercise in n= 12 veterans with Gulf War Illness n=11 healthy veterans. In an effort to cast this data in the context of *a priori* knowledge, we apply as a mechanistic scaffold an extension of a literature-based model of immune signaling [23] previously reported by our group. We project individual cytokine and chemokine measurements on to functional sets used in Folcik et al. (2007; 2011) [24, 25] and apply a rate equation framework which favors the identification of directed control actions over naïve fit to data [22]. Candidate causal relationships inferred from the data are then compared to the documented signaling mechanisms in the literature-based model. Results of this analysis again suggest that immune response to exercise challenge in GWI veterans draws on a set of known immune signaling mechanisms that differ significantly from the signaling pattern expressed in healthy veterans. Of the 50 immune signaling interactions extracted from the literature, roughly half (19) were found

active in the combined exercise response data. However, only 4 signals were common to both illness and healthy groups while 7 were uniquely active in GWI and 10 uniquely active in healthy veterans. Many of these differences involved mechanisms mediating the coordinated activity of innate immune response with the Th1 and Th17 adaptive immune axes. In addition to documented signaling mechanisms several undocumented empirical interactions were identified from the data. Though many may represent false positive events, others may constitute candidates for further experimentation and analysis. Simulations where the immune sub-circuit in GWI was remodeled by abrogating the actions of MK6 (IL-6) concurrently with CK1 (principally IL-2, TNFa) or MK1A (IL-1a) predicted only partial rescue of immune response during recovery from exercise. These data-informed predictions are consistent with earlier theoretical results from our group suggesting that lasting remission in GWI may require acting on a broader physiology, namely one that includes endocrine oversight of immune function [26].

3.2 Material and Methods

3.2.1 Cohort recruitment

A subset of n=12 GWI subjects and n=12 healthy but sedentary Gulf War era veterans were recruited from a larger ongoing study at the Miami Veterans Administration Medical Center. Subjects were male and ranged in age between 40 and 60, and of comparable body mass index (BMI), ethnicity and duration of illness. Inclusion criteria was derived from Fukuda et al. (1998) [27] and consisted in identifying veterans deployed to the theater of operations between August 8, 1990 and July 31, 1991, with one or more symptoms present after 6 months from at least 2 of the following: fatigue; mood and cognitive complaints; and musculoskeletal complaints. Subjects were in good health prior to 1990, and had no current exclusionary diagnoses [28]. Medications that could have impacted immune function were excluded. Use of the Fukuda definition in GWI is

supported by Collins and coworkers in 2002 [29]. Summary results of the included subset of subject demographics and exercise performance are listed in Table 3.1. Additional details about this cohort can be found in [19].

3.2.2 Graded eXercise Test (GXT)

All subjects included in the study (HC and GWI) underwent a maximal Graded eXercise Test (GXT) to stimulate immune response. A Vmax Spectra 29c Cardiopulmonary Exercise Testing Instrument, Sensor-Medics Ergoline 800 fully automated cycle ergometer, and SensorMedics Marquette MAX 1 Sress ECG were used during the GXT. Following the McArdle protocol [30], subjects pedaled at an initial output of 60W for 2 min, followed by an increase of 30W every 2 min until the subject reached: (1) a plateau in maximal oxygen consumption (VO_2); (2) a respiratory exchange ratio >1.15; or (3) the subject stopped the test. A total of 8 blood draws were conducted on each subject. First blood draw (T_0) was conducted prior to exercise following a 30-min rest. Second and third blood draws were conducted ~3-5 min. after starting the exercise test (T_0+3) and upon reaching peak effort (VO2 max) (T_1) respectively, followed by blood draws at 10, 20, 30, 60 min., and 4 hours after VO2 max (T_1+10, T_1+20, T_1+30, T_1+60, and T_2). All control subjects were screened as sedentary upon recruitment on the basis of their response to a questionnaire [31]. Analysis in this same cohort [16] of the weight-adjusted maximum VO2 measured in L/min/kg indicated a decline in the average maximum VO_2 achievable with healthy controls performing best ($p=0.04$). In light of this finding we suggest that results presented here be interpreted as immune response at maximum perceived exertion but not necessarily at equivalent exercise intensity. We consider reduced exercise capacity to be another symptom of GWI. The characteristic immune response patterns measured at maximum perceived exertion capture this implicitly.

Table 3.1 Summary of demographic variables and exercise performance for Healthy control and GWI subjects.

Demographic Variable		HC	GWI
Subjects		12	12
Race			
	0	4	2
	1	6	4
	2	2	6
Age (years)		47.08(1.31)	45(1.16)
Body mass Index (BMI)		30.14(1.45)	33.38(1.59)
Time to VO_2 max		17(1.8)	14(1.01)

Ethics statement. All subjects signed an informed consent approved by the Institutional Review Board of the University of Miami and the Miami Veterans Affairs Medical Center. Ethics review and approval for data analysis was also obtained by the IRB of the University of Alberta.

3.2.3 Cytokine profiling

Plasma was separated from each sample within 2 h of collection and stored at -80° C until assayed. Concentration levels of 16 cytokines were measured in plasma using Quansys reagents and 96 well plates based chemiluminescent imaging instrument (Quansys Biosciences, Logan, Utah). The Q-Plex™ Human Cytokine- Screen (16-plex) is a quantitative enzyme-linked immunoabsorbent assay (ELISA), where 16 distinct capture antibodies have been absorbed to each well of a 96-well plate in a defined array. The range of the standard curves and exposure time were adjusted previously to provide reliable comparisons between subject groups in this illness population at both low and high cytokine concentrations in plasma. Quadruplicate determinations were made, i.e., each sample was run in duplicate in two separate assays. The standard sample concentrations used to establish second order polynomial calibration curves for each cytokine as well as the detection limits for this assay have been described in detail in

previous work by our group [32]. In brief, these support an average coefficient of variability (CV) of 0.20 for inter-assay comparisons and a value of 0.09 for intra-assay repeatability.

3.2.4 Quantitative analysis

3.2.4.1 Statistical evaluation of cytokine data

Prior to analysis, the raw cytokine concentration data was filtered and normalized. All the cytokine levels that were undetectable (zeros) were replaced by the minimum concentration level of that particular cytokine observed across all the subjects (HC and GWI). The raw cytokine data was linearly interpolated across the entire time course using the minimum time interval (i.e. ~3 min) to provide equally spaced sample estimates. Further, interpolated data was log2 transformed and normalized for every cytokine across both groups by subtracting the average log2 transformed cytokine levels at rest (T0) in the HC group for each cytokine. This normalized log2 transformed data is finally converted to fold change by calculating the log2 normalized cytokine concentration exponent of 2. Summary statistics of the filtered and normalized cytokine concentration levels (pg/ml) are reported in Appendix 3.1 and presented graphically in Appendix 3.2. We identified an outlier in the healthy control subjects with out-of-range expression levels in several cytokines, namely IL-2, IL-6 and IL-13. This subject was removed from further study leaving n=11 healthy control subjects.

Differences in the time course trajectory of individual cytokines from one subject to the next were characterized using the SMETS (Semi Metric Ensemble Time Series) measure developed for the comparison of multiple time series of arbitrary length [33]. In order to generate distribution statistics for this measure of divergence in trajectory we combined a leave-one-out cross-validation strategy with standard bootstrapping. More precisely, a group of n=10 of 11 (HC) time series randomly sub-sampled without

replacement were compared with another group of n=10 of 12 (GWI) time series also randomly sub-sampled without replacement. This was done repeatedly (100 times) for each of the 16 cytokines. Intra-group and inter-group SMETS values were calculated by comparing each of the 10 subsampled time series from one group with each other as well as with each of the 10 subsampled time series from the opposing group. Differences in the resulting distributions of intra and inter-group SMETS values were tested for significance using the t test and the Wilcoxon ranksum test. The SMETS algorithm and sub-sampling technique are described further in Appendix 3.3.

3.2.4.2 Aggregating cytokines into functional sets

In previous work, our group updated and further developed the network of documented immune signaling interactions used by the agent-based Basic Immune Simulator [24] to create an augmented model of innate and adaptive immune cell signaling [23]. In this model, aggregated functional groups were used to represent various adaptive immune cell subsets (namely, Th1, Th2, Th17 for T helper cell populations and cytotoxic T lymphocytes as CTL), as were sub-populations of innate immune cells (natural killer cells or NK and dendritic cells or DC). In much the same way individual cytokines were grouped based on the predominant cell population of origin and mode of action. For example, cytokines released primarily by monocytes (DCs) were grouped into a monokine (MK) group whereas cytokines released by lymphocytes such as NKs, Th1, Th2, and CTLs are grouped into a lymphokine group (CK). These groups were further subdivided into monokine MK1 and cytokine CK1 forming the pro-inflammatory cytokine functional sub-groups, with MK2 and CK2 comprising the corresponding anti-inflammatory sets. The remaining cytokine groups were composed of individual cytokines (e.g., MK15 contains only IL-15) (Table 3.2).

Table 3.2: Aggregated Cytokine groupings. Resulting aggregated variables used in the extracted cytokine network from the immune signaling model reported in Fritsch et al. (2013) [23]. MK1A and MK1B represent the first and second principal components respectively obtained from individual cytokines.

Node ID	Group	Cytokines
1.	MK1A	IL-1α, IL-1β, IL-8 and IL-12
2.	MK1B	IL-1α, IL-1β, IL-8 and IL-12
3.	MK2	IL-10
4.	MK6	IL-6
5.	MK15	IL-15
6.	MK23	IL-23
7.	CK1	IL-2, IFNγ, TNFα and TNFβ
8.	CK2	IL-4, IL-5 and IL-13
9.	CK17	IL-17

In order to take advantage of this documented signaling network it was necessary to aggregate the individual cytokines measured experimentally in this work into their corresponding functional sets as defined in [23]. In cases where the functional sets contained multiple cytokines, such as MK1, CK1 and CK2, the activation level for the aggregate set was estimated by applying principal component analysis (PCA) to the concentration levels of the constituent cytokines and using the first component score as a joint measure of expression. As a general rule, a second additional principal component was used only if the first component captured less than 80% of the variability in the aggregate set. This was the case for MK1 that was scored as two separate co-expression patterns MK1A and MK1B (Table 3.2, 3.3). As shown in Table 3.3, cytokine co-expression patterns were relatively consistent across subject groups for sets MK1A and B, with over 75% and 10% of the overall variability captured by the first and second latent vectors respectively. This was not the case for CK1 and CK2 where the shared variability captured by PC1 was visibly - lower in GWI (0.41 and 0.68 respectively) suggesting that cytokines aggregated under CK1 and CK2 behaved less cohesively in the illness group. With the exception of set CK2, the loading coefficients for PC1 were

consistent in sign (positive or negative) across both subject groups. Accordingly, in order to create a common coordinate system and facilitate the comparison of network structures across groups, aggregate expression for these sets was estimated using a PCA model based on profiles from all subjects thereby capturing co-expression patterns shared by both groups (HC and GWI).

Table 3.3: Variance captured by the first principal component (PC1) for aggregated cytokine variables and their respective loadings. In healthy and GWI models data from respective individual groups was used for PCA whereas all the data was combined in HC+GWI model for PCA. Variance for MK1b represents the fractional variance covered by second principal component (PC2). Data was normalized, interpolated and converted to fold change before the PCA calculations.

Variable	Aggregated cytokines	Healthy	GWI	Healthy+GWI
MK1a	**Tot Variance** (PC1)	**0.7568**	**0.8292**	**0.7873**
	IL-1a	0.9877	0.9974	0.9931
	IL-1b	-0.0594	-0.0447	-0.0536
	IL-8	-0.1386	-0.0502	-0.0968
	IL-12	-0.0424	-0.0267	-0.0378
MK1b	**Fract. Tot Variance** (PC2)	**0.1321**	**0.1075**	**0.121**
	IL-1a	0.1437	0.0513	0.0984
	IL-1b	0.2803	0.3054	0.2972
	IL-8	0.9413	0.9039	0.9267
	IL-12	-0.1218	-0.2950	-0.2078
CK1	**Tot Variance** (PC1)	**0.9234**	**0.4105**	**0.8874**
	IL-2	0.9917	0.5938	0.9913
	IFN-y	-0.0245	-0.2533	-0.0269
	TNF-a	0.0031	0.7621	0.0149
	TNF-b	0.1261	0.0492	0.1278
CK2	**Tot Variance** (PC1)	**0.9811**	**0.6788**	**0.9613**
	IL-4	0.0963	0.9225	0.0921
	IL-5	0.7585	-0.0470	0.7568
	IL-13	0.6445	-0.3832	0.6471

3.2.4.3 Creation of literature-based reference networks

Building on our earlier literature-based model describing cytokine-cell immune signaling [23], we removed immune cell nodes lying between any two cytokines to create an abstracted graph of cytokine-cytokine interaction. Only edges connecting first (cytokine-cytokine) and second neighbour cytokines (cytokine-cell-cytokine) were included in the final network. In the latter case, the aggregate mode of action linking cytokines was determined by multiplying the sign of the intervening edges. For example, in Fritsch et al. (2013) [23] the MK2 cytokine set inhibits the dendritic cell set (DC1) which typically promotes the secretion of MK15. In the abstraction presented here this translates into a direct inhibition of MK15 by MK2. In addition, as MK1 was divided into two subsets, note that all outgoing and incoming edges for MK1 were directly propagated to MK1A and MK1B nodes.

To further consolidate this network, we also extracted interactions linking the 16 cytokines measured in our experiments using the "Search Tool for the Retrieval of Interacting Genes" (STRING) database [34]. Interactions in the STRING database are included and scored on the basis of several supporting sources such as co-occurrence in manually curated literature and co-expression in available experimental databases to name a few. Every interaction in the STRING database was assigned a confidence score with direction and type of regulation predicted for most edges (except direct physical binding) based on natural language processing (NLP) [34]. It is important to note that these scores do not indicate the strength or the specificity of the interaction. Instead, they are indicators of confidence, i.e. how likely STRING judges an interaction to be true, given the available evidence. All scores rank from 0 to 1, with 1 being the highest possible confidence. A score of 0.5 would indicate that roughly every second interaction might be erroneous (i.e., a false positive). Scores are assigned to individual evidences and a combined score is computed using the weightage of every score. It is

important to note that all the interactions retained in the extracted cytokine network had a confidence score of ≥0.80 with respect to their predicted direction based on human studies. Source and target cytokine nodes associated with each edge along with supporting evidence and confidence scores are summarized in Appendix 3.4. We then translated this basic cytokine-cytokine network into one linking the 9 cytokine sets described in [23]. Since MK1A, MK1B, CK1 and CK2 individually represent several cytokines in one aggregated variable multiple edges among constituent cytokines within or between aggregate sets were also rationalized using the union of all incoming and outgoing edges for that cytokine sub-network. This yielded an abstracted network with 38 edges linking 9 aggregate sets from an initial directed network of 47 edges linking 16 individual cytokines extracted from STRING database. As might be expected these two reference networks overlapped substantially with 30 interactions sharing source, target and direction across both networks. Building on this consensus and including interactions unique to each, we created a single unified reference network with 50 directed edges linking 9-aggregate cytokine nodes (Appendix 3.5).

3.2.4.4 Inferring directed cytokine networks from data

An ordinary differential equation (ODE) based model was used to infer directed interactions among the grouped cytokine variables. These models have been widely used for the inference of regulatory networks. In this model, we use a simple linear rate equation to describe the rate of change of concentration of every aggregated cytokine variable as described in Equation 1:

$$\frac{\partial x_i}{\partial t} = a_{i,1}x_1 + a_{i,2}x_2 + \cdots + a_{i,n}x_n \qquad (3.1),$$

where $a_{i,j}$ describes the influence of node *j* on the rate of change of expression of node *i*. A positive value of $a_{i,j}$ represents activation of node *i* by node *j*, negative value

represents inhibition and zero value represents no interaction between node *j* and *i* . Eq. 1 can also be rewritten in the matrix form (Eq.2).

$$\dot{X}(t) = A \cdot X(t) \quad (3.2),$$

where *X* is an n x 1 vector and A is an *n x n* matrix containing the weight of all the edges of the network.

Consistent with our recent work [22], we used an extension of standard PCA called partial least squares (PLS) regression [35, 36] for the estimation of latent vectors. Furthermore, we used the broken-stick technique, a variant of the Horn's technique (Horn, 1965 [37]) to select appropriate number of latent vectors to be retained for identification of unknown parameter set A in Eq 2. Note that this method was chosen over Bartlett's method (Bartlett, 1950 [38]), which is more permissive and therefore more prone to false positives in the inference of interactions [22, 39]. Parameters of the broken stick method were tuned to provide the maximum F score values for the inference of the combined literature-based reference network described in the previous section (Appendix 3.5). A global optimization method, constrained simulated annealing, was used to balance computational cost and thoroughness.

All algorithms were encoded in MatLab using the functions available in the Statistics, Machine learning and Global Optimization toolboxes (The MathWorks, Inc., Natick, MA). For more details about parameter tuning we refer the reader to [22].

3.2.4.5 Network analysis

3.2.4.5.1 Graph edit distance (GED)

Weighted Graph edit distances (GED) (Bunke, 2000 [40]) were calculated to quantify the topological differences among the networks of same group (intra GEDs) as well as between networks of two groups (inter GEDs). A weighted Graph Edit Distance (GED)

corresponds to the “cost” associated with the edit operations to transform a graph into the other [41, 42]. Here, we make the cost of these edit operations proportional to the differences in the edge weights. The weighted GED between two networks of order N with adjacency matrices A and B is:

$$GED = \sum_{i=1}^{N} \sum_{j \geq i}^{N} \left| a_{ij} - b_{ij} \right| \quad (3.3),$$

where, a_{ij} and b_{ij} are the weights for an element in adjacency matrix A and B respectively. Statistical significance of the edit costs separating networks across illness groups compared to networks within groups was based on repeated random sub-sampling of subjects. Local restructuring of the networks that drive these global topological differences was described in terms of node centrality measures such as betweenness centrality, degree centrality and closeness centrality. Furthermore, ‘hubs’ and ‘authority’ centrality scores were used to further differentiate the local topological features of healthy networks from GWI networks. Details of these metrics are described in Appendix 3.6. A general review of basic metrics used to describe global and local network structure and their applications in biology may also be found in [43] and [44].

All calculations related to network identification and rationalization as well as the analysis of network attributes were conducted with the MATLAB software environment (The MathWorks Inc., Natick, MA). Note that, MatLab 2016a was used for node centrality measures calculations. The graphical rendering of directed networks was performed using ‘Orthogonal’ layout of yEd graph editor program (yWorks Gmbh, Germany).

3.2.4.5.2 Simulation engine

The dynamic behaviour supported by the directed cytokine networks identified in this work was explored by using the discrete state simulation engine NetSim [45] where the target transition state for any given cytokine node at time t+1 is determined by resolving the fuzzy logic statement describing the regulation of that node. A sigmoidal activation

function is then used by NetSim to modulate the incremental transition from the node's current state in the direction of its target state. This incremental change in state is weighted by a time constant capturing both synthesis and degradation dynamics. In all simulations the parameters describing node dynamics were sampled from Gaussian distributions with mean and standard deviation as recommended by the authors. As recovery dynamics are of specific interest here, the initial states for each simulation were set to values measured at peak exercise effort.

3.3 Results

Although the exercise capacity of GWI veterans approaches that of healthy controls in terms of % peak effort and the time required to reach maximal VO2, they differ significantly in their ability to recover from this challenge. This impaired recovery presents as an exacerbation of GWI symptoms and has been documented in several studies as post-exertional malaise [10, 46]. Therefore, we have focused in this work on isolating and comparing the networked response of the immune system in GWI subjects to that of HC subjects in the recovery phase. Specifically, we consider the 4-hour time period starting at the VO2 max time point and described by 6 out of the 8 time points measured.

3.3.1 Divergence in exercise response of individual cytokines

The distribution of SMETS values describing the separation of time course response in the recovery phase for each individual cytokine both within and between subject groups was calculated using a leave-one-out repeated sub-sampling scheme. The mean values and standard error for intra-group, pooled intra-group (HC+GWI) and inter-group SMETS divergence values are reported in Appendix 3.7A. The corresponding SMETS median values and the median absolute deviation from the median (MADM) are reported in

Appendix 3.7B. Results show that individual cytokine response trajectories differed significantly between subject groups for most cytokines surveyed based on a Wilcoxon ranksum and Students's t tests (Appendix 3.7C). The between group SMETS divergence values were significantly greater than within group values among healthy control subjects, GWI subjects or both groups pooled. The only exceptions were IL-1α, IL-23, TNF-α and TNF-β that did not differ significantly between groups when compared to the distribution of SMETS values separating subjects within the healthy control group. Among the cytokines that differed significantly in trajectory between groups, average (or median) SMETS values in IL-2, 13 and 17 separating GWI from HC subjects were at least 1.5 times the corresponding SMETS values separating subjects within the same group. It should be noted that in general, cytokine dynamics were more diverse in HC subjects, with higher mean intra-group SMETS values in 11 of 16 cytokines. Only in the case of IL-5, 10, 17, 23 and TNF-β were these within group differences statistically significant.

3.3.2 Remodeling of cytokine networks inferred from experimental data

In order to align the empirical analysis with the data mined mechanistic model we first projected the cytokine profiles measured at the 6 recovery phase time points into the space defined by the aggregate sets described in Table 3.2 and 3.3, then captured the dynamic trajectories of these sets by fitting the parameters of a first order linear ODE (Eq.1). This was performed for each individual subject in each group yielding subject-specific directed immune response networks. To emphasize network features characteristic of each illness group a combination of leave-one-out and bootstrapping is applied as described in the Methods section. We re-sampled 100 random subsets of 10 subjects without replacement from 11 in HC and 12 subjects in the GWI group respectively. Individual cytokine networks were inferred for every subject of each subset.

Within each subsample a consensus network was identified by majority rule whereby only edges shared by at least 6 out of the 10 networks were retained. These 100 consensus networks identified for each illness group were used to support comparative statistics directed at establishing the significance of network remodeling in GWI. Comparing these empirical networks in terms of graph edit distance (GED) we found significant remodeling of the topology across groups compared to the pooled within group variability (HC and GWI) (p_{inter}<<<0.01) (Figure 3.1).

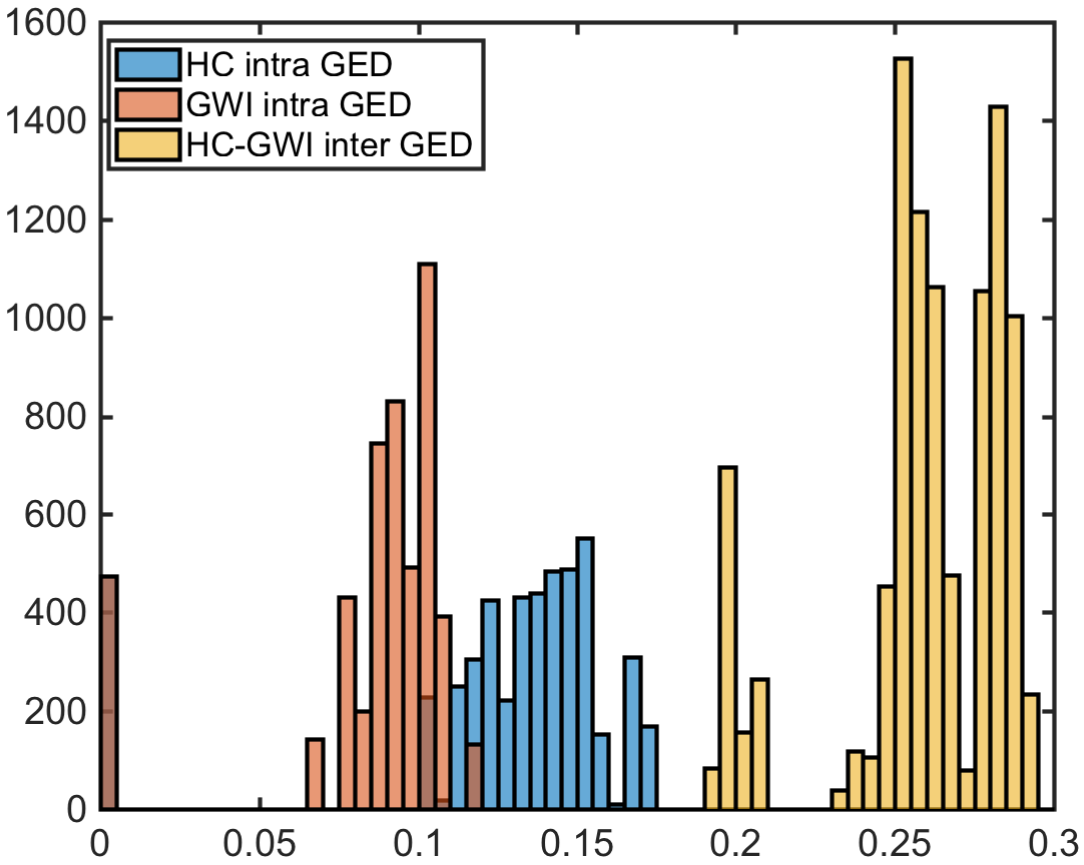

Figure 3.1: Significantly altered immune circuitry. Graph edit distance (GED) distributions comparison between HC (blue) and GWI (orange) intra GEDs and inter group GEDs (yellow).

Moreover, within group GED was significantly higher in HC compared to GWI (p_{intra}<<<0.01) indicating that consensus networks were more topologically diverse in this group. To assess the nature of this remodeling we quantified the role of each cytokine in the signaling network in terms of centrality measures such as node degree, betweenness centrality and closeness centrality. In addition, hub and authority scores were also calculated to further highlight dominant contributors to the topology (Table 3.4; Appendix 3.8; Appendix 3.9 A-D). These measures point to a major reshuffling of roles for each cytokine in the GWI consensus networks. The differences between weighted median betweenness centrality scores were significant for all cytokine functional sets except MK1B ($p<0.05$) (Appendix 3.9A). In general, weighted median betweenness centrality scores were higher in HC consensus networks (Appendix 3.8) with MK6 (0.25),

Table 3.4: Summary of changes in cytokine node centrality. Increase or decrease in fold change for individual node centrality measures (GWI/HC) highlighting $p < 0.05$ and FC<0.5 (red star) and FC > 2 (green star). Results show significant change in the roles of a broad majority of aggregate cytokine sets used in the immune signaling model of Fritsch et al. (2013) [23], including MK2, 6 and 15, key components of the GWI regulatory motif. Recall MK1A and B represent the first and second principal components respectively derived from the co-expression patterns of IL-1α, IL-1β, IL-8 and IL-12.

Node names	Weight. betw cent	Weight. Inclose ness	Weight. Outclose ness	Weight. Indeg	Weight. Outdeg	Weight. Hub ranks	Weight. Auth. ranks
MK1A	1.6	1.97	1.05	1.67	1.5	4.75*	0.86
MK1B		1.98	1.45	2	1.25	2.72*	0.72
MK2	2.25*	1.56	2.25*	0.83	3.00*	3.76*	0.84
MK6	0.14*	1.78	0.95	2.33*	1	1.25	2.38*
MK15	0.17*	1.18	1.57	1.33	1	0.49*	1.98
MK23	0.57	1.09	1.91	0.9	1	0.40*	1.21
CK1	**	2.96*	1.5	1.5	1.5	2.22*	0.22*
CK2	0.20*	1.1	1.57		1	0.56	5.23*
CK17	**	1.18	1.63	0.33	1.33	1.43	0.41*

MK15 (0.21) and CK2 (0.18) nodes being most influential and differing significantly from corresponding values in GWI ($p<0.01$) (Appendix 3.8; Appendix 3.9A). Conversely in GWI, MK1B (0.20), MK2 (0.16) and MK1A (0.14) nodes had the highest median betweeness centrality values but these differed from HC only in the case of MK2 ($p<0.01$). In keeping with a less centralized topology in GWI, node accessibility from other nodes (Incloseness centrality) and access to other nodes (Outcloseness centrality) was generally higher in GWI consensus networks ($p<0.05$) (Appendix 3.8; Appendix 3.9B). For example, MK23 (3.74), CK2 (2.75) and MK2 (2.57) were the most accessible nodes (weighted incloseness centralities) to the other nodes of immune network in HC. These nodes were replaced in terms of accessibility by MK1B (4.38), CK1 (4.35) and MK1A (4.24) in GWI. Conversely, MK6 (2.96), MK1B (2.67) and MK15 (2.61) have the three highest median weighted outcloseness or access to the network in HC whereas MK2 (4.25), MK15 (4.11) and MK23 (3.94) nodes have best access in GWI consensus networks. Not surprisingly these differences are in close alignment with median indegree and outdegree values, which were also generally higher in GWI consensus networks (Appendix 3.9C). With the exception of CK2, all nodes differed significantly in indegree and outdegree between HC and GWI with MK6 undergoing the biggest shift in indegree and MK2 the largest in outdegree centrality.

Hub and authority metrics offer a summary measure of these changes in incoming and outgoing connectivity at each node that also takes into consideration the impact of these changes in terms of reach across the broader network and the shifting involvement of influential nodes (Appendix 3.9D). For example, increased hub-rank for node CK1 suggest increased regulatory broadcasting in GWI despite less prompting by incoming signals or lower authority score. Similarly, nodes MK1A, MK1B and MK2 show increased regulatory broadcasting with only modest ($FC<2$) changes in authority score. Conversely MK15 and MK 23 show markedly lower levels of broadcasting to influential

nodes despite similar or higher prompting. Differences across these metrics are summarized in Table 3.4.

3.3.3 Concordance with a literature-based reference network

Based on the subsampling scheme described above, 100 subsamples were created in each of the HC and GWI clinical phenotypes. These 100 subsamples each consisted of 10 subject-specific empirical networks. When casting these against documented signalling mechanisms we found that they were sufficiently diverse in both GWI and HC to collectively canvas over 80% of the documented immune circuitry during exercise in at least half of the instances (median recall 0.82 HC, 0.84 GWI). Similarly, roughly 60% of the regulatory interactions predicted from the data were also documented in the literature in at least half of the cases (median PPV=0.61 HC, 0.60 GWI) (Appendix 3.10A). If we restrict this to only those interactions shared across subjects within each subsample the proportion of documented immune circuitry inferred as active from the data decreases comparably in both HC and GWI subject groups to just below 40% (Appendix 3.10B; median recall 0.37 HC, 0.39 GWI). Finally, by enforcing unanimity across all individual samples in all subsample sets we obtain empirical networks derived from the data in each group, which converge to a similar number of interactions (Appendix 3.10C; 19 HC, 24 GWI) supporting a connection or edge density of roughly 20-30%. In both HC and GWI groups, the proportion of documented interactions inferred as active across networks decreased almost in step as increasing levels of agreement were applied, falling from initial levels >80% to settle at somewhat similar values of 29% in HC and 22% in GWI. In contrast, while the proportion of predicted interactions validated by the literature-based model increased in the healthy control group from 61 to 74%, it decreased substantially from 60 to 46% in the GWI group with increased consensus (Appendix 3.10C; median PPV 0.74 HC, 0.46 GWI). Notwithstanding

spurious false positives expected of this limited group size, this would suggest that in GWI a higher proportion of immune signaling diverges from patterns commonly associated with healthy physiology. Focusing our analysis on only those interactions represented unanimously in the data collected in each group and documented in the literature-based model, we obtain conserved characteristic motifs for HC and GWI consisting of 14 and 11 regulatory interactions respectively (Table 3.5). Only 4 of these interactions were shared across illness groups leaving 7 documented regulatory interactions characteristically active in GWI alone. Of these 4 shared interactions, only the positive regulation of MK1A by CK2 retained the same mode of action, the remaining 3 took on opposing regulatory actions across groups suggesting involvement of unobserved intermediate regulatory elements. In addition, we notice that CK17 is uniquely targeted for active regulation by several mediators in GWI whereas it is an active regulator in the HC circuit. One such regulator of CK17 in GWI is MK23, which is also involved in a characteristic positive feedback loop with MK2 in GWI (Figure 3.2B). Positive feedback regulation is characteristic of self-sustaining cascades and the emergence of multiple stable resting states. In contrast, no positive feedback loops were identified as active during recovery from exercise in HC (Figure 3.2A). In addition to feedback regulation, feed-forward control circuits are found extensively in nature and serve very specific regulatory functions. Alon (2007) [47] defines 8 such recurring regulatory building blocks or network motifs, classifying them as coherent or incoherent controllers. The latter motif serves as a basic pulse generator and response accelerator whereas the former responds to persistent input with a 'sign-sensitive delay', i.e. delaying activation but allowing rapid deactivation.

Table 3.5: Documented immune signals represented in experimental data. Immune signaling interactions documented in the literature (Fritsch et al., (2013)) [23] and the STRING database (Szklarczyk et al. (2015)) [34] that were also represented in the experimental data collected under exercise challenge in Gulf War Illness (GWI) veterans as well as healthy control veterans (HC). Shaded source-target interactions are shared between both illness groups in direction but not necessarily mode of action. Cytokine sets appearing as unique sources or targets in each group are underlined and *italicized*.

Source	Target	Agonist (+1) / Antagonist (-1)	Active in Illness Group
CK1	MK6	-1	GWI
CK1	MK15	-1	GWI
CK2	MK1A	1	GWI
MK1A	*CK17*	-1	GWI
MK1B	CK1	1	GWI
MK1B	MK23	1	GWI
MK6	*CK17*	-1	GWI
MK15	CK1	1	GWI
MK15	MK2	1	GWI
MK23	MK1B	-1	GWI
MK23	MK2	1	GWI
CK1	MK15	1	HC
CK1	MK23	1	HC
CK2	MK1A	1	HC
CK2	MK1B	1	HC
CK17	MK6	-1	HC
MK1A	MK1B	-1	HC
MK2	CK1	-1	HC
MK2	MK2	-1	HC
MK2	MK15	-1	HC
MK6	*CK2*	1	HC
MK23	MK1B	1	HC
MK23	MK2	-1	HC
MK23	MK15	-1	HC
MK23	MK23	-1	HC

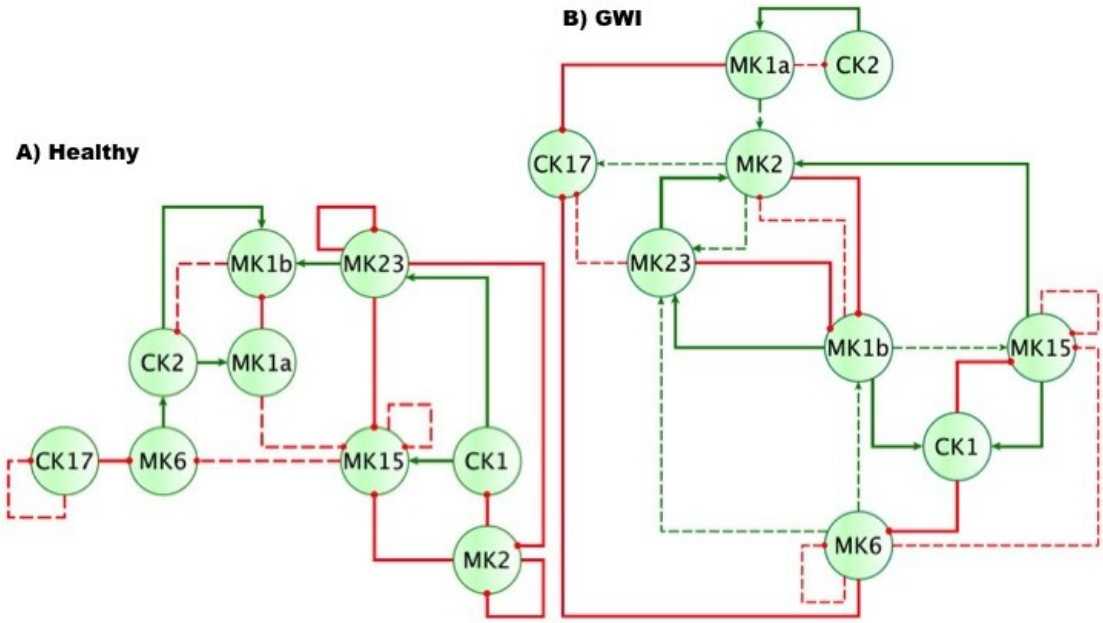

Figure 3.2: Mechanistically informed regulatory motif in A) Healthy control and B) GWI. Regulatory interactions extracted from documented prior knowledge that are uniquely represented in the experimental data in A) healthy and B) GWI during recovery from maximum exercise. Solid lines represent documented interactions and dashed lines show undocumented interactions in literature. Green arrows indicate a stimulatory action while red "T" terminators indicate suppressive actions.

Interestingly, the only coherent type 2 motif identified was characteristic of the active HC sub-circuit, suggesting increased robustness to rapid fluctuations in the delayed down-regulation of MK15 by MK2 (Figure 3.3). While incoherent type 1 FFL pulse-generating motifs were found active in both illness and healthy groups, the GWI sub-circuit presented with a unique incoherent type 1 regulation of CK17 by MK23. Incoherent feed-forward control motifs produce bimodal behaviour [48] as well as supporting a ratio-based control function e.g. fold change over background [49]. Of note, CK17 was also the object of coherent type2 control in GWI only. In both motifs we find an apparent inhibitory action of MK23 on CK17, which contradicts the well-documented positive contribution of IL-23 to the maintenance and development of Th17 cells [50]. It is important to note that the control action in question was inferred from the experimental data only and was not supported by the literature-based model.

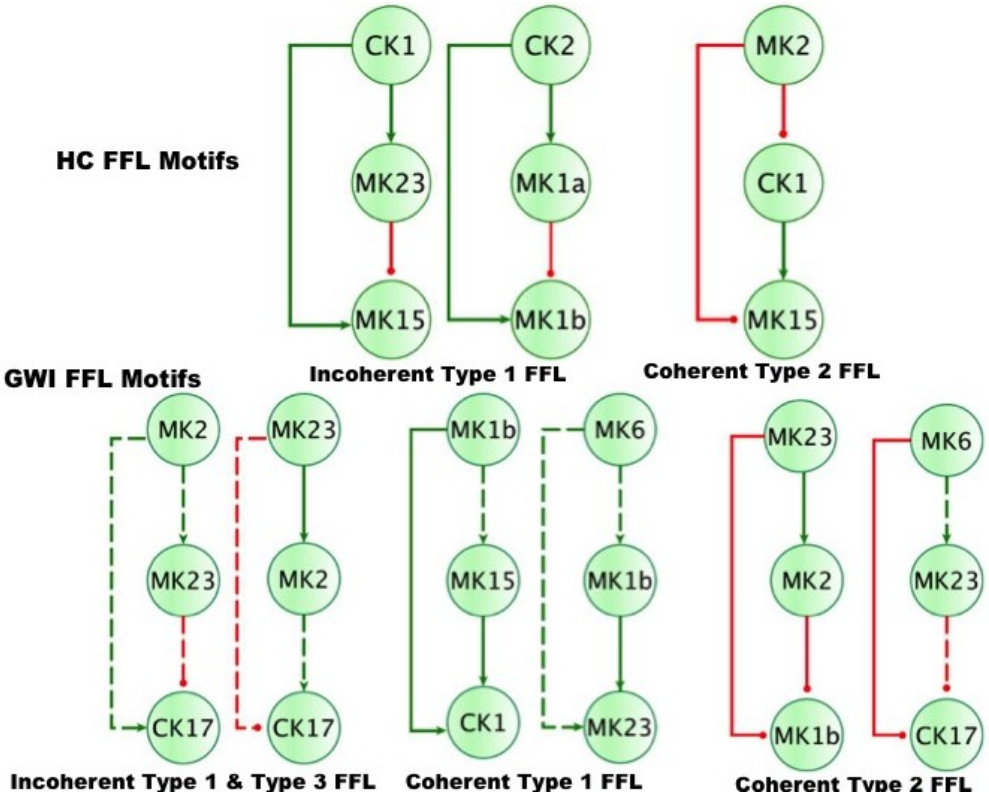

Figure 3.3: Basic regulatory control motifs in HC and GWI. Minimal regulatory component feed-forward control motifs suggested by Alon (2007) [47]; emerge as unique features in the sub-circuits for Healthy and GWI groups. Specifically, incoherent type 1 and coherent type 2 feed-forward loops (FFL) unique to HC (upper lane), indicating robustness to sudden disturbances. The GWI circuit however presents with the incoherent type 1 and 3 and coherent type 1 and type 2 FFLs.

Indeed, if we consider the documented control actions in the GWI circuit (Figure 3.2B), we find a cascade linking MK23 to CK17 through the intermediaries MK1B, CK1, and MK6 with alternating control actions such that the net effect is an indirect inhibition of CK17 (Appendix 3.11). The incoherent FFL motifs identified should therefore be considered apparent motifs that summarize the net control effects.

3.3.4 Simulated ad hoc cytokine inhibition

In the previous section we identify a characteristic control sub-circuitry active during recovery from exercise in each illness group. This active sub-circuitry consists of control

actions inferred for experimental data with some of these being further validated against a literature-informed template consisting of known documented mechanistic interactions (Figure 3.2A, B). One could now ask if there exist minor changes to this circuitry that might allow the GWI sub-circuit to perform at least partially like the healthy control sub-circuit in response to exercise. Mainstream pharmaceutical immune-therapy often involves delivering small molecules that act as immune agonists or antagonists. As the GWI circuit is de facto more abundantly connected we simulate the effects of a pharmaceutical blockade of receptors for a specific cytokine functional group by removing all outgoing edges from that network node. This was applied to all nodes in the GWI circuit individually and in pairs with the objective of minimizing the topological differences with the healthy control circuit quantified as the graph edit distance. The original GWI circuit diverges topologically from the HC circuit with a weighted graph edit distance (GED) of 0.2569 (0.0021 Std. Err). Results presented in Appendix 3.12 suggest that attenuating MK6 signaling is the single best intervention target, reducing the deviation in GWI network topology from HC to 0.2427, a small but statistically significant reduction (~5%). Similarity to the healthy control circuit architecture is further improved slightly by combining MK6 blockade with a CK1 antagonist (GED 0.2338). The effects of these changes in GWI network signaling on expected immune response behaviour were then simulated using the NetSim environment in order to provide a data agnostic perspective. Results presented in Figure 3.4 suggest that this topologically motivated approach nonetheless produced a rescue of the MK1B and CK17 response, a characteristic component in GWI. Transient restorative effects on MK2 and MK15 responses were also produced but were accompanied by a significant abrogating the otherwise normal MK6 response.

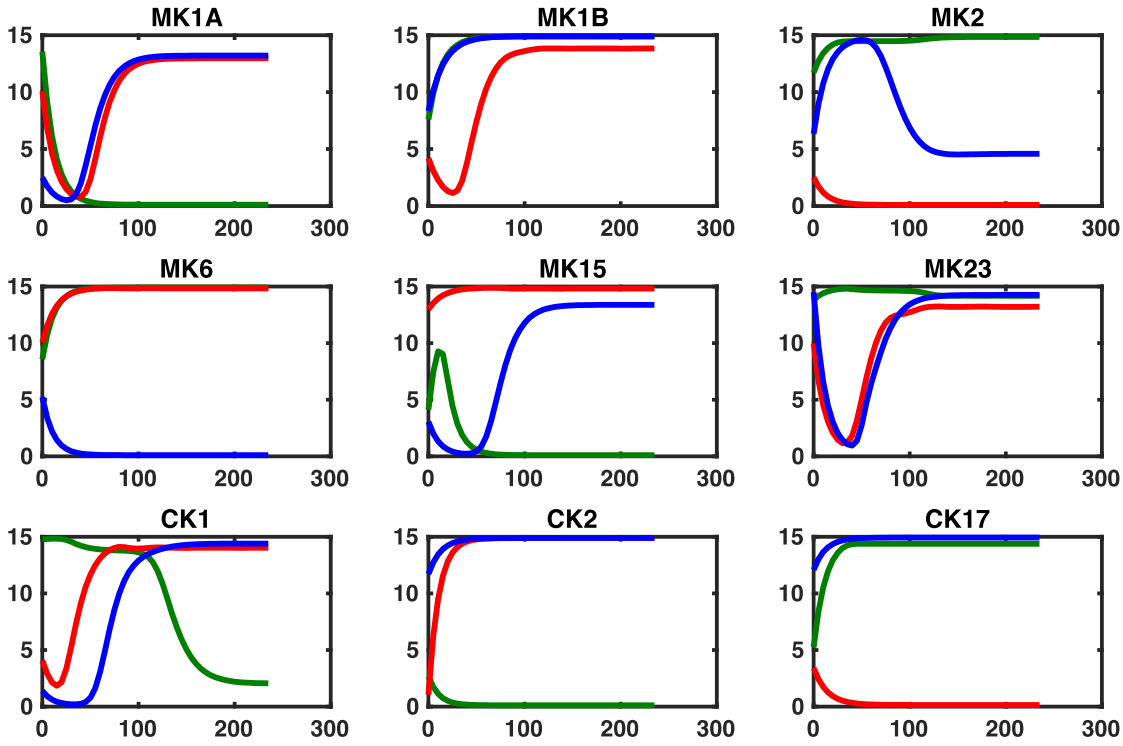

Figure 3.4: Simulating regulatory circuit response to MK6 and CK1 antagonism. Simulated response to a step perturbation applied to the characteristic circuits for GWI (GWI, red line), healthy control (HC, green line), as well as the pharmaceutically edited GWI network (Treated, blue line). Improved adherence to output from the healthy control circuit is produced for cytokine sets **CK17**and **MK1B**, with transient restorative effects on **MK2** and **MK15**. This is accompanied by significant worsening in **MK6** response.

The second leading alteration to the GWI immune circuitry consisted in a concurrent blockade of MK6 and MK23 receptor function. Response of this modified GWI immune circuit to a simulated relaxation is described in Figure 3.5. Results indicate that this strategy would improve adherence to the predicted healthy control circuit response in cytokine sets MK1A, MK1B, and CK2 without inducing significant negative effects in other cytokine responses. It is important to note that these simulations assume that with the exception of pharmaceutically targeted cytokine signals the remainder of the circuitry is still active.

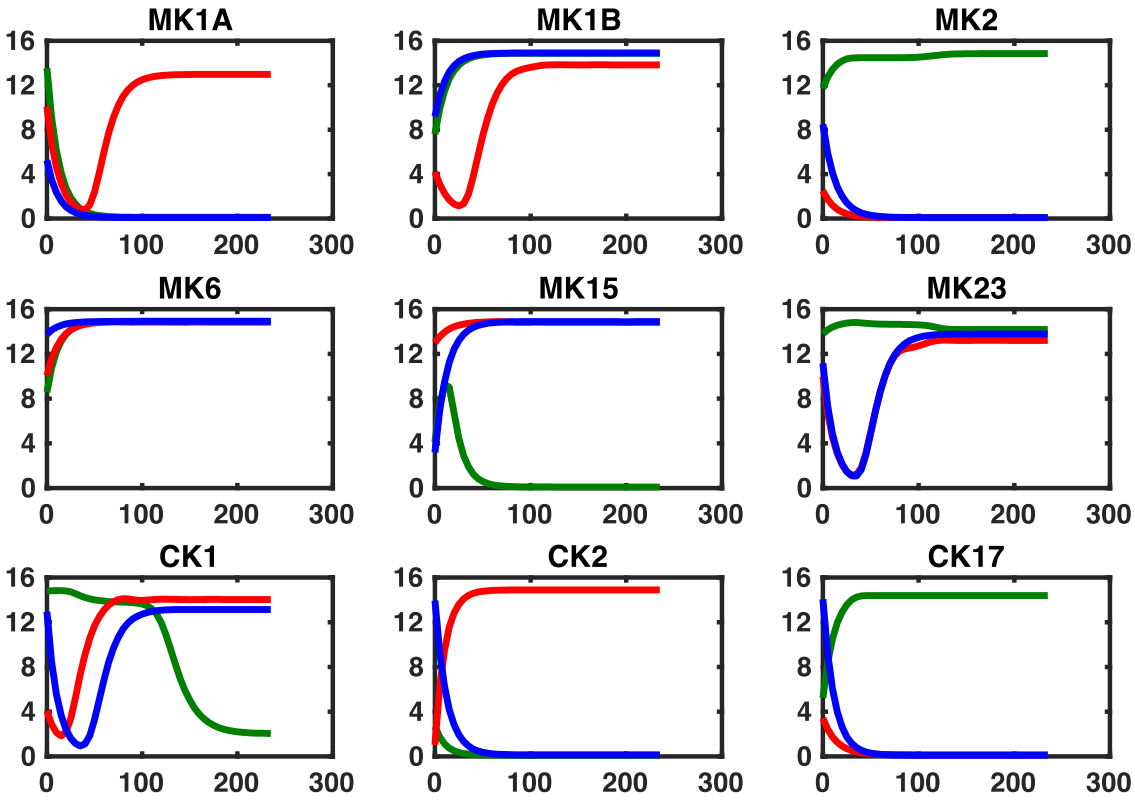

Figure 3.5: Simulating regulatory circuit response to MK6 and MK23 antagonism. Simulated response to a step perturbation applied to the characteristic circuits for GWI (GWI, red line), healthy control (HC, green line), as well as the pharmaceutically edited GWI network (Treated, blue line). Improved adherences to output from the healthy control circuit are produced for cytokine sets MK1A, MK1B, and CK2 without significant negative effects on other sets.

Moreover, it also assumes that although some corrective results are produced at the level of individual cytokine sets that the overall immune network continues to operate in the vicinity of the GWI regulatory regime and as such does not significantly activate any new cytokine signaling mechanisms. We have shown previously that certain cytokine sets act as primary drivers of symptom burden, including IL-1a (MK1A) and IL-10 (MK2), and though not curative that mediating these may reduce illness severity [19].

3.4 Discussion

In this study, we used a Graded eXercise Test (GXT) to stimulate immune signaling in a group of N=12 veterans with Gulf War Illness (GWI) and N= 11 healthy control subjects.

Cytokine levels in blood serum were measured at 8 time points spanning from initial time point at rest to 4 hours post-effort. Statistical analysis using the SMETS metric of the differences in response dynamics for individual cytokines during recovery confirmed that the majority of these differed significantly in GWI compared to HC. The only exceptions to this were responses in IL-1α, IL-23, TNF-α and TNF-β, which did not differ significantly between groups compared to the distribution SMETS distances separating HC subjects from one another. Considering the smaller cohort and heterogenous nature of GWI, we explored the underlying candidate mechanisms driving these divergent choreographed behaviours, rather than the highly variable expression profiles they support. In particular, we identified directed interaction networks from the data collected in each group, aggregating these cytokines into functional sets to facilitate the integration of these empirical interactions with documented immune signals described in work by Folcik and colleagues [24, 25] and used subsequently in simulations by our group [23]. This literature-based network was further reinforced by including immune signaling interactions reported in the latest version of the STRING database [34]. Integration of literature-based and data-derived signaling components indicated that vastly different subsets of immune circuitry become active in each group during recovery with a smaller proportion of these being documented in our reference circuit for GWI than HC. Significant differences in topology occurred specifically regarding involvement of MK2, MK6 and MK15 in the broader network, key components of the GWI regulatory motif. This remodeling of the signaling networks manifested in part through the emergence of characteristic feed-forward control motifs proposed as basic regulatory building blocks by Alon (2007) [47]. Not surprisingly feed-forward mediation of MK23 and CK17 by MK2 and MK6 emerged as distinguishing control elements that were characteristically active in GWI during recovery from exercise. Interestingly, when assessing topological changes that might be imparted to the GWI sub-circuit to produce

a circuitry that best resembles that of HC, abrogating MK6 (IL-6) signaling arose the single most impactful modification. Combining this with a concurrent blockade of inflammatory Th1 cytokine under CK1 (IL-2, IFN-γ, TNF-α, TNF-β) further improved alignment in topology between the GWI and HC active sub-circuits. Simulating the effects of these changes in connectivity suggested that this joint blockade of MK6 and CK1 might allow for the recovery of normal response dynamics in MK1B (primarily IL-1b and IL-8), MK2 (IL-10) and CK17 (IL-17) response dynamics albeit while worsening MK6 (IL-6) response. In previous work by our group [19], IL-10 (MK2) arose as a strong correlate of increased illness severity, specifically multidimensional fatigue inventory (MFI) [51] describing increased general and physical fatigue accompanied by reduced activity and motivation scores. Increases in IL-10 also correlated with decreased general well being scores under the SF-26, a 36-item short-form survey [52] assessing health-related quality of life. In addition to reducing symptom burden, theoretical simulations by our group [26] identified inhibition of Th1 (CK1) inflammatory cytokines as a main component in a two-pronged intervention that could potentially deliver lasting remission from GWI.

The pharmaceutical blockade strategy that delivered the next best topological alignment of GWI and HC sub-circuits consisted of jointly inhibiting MK6 (IL-6) and MK23 (IL-23) receptors. Interestingly IL-23 modulation has recently attracted interest as a potentially important therapeutic target relevant to a broad range of autoimmune illnesses [50, 53, 54]. Moreover, activation of STAT3 [55], a key component of IL-23/ IL-17 signaling has been linked to neurotoxin induced neuro-inflammatory hyper-responsiveness in a mouse model of GWI. Similarly, selective antagonism of IL-6 receptor signaling has shown established efficacy in treating several autoimmune illnesses and in repairing Th17 /Treg imbalance [56]. Moreover, anti-IL-6 therapies have proven especially useful for example in treating rheumatoid arthritis in patients

unresponsive to TNF inhibitors [57]. Simulation of this dual IL-6/ IL-23 blockade suggests that this strategy might support the rescue of MK1A and MK1B (IL-1α, IL-1 β, IL-8 and IL-12) as well as responses in Th2 cytokines under CK2 (IL-4, 5 and 13). This is accomplished under this scenario without negatively impacting other responses. Once again, our previous work indicated that changes in IL-4 and IL-12 correlated significantly with changes in MFI scores for motivation and the Krupp Fatigue Severity Inventory (Krupp FSI) [58]. Likewise changes in IL-1α and IL-5 correlated with changes in SF36 measures for physical function, physical limit, pain, and vitality. Moreover, results of another analysis by our group [17] suggested that initial variations in IL-1α levels might catalyze much broader immune activation during exercise and serve as an important driver of exacerbation in GWI.

Collectively these results suggest that pharmacologically altering active immune circuit topology can inform on strategies that while not curative may nonetheless deliver reduction in symptom burden in GWI. Moreover, the numerical protocol used in this work is currently serving as the basis for the study of larger cohort of n=300 directed at further verifying these characteristic changes in immune signaling network structure. Importantly, predictions made on the basis of interventional restoration of network structure, e.g. Th1 blockade, is being tested in an animal model of GWI and being translated to human clinical trials. It is important to recall that these characteristic circuits represent immune signaling that is predominantly active within the stable regulatory regime that we propose perpetuates GWI [59]. As such we also propose that although a broader response circuitry is available in principle, that for the most part, the topology of this active sub-circuitry will remain dominant within this homeostatic regime and these pharmaceutical interventions are reasonably well represented by edits to this characteristic circuit. This assumption becomes less valid the greater the deviation from the chronic stable state. Nonetheless, this simple approach offers not only a

mechanistically informed molecular motif for GWI but may also inform on beneficial strategies for illness management.

3.5 References

1. Wolfe, J., Proctor Susan, P., Davis Jennifer, D., Borgos Marlana, S. & Friedman Matthew, J. (1998) Health symptoms reported by Persian Gulf War veterans two years after return, *Am J Ind Med.* **33**, 104-113.

2. Unwin, C., Blatchley, N., Coker, W., Ferry, S., Hotopf, M., Hull, L., Ismail, K., Palmer, I., David, A. & Wessely, S. (1999) Health of UK servicemen who served in Persian Gulf War, *The Lancet.* **353**, 169-178.

3. Bourdette, D. N., McCauley, L. A., Barkhuizen, A., Johnston, W., Wynn, M., Joos, S. K., Storzbach, D., Shuell, T. & Sticker, D. (2001) Symptom Factor Analysis, Clinical Findings, and Functional Status in a Population-Based Case Control Study of Gulf WarUnexplained Illness, *J Occup Environ Med.* **43**, 1026-40.

4. Kang, H. K., Natelson, B. H., Mahan, C. M., Lee, K. Y. & Murphy, F. M. (2003) Post-traumatic stress disorder and chronic fatigue syndrome-like illness among Gulf War veterans: a population-based survey of 30,000 veterans, *Am J Epidemiol.* **157**, 141-148.

5. Golier, J. A., Legge, J. & Yehuda, R. (2006) The ACTH Response to Dexamethasone in Persian Gulf War Veterans, *Ann N Y Acad Sci.* **1071**, 448-453.

6. Golier, J. A., Schmeidler, J., Legge, J. & Yehuda, R. (2007) Twenty-four Hour Plasma Cortisol and Adrenocorticotropic Hormone in Gulf War Veterans: Relationships to Posttraumatic Stress Disorder and Health Symptoms, *Biol Psychiatry.* **62**, 1175-1178.

7. Rice, M. A., Craddock, T. J. A., Folcik, V. A., del Rosario, R. M., Barnes, Z. M., Klimas, N. G., Fletcher, M. A., Zysman, J. & Broderick, G. (2014) Gulf War Illness: Is there lasting damage to the endocrine-immune circuitry?, *Sys Biomed.* **2**, 80-89.

8. Duclos, M. & Tabarin, A. (2016) Exercise and the Hypothalamo-Pituitary-Adrenal Axis in *Sports Endocrinology* (Lanfranco, F. & Strasburger, C., eds) pp. 12-26, Front Horm Res.

9. Nagelkirk, P. R., Cook, D. B., Peckerman, A., Kesil, W., Sakowski, T., Natelson, B. H. & LaManca, J. J. (2003) Aerobic capacity of Gulf War veterans with chronic fatigue syndrome, *Mil Med.* **168**, 750-55.

10. Cook, D. B., Nagelkirk, P. R., Peckerman, A., Poluri, A., Lamanca, J. J. & Natelson, B. H. (2003) Perceived Exertion in Fatiguing Illness: Gulf War Veterans with Chronic Fatigue Syndrome, *Med Sci Sports Exerc.* **35**, 569-574.

11. Rayhan, R. U., Stevens, B. W., Raksit, M. P., Ripple, J. A., Timbol, C. R., Adewuyi, O., VanMeter, J. W. & Baraniuk, J. N. (2013) Exercise Challenge in Gulf War Illness Reveals Two Subgroups with Altered Brain Structure and Function, *PLOS ONE.* **8**, e63903.

12. Chalder, T., G, B., Pawlikowska, T., Watts, L., Wessely, S., Wright, D. & Wallace, E. P. (1993) Development of a fatigue scale, *J Psychosom Res.* **37**, 147-53.

13. McManimen, S. L., Sunnquist, M. L. & Jason, L. A. (2016) Deconstructing post-exertional malaise: An exploratory factor analysis, *J health psychol*, 1359105316664139.

14. Snell, C. R., Stevens, S. R., Davenport, T. E. & Van Ness, J. M. (2013) Discriminative Validity of Metabolic and Workload Measurements for Identifying People With Chronic Fatigue Syndrome, *Phys Ther.* **93**, 1484-1492.

15. Broderick, G., Fletcher, M. A., Gallagher, M., Barnes, Z., Vernon, S. D. & Klimas, N. G. (2012) Exploring the Diagnostic Potential of Immune Biomarker Coexpression in Gulf War Illness in *Psychoneuroimmunology Methods Mol Biol (Methods and Protocols)* (Yan, Q., ed) pp. 145-164, Humana Press, Totowa, NJ.

16. Smylie, A. L., Broderick, G., Fernandes, H., Razdan, S., Barnes, Z., Collado, F., Sol, C., Fletcher, M. A. & Klimas, N. (2013) A comparison of sex-specific immune signatures in Gulf War illness and chronic fatigue syndrome, *BMC Immunology.* **14**, 29.

17. Broderick, G., Kreitz, A., Fuite, J., Fletcher, M. A., Vernon, S. D. & Klimas, N. (2011) A pilot study of immune network remodeling under challenge in Gulf War Illness, *Brain Behav Immun.* **25**, 302-313.

18. Whistler, T., Fletcher, M. A., Lonergan, W., Zeng, X.-R., Lin, J.-M., LaPerriere, A., Vernon, S. D. & Klimas, N. G. (2009) Impaired immune function in Gulf War Illness, *BMC Med Genomics.* **2**, 12.

19. Broderick, G., Ben-Hamo, R., Vashishtha, S., Efroni, S., Nathanson, L., Barnes, Z., Fletcher, M. A. & Klimas, N. (2013) Altered immune pathway activity under exercise challenge in Gulf War Illness: An exploratory analysis, *Brain Behav Immun.* **28**, 159-169.

20. Koslik, H. J., Hamilton, G. & Golomb, B. A. (2014) Mitochondrial Dysfunction in Gulf War Illness Revealed by 31Phosphorus Magnetic Resonance Spectroscopy: A Case-Control Study, *PLOS ONE.* **9**, e92887.

21. Lengert, N. & Drossel, B. (2015) In silico analysis of exercise intolerance in myalgic encephalomyelitis/chronic fatigue syndrome, *Biophys Chem.* **202**, 21-31.

22. Vashishtha, S., Broderick, G., Craddock, T. J. A., Fletcher, M. A. & Klimas, N. G. (2015) Inferring Broad Regulatory Biology from Time Course Data: Have We Reached an Upper Bound under Constraints Typical of *In Vivo* Studies?, *PLOS ONE.* **10**, e0127364.

23. Fritsch, P., Craddock, T. J. A., del Rosario, R. M., Rice, M. A., Smylie, A., Folcik, V. A., de Vries, G., Fletcher, M. A., Klimas, N. G. & Broderick, G. (2013) Succumbing to the laws of attraction, *Sys Biomed.* **1**, 179-194.

24. Folcik, V. A., An, G. C. & Orosz, C. G. (2007) The Basic Immune Simulator: An agent-based model to study the interactions between innate and adaptive immunity, *Theor Biol Med Model.* **4**, 39.

25. Folcik, V. A., Broderick, G., Mohan, S., Block, B., Ekbote, C., Doolittle, J., Khoury, M., Davis, L. & Marsh, C. B. (2011) Using an agent-based model to analyze the dynamic communication network of the immune response, *Theor Biol Med Model.* **8**, 1.

26. Craddock, T. J. A., Del Rosario, R. R., Rice, M., Zysman, J. P., Fletcher, M. A., Klimas, N. G. & Broderick, G. (2015) Achieving Remission in Gulf War Illness: A Simulation-Based Approach to Treatment Design, *PLoS ONE.* **10**, e0132774.

27. Fukuda, K., Nisenbaum, R., Stewart, G. Thompson, W. W., Robin, L., Washko, R. M., Noah, D. L., Barrett, D. H., Randall, B., Herwaldt, B. L., Mawle, A. C., Reeves, W. C., (1998) Chronic multisymptom illness affecting air force veterans of the gulf war, *JAMA.* **280**, 981-988.

28. Reeves, W. C., Lloyd, A., Vernon, S. D., Klimas, N., Jason, L. A., Bleijenberg, G., Evengard, B., White, P. D., Nisenbaum, R., Unger, E. R. & the International Chronic Fatigue Syndrome Study, G. (2003) Identification of ambiguities in the 1994 chronic fatigue syndrome research case definition and recommendations for resolution, *BMC Health Serv Res.* **3**, 25-25.

29. Collins, J. F., Donta, S. T., Engel, C. C., Baseman, J. B., Dever, L. L., Taylor, T., Boardman, K. D., Martin, S. E., Wiseman, A. L. & Feussner, J. R. (2002) The Antibiotic Treatment Trial of Gulf War Veterans' Illnesses: issues, design, screening, and baseline characteristics, *Control Clin Trials.* **23**, 333-353.

30. McArdle, W. D., Katch, F. L. & Katch, V. L. (2007) *Exercise Physiology: Nutrition, Energy, and Human Performance* Lippincott Williams & Wilkins, London.

31. Hurwitz, Barry E., Coryell, Virginia T., Parker, M., Martin, P., LaPerriere, A., Klimas, Nancy G., Sfakianakis, George N. & Bilsker, Martin S. (2009) Chronic fatigue syndrome: illness severity, sedentary lifestyle, blood volume and evidence of diminished cardiac function, *Clin Sci (Lond).* **118**, 125-135.

32. Broderick, G., Fuite, J., Kreitz, A., Vernon, S. D., Klimas, N. & Fletcher, M. A. (2010) A Formal Analysis of Cytokine Networks in Chronic Fatigue Syndrome, *Brain Behav Immun.* **24**, 1209-1217.

33. Tapinos, A. & Mendes, P. (2013) A Method for Comparing Multivariate Time Series with Different Dimensions, *PLOS ONE.* **8**, e54201.

34. Szklarczyk, D., Franceschini, A., Wyder, S., Forslund, K., Heller, D., Huerta-Cepas, J., Simonovic, M., Roth, A., Santos, A., Tsafou, K. P., Kuhn, M., Bork, P., Jensen, L. J. & von Mering, C. (2015) STRING v10: protein–protein interaction networks, integrated over the tree of life, *Nucleic Acids Res.* **43**, D447-D452.

35. Wold, S., Sjöström, M. & Eriksson, L. (2001) PLS-regression: a basic tool of chemometrics, *Chemom Intell Lab Syst.* **58**, 109-130.

36. Wold, S., Trygg, J., Berglund, A. & Antti, H. (2001) Some recent developments in PLS modeling, *Chemom Intell Lab Syst.* **58**, 131-149.

37. Horn, J. L. (1965) A rationale and test for the number of factors in factor analysis, *Psychometrika.* **30**, 179-185.

38. Bartlett, M. S. (1950) Tests of significance in factor analysis, *Br J Psych Stat Sec.* **3**, 77-85.

39. Jackson, J. E. (1991) PCA with more than Two Variables in *A User's Guide to Principal Components* (Shewhart, W. A., Wilks, S. S., ed) pp. 26-62, Wiley-Interscience, Hoboken, NJ.

40. Bunke, H. (2000). Graph matching: Theoretical foundations, algorithms, and applications. Paper presented at the *Proc Vision Interface*, Montreal.

41. Dickinson, P. J., Bunke, H., Dadej, A. & Kraetzl, M. (2004) Matching graphs with unique node labels, *Pattern Anal Applic.* **7**, 243-254.

42. Harper, G., Bravi, G. S., Pickett, S. D., Hussain, J. & Green, D. V. S. (2004) The Reduced Graph Descriptor in Virtual Screening and Data-Driven Clustering of High-Throughput Screening Data, *J Chem Inform Comput Sci.* **44**, 2145-2156.

43. Barabasi, A.-L. & Oltvai, Z. N. (2004) Network Biology: Understanding the cell's functional organization, *Nat Rev Genet.* **5**, 101-113.

44. Huber, W., Carey, V. J., Long, L., Falcon, S. & Gentleman, R. (2007) Graphs in molecular biology, *BMC Bioinformatics.* **8**, S8.

45. Di Camillo, B., Toffolo, G. & Cobelli, C. (2009) A Gene Network Simulator to Assess Reverse Engineering Algorithms, *Annals New York Acad Sci.* **1158**, 125-142.

46. Rayhan, R. U., Raksit, M. P., Timbol, C. R., Adewuyi, O., VanMeter, J. W. & Baraniuk, J. N. (2013) Prefrontal lactate predicts exercise-induced cognitive dysfunction in Gulf War Illness, *Am J Trans Res.* **5**, 212-223.

47. Alon, U. (2007) Network motifs: theory and experimental approaches, *Nat Rev Genet.* **8**, 450-461.

48. Hart, Y. & Alon, U. (2013) The Utility of Paradoxical Components in Biological Circuits, *Mol Cell.* **49**, 213-221.

49. Goentoro, L., Shoval, O., Kirschner, M. & Alon, U. (2009) The incoherent feedforward loop can provide fold-change detection in gene regulation, *Mol cell.* **36**, 894-899.

50. Gaffen, S. L., Jain, R., Garg, A. V. & Cua, D. J. (2014) IL-23-IL-17 immune axis: Discovery, Mechanistic Understanding, and Clinical Testing, *Nat Rev Immunol.* **14**, 585-600.

51. Smets, E. M. A., Garssen, B., Bonke, B. & De Haes, J. C. J. M. (1995) The multidimensional Fatigue Inventory (MFI) psychometric qualities of an instrument to assess fatigue, *J Psychosom Res.* **39**, 315-325.

52. Ware, J. E., Jr. & Sherbourne, C. D. (1992) The MOS 36-item short-form health survey (SF-36). I. Conceptual framework and item selection, *Med Care.* **30**, 473-483.

53. Sasaki-Iwaoka, H., Ohori, M., Imasato, A., Taguchi, K., Minoura, K., Saito, T., Kushima, K., Imamura, E., Kubo, S., Furukawa, S. & Morokata, T. (2018) Generation and characterization of a potent fully human monoclonal antibody against the interleukin-23 receptor, *Eur J Pharmacol.* **828**, 89-96.

54. Yang, J., Sundrud, M. S., Skepner, J. & Yamagata, T. (2014) Targeting Th17 cells in autoimmune diseases, *Trends Pharmacol Sci.* **35**, 493-500.

55. Locker, A. R., Michalovicz, L. T., Kelly, K. A., Miller, J. V., Miller, D. B. & O'Callaghan, J. P. (2017) Corticosterone primes the neuroinflammatory response to Gulf War Illness ‐ relevant organophosphates independently of acetylcholinesterase inhibition, *J Neurochem.* **142**, 444-455.

56. Tanaka, T., Narazaki, M. & Kishimoto, T. (2012) Therapeutic Targeting of the Interleukin-6 Receptor, *Annu Rev Pharmacol Toxicol.* **52**, 199-219.

57. Tanaka, Y. & Martin Mola, E. (2014) IL-6 targeting compared to TNF targeting in rheumatoid arthritis: studies of olokizumab, sarilumab and sirukumab, *Ann Rheum Dis.* **73**, 1595-1597.

58. Krupp, L. B., LaRocca, N. G., Muir-Nash, J. & Steinberg, A. D. (1989) The fatigue severity scale: Application to patients with multiple sclerosis and systemic lupus erythematosus, *Arch Neurol.* **46**, 1121-1123.

59. Craddock, T. J. A., Fritsch, P., Rice, M. A., Jr., del Rosario, R. M., Miller, D. B., Fletcher, M. A., Klimas, N. G. & Broderick, G. (2014) A Role for Homeostatic Drive in the Perpetuation of Complex Chronic Illness: Gulf War Illness and Chronic Fatigue Syndrome, *PLOS ONE.* **9**, e84839.

4 Chapter 4: Potentiation of a persistent immune response to Gulf war related exposures by prior physiological stress is conserved across species: A network study

4.1 Introduction

Gulf war illness (GWI) is an archetypal, medically unexplained chronic condition occurring in approximately one third of the veterans of the 1990-91 Gulf War and affecting multiple systems of the body including nervous, endocrine and immune systems resulting in a fully or partially coordinated set of symptoms: fatigue, musculoskeletal pain, cognitive dysfunction, chemical sensitivities, loss of memory and sleep disruption [1-4]. The resemblance of these symptoms to 'sickness behaviour,' a behavioural condition associated with brain inflammatory responses [5, 6], has led to a neuro-immune-based hypothesis on the underlying pathobiology of GWI [2, 7-9]. While the underlying changes in neurochemistry driving these symptoms are difficult to observe directly they may manifest indirectly through changes in the periphery. Indeed, it is now well known that the peripheral immune system and central nervous system (CNS) work in close collaboration to maintain the homeostasis, appropriate responsiveness at increased metabolic demand, as well as to coordinate an appropriate inflammatory response to physical, psychological or immune stresses [10, 11]. Cytokines play an important role as messengers in the peripheral immune system and transmit signals to the CNS. In fact, several mechanisms exist for the communication between peripheral cytokines and the CNS. Many cytokines can directly cross the Blood Brain Barrier (BBB) with the help of a saturable transport system that consists of cytokine transporters capable of altering the permeability of the BBB [5, 12, 13]. Of course, primary afferent nerves, such as vagal nerves during abdominal and visceral infections and trigeminal nerves during oro-lingual infections, can also be directly activated by peripheral cytokines to transmit signals to the CNS [14, 15]. In another mechanism, proinflammatory cytokines, such as IL-1β, produced in response to pathogen-associated molecular patterns sensed by toll-like receptors of macrophage-like cells residing in the

circumventricular organs and choroid plexus can diffuse through the BBB into the CNS [5, 16]. In addition, IL-1 receptors have been observed on perivascular macrophages and endothelial cells of brain venules [5]. Activation of these IL- 1 receptors by circulating cytokines results in the local production of prostaglandin E2 (PGE2). This communication between peripheral cytokines and the brain can lead to the activation of microglial cells that eventually produce proinflammatory cytokines and chemokines in the brain [5]. It has been demonstrated that an immune system activated by peripheral lipopolysaccharide (LPS) administration leads to increased cytokine levels in the brain, especially proinflammatory cytokines, such as IL-1β, IL-6 and TNFα [17, 18]. In addition, peripheral immune challenge and pain stimulation can lead to the activation of microglial cells [17, 19].

Consistent with this ongoing collaborative exchange between the CNS and peripheral immune signaling, several human studies have reported alterations in the immune and endocrine response in GWI veterans. For example, significantly higher levels of IL-2, IL-10, IFN-γ, and TNF-α transcripts in peripheral blood mononuclear cells (PBMC) were reported in early studies of GW veterans experiencing chronic fatigue when compared to healthy veteran control subjects, while non-veterans with ME/CFS were much more difficult to distinguish [20]. Similarly, significantly elevated levels of IL-2 and IFN-γ expression were reported in unstimulated PBMCs from GWI compared to asymptomatic veterans [21]. Moreover, members of our group reported concurrent expression of IFN-γ with Th2 cytokine IL-5 in Phytohaemagglutinin (PHA)-stimulated PBMC culture during the course of a standardized exercise challenge [22]. In a limited number of studies, these characteristic differences in peripheral immune signature have been linked to symptom burden. In a recent preliminary study, IL-1β and IL-15 levels in blood were associated with increased fatigue in pilot cohort of GWI veterans [23]. This is consistent with an earlier study by our group where we found Short Form 36 (SF36)

measures for physical function, physical limit, pain severity, and vitality cluster together and were linked to IL-1α, IL-2 and IL-5 levels [24]. We also found that changes in peripheral expression of IL-10 had the broadest effects on illness severity, including direct correlation with 4 of the 5 constructs for multidimensional fatigue index (MFI). These effects correlated with the activation of pathways related to neuronal development and androgen mediated NF-κB signaling as intracellular markers of GWI symptom burden in peripheral blood. Currently, an animal model that mimics the etiology of GWI remains the best opportunity of capturing how these correlates of severity in the periphery are reflected by changes in the brain.

While the etiology of this illness remains elusive more than two decades after the war, observations in several animal and human studies have supported the involvement of neuroimmune and/or neuroinflammatory dysfunction as a plausible cause of GWI [6, 25]. Multiple exposures and conditions have been hypothesized as the causal agents to instigate the symptoms of GWI. Of these, nerve agent exposure in the war zone, prophylactic treatments with the pyridostigmine bromide (PB), and continuous exposure to pesticides/insect repellants in theater exacerbated by combat stress have been put forth as the leading causes of GWI [26, 27]. Many of these exposures involved either reversible or irreversible acetylcholinesterase (AChE) inhibitors; prophylactic PB is a reversible AChE inhibitor, whereas the nerve gas Sarin, its surrogate diisopropyl fluorophosphate (DFP), and a broad class of pesticides including chlorpyrifos and dichlorvos are organophosphates that act as irreversible AChE inhibitors. Importantly the widely used insect repellent DEET (N, N-diethyl-meta-toluamide) is a weak AChE inhibitor that may also increase the activity of other AChE antagonists [28]. Therefore, a combined effect of exposure to AChE inhibitors, in the context of combat stress and corresponding physiological effects has been widely hypothesized as a cause of GWI and examined in several animal models [6-8, 29-35].

Stress has long been associated with various physical and psychiatric pathologies in humans. In response to stressors, the adrenal cortex secretes stress hormones, such as glucocorticoids (i.e. cortisol), that are well known for their immunosuppressive or anti-inflammatory properties [36]. However, recent findings of animal studies suggest that duration (acute or chronic) and timing (before or after an immune challenge) of exposure determine the type of inflammatory response to glucocorticoids (GCs) [37-39]. Specifically, GCs are known to suppress the expression of IL-1β in both the periphery and the CNS [40]. Conversely, glucocorticoids were shown to cause sensitization of isolated hippocampal microglia through an increased proinflammatory response to peripheral LPS as measured through IL-β and IL-6 levels [41]. Interestingly, while prior exposure to GCs enhanced the inflammatory response to LPS injection in both the liver (peripheral) and hippocampus (central), exposure to GCs post-LPS leads to suppression of the inflammatory response [42]. Similar patterns of response to the acute and chronic exposure to GCs prior to a challenge are extended from CNS to HPA axis [37-39]. Consistent with this, we have recently shown that the prior exposure to corticosterone (CORT) equivalent to levels expected under conditions of high physiological stress [36, 43] exacerbates the neuroinflammation caused by acute exposure to DFP, a surrogate of Sarin, in mice as well as rats [6-8]. Similar neuroinflammatory effects and their exacerbation by the prior exposure to CORT have also been observed in response to exposure to other irreversible AChE inhibitors such as CPO (chlorpyrifos Oxon) [7], methamphetamines [44], as well as bacterial LPS and viral dsRNA [45]. These observations suggest that chronic/subchronic prior exposure to high levels of CORT exerts a priming effect on the CNS leading to a hyper-responsiveness to subsequent neurotoxic or neuroinflammatory stimuli. Many other studies have also demonstrated that CORT has a synergistic effect on the proinflammatory response induced by LPS in different compartments as shown through

increased expression of proinflammatory cytokines such as IL-1β, IL-6 and TNFα, increased core body temperature and activation of the NFκ-B signaling pathway [41, 45-49]. Overall, these studies demonstrate that peripheral exposure to CORT has proinflammatory effects in the periphery and the CNS, especially when administered before a potent immune challenge. Indeed, these observations in animal models together suggest that the prior physiological stress and exposure to irreversible AchE inhibitors could be the potential instigating agents for the neuroinflammation in GWI. While it remains difficult to examine broadly the expression of neuroinflammatory cytokines in human brain, structural and functional alterations observed in brain-imaging studies of GWI offer evidence of persistent neuroinflammation in these affected veterans. For example, significantly elevated cerebral blood flow (CBF) was observed in the hippocampus, amygdala, caudate and thalamic areas in the brain of symptomatic Gulf war veterans, when peripherally challenged with a reversible cholinesterase inhibitor, Physostigmine [50, 51]. Moreover, reduction in the grey and white matter of ill veterans has been consistently reported in several MRI studies [52, 53].

Though these animal models provided key insights into the effects of different individual or combination of exposures, confirming their relevance to GWI will require additional validation alignment in immune and endocrine marker expression in a compartment that is accessible in both human and mouse, namely in peripheral blood. Ideally this would extend beyond the conventional comparison of expression levels in individual markers, as these are manifest in specific patterns that evolve across time as a result of the underlying regulatory mechanisms. Indeed, one could argue that recovery of the same regulatory interactions in the animal model is a more valid measure of fidelity since treatment will be focused on mediating these illness mechanisms. In the present study, we try to emulate the age of human subjects at the time of exposure by using the mice of 8-12 weeks of age. This age is considered as the 20-26 years of age in

human equivalent years. Moreover, 8-12 weeks is more commonly used age in animal model because of two important limiting factors: increased cost associated with using older animals and maintenance of historical data comparability [54]. Further, we emulated the current condition in Gulf War veterans, 25 years after war by extending the observation period of a previously published mouse model of acute exposure of 1-week to more chronic exposure conditions of 3- and 12-week. Further, we applied graph theoretical methods to identify and analyze the alterations in cytokine signaling patterns due to the individual and combination of exposures in a mouse model of GWI. Further, these patterns of immune cytokine signaling in mice were compared to the co-activity patterns among same cytokines in GW veterans in response to a graded exercise challenge.

4.2 Materials and Methods

4.2.1 Mouse sample collection and processing

4.2.1.1 Animals

Adult male C57BL/6J mice (n = 5 mice per group; 8-12 weeks of age) were purchased from Jackson Labs (Bar Harbor, ME, USA). All procedures were performed under protocols approved by the Institutional Animal Care and Use Committee of the Centers for Disease Control and Prevention, National Institute for Occupational Safety and Health and U.S. Army Medical Research and Materiel Command Animal Care and Use Review Office and the animal facility was certified by AAALAC International. Upon receipt, the mice were housed individually in a temperature-controlled (21 ± 1°C) and humidity-controlled (50 ± 10%) colony room maintained under filtered positive pressure ventilation on a 12-h light/12-h dark cycle beginning at 06:00 EDT. Food (Harlan 7913 irradiated NIH-31 modified 6% rodent chow) and water were available ad libitum.

4.2.1.2 Materials

The following chemicals were kindly provided by or obtained from the sources indicated: DFP and LPS from *Escherichia coli* serotype 055:B5: Cat. Number L2880, Sigma-Aldrich, St. Louis, MO, USA, CORT: Steraloids, Inc., Newport, RI, USA. All other reagents were of at least analytical grade and obtained from a variety of commercial sources.

4.2.1.3 Dosing

Similar to our previous studies [7, 9], CORT was given in the drinking water (200 mg/L in 0.6% ethanol, EtOH) for 4 days prior to DFP (3 mg/kg, s.c.) or saline (0.9%) injection. For 3- or 12-week exposures, CORT was given every other week prior to LPS or vehicle injection on day 18 or 87, respectively. It is important to note that the dose of LPS we used here, was chosen for it's inability to mount a significant immune response without prior CORT exposure. We did this, because we were hoping to avoid a situation where the combined response to CORT and LPS would wash out any additive effect introduced by DFP exposure. The schematic view of the dosing paradigm has been presented in Figure 4.1.

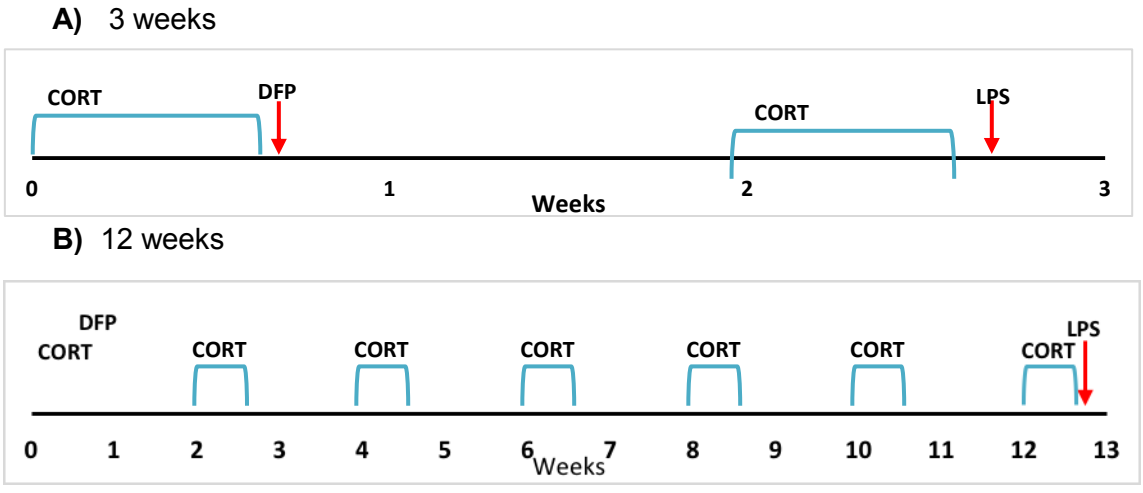

Figure 4.1: Dosing paradigm in 3 weeks and 12 weeks exposure. CORT was given prior to DFP/ Saline injection and CORT was repeated every other week in 3-weeks and 12-weeks regimen before LPS or vehicle injection.

4.2.1.4 Serum cytokine measurement

Mice were killed by decapitation at 6 hours post LPS exposure. Trunk blood was collected from the decapitated animals for serum isolation as described previously in [54]. Serum was frozen at -85°C until subsequent cytokine analysis. Serum cytokine expression was measured as previously described in [55].

4.2.2 Human Sample collection and processing

4.2.2.1 Cohort recruitment & assessment

As part of a larger ongoing study a subset GWI subjects (n = 27) and healthy but sedentary Gulf War era veterans (n = 27) were recruited from the Miami Veterans Administration Medical Center. All subjects were comparable in age, body mass index (BMI), ethnicity and duration of illness. Subjects were male and ranged in age between 40 and 55. Inclusion criteria was derived from [1], and consisted in identifying veterans deployed to the theater of operations between August 8, 1990 and July 31, 1991, with one or more symptoms present after 6 months from at least 2 of the following: fatigue; mood and cognitive complaints; and musculoskeletal complaints. Subjects were in good health prior to 1990, and had no current exclusionary diagnoses [56]. Medications that could have impacted immune function were excluded. In 2002, Collins and coworkers [57] also supported the use of the Fukuda definition in GWI. Summary results of subject demographics and exercise performance are listed in Appendix 4.1.

All subjects underwent a physical examination and medical history including the GWI symptom checklist as per the case definition. Assessments included fatigue measurement through a 20-item self-report instrument Multidimensional Fatigue Inventory (MFI) [58], quality of life assessment through the Medical Outcomes Study 36-item short-form survey (SF-36) [59], The Krupp Fatigue Severity Inventory (Krupp FSI) for measurement of the perceptions of fatigue severity [60] while the impact of symptoms

on the activities of daily life was measured with the Sickness Impact Profile (SIP) [61]. Subjects were screened for quantity and quality of sleep, and evaluated for the likelihood of primary sleep disorders using the Pittsburgh Sleep Quality Index (PSQI) [62]. Designed to assess symptoms of post-traumatic stress disorder (PTSD), the Davidson Trauma Scale (DTS) [63] was applied to those subjects who reported a traumatic experience (death of loved one, assault, injury, etc.). This instrument is divided into three components: intrusion, avoidance, and hyper-arousal. The DTS for all three components are mentioned in Appendix 4.2. While 66% of the GWI cohort presented DTS scores consistent with PTSD, this data is available only for a small fraction of healthy control subjects. Finally, aspects of cognitive impairment were assessed using the Paced Auditory Serial Addition Task (PASAT). This serial-addition task is used to assess the rate of information processing, sustained attention, and working memory [64].

A standard maximal Graded eXercise Test (GXT) was used to stimulate the immune response. V_{max} Spectra 29c Cardiopulmonary Exercise Testing Instrument, Sensor-Medics Ergoline 800 fully automated cycle ergometer, and SensorMedics Marquette MAX 1 Sress ECG were used for the test. Subjects pedaled at an initial output of 60W for 2 min, followed by an increase of 30W every 2 min until the subject reached: (1) a plateau in maximal oxygen consumption (VO2); (2) a respiratory exchange ratio >1.15; or (3) the subject stopped the test [65]. A first blood draw was conducted prior to exercise following a 30-min rest. Second and third blood draws were conducted upon reaching peak effort (VO2 max) and at 4-h post exercise respectively. Summary exercise performance results are also presented in Appendix 4.1. All control subjects were screened as sedentary based on their response to a questionnaire upon recruitment. This was subsequently confirmed by the aerobic capacities obtained (VO2 max) [66]. Adjusted maximum VO2 levels were comparable between GWI and control groups but were significantly lower for the CFS disease control group ($p < 0.05$). Trends

existed towards shorter exercise bouts in both illness groups but these did not achieve statistical significance.

4.2.2.2 Cytokine profiling

Plasma was also separated from each human sample within 2 h of collection and stored at -80°C until assayed. We measured 16 cytokines in plasma using Quansys reagents and instrument (Quansys Biosciences, Logan, Utah). The Quansys Imager, driven by an 8.4 megapixel Canon 20D digital SLR camera, supports 96 well plate based chemiluminescent imaging. The Q-Plex™ Human Cytokine-Screen (16-plex) is a quantitative enzyme-linked immunoabsorbent assay (ELISA) where sixteen distinct capture antibodies have been absorbed to each well of a 96-well plate in a defined array. The range of the standard curves and exposure time were adjusted previously to provide reliable comparisons between subject groups in this illness population at both low and high cytokine concentrations in plasma. Second order polynomial regression models were used as standard calibration curves. Quadruplicate determinations were made, i.e., each sample was run in duplicate in two separate assays. Statistics reported previously in Broderick et al. (2010) [67] indicated an average coefficient of variability (CV) of 0.20 for inter-assay and 0.09 for intra-assay repeatability.

4.3 Numerical analysis

4.3.1 Statistical analysis

Prior to analysis, the raw cytokine expression data from mice challenged with LPS at 3 and 12 weeks following all permutations of priming with Corticosterone, exposure to DFP, or both was log2 transformed along with data from saline treated control mice. The average log2 transformed cytokine levels for the saline control animals were subtracted from the log2-transformed cytokine levels for each individual combination of priming and

neurotoxic exposure. This normalized log2 transformed data is finally converted to fold change levels by calculating the log2 normalized cytokine concentration exponent of 2. Further, one-way ANOVA (Analysis of variance) was performed to analyze the effects of different individual and combinations of CORT priming and exposure.

Similar to the mice, the average log2 transformed data for healthy human subjects at rest (T0) was subtracted from log2 transformed cytokine concentrations for healthy controls (HC) and GWI at rest (T0), peak effort (T1) and recovery (T2) time points and finally converted to fold change levels by calculating the log2 normalized cytokine concentration exponent of 2. Further, the fold change levels for healthy and GWI subjects were compared for the equality of medians at each time point using Mann-Whitney-Wilcoxon ranksum test. A two-way ANOVA was also performed to evaluate the significance of group, time and combined effects.

4.3.2 Identification of cytokine co-expression networks

A simple linear correlation was used as a measure of association to describe the co-expression of cytokines. It is important to note that because of the high degree of concordance between genetically identical mice we concatenated groups of control (n=5) and exposed (n=5) animals to incorporate the perturbation and create a stronger basis for the correlation analysis. Further, a leave-one-out subsampling strategy was applied to the concatenated data of N=10 (n=5 control and n=5 exposed) mice and a mouse from each group i.e. exposed as well unexposed was left out in each subsample set of N=8 (n=4 exposed and n=4 control) mice. Within each of the resulting 25 (15 in cases where n=3) subsampled sets correlation coefficients between cytokine pairs were computed along with their respective null probability estimates. Null probability p was computed by transforming the correlation to create a t statistic having n-2 degrees of freedom for n observations. Confidence bounds were based on an asymptotic normal

distribution of $0.5*log\ ((1+r\ (x_i\ x_j \mid x_k))/(1-r\ (x_i\ x_j \mid x_k)))$, with an approximate variance equal to 1/(n-3) when variables have a multivariate normal distribution. As there exist 66 (n (n-1)/2) possible pair-wise interactions, null probability values were adjusted for multiple comparisons using the Benjamini Hochberg method for estimating the false discovery rate (FDR). Further, correlation networks for each group were generated with a 75% consensus across sub-sampled networks to ensure the existence of at least one edge in each consensus network. More precisely, only edges that were assigned a significant correlation ($p<0.05$) at a low false discovery rate ($FDR<0.05$) in 3 out of 4 subsample networks were included in the consensus co-expression networks.

Since human subjects, unlike mice, are not genetically identical a slightly different strategy was used for the concatenation and subsampling of data to deal with the added biological variability. A set of n=10 healthy and n=10 GWI subjects were randomly selected without replacement and concatenated to make a combined set of N=20. This random selection without replacement is performed 100 times. Further, we constructed 100 subsampled correlation networks with a null probability of $p<0.05$ and $FDR<0.05$ as described in the case of mice. Once again, a 75% agreement across subsample networks was used to construct the consensus correlation network.

4.3.3 Network analysis

General topological differences in networks were evaluated using graph edit distance [68] generalized for continuously weighted graphs. The graph edit distance is based on the minimum summed ‘‘cost” involved in removing and inserting graph edges to transform one network into another. The distance implied is proportional to the magnitude of the weighted change in each edge. The weighted graph edit distance, dGED, between two undirected networks of order N with adjacency matrices, A and B, can be described as follows:

$$d_{GED} = \sum_{i=1}^{N} \sum_{j \geq i}^{N} |a_{ij} - b_{ij}| \quad (4.1).$$

The null probabilities of significance of differences in graph edit distances (GED) were calculated by comparing the GEDs of different subsampled networks. In addition to general topological changes, changes that occur in a node are also of significance since they derive these general topological differences. Median node centrality measures such as degree centrality, betweenness centrality, and closeness centrality are also reported to describe the local changes in the networks around each node. Moreover, we also reported the importance of nodes in terms of hubs and authorities in the networks. Further details about these node centrality measures could be seen in Appendix 3.6.

4.4 Results

4.4.1 Distinctive cytokine profiles in mice

In this study, we have expanded upon our previously published acute exposure model [6, 7, 9] to evaluate a more chronic exposure condition in 3- and 12-week paradigms. The rationale behind evaluating these more extended time points is to try to emulate a condition in the animal model that is more relevant to the current state of the affected Gulf war veterans, now over 25 years removed from the 1991 conflict. Furthermore, we have found previously that repeated exposure to weeklong bouts of CORT results in a compounding increase in LPS-induced neuroinflammation [45]. By layering this effect with an early exposure to DFP by using our acute GWI model, we can evaluate persistent GWI-related alterations in immune signaling by also attempting to mimic cumulative and exacerbating effects of random stressors occurring in day-to-day lives of the returning veterans.

The median cytokine expression fold change measured in response to every individual or combination of exposures was compared to the median cytokine expression fold change in saline-treated animals using a non-parametric Mann Whitney test

(Appendix 4.3). Further, one-way Analysis of Variance (ANOVA) was used to compare the cytokine response in FC levels of different exposures with each other as well as with the cytokine FC levels in response to saline to identify significant exposure effects (Figure 4.2). As shown in Appendix 4.3, the median fold change (FC) levels for the IL-6, TNF-α and KC in mice challenged with LPS, with or without priming with CORT and with or without exposure to DFP, were all significantly different from the median FC levels measured in saline-treated animals at 3 weeks ($p<0.05$). Significant effects of LPS challenge were also evident in the same cytokines in one-way ANOVA (Figure 4.2). Furthermore, median FC levels of these same cytokines were found significantly different with an inclusion of IL-10 in Mann Whitney as well as ANOVA tests even at 12 weeks in response to all LPS challenges except DFP LPS challenge (Figure 4.2). Conversely, delayed effects of DFP exposure were evident on IL-1β cytokine profile in one-way analysis of variance (ANOVA) comparison of the 12-week LPS and DFP LPS cytokine profiles (Figure 4.2). Prior inclusion of CORT in the dosing regimen significantly amplified the effects caused by LPS and DFP+LPS exposures, evident from significant differences in the cytokine profiles of many of the surveyed cytokines.

In all of the comparisons, there were definitely some individual effects of DFP exposure however these effects were so subtle that they were not clearly evident. Therefore, we compared the cytokine FC levels in response to LPS challenge in the 3-week as well as the 12-week paradigms with and without prior DFP exposure in the absence of CORT priming and performed one-way ANOVA to isolate the effects of DFP. A significant group effect of DFP exposure was observed on IL-1β FC levels in the 3-week profiles, this effect on IL-1β persisted to 12 weeks but did not achieve significance (Appendix 4.3). In addition, we compared the profiles in response to LPS challenge with and without DFP exposure but with prior CORT priming i.e. CORT LPS and Cort DFP LPS at 3 weeks and 12 weeks, respectively. Significant group effects for DFP exposure

were obtained when CORT priming was present for IL-1α and IL-4 cytokine profiles at 3 weeks; however, none of the cytokines showed significant group effects in the 12-week cytokine profiles.

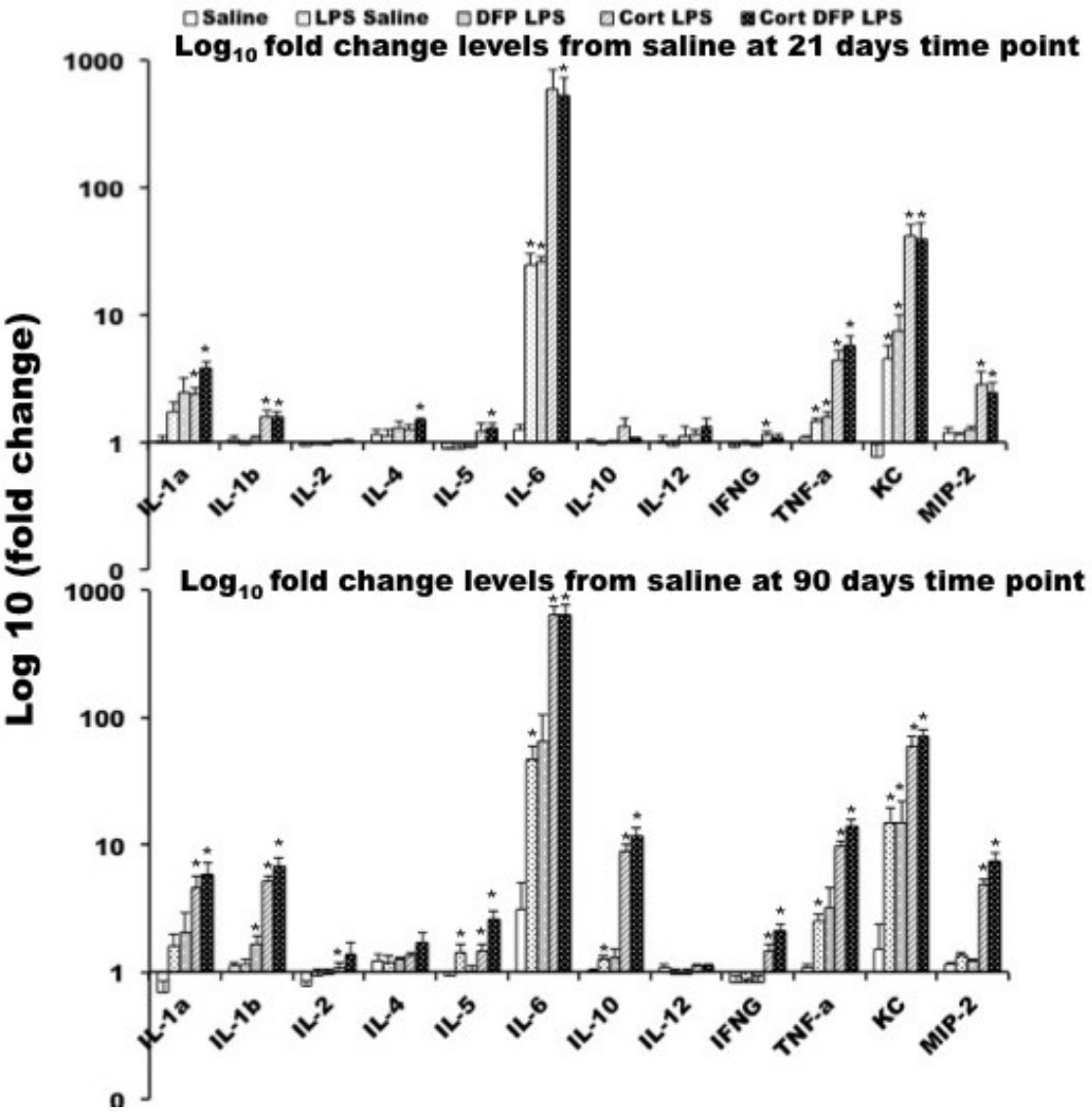

Figure 4.2: Persistent cytokine expression. Fold change in response to LPS challenge following DFP exposure with repeated CORT priming compared to saline control animals have shown broad group effects (one-way ANOVA) in the same cytokines after 21 days and even after 90 days (with some additional ones). DFP exposure was a specific driver of early IL-1b, these differences in IL-1b was persistent but could not achieve the significance level. Error bars represent standard error, * sign represents significant effects of exposure in comparison to saline control fold change levels.

ANOVA results show that CORT priming affected several of the cytokines significantly namely, IL-1β, IL-5, IL-6, IL-10, TNF-α, KC and MIP-2 irrespective of the observation time and IFN-γ in day 90 profiles only. The inclusion of DFP with CORT expanded the breadth of these effects to several other cytokines namely, IL-1α, IL-1β and IL-4 in the 3-week profiles whereas the effects of DFP in the 12 week profiles were so subtle that no significant change in the effect of CORT was discernable (Appendix 4.3).

4.4.2 Immune co-expression patterns in mice

As shown in the previous section, traditional analysis of individual cytokine profiles can only reveal subtle effects of DFP on cytokine fold change in mice. However, cytokines are expressed via underlying mechanisms in a coordinated manner by a diverse community of immune cells to mount responses to immune challenge. To glimpse these underlying mechanisms of action, we constructed co-expression networks using linear correlation as a robust measure of association among markers of immune signaling in mice challenged with LPS with and without DFP exposure and CORT priming. As mentioned earlier in the methods section, subsamples of exposed and unexposed mice were created by concatenating cytokine profiles from both groups and a correlation response network was constructed for each subsample. Further, all the cytokine-cytokine associations (edges) that were present in 75% or more networks were used to construct a consensus correlation network for each condition and compared to elucidate the individual effects.

No uniformly conserved edges were identified in response to LPS challenge alone at 3 weeks that were present in 75% of networks and only one edge was identified as conserved in 75% of the networks in response to LPS challenge with prior exposure to DFP in the 3-week paradigm. Similarly, only two conserved connections were

observed in each LPS and DFP LPS response network at 12 weeks. It is not surprising considering the dose of LPS that we are using in these experiments was chosen for it's inability to mount a significant immune response without prior CORT exposure. In other words, LPS challenge alone or with prior DFP exposure were not capable of triggering a strong coordinated immune response that was also consistent across subsets of animals. Therefore, these exposure-challenge conditions were not included in further analysis. Interestingly, inclusion of CORT to the dosing regimen prior to LPS challenge with and without DFP exposure not only primed the immune response but also made the co-activity patterns of these cytokines very consistent (Figure 4.3 and 4.4).

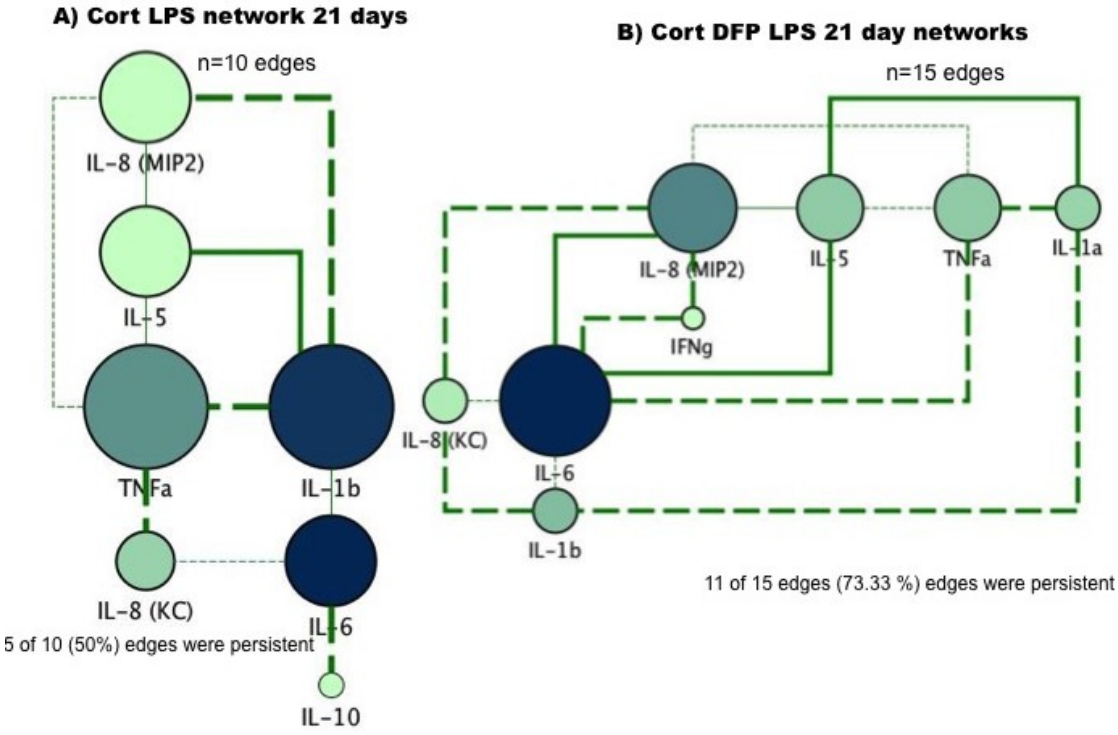

Figure 4.3: Effects of prior DFP exposure on consensus networks. Consensus of 75% of networks in mouse exposed to LPS challenge on day 21 (3 weeks) after repeated periodic exposure to CORT (A) without and (B) with prior exposure to DFP. Thin edges (dashed/solid) represent the edges shared in the both networks. Dashed lines represent edges that were also present in 90-day network in response to same exposure. Node sizes represent the degree and node colour represents the node betweenness centralities.

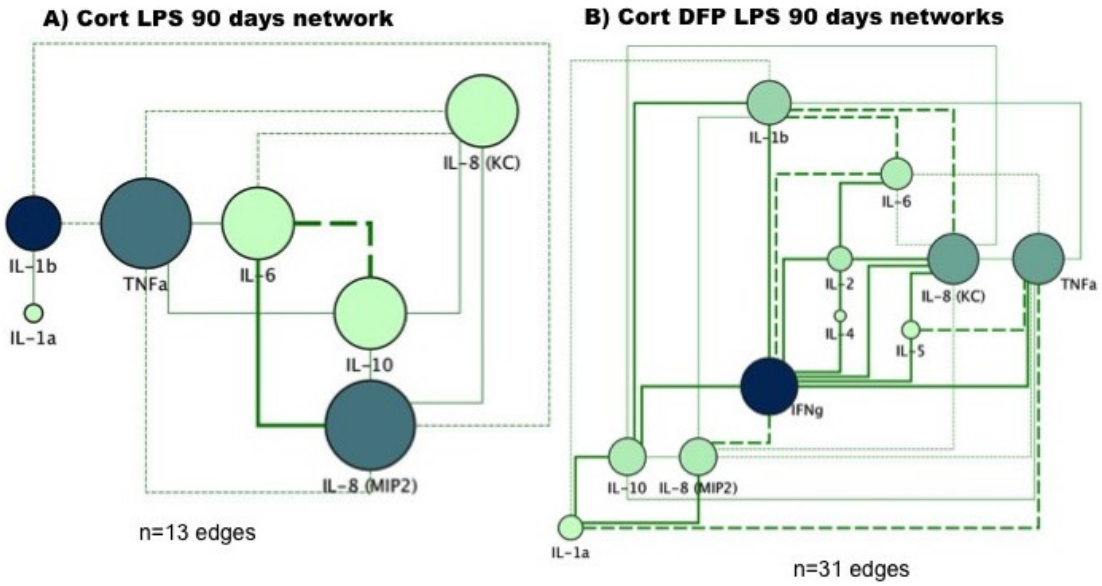

Figure 4.4: Effects of prior DFP exposure on consensus networks. Consensus of 75% of networks in mouse exposed to LPS challenge on day 90 (12-weeks) after repeated periodic exposure to CORT without (A) and with (B) prior exposure to DFP. Thin edges represent the edges shared in the both networks. Thick edges represent the edges unique to each network. Dashed lines represent the persistent edges in the networks. Node sizes represent the degree and node color represents the node betweenness centralities.

Figures 4.3 (A & B) and 4.4 (A & B) represent the consensus of 75% response networks to the prior CORT priming followed by LPS challenge at 3 weeks and repeated to 12 weeks without and with DFP exposure, respectively. These networks were visibly very different in their architecture. The results in Figures 4.3 and 4.4 indicate that the consensus immune networks in response to CORT priming and LPS challenge without DFP exposure were generally smaller than the networks obtained with DFP exposure. While extending the CORT priming to 12 weeks increased the size of the CORT LPS response networks by 30%, this effect was amplified by DFP exposure leading to a doubling of network size. To describe the structural changes of the consensus networks in statistical terms, we compared the individual response networks obtained for each subsampled set of subjects. First, networks describing the response in CORT DFP LPS groups at 3- and 12-weeks were compared to networks obtained without DFP exposure (CORT LPS) to elucidate the topological separation introduced by this neurotoxin. The 3-

week CORT DFP LPS and CORT LPS response networks were separated by a median graph edit distance (GED) of 3.58 (14.5 times the within-group median absolute deviation (MAD) of 0.2470). This median inter-group GED separation was increased further to 3.92 (MAD=0.42) at 12 weeks. These topological differences suggest a role of DFP exposure in the alteration of co-activity patterns. Further, the median inter-group GED between the 12 week response networks (3.92) was significantly different ($p<<<0.001$) from the median inter group GED at 3 weeks response networks (3.58), suggesting a measurable exacerbation of topological differences as a result of extending the repeated CORT priming regimen to 12 weeks.

Next, networks obtained for CORT LPS and CORT DFP LPS groups at 3 weeks were compared directly to their counterparts at 12 weeks. The CORT LPS networks obtained in the 3-week paradigm were separated by median GED of 3.81 (MAD=0.34) from the networks obtained in response to the extended, 12-week CORT regimen. Further, the median GED between the networks in response to CORT DFP LPS exposure at 3 and 12 weeks were significantly ($p<<<0.001$) increased to 4.41 (MAD=0.26) suggesting a greater role of extended CORT regimen in the exacerbation of topological differences caused by DFP. This separation of structure is also evident in the consensus response networks.

Part of these topological differences resulted from the emergence of new signaling connections in consensus networks. Indeed, a large part of the topology in these consensus networks was unique to individual exposures. For example, all the thick edges i.e. 10 of 15 edges in Figure 4.3B and 20 of 31 edges in Figure 4B were unique to the inclusion of DFP in the dosing regimen and all the solid edges were unique to the extension of CORT priming to 12 weeks. Conversely, extension of the CORT dosing regimen played a role in galvanizing the persistence of core components in the immune response. Several connections that were observed in the CORT LPS and CORT DFP

LPS response networks at 3 weeks were also present in the response networks at 12 weeks in the CORT LPS (i.e. 6 of 10 edges) and CORT DFP LPS (i.e. 11 of 15 edges) exposure groups (dashed lines in Figure 4.3 & 4.4A; Figure 4.3 & 4.4B). This redistribution in the local network structure has also caused a shift in the importance of individual nodes. To identify areas of the immune network where most of this redistribution occurred, we calculated node centrality measures such as node degree centrality, betweenness centrality, closeness centrality and eigenvector centrality.

Based on these centrality measures, important changes in the role of individual cytokines were observed as a result of DFP exposure as well as extended priming with CORT (Appendix 4.4; Figure 4.3 and 4.4). Exhibiting the highest betweenness centrality scores, IL-6 and IL-1β emerged as the most central information propagators in response to CORT LPS exposure at 3 weeks. Though, IL-6 maintained this central role under exposure to DFP (CORT DFP LPS), IL-1β was no longer among the most central nodes in the 3 week consensus network (Figure 4.3 A, B). The importance of IL-6 in the early response was fleeting, however, as repeated CORT priming up to 12 weeks saw this cytokine decline in importance, becoming the least central node in the 12 week CORT LPS challenge consensus response network in the absence of DFP exposure (Figure 4.3A; 4.4A). Inclusion of DFP exposure shifted the movement of information at the 12-week challenge through IFN-γ away from IL-1β (Figure 4.4A, B). Once again, extended CORT priming with prior DFP (CORT DFP LPS) exposure saw IL-6 slip from the most central to one of the least central nodes in terms of betweenness centrality (Figure 4.3B; 4.4B). To determine the statistical significance of these alterations in node centrality observed in the conserved consensus networks, we computed these same node centrality measures for each individual response network from subset of subsampled mice (Appendix 4.5).

General trends in individual networks follow the trends in consensus networks. Namely, there were very few nodes with high median betweenness centralities in response networks for CORT LPS at 3 weeks, as well as 12 weeks. Inclusion of DFP in the dosing regimen (CORT DFP LPS) redistributed this information-processing load more broadly as reflected by the reduction in the betweenness centrality of the previously high centrality nodes and a corresponding increase in the previously low betweenness centrality nodes in the 3-week response networks. For instance, at 3 weeks the largest reductions were seen in the betweenness centrality of IL-6 and IL-1β whereas IL-8 (MIP-2) saw the largest increase in median betweenness centrality with DFP exposure. Despite this redistribution, IL-6 remained the most central node in these networks in response to CORT DFP LPS exposure at 3 weeks, with IL-8 (MIP-2) replacing IL-1β as the second most central node. Interestingly, this redistribution continued in the 12-week response networks, but this time the betweenness centrality of most nodes was increased. IFN-γ and IL-8 (KC) gained the most in terms of betweenness centrality and emerged as the most central nodes in 12-week networks in response to CORT DFP LPS exposure (Appendix 4.5). Even in the absence of DFP exposure, extended CORT priming significantly affected the betweenness centrality of several cytokines namely, IL-1α, IL-6 and IL-10 in the 12-week response networks. However this effect was broadened significantly with inclusion of DFP exposure in the regimen, excluding only IL-4, IL-12p70 and TNF-α. This very broad reshuffling in the role of individual cytokines under CORT DFP LPS exposure conditions suggests a further heightening of the effects of DFP under conditions mimicking chronic stress. Not surprisingly, exposure to DFP as well as repeated administration of Cort also significantly impacted other node centrality measures such as eigenvector centrality, closeness centrality and degree centrality in several cytokines further confirming a major redistribution of involvement in the activation of response mechanisms to the nerve

agent DFP and physiological stress. The detailed comparisons of these centrality scores in response to different combinations of exposure and priming are reported in Appendix 4.5.

4.4.3 Cytokine profiles in GWI human cohort

Human data collected from GWI subjects was analyzed by first considering all the GWI subjects (n=27) and secondly by focusing on a sub-group of GWI subjects with a Davidson Trauma Score (DTS) of 50 indicative of a higher exposure to trauma (n=17). All data was converted to fold change with respect to healthy veteran control subjects at each of 3 time points, namely at rest (T0), at peak exercise effort (T1) and 4 hours post exercise (T2). As mentioned earlier, 16 peripheral cytokines were measured in humans whereas 12 cytokines were measured in mice. Therefore, data for only those human cytokines or cytokine homologues that were also measured in mice were used in this analysis.

Of the 12 cytokines measured in mice, 10 cytokines were also measured in the humans. As KC and MIP-2 are not found in humans, we used their homologue IL-8 in humans and duplicated it to use it as KC and MIP-2. While less than ideal, the documented importance of IL-8 in exercise response is such that signaling events around IL-8 were considered important to retain in the analysis. Hereafter, we refer to IL-8 as IL-8 (MIP-2/KC). Therefore, we present only 11 cytokines in the descriptive statistical analysis of human data (Figure 4.5). The mean fold change levels and standard error along with null probability p values obtained from a non-parametric Mann-Whitney Wilcoxon ranksum test are reported in Appendix 4.6A &B and shown in the Figure 4.5 A & B.

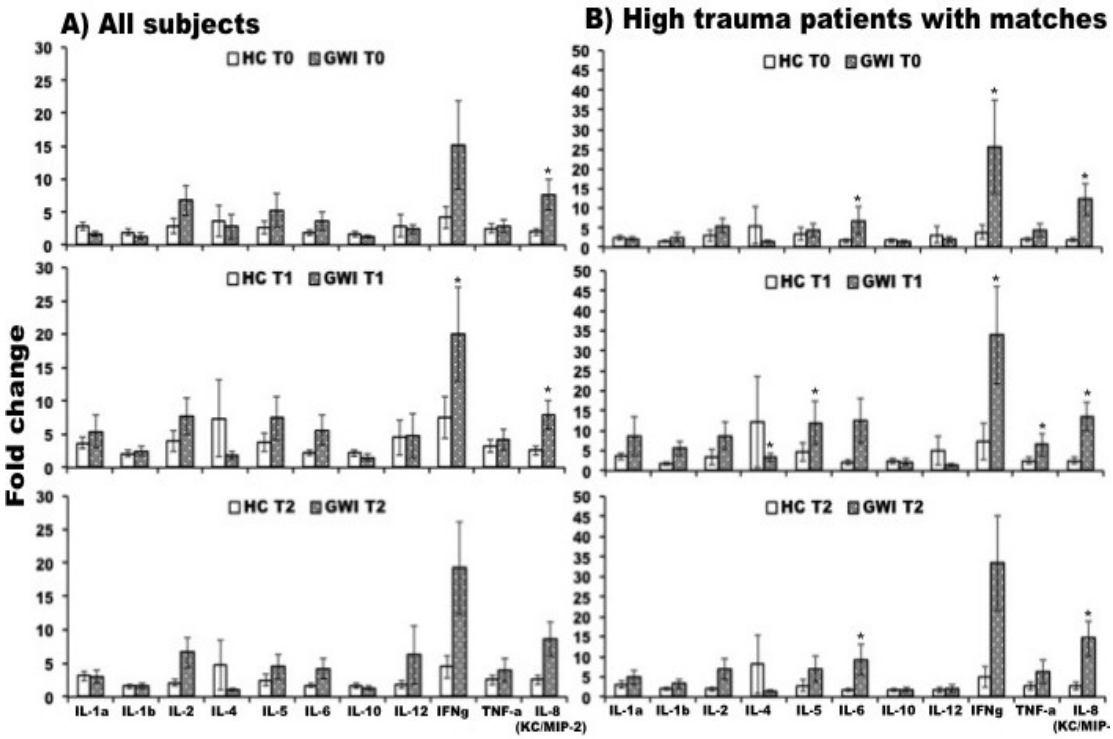

Figure 4.5: Effect of exercise on Mean fold change levels: Mean fold change level comparison in A) All GWI subjects and, B) high trauma GWI subjects and HC controls; '*' represents the statistically significant difference in GWI and HC median FC levels using Wilcoxon ranksum test. Error bars represent standard error.

Differences between the median FC levels of all GWI with respect to healthy control subjects were not significant for most cytokines. However, when we took only high trauma GWI subjects into consideration and compared them with their matching healthy controls, significant differences were observed in the median FC levels of IL-6, IFN-γ and IL-8 at rest, IL-4, IL-5, IL-6, IFN-γ, TNF-α and IL-8 at peak effort and IL-6 and IL-8 during recovery (Figure 4.5B). Further, we performed a two-way analysis of variance (ANOVA) and compared FC levels of all GWI as well as high trauma GWI with their healthy counterparts. Interestingly, GWI subjects with or without suspected high trauma exposure did not show any significant time or interaction effects (Appendix 4.7). However, significant group effects were observed in the GWI subjects with and without a trauma-based stratification. More precisely, IL-2, IL-6, IFN-γ and IL-8 (KC/MIP-2) showed significant group effects in the overall set of all GWI subjects. In addition to

these cytokines IL-1β and TNF-α also show significant group effects in subset of high trauma GWI subjects (Appendix 4.7).

4.4.4 Immune co-activity patterns overlap across species

While animal models have been serving as important predictors of human immune responses for several decades, there is surprisingly little literature where immune responses have been directly and broadly compared across species in the context of a particular disease. Here, we attempt to compare directly and quantitatively peripheral cytokine immune response networks in a mouse model of GWI with the corresponding peripheral immune response networks identified from GWI human subjects. As mentioned earlier, a "leave-two-out" strategy of subsampling was applied to concatenated subsets of mouse cytokine profiles. On the other hand, GWI human subjects were either stratified as high trauma (HT) or were not stratified at all. Ten GWI subjects from the overall set of all GWI subjects were concatenated with healthy controls and randomly subsampled 100 times without replacement. This same procedure of concatenation and random subsampling was followed for the HT GWI subjects. The larger number of subjects, as well as the larger subsample size, served to mitigate the higher variability in the human data relative to the genetically identical mice. A response network was identified for each subset sampled either from all GWI subjects or the HT subjects only. Consensus networks were constructed from interactions that were conserved in at least 75% or more of the individual subsampled networks similar to the approach applied to the mouse data.

The response networks obtained for individual subsets sampled from the overall GWI group were significantly smaller in size than the response networks obtained in subsets of HT GWI veterans at all three exercise challenge time points ($p<0.05$). The median sizes of networks generated using all GWI subjects at each time point were 21,

32, and 29 edges at rest, peak effort and during recovery, respectively. In contrast, median sizes of response networks for HT subjects were 27, 36 and 31 edges at rest, peak effort and recovery time points, respectively. Moreover, only 4, 7, and 7 edges, respectively, were present in the 75% consensus networks for all subjects. However, 11, 22 and 24 edges were identified in the HT subject group at rest, peak effort and recovery time points, respectively, suggesting a more consistent response across HT subjects.

Next, human and mouse networks obtained for individual subsamples were compared to each other and median GEDs were computed to quantify the topological separation within and between groups (Figure 4.6). The response networks in the CORT LPS and CORT DFP LPS exposed mice at 3 weeks were significantly ($p<<<0.05$) closer to GWI response networks in comparison to the 12-week response networks irrespective of exercise challenge time points.

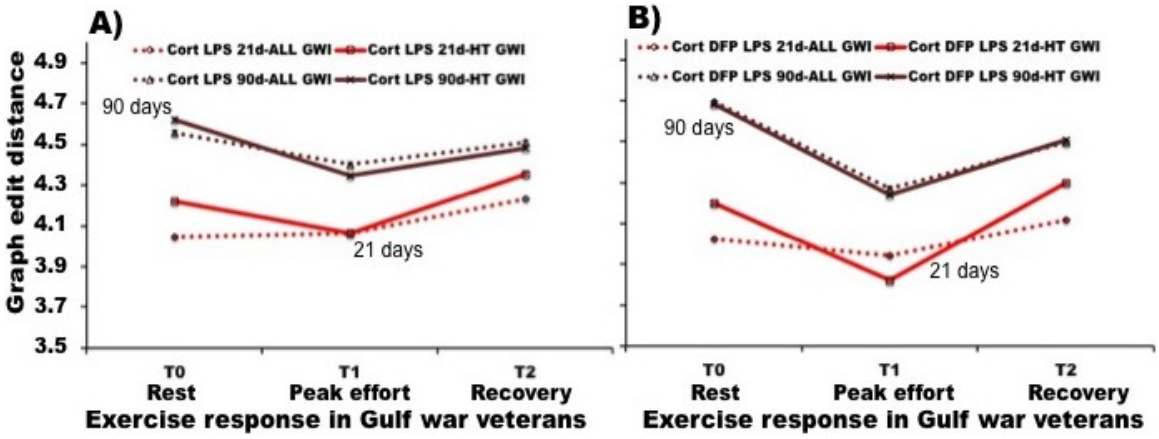

Figure 4.6: Graph edit distances in mouse and human networks: Graph edit distances obtained from the comparison of the networks in response to an LPS challenge without (A) and with (B) DFP exposure after repeated priming with CORT on day 21 (3-week) and again on day 90 (12-week) with the networks in response to a graded exercise challenge in all (HT+LT) human subjects as well as subjects with high trauma (HT). 3-weeks exposure networks in mouse were significantly closer to human response networks at peak effort ($p<<<0.05$; Wilcoxon ranksum) irrespective of exposure.

Indeed, networks obtained in response to CORT LPS or CORT DFP LPS at 3 weeks were closest to the GWI response networks obtained at peak effort (Figure 4.6). Furthermore, the 3-week, CORT DFP LPS networks offered the closest topological match to networks identified at peak effort in the HT GWI subgroup (Figure 4.6). Based on the results of the analysis described above, we compared the 75% consensus response network obtained at peak effort in HT humans (22 edges) with the 75% consensus networks obtained in mice in response to CORT DFP LPS exposure at 3 weeks (15 edges). A significant part of the consensus response network in mice (13 edges) was also shared with HT human networks at peak effort (T1). Since, 11 of the 15 edges expressed in the mouse consensus response network at 3 weeks were persistently expressed in the response network at 12 weeks, we also compared the latter with the consensus response network in HT humans at peak effort (T1). Interestingly, 14 of the 31 edges in the mouse consensus response network obtained for the CORT DFP LPS exposure group at 12 weeks were shared with the HT human response network at peak effort (T1).

Encouraged by these results, we further evaluated how many of the 11 edges persisting in the mouse from 3 to 12 weeks might be active in the human subjects during and after exercise. We found that 8 of 11 persistent edges in the mouse response networks to the CORT DFP LPS exposure were also present in the HT human exercise response networks at peak effort (T1) and 5 of these 8 edges persisted into the recovery phase (T2) (Figure 4.7). These edges capture interactions between IL-6, IL-8, TNFα and IFNγ. At peak effort, additional interactions with IL-1β and IL-5 also emerge as persistent interactions in mouse that are shared with the human immune response in the HT GWI group.

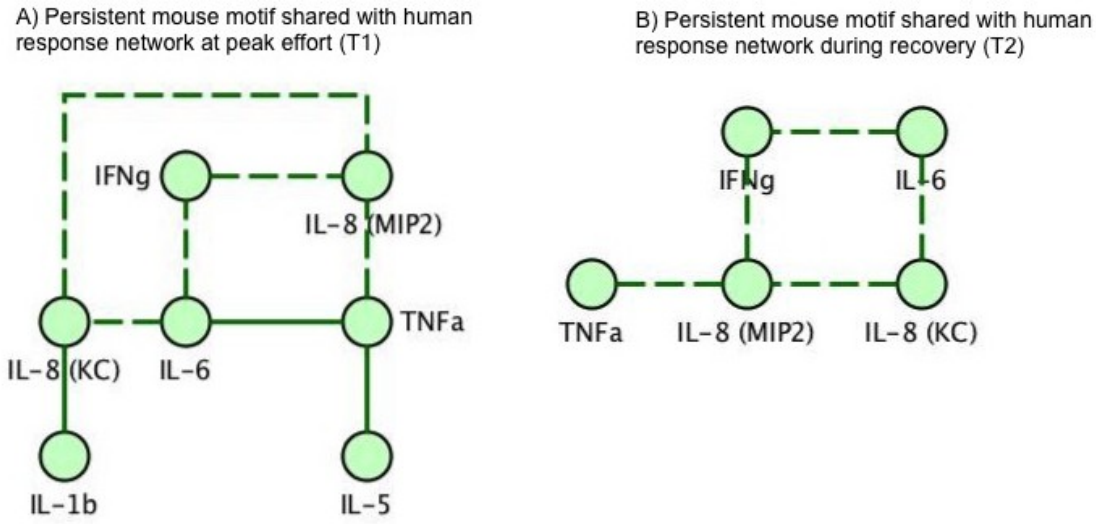

Figure 4.7: Persistently shared motifs across species and time. Edges that were shared in mice exposed to DFP and CORT prior to LPS immune challenge after 3 weeks and 12 weeks with response networks in high trauma affected GWI subjects at (A) peak effort and (B) recovery. Dashed edges represent the edges shared in mice across 3 and 12-week time points as well as in response networks in HT GWI subjects at peak effort and recovery.

4.5 Discussion

In this work, we use an enhancement of the previously described acute GWI exposure model [6-9, 55] that captures the short-term effects of stress potentiated exposure, but also describes a time horizon compatible with the time out-of-theatre of GWI veterans and their current health status. Implicit to this, the animal model also mimics the periodic sub-chronic stress experienced by the affected veterans over the period of two decades since their active duty, in addition to the exposure and stressors experienced in theatre. In this work specifically, we extend our previous analysis of neuroinflammatory markers in brain [6, 7, 9] and blood [55] with a comprehensive profiling of inflammatory markers in the peripheral blood in order to support direct comparison with these immune responses more suitably surveyed in this compartment in human subjects.

We have shown here that though the effects of DFP remain subdued and are not clearly evident in the peripheral cytokine profiles after a considerably long period of time,

these effects are clearly reflected by considerable alterations in consensus co-activity patterns expressed in response to an immune challenge in mice. While conventional comparison of cytokines pointed towards the limited effects of DFP on only IL-1β levels in mice that were persistent but not significant (Appendix 4.3), In contrast, inclusion of DFP exposure to CORT LPS enlarged the size of cytokine co-expression networks. The effects of DFP were not only limited to the global structure of networks but also affected the local topological patterns in these networks. More specifically, DFP also broadly distributed the information-processing load among cytokines, an effect that is even more pronounced following 12 weeks of repeated CORT priming. Moreover, these alterations are only exacerbated with the extended exposure to periodic CORT. In addition, we have also shown that the CORT DFP LPS exposure enlarged the persistent immune response motif in mice. Snapshots at 3 and 12 weeks also indicate a gradual alteration in the mechanism of response to immune challenge by the alterations in the centralities of nodes. For example, IL-6 was the most central node in immune response networks in response to CORT LPS and CORT DFP LPS at 3 weeks, but was replaced by IFN-γ and IL-1β at 12 weeks in CORT DFP LPS and CORT LPS groups, respectively.

Despite the fact that we used a low level LPS challenge to activate the immune system in mice and maximal exercise to prompt the immune response in human subjects, we observed highly conserved elements across species unique to the GWI condition. Specifically, we observed that the immune response co-activity patterns in mice exposed to DFP were topologically more similar to the GWI response networks in human subjects, specifically at peak exercise effort, and that this was especially true of GWI veterans with high trauma exposure scores. Indeed, a significantly large part of the persistent consensus motif in CORT DFP LPS exposed mice was shared with the GWI consensus response network at peak effort and persisted in large part during recovery from exercise.

While we can only largely speculate what any individual veteran with GWI was exposed to in theater, the current results validate our theory that chronic high levels of physiological stress combined with exposure to nerve agent or other organophosphate, AChE inhibitors was a likely initiating event that is perpetuated through periodic exposure to physiological stress and subsequent immune challenges. An important finding of the current study is that the peripheral cytokine profiles generated in the 3-week co-expression networks more closely associate with current immune profiles from veterans with GWI than the 12-week networks. This result is interesting because many other animal models of GWI that do not use repeated CORT priming see significant results only months after exposure [69, 70]. Indeed, longer post-exposure time points are sought after to better correlate animal age and time post-exposure to the current condition of GWI-suffering veterans who were exposed over 25 years ago. However, using our intermittent CORT exposure, we have shortened the time frame of exposure in our GWI paradigm, allowing for more timely and efficient evaluation of inflammatory response, as well as a paradigm that is more conducive to therapeutic testing and evaluation.

These robust and persistent co-expression motifs included interactions between cytokines not typically associated with exercise response in addition to exercise-relevant cytokines. Cytokines such as IL-6 and IL-8 are well known myokines and expected to be a part of the exercise response network motif, however presence of IL1β, TNF-α, IL-5 and IFN-γ in a GWI-specific motif is interesting. In fact, IL-1β and TNF-α are not normally recruited during exercise in healthy subjects [71]. Moreover, elevated IL-1β is widely associated with psychological stress, depression, neuropathic pain and other cognitive issues [72, 73], all of which are symptoms associated with GWI. Moreover, exercise has been shown to attenuate the IL-1β levels in subjects affected with major depressive disorder (MDD) and to relieve the symptoms of hypersomnia [74]. Similarly, attenuation

of IL-5 has been reported in response to exercise in several autoimmune or inflammatory illnesses, e.g. asthma [75]. Moreover, the presence of IL-5 is consistent with our previous findings of involvement of the Th2-component of the immune system [24]. Similarly, the presence of TNF-α as a highly conserved, central signaling element in these response networks aligns with data naïve, mechanistic work by our group where simulations showed that TNF would be a target of interest to produce immune-based homeostatic reset as a potential treatment for GWI [76].

These results together show that the basic immune response mechanisms activated under challenge in exposed mice overlap with those in GWI subjects. These mechanisms are persistent and unique to the illness group, especially in veterans with high trauma exposure. Although, a diversion from the conventional approach, the validation of an animal model using graph theoretical principles is more valid than transient expression profiles as it directly represents our ability to reproduce illness mechanisms.

4.6 References

1. Fukuda, K., Nisenbaum, R., Stewart, G. & et al. (1998) Chronic multisymptom illness affecting air force veterans of the gulf war, *JAMA.* **280**, 981-988.

2. Steele, L. (2000) Prevalence and Patterns of Gulf War Illness in Kansas Veterans: Association of Symptoms with Characteristics of Person, Place, and Time of Military Service, *Am J Epidemiol.* **152**, 992-1002.

3. Dursa, E. K., Barth, S. K., Schneiderman, A. I. & Bossarte, R. M. (2016) Physical and Mental Health Status of Gulf War and Gulf Era Veterans: Results From a Large Population-Based Epidemiological Study, *J Occup Environ Med.* **58**, 41-46.

4. White, R. F., Steele, L., O'Callaghan, J. P., Sullivan, K., Binns, J. H., Golomb, B. A., Bloom, F. E., Bunker, J. A., Crawford, F., Graves, J. C., Hardie, A., Klimas, N., Knox, M., Meggs, W. J., Melling, J., Philbert, M. A. & Grashow, R. (2016) Recent research on Gulf War illness and other health problems in veterans of the 1991 Gulf War: Effects of toxicant exposures during deployment, *Cortex.* **74**, 449-475.

5. Dantzer, R., O'Connor, J. C., Freund, G. G., Johnson, R. W. & Kelley, K. W. (2008) From inflammation to sickness and depression: when the immune system subjugates the brain, *Nat Rev Neurosci.* **9**, 46-56.

6. O'Callaghan, J. P., Kelly, K. A., Locker, A. R., Miller, D. B. & Lasley, S. M. (2015) Corticosterone primes the neuroinflammatory response to DFP in mice: potential animal model of Gulf War Illness, *J Neurochem.* **133**, 708-721.

7. Locker, A. R., Michalovicz, L. T., Kelly, K. A., Miller, J. V., Miller, D. B. & O'Callaghan, J. P. (2017) Corticosterone primes the neuroinflammatory response to Gulf War Illness - relevant organophosphates independently of acetylcholinesterase inhibition, *J Neurochem.* **142**, 444-455.

8. Koo, B.-B., Michalovicz, L. T., Calderazzo, S., Kelly, K. A., Sullivan, K., Killiany, R. J. & O'Callaghan, J. P. (2018) Corticosterone potentiates DFP-induced neuroinflammation and affects high-order diffusion imaging in a rat model of Gulf War Illness, *Brain Behav Immun.* **67**, 42-46.

9. Miller, J. V., LeBouf, R. F., Kelly, K. A., Michalovicz, L. T., Ranpara, A., Locker, A. R., Miller, D. B. & O'Callaghan, J. P. (2018) The Neuroinflammatory Phenotype in a Mouse Model of Gulf War Illness is Unrelated to Brain Regional Levels of Acetylcholine as Measured by Quantitative HILIC-UPLC-MS/MS, *Toxicol Sci.* **165**, 302-313.

10. Xanthos, D. N. & Sandkühler, J. (2013) Neurogenic neuroinflammation: inflammatory CNS reactions in response to neuronal activity, *Nat Rev Neurosci.* **15**, 43-53.

11. Chiu, I. M., von Hehn, C. A. & Woolf, C. J. (2012) Neurogenic inflammation and the peripheral nervous system in host defense and immunopathology, *Nat Neurosci.* **15**, 1063-1067.

12. Banks, W. A. & Erickson, M. A. (2010) The blood–brain barrier and immune function and dysfunction, *Neurobiol Dis.* **37**, 26-32.

13. Procaccini, C., Pucino, V., De Rosa, V., Marone, G. & Matarese, G. (2014) Neuro-Endocrine Networks Controlling Immune System in Health and Disease, *Front Immunol.* **5**, 143.

14. Goehler, L. E., Gaykema, R. P. A., Hansen, M. K., Anderson, K., Maier, S. F. & Watkins, L. R. (2000) Vagal immune-to-brain communication: a visceral chemosensory pathway, *Auton Neurosci.* **85**, 49-59.

15. Romeo, H. E., Tio, D. L., Rahman, S. U., Chiappelli, F. & Taylor, A. N. (2001) The glossopharyngeal nerve as a novel pathway in immune-to-brain communication: relevance to neuroimmune surveillance of the oral cavity, *J Neuroimmunol.* **115**, 91-100.

16. Quan, N., Whiteside, M. & Herkenham, M. (1998) Time course and localization patterns of interleukin-1β messenger rna expression in brain and pituitary after peripheral administration of lipopolysaccharide, *Neurosci.* **83**, 281-293.

17. Biesmans, S., Meert, T. F., Bouwknecht, J. A., Acton, P. D., Davoodi, N., De Haes, P., Kuijlaars, J., Langlois, X., Matthews, L. J. R., Ver Donck, L., Hellings, N. & Nuydens, R. (2013) Systemic Immune Activation Leads to Neuroinflammation and Sickness Behavior in Mice, *Mediators Inflamm.* **2013**, 14.

18. Nguyen, K. T., Deak, T., Owens, S. M., Kohno, T., Fleshner, M., Watkins, L. R. & Maier, S. F. (1998) Exposure to Acute Stress Induces Brain Interleukin-1β Protein in the Rat, *J Neurosci.* **18**, 2239-2246.

19. Hathway, G. J., Vega-Avelaira, D., Moss, A., Ingram, R. & Fitzgerald, M. (2009) Brief, low frequency stimulation of rat peripheral C-fibres evokes prolonged microglial-induced central sensitization in adults but not in neonates, *PAIN.* **144**, 110-118.

20. Zhang, Q., Zhou, X.-D., Denny, T., Ottenweller, J. E., Lange, G., LaManca, J. J., Lavietes, M. H., Pollet, C., Gause, W. C. & Natelson, B. H. (1999) Changes in Immune Parameters Seen in Gulf War Veterans but Not in Civilians with Chronic Fatigue Syndrome, *Clin Diagn Lab Immunol.* **6**, 6-13.

21. Skowera, A., Hotopf, M., Sawicka, E., Varela-Calvino, R., Unwin, C., Nikolaou, V., Hull, L., Ismail, K., David, A. S., Wessely, S. C. & Peakman, M. (2004) Cellular Immune Activation in Gulf War Veterans, *J Clin Immunol.* **24**, 66-73.

22. Whistler, T., Fletcher, M. A., Lonergan, W., Zeng, X.-R., Lin, J.-M., LaPerriere, A., Vernon, S. D. & Klimas, N. G. (2009) Impaired immune function in Gulf War Illness, *BMC Med Genomics.* **2**, 12.

23. Parkitny, L., Middleton, S., Baker, K. & Younger, J. (2015) Evidence for abnormal cytokine expression in Gulf War Illness: A preliminary analysis of daily immune monitoring data, *BMC Immunol.* **16**, 57.

24. Broderick, G., Kreitz, A., Fuite, J., Fletcher, M. A., Vernon, S. D. & Klimas, N. (2011) A pilot study of immune network remodeling under challenge in Gulf War Illness, *Brain Behav Immun.* **25**, 302-313.

25. Broderick, G., Ben-Hamo, R., Vashishtha, S., Efroni, S., Nathanson, L., Barnes, Z., Fletcher, M. A. & Klimas, N. (2013) Altered immune pathway activity under exercise challenge in Gulf War Illness: An exploratory analysis, *Brain Behav Immun.* **28**, 159-169.

26. Illnesses, R. A. C. R. o. G. W. V. (2008) Gulf War Illness and the Health of Gulf War Veterans: Scientific Findings and Recommendations in, U.S. Government Printing Office, Washington, DC.

27. Illnesses, R. A. C. R. o. G. W. V. (2014) Gulf War Illness and the Health of Gulf War Veterans: Research Update and Recommendations, 2009-2013 in, U.S. Government Printing Office, Washington, DC.

28. Corbel, V., Stankiewicz, M., Pennetier, C., Fournier, D., Stojan, J., Girard, E., Dimitrov, M., Molgó, J., Hougard, J.-M. & Lapied, B. (2009) Evidence for inhibition of cholinesterases in insect and mammalian nervous systems by the insect repellent deet, *BMC Biol.* **7**, 47.

29. Kerr Kathleen, J. (2015) Gulf War illness: an overview of events, most prevalent health outcomes, exposures, and clues as to pathogenesis in *Rev Environ Health* pp. 273-286

30. Zakirova, Z., Tweed, M., Crynen, G., Reed, J., Abdullah, L., Nissanka, N., Mullan, M., Mullan, M. J., Mathura, V., Crawford, F. & Ait-Ghezala, G. (2015) Gulf War Agent Exposure Causes Impairment of Long-Term Memory Formation and Neuropathological Changes in a Mouse Model of Gulf War Illness, *PLOS ONE.* **10**, e0119579.

31. Abdullah, L., Evans, J. E., Bishop, A., Reed, J. M., Crynen, G., Phillips, J., Pelot, R., Mullan, M. A., Ferro, A., Mullan, C. M., Mullan, M. J., Ait-Ghezala, G. & Crawford, F. C. (2012) Lipidomic Profiling of Phosphocholine Containing Brain Lipids in Mice with Sensorimotor Deficits and Anxiety-Like Features After Exposure to Gulf War Agents, *NeuroMol Med.* **14**, 349-361.

32. Pierce, L. M., Kurata, W. E., Matsumoto, K. W., Clark, M. E. & Farmer, D. M. (2016) Long-term epigenetic alterations in a rat model of Gulf War Illness, *NeuroToxicol.* **55**, 20-32.

33. Steele, L., Sastre, A., Gerkovich, M. M. & Cook, M. R. (2012) Complex Factors in the Etiology of Gulf War Illness: Wartime Exposures and Risk Factors in Veteran Subgroups, *Environ Health Perspect.* **120**, 112-118.

34. Golomb, B. A. (2008) Acetylcholinesterase inhibitors and Gulf War illnesses, *Proc Natl Acad Sci.* **105**, 4295-4300.

35. Sullivan, K., Krengel, M., Bradford, W., Stone, C., Thompson, T. A., Heeren, T. & White, R. F. (2018) Neuropsychological functioning in military pesticide applicators

from the Gulf War: Effects on information processing speed, attention and visual memory, *Neurotoxicol Teratol.* **65**, 1-13.

36. O'Callaghan, J. P., Brinton, R. E. & McEwen, B. S. (1991) Glucocorticoids Regulate the Synthesis of Glial Fibrillary Acidic Protein in Intact and Adrenalectomized Rats but Do Not Affect Its Expression Following Brain Injury, *J Neurochem.* **57**, 860-869.

37. Grippo, A. J. & Scotti, M. A. L. (2013) Stress and Neuroinflammation, *Mod Trends PharmacoPsychiatry.* **28**, 20-32.

38. Sorrells, S. F. & Sapolsky, R. M. (2007) An inflammatory review of glucocorticoid actions in the CNS, *Brain Behav Immun.* **21**, 259-272.

39. Sorrells, S. F., Caso, J. R., Munhoz, C. D. & Sapolsky, R. M. (2009) The Stressed CNS: When Glucocorticoids Aggravate Inflammation, *Neuron.* **64**, 33-39.

40. Goujon, E., Layé, S., Parnet, P. & Dantzer, R. (1997) Regulation of cytokine gene expression in the central nervous system by glucocorticoids: Mechanisms and functional consequences, *Psychoneuroendocrinol.* **22**, S75-S80.

41. Frank, M. G., Thompson, B. M., Watkins, L. R. & Maier, S. F. (2012) Glucocorticoids mediate stress-induced priming of microglial pro-inflammatory responses, *Brain Behav Immun.* **26**, 337-345.

42. Frank, M. G., Miguel, Z. D., Watkins, L. R. & Maier, S. F. (2010) Prior exposure to glucocorticoids sensitizes the neuroinflammatory and peripheral inflammatory responses to E. coli lipopolysaccharide, *Brain Behav Immun.* **24**, 19-30.

43. Gannon, M. N. & McEwen, B. S. (1990) Calmodulin Involvement in Stress- and Corticosterone-Induced Down-Regulation of Cyclic AMP-Generating Systems in Brain, *J Neurochem.* **55**, 276-284.

44. Kelly, K. A., Miller, D. B., Bowyer, J. F. & O'Callaghan, J. P. (2012) Chronic exposure to corticosterone enhances the neuroinflammatory and neurotoxic responses to methamphetamine, *J Neurochem.* **122**, 995-1009.

45. Kelly, K. A., Michalovicz, L. T., Miller, J. V., Castranova, V., Miller, D. B. & O'Callaghan, J. P. (2018) Prior exposure to corticosterone markedly enhances and prolongs the neuroinflammatory response to systemic challenge with LPS, *PLOS ONE.* **13**, e0190546.

46. de Pablos, R. M., Villarán, R. F., Argüelles, S., Herrera, A. J., Venero, J. L., Ayala, A., Cano, J. & Machado, A. (2006) Stress Increases Vulnerability to Inflammation in the Rat Prefrontal Cortex, *J Neurosci.* **26**, 5709-5719.

47. Johnson, J. D., O'Connor, K. A., Hansen, M. K., Watkins, L. R. & Maier, S. F. (2003) Effects of prior stress on LPS-induced cytokine and sickness responses, *Am J Physiol Regul Integr Comp Physiol.* **284**, R422-R432.

48. Munhoz, C. D., Lepsch, L. B., Kawamoto, E. M., Malta, M. B., Lima, L. d. S., Werneck Avellar, M. C., Sapolsky, R. M. & Scavone, C. (2006) Chronic

Unpredictable Stress Exacerbates Lipopolysaccharide-Induced Activation of Nuclear Factor-κB in the Frontal Cortex and Hippocampus via Glucocorticoid Secretion, *J Neurosci.* **26**, 3813-3820.

49. Munhoz, C. D., Sorrells, S. F., Caso, J. R., Scavone, C. & Sapolsky, R. M. (2010) Glucocorticoids Exacerbate Lipopolysaccharide-Induced Signaling in the Frontal Cortex and Hippocampus in a Dose-Dependent Manner, *J Neurosci.* **30**, 13690-13698.

50. Liu, P., Aslan, S., Li, X., Buhner, D. M., Spence, J. S., Briggs, R. W., Haley, R. W. & Lu, H. (2011) Perfusion deficit to cholinergic challenge in veterans with Gulf War Illness, *NeuroToxicol.* **32**, 242-246.

51. Haley, R. W., Spence, J. S., Carmack, P. S., Gunst, R. F., Schucany, W. R., Petty, F., Devous, M. D., Bonte, F. J. & Trivedi, M. H. (2009) Abnormal brain response to cholinergic challenge in chronic encephalopathy from the 1991 Gulf War, *Psychiatry Res.* **171**, 207-220.

52. Chao, L. L., Abadjian, L., Hlavin, J., Meyerhoff, D. J. & Weiner, M. W. (2011) Effects of low-level sarin and cyclosarin exposure and Gulf War Illness on Brain Structure and Function: A study at 4T, *Neurotoxicology.* **32**, 814-822.

53. Rayhan, R. U., Stevens, B. W., Timbol, C. R., Adewuyi, O., Walitt, B., VanMeter, J. W. & Baraniuk, J. N. (2013) Increased Brain White Matter Axial Diffusivity Associated with Fatigue, Pain and Hyperalgesia in Gulf War Illness, *PLOS ONE.* **8**, e58493.

54. Jackson, S. J., Andrews, N., Ball, D., Bellantuono, I., Gray, J., Hachoumi, L., Holmes, A., Latcham, J., Petrie, A., Potter, P., Rice, A., Ritchie, A., Stewart, M., Strepka, C., Yeoman, M. & Chapman, K. (2017) Does age matter? The impact of rodent age on study outcomes, *Lab Anim.* **51**, 160-169.

55. Michalovicz, L. T., Locker, A. R., Kelly, K. A., Miller, J. V., Barnes, Z., Fletcher, M. A., Miller, D. B., Klimas, N. G., Morris, M., Lasley, S. M. & O'Callaghan, J. P. (2019) Corticosterone and pyridostigmine/DEET exposure attenuate peripheral cytokine expression: Supporting a dominant role for neuroinflammation in a mouse model of Gulf War Illness, *NeuroToxicology.* **70**, 26-32.

56. Reeves, W. C., Lloyd, A., Vernon, S. D., Klimas, N., Jason, L. A., Bleijenberg, G., Evengard, B., White, P. D., Nisenbaum, R., Unger, E. R. & the International Chronic Fatigue Syndrome Study, G. (2003) Identification of ambiguities in the 1994 chronic fatigue syndrome research case definition and recommendations for resolution, *BMC Health Serv Res.* **3**, 25-25.

57. Collins, J. F., Donta, S. T., Engel, C. C., Baseman, J. B., Dever, L. L., Taylor, T., Boardman, K. D., Martin, S. E., Wiseman, A. L. & Feussner, J. R. (2002) The Antibiotic Treatment Trial of Gulf War Veterans' Illnesses: issues, design, screening, and baseline characteristics, *Control Clin Trials.* **23**, 333-353.

58. Smets, E. M. A., Garssen, B., Bonke, B. & De Haes, J. C. J. M. (1995) The multidimensional Fatigue Inventory (MFI) psychometric qualities of an instrument to assess fatigue, *J Psychosom Res.* **39**, 315-325.

59. Ware, J. E., Jr. & Sherbourne, C. D. (1992) The MOS 36-item short-form health survey (SF-36). I. Conceptual framework and item selection, *Med Care.* **30**, 473-483.

60. Krupp, L. B., LaRocca, N. G., Muir-Nash, J. & Steinberg, A. D. (1989) The fatigue severity scale: Application to patients with multiple sclerosis and systemic lupus erythematosus, *Arch Neurol.* **46**, 1121-1123.

61. Bergner M, B. R., Carter WB, Gilson BS (1981) The Sickness Impact Profile: development and final revision of a health status measure, *Med Care.* **19**, 787-805.

62. Buysse, D. J., Reynolds, C. F., Monk, T. H., Berman, S. R. & Kupfer, D. J. (1989) The Pittsburgh sleep quality index: A new instrument for psychiatric practice and research, *Psychiatry Res.* **28**, 193-213.

63. Davidson, J. R. T. B., S. W.; Colket, J. T.; Tupler, L. A.; Roth, S.; David, D.; Hertzberg, M.; Mellman, T.; Beckham, J. C.; Smith, R. D.; Davison, R. M.; Katz, R.; Feldman, M. E. (1997) Assessment of a new self-rating scale for post-traumatic stress disorder, *Psychol Med.* **27**, 153-160.

64. Gronwall, D. M. A. (1977) Paced Auditory Serial-Addition Task: A Measure of Recovery from Concussion, *Percept Mot Skills.* **44**, 367-373.

65. McArdle, W. D., Katch, F. L. & Katch, V. L. (2007) *Exercise Physiology: Nutrition, Energy, and Human Performance* Lippincott Williams & Wilkins, London.

66. Hurwitz, Barry E., Coryell, Virginia T., Parker, M., Martin, P., LaPerriere, A., Klimas, Nancy G., Sfakianakis, George N. & Bilsker, Martin S. (2009) Chronic fatigue syndrome: illness severity, sedentary lifestyle, blood volume and evidence of diminished cardiac function, *Clin Sci (Lond).* **118**, 125-135.

67. Broderick, G., Fuite, J., Kreitz, A., Vernon, S. D., Klimas, N. & Fletcher, M. A. (2010) A Formal Analysis of Cytokine Networks in Chronic Fatigue Syndrome, *Brain Behav Immun.* **24**, 1209-1217.

68. Bunke, H. (2000). Graph matching: Theoretical foundations, algorithms, and applications. Paper presented at the *Proc Vision Interface*, Montreal.

69. Abdullah, L., Evans, J. E., Joshi, U., Crynen, G., Reed, J., Mouzon, B., Baumann, S., Montague, H., Zakirova, Z., Emmerich, T., Bachmeier, C., Klimas, N., Sullivan, K., Mullan, M., Ait-Ghezala, G. & Crawford, F. (2016) Translational potential of long-term decreases in mitochondrial lipids in a mouse model of Gulf War Illness, *Toxicology.* **372**, 22-33.

70. Abdullah, L., Evans, J. E., Montague, H., Reed, J. M., Moser, A., Crynen, G., Gonzalez, A., Zakirova, Z., Ross, I., Mullan, C., Mullan, M., Ait-Ghezala, G. & Crawford, F. (2013) Chronic elevation of phosphocholine containing lipids in mice

exposed to Gulf War agents pyridostigmine bromide and permethrin, *Neurotoxicol Teratol.* **40**, 74-84.

71. Brandt, C. & Pedersen, B. K. (2010) The Role of Exercise-Induced Myokines in Muscle Homeostasis and the Defense against Chronic Diseases, *J Biomed Biotechnol.* **2010**, 6.

72. Brydon, L., Edwards, S., Jia, H., Mohamed-Ali, V., Zachary, I., Martin, J. F. & Steptoe, A. (2005) Psychological stress activates interleukin-1β gene expression in human mononuclear cells, *Brain Behav Immun.* **19**, 540-546.

73. Gui, W.-S., Wei, X., Mai, C.-L., Murugan, M., Wu, L.-J., Xin, W.-J., Zhou, L.-J. & Liu, X.-G. (2016) Interleukin-1β overproduction is a common cause for neuropathic pain, memory deficit, and depression following peripheral nerve injury in rodents, *Mol Pain.* **12**, 1744806916646784.

74. Rethorst, C. D., Greer, T. L., Toups, M. S. P., Bernstein, I., Carmody, T. J. & Trivedi, M. H. (2015) IL-1β and BDNF are associated with improvement in hypersomnia but not insomnia following exercise in major depressive disorder, *Transl Psychiatry.* **5**, e611.

75. Pastva, A., Estell, K., Schoeb, T. R., Atkinson, T. P. & Schwiebert, L. M. (2004) Aerobic Exercise Attenuates Airway Inflammatory Responses in a Mouse Model of Atopic Asthma, *J Immunol.* **172**, 4520-4526.

76. Craddock, T. J. A., Del Rosario, R. R., Rice, M., Zysman, J. P., Fletcher, M. A., Klimas, N. G. & Broderick, G. (2015) Achieving Remission in Gulf War Illness: A Simulation-Based Approach to Treatment Design, *PLoS ONE.* **10**, e0132774.

5 Chapter 5: Conclusions and future perspectives

5.1 General Discussion

Over the years, the focus of the most immunological studies has been on studying the individual biological entities such as genes, proteins, metabolites, cells etc..., however, technological advances in the last two decades are moving our understanding of health and disease from individual entities to their microenvironment. With the advent of high throughput technologies such as microarray, next generation sequencing, flow cytometry and multiplex bead assays, now we have capability to query the whole transcriptome, and broad swaths of the proteome, metabolome and microbiome in an organism. The traditional piecewise approaches of comparing individual expressions/concentrations of biological entities (genes, proteins, metabolites etc.) are not able to adequately represent and support the interpretation of the complex interactions underlying cellular communications that manifest in the data generated from these advanced experimental techniques. As a result, the development and application of such mathematical and computational concepts had also been greatly evolved in last two decades to better infer the complex interactions of this myriad of interdependent cellular components (cells, genes, proteins, metabolites etc.), the evolution of these system-wide relationships with time and the emergent behaviours they support in response to external perturbations at various levels of biological complexity. Accordingly, a large number of studies now consider the coexistence of relevant cells, genes, proteins, cytokines, metabolites and even microbiota in a community structure as an inherent characteristic of biological and physiological systems and use relevant mathematical models to infer the regulatory or co-expression networks from the measured experimental data.

In the past two decades, the reverse engineering of causal regulatory networks from time course expression profiles has received special attention with a number of methods and mathematical formulations being proposed for network inference. Although

competitions such as the DREAM challenges [1-4] provide an ongoing forum for evaluating new iterations of these methods, several important questions regarding their suitability and performance, their data requirements, and the optimal identification of parameters remain areas of active research. The first part of this thesis (Chapter 2 and 3) is focused on addressing some of the questions mentioned above, specifically regarding the identification of directed regulatory networks under constraints applicable to in-vivo studies. The insights obtained were used for the inference from time series data of directed regulatory interaction patterns among cytokines in the peripheral immune system in human subjects with a debilitating condition also known as, 'Gulf War illness' (GWI). This reverse engineering of mechanisms controlling the dynamics of cytokine expression in turn allow us to identify characteristic immune regulatory motifs of GWI that may serve as potential therapeutic avenues.

In the chapter 2 of the thesis, we surveyed a number of reverse engineering methods and selected some basic classes of these methods suitable for data collected under constraints specific to in-vivo studies where the range of allowable perturbations (e.g. virtual absence of knockout data), the sampling frequency and the number of subjects are all significantly limited. Artificial perturbation time course data with the same basic network properties found in biological systems was generated through NetSim simulations [5] and used to assess the performance of conventional gradient-based ODE model, equivalent time-lagged difference equation (TSNI integral) [6] and an information theoretic method adapted for use with time course experiments, TD-ARACNE (Time delay-ARACNE) [7]. In particular, the components of conventional ODE-based methods were constructed and reassembled *de-novo* by applying two popular classes of feature selection namely the truncation of candidate terms (stepwise method) or their projection onto composite constructs (broken stick and Bartlett's methods). These models were then used to explore how performance might be affected by design choices in these

component parts. Finally, the general applicability of simulation results was explored by reconstructing in silico networks using data from the DREAM3 challenge, from the synthetic IRMA network [8] as well as from 9-gene HeLa cell cycle network [9, 10].

None of the methods evaluated in chapter 2 matched their reported average performance on single simulated time courses created using the logic-based NetSim [5]. In general, ODE-based methods performed better than the information-theoretic TD-ARACNE under conditions that approximated *in vivo* time-course studies. Among the ODE based methods, projection-based methods typically performed better though all exhibited a high rate of false positive calls.

These more classical projection-based feature selection techniques (broken stick, Bartlett' s and TSNI integral) did not however outperform the method proposed in Yip et al. (2010) [11] on DREAM3 data. It is important to note however that most of the correct identifications made by the latter were obtained on the basis of homozygous deletion (knock out) data by applying a null hypothesis noise model [12, 13]. Unfortunately, knock out/knock down data are not easily available from *in vivo* studies of *human subjects*. Indeed when applied to the DREAM3 perturbation time series data, the projection techniques mentioned above outperformed the predictions of linear and nonlinear ODE models used in Yip et al. (2010) [11] for all networks. Further, we have shown that the performance of projection-based methods namely, broken stick and Bartlett's method not only outperform the TSNI integral for the inference of 5-node IRMA network as well as 9-gene HeLa cell cycle network but also match the performance of best performing methods reported for the inference of these networks [8-10, 14]. These results re-affirm that even simple models have the potential to perform as well as more complex methods, if tuned *a priori* with simulated data.

Not surprisingly, we also show that inferring networks from a set of multiple expression time course profiles can improve the performance of all selected methods

though sample size effects are not well quantified in the literature. Our analysis suggests that at least 10 time courses would be required for the inference of a representative network for a group of individuals. Moreover, we found that the more parsimonious of the projection approaches i.e., broken stick and TSNI performed consistently when at least 10 time points were used. This analysis in chapter 2 not only offers a comparative survey of reverse engineering methods for the inference of *in vivo* network regulatory kinetics but also attempts to quantitatively delineate the type and amount of data that might be required under the narrow experimental conditions that can be safely deployed in human subjects. Moreover, this analysis offers a reasonably robust numerical protocol with an approximate set of best practices that might be applied to the design of such studies for example, the selection of a suitable inference method, their data requirements in terms of sampling frequency and replicate experiments. Importantly, we propose a model-based optimization of tuning parameters conducted prior to inference using simulated data designed to mimic the anticipated *in vivo* perturbation study.

The numerical protocol developed in Chapter 2 was used to inform key elements in the analysis of human data in Chapter 3. Specifically, the method that consistently performed best in *a priori* analysis was selected for the inference of directed networks. Prior knowledge of the experimental design was used to direct the simulation of time course data with parameter setting predicted to support optimal network recovery used to improve the inference the actual immune networks being surveyed in the human subject data. Using simulations to inform these choices, 16 blood-borne immune markers were measured to interrogate the immune response to physiological stress at 9 time points before, during and after maximum exercise challenge in n=12 GWI veterans and n=12 healthy veteran controls deployed to the same theatre.

Statistical analysis using the SMETS metric [15] of the differences in response dynamics for individual cytokines during recovery confirmed that the majority of these

differed significantly in GWI compared to HC with the exception of IL-1α, IL-23, TNF-α and TNF-β. Individual immune markers were then combined into 9 functional cytokine sets in order to facilitate the integration of interactions identified empirically from the time course data with documented immune signaling mechanisms described in work by [16, 17] and explored further in simulation work by our group [18]. Classical rate equations capturing cytokine expression dynamics observed in the data were further informed by prior structural knowledge obtained from the literature to produce directed networks for the healthy and GWI subject groups separately. Using sub-sampling as a means of estimating the stability of these networks, statistically significant topological differences were observed in the networks for healthy and GWI group networks. This was supported by significantly higher inter-group Graph Edit Distances (GED) (p_{inter}<<<0.01) compared to intra-group variability. Similarly, node centrality measures showed a major reshuffling around functional nodes including IL-10 (MK2), IL-6 (MK6) and IL-15 (MK15) suggesting significant changes in terms of their role as immune information propagators. Interestingly, these nodes form the major component of a characteristic GWI regulatory motif. Indeed, a close inspection of directed networks for each subject group supported the identification of feed-forward mediation of IL-23 (MK23) and IL-17 (MK17) by IL-6 (MK6) and IL-10 (MK2) characteristically active in GWI. Consistent with this observation in human subjects, activation of STAT3, a key component of IL-23/ IL-17 signaling has been linked to neurotoxin induced neuro-inflammatory hyper-responsiveness in a mouse model of GWI [19].

Moreover, simulations of IL-6 (MK6) receptor inhibition along with that of a Th1 cytokine under the set CK1 (IL-2, IFN-γ, TNF-α, TNF-β) or that of the IL-23 receptor was predicted to support a partial rescue of immune response elements. Interestingly, these same elements were associated with illness severity in our previous study [20]. Indeed, simulations mimicking a joint blockade of IL-6 (MK6) and Th1 cytokine activity (CK1)

indicate the recovery of normal response dynamics in inflammatory mediators, primarily IL-1b and IL-8 (MK1B), as well as anti-inflammatory IL-10 (MK2) and Th17 mediator IL-17 (CK17) albeit while worsening IL-6 (MK6) response. Anti-IL-6 therapies have proven especially useful for example in treating rheumatoid arthritis in patients unresponsive to TNF inhibitors [21]. Moreover, IL-10 (MK2) has been strongly correlated with increased illness severity in GWI [20], reported in measures such as multidimensional fatigue inventory (MFI) [22] and SF-26, a 36-item short-form survey [23] assessing health-related quality of life. Restoration of IL-10 might reduce the symptom burden of GWI subjects and could improve quality of life.

Similarly, simulation of the dual IL-6/ IL-23 blockade suggests that this strategy might support the rescue of MK1A and MK1B functional sets which include IL-1α, IL-1β, IL-8 and IL-12 as well as responses in Th2 cytokines IL-4, 5 and 13 included in set CK2. This is accomplished without negatively impacting other cytokine responses. Once again, changes in IL-4 and IL-12 correlated significantly in GWI [20] with changes in MFI scores for motivation and the Krupp Fatigue Severity Inventory (Krupp FSI) [24]. Likewise changes in IL-1α and IL-5 correlated with changes in SF36 measures for physical function, physical limit, pain, and vitality. Moreover, results of another analysis by our group [25] suggested that initial variations in IL-1α levels might catalyze much broader immune activation during exercise and serve as an important driver of exacerbation in GWI.

In the final study of this thesis work, we extend study of cytokine signaling networks to the immune system of animal models of GWI. In particular, we propose that the recovery of like network structures representing immune response is more mechanistically meaningful than alignment of expression profiles in supporting the validity of an animal exposure model for GWI. We compare the peripheral immune response networks identified from data collected in human subjects with that measured

in an extended version of mouse model developed by colleagues at the CDC and consisting of exposure to a Sarin gas surrogate under conditions simulating environmental stress. Network signatures are identified from animal data both for early response (3-weeks) and prolonged chronic response (12 weeks), as time frame more appropriately emulating the current-day condition of GWI subjects more than two decades after their exposure in theatre. The effects on immune signaling of Gulf War related exposures such as DFP, a surrogate of nerve gas Sarin were evaluated by constructing undirected co-expression response networks linking 12 cytokines after 3 and 12-weeks. This was done in the presence and absence of the stress hormone corticosterone (CORT) simulating physiological stress and assessed as changes in the normal immune response to the common bacterial protein lipopolysaccharide (LPS), namely: wild type LPS response, CORT-potentiated LPS, LPS response following exposure to the neurotoxicant DFP with and without CORT potentiation. Graph theoretical principles were used to compare the structure of undirected networks identified under each protocol with each other to identify stress and exposure-related alterations. In addition, undirected networks inferred from responses to LPS challenge in the wake of CORT and combined CORT-DFP exposures after 3 and 12-weeks were compared to undirected networks linking the same cytokines in human GWI subjects. This served to highlight active immune mechanisms that are conserved across the species under specific conditions of stress hormone priming and neurotoxic exposure, thereby supporting the validity and applicability of the proposed animal exposure protocol.

Consistent with the hypothesis that stress potentiates a shift in signaling patterns imparted by neurotoxic exposure, only subdued effects of DFP were observed in the conventional comparison of cytokine profiles. In contrast, significant alterations in global as well as local topological features of the cytokine association networks were clearly

visible when comparing CORT LPS and CORT DFP LPS response networks at the 3-week and 12-week time points respectively. For example, IL-6 was the most central node in LPS immune response networks following CORT and CORT DFP treatment at 3 weeks, but was replaced as a central mediator by IFN-γ and IL-1β at 12 weeks in CORT DFP and CORT treatment groups, respectively. In general, CORT DFP LPS response networks at 3 weeks were significantly ($p<<<0.05$) closer to GWI response networks irrespective of exercise challenge time point (rest, maximum effort, recovery). However, the 3-week combined CORT DFP LPS response networks offered the closest topological match to networks identified at peak exercise effort in the high-trauma (HT) subgroup of veterans with GWI. Furthermore, a persistent motif of interactions linking IL-6, IL-8, TNFα, IFNγ, IL-1β and IL-5 in mouse was also shared with the human immune response network in the HT GWI group at peak effort. Interestingly, the inhibition of receptors for IL-6 and any of the Th1 cytokines under the CK1 functional set (IL-2, IFN-γ, TNF-α, TNF-β) was predicted to support a partial remission from illness severity in GWI in Chapter 3 of this thesis. The presence of IL-1β and TNF-α in motif conserved across exposed mice and human GWI subjects is even more noteworthy because these cytokines are not normally recruited in healthy subjects during exercise [26].

5.2 Conclusions and Future perspectives

The contribution of this thesis work to the ongoing research of GWI is several fold. The work in chapter 2 of the thesis sets the stage for the chapter 3. In particular, an ever-increasing variety of methods are proposed regularly for the inference of regulatory networks each claiming to perform better than the others. However, with the exception of DREAM challenges, there are very limited efforts to independently evaluate the performance of these methods in quantitative terms. In chapter 2, we have specifically focused on methods that are robust to the constraints of *in vivo* human studies. This type

of standardized comparison, especially one conducted at the level of component parts of the methods, has not been previously conducted to the best of our knowledge. Also novel is the use of such analyses to provide general guidelines for the experimental design of human pilot studies. Leveraging these contributions to the methodology, Chapter 3 of the thesis offers the first ever study of directed networks in GWI literature. Identification of characteristic feed-forward regulatory motif in GWI offers new insight into illness specific mechanisms of immune signaling and points towards the involvement of IL-23 IL-17 dysregulation. This finding can and should be further tested in animal models of GWI. In the end, chapter 4 of this thesis offers a unique comparison of co-expression networks across species in GWI, supporting the applicability of an exposure model in mouse to the human condition. To our knowledge, this type of network based comparison highlighting the mechanistic overlap between human condition and animal model has also been never attempted before in GWI, or other complex conditions. This type of graph theoretical analysis not only recovers the common active elements across species but also provides a better resolution for the validation of animal models.

As mentioned earlier, this research work provides a robust framework to move further in ongoing GWI research. First, the findings of Chapter 3 should also be validated in the animal model of GWI as the one evaluated and validated in Chapter 4. In addition, this analysis is restricted to the immune dysregulaiton in human male veterans. Therefore, a similar study of female veterans should be undertaken to elucidate the differences between the male and female hormone-mediated immunity. Moreover, the analysis performed in Chapter 4 should be further extended to a comprehensive survey of the neuroinflammatory markers along with peripheral immune markers in animal models of GWI. This would allow for a much more comprehensive view of illness across the blood brain barrier as well as supporting the identification of key elements that play role in affecting balance between physiological compartments. In addition, an interesting

avenue would be to investigate the involvement of a single cell population in GWI. The involvement of NK cells has been suspected since long time [27]. Latest advancements in technology such as Single- cell RNA-seq would allow us to use transcript abundance in each immune cell sub-population to better determine the specific cell populations responsible for changes in overall cytokine expression as well as look within these cells at changes in pathway activation. Finally, further time course evaluations in animal models of GWI with added sampling both in the short term and long-term responses support a more robust identification of directed circuitry and the mechanistic shift towards persistent illness.

5.3 References

1. Stolovitzky, G., Monroe, D. O. N. & Califano, A. (2007) Dialogue on Reverse-Engineering Assessment and Methods, *Ann N Y Acad Sci.* **1115**, 1-22.

2. Stolovitzky, G., Prill, R. J. & Califano, A. (2009) Lessons from the DREAM2 Challenges, *Ann N Y Acad Sci.* **1158**, 159-195.

3. Madar, A., Greenfield, A., Vanden-Eijnden, E. & Bonneau, R. (2010) DREAM3: Network Inference Using Dynamic Context Likelihood of Relatedness and the Inferelator, *PLoS ONE.* **5**, e9803.

4. Greenfield, A., Madar, A., Ostrer, H. & Bonneau, R. (2010) DREAM4: Combining Genetic and Dynamic Information to Identify Biological Networks and Dynamical Models, *PLoS ONE.* **5**, e13397.

5. Di Camillo, B., Toffolo, G. & Cobelli, C. (2009) A Gene Network Simulator to Assess Reverse Engineering Algorithms, *Annals New York Acad Sci.* **1158**, 125-142.

6. Bansal, M. & di Bernardo, D. (2007) Inference of gene networks from temporal gene expression profiles, *IET Syst Biol.* **1**, 306-312.

7. Zoppoli, P., Morganella, S. & Ceccarelli, M. (2010) TimeDelay-ARACNE: Reverse engineering of gene networks from time-course data by an information theoretic approach, *BMC Bioinform.* **11**, 154.

8. Cantone, I., Marucci, L., Iorio, F., Ricci, M. A., Belcastro, V., Bansal, M., Santini, S., di Bernardo, M., di Bernardo, D. & Cosma, M. P. (2009) A Yeast Synthetic Network for *in vivo* Assessment of Reverse-Engineering and Modeling Approaches, *Cell.* **137**, 172-181.

9. Sambo, F., camillo, B. D. & Toffolo, G. (2008) CNET: an algorithm for reverse engineering of causalgene networks in *8th Workshop on Network Tools and Applications in Biology NETTAB 2008* pp. 134-136 National Research Council, Milan, Italy.

10. Lozano, A. C., Abe, N., Liu, Y. & Rosset, S. (2009) Grouped graphical Granger modeling for gene expression regulatory networks discovery, *Bioinformatics.* **25**, 110-118.

11. Yip, K. Y., Alexander, R. P., Yan, K.-K. & Gerstein, M. (2010) Improved Reconstruction of In Silico Gene Regulatory Networks by Integrating Knockout and Perturbation Data, *PLoS ONE.* **5**, e8121.

12. Prill, R. J., Marbach, D., Saez-Rodriguez, J., Sorger, P. K., Alexopoulos, L. G., Xue, X., Clarke, N. D., Altan-Bonnet, G. & Stolovitzky, G. (2010) Towards a Rigorous Assessment of Systems Biology Models: The DREAM3 Challenges, *PLoS ONE.* **5**, e9202.

13. Marbach, D., Prill, R. J., Schaffter, T., Mattiussi, C., Floreano, D. & Stolovitzky, G. (2010) Revealing strengths and weaknesses of methods for gene network inference, *Proc Natl Acad Sci USA*. **107,** 6286-6291.

14. ElBakry, O., Ahmad, M. O. & Swamy, M. N. S. (2013) Inference of Gene Regulatory Networks with Variable Time Delay from Time-Series Microarray Data, *IEEE/ACM Trans Comp Biol Bioinform* **10**, 671-687.

15. Tapinos, A. & Mendes, P. (2013) A Method for Comparing Multivariate Time Series with Different Dimensions, *PLOS ONE.* **8**, e54201.

16. Folcik, V. A., An, G. C. & Orosz, C. G. (2007) The Basic Immune Simulator: An agent-based model to study the interactions between innate and adaptive immunity, *Theor Biol Med Model.* **4**, 39.

17. Folcik, V. A., Broderick, G., Mohan, S., Block, B., Ekbote, C., Doolittle, J., Khoury, M., Davis, L. & Marsh, C. B. (2011) Using an agent-based model to analyze the dynamic communication network of the immune response, *Theor Biol Med Model.* **8**, 1.

18. Fritsch, P., Craddock, T. J. A., del Rosario, R. M., Rice, M. A., Smylie, A., Folcik, V. A., de Vries, G., Fletcher, M. A., Klimas, N. G. & Broderick, G. (2013) Succumbing to the laws of attraction, *Sys Biomed.* **1**, 179-194.

19. Locker, A. R., Michalovicz, L. T., Kelly, K. A., Miller, J. V., Miller, D. B. & O'Callaghan, J. P. (2017) Corticosterone primes the neuroinflammatory response to Gulf War Illness ‐ relevant organophosphates independently of acetylcholinesterase inhibition, *J Neurochem.* **142**, 444-455.

20. Broderick, G., Ben-Hamo, R., Vashishtha, S., Efroni, S., Nathanson, L., Barnes, Z., Fletcher, M. A. & Klimas, N. (2013) Altered immune pathway activity under exercise challenge in Gulf War Illness: An exploratory analysis, *Brain Behav Immun.* **28**, 159-169.

21. Tanaka, Y. & Martin Mola, E. (2014) IL-6 targeting compared to TNF targeting in rheumatoid arthritis: studies of olokizumab, sarilumab and sirukumab, *Ann Rheum Dis.* **73**, 1595-1597.

22. Smets, E. M. A., Garssen, B., Bonke, B. & De Haes, J. C. J. M. (1995) The multidimensional Fatigue Inventory (MFI) psychometric qualities of an instrument to assess fatigue, *J Psychosom Res.* **39**, 315-325.

23. Ware, J. E., Jr. & Sherbourne, C. D. (1992) The MOS 36-item short-form health survey (SF-36). I. Conceptual framework and item selection, *Med Care.* **30**, 473-483.

24. Krupp, L. B., LaRocca, N. G., Muir-Nash, J. & Steinberg, A. D. (1989) The fatigue severity scale: Application to patients with multiple sclerosis and systemic lupus erythematosus, *Arch Neurol.* **46**, 1121-1123.

25. Broderick, G., Kreitz, A., Fuite, J., Fletcher, M. A., Vernon, S. D. & Klimas, N. (2011) A pilot study of immune network remodeling under challenge in Gulf War Illness, *Brain Behav Immun.* **25**, 302-313.

26. Brandt, C. & Pedersen, B. K. (2010) The Role of Exercise-Induced Myokines in Muscle Homeostasis and the Defense against Chronic Diseases, *J Biomed Biotechnol.* **2010**, 520528.

27. Whistler, T., Fletcher, M. A., Lonergan, W., Zeng, X. R., Lin, J. M., LaPerriere, A., Vernon, S. D., Klimas, N. G.(2009) Impaired immune function in Gulf War Illness, *BMC Med. Genomics.* **2**, 12.

Bibliography

Chapter 1: Introduction and Background

1. Haley, R. W. (1997) Is Gulf War Syndrome Due to Stress? The Evidence Reexamined, *Am J Epidemiol.* **146**, 695-703.

2. Fukuda, K., Nisenbaum, R., Stewart, G. Thompson, W. W., Robin, L., Washko, R. M., Noah, D. L., Barrett, D. H., Randall, B., Herwaldt, B. L., Mawle, A. C., Reeves, W. C., (1998) Chronic multisymptom illness affecting air force veterans of the gulf war, *JAMA.* **280**, 981-988.

3. Steele, L. (2000) Prevalence and Patterns of Gulf War Illness in Kansas Veterans: Association of Symptoms with Characteristics of Person, Place, and Time of Military Service, *Am J Epidemiol.* **152**, 992-1002.

4. Haley, R. W., Kurt, T. L. & Hom, J. (1997) Is there a gulf war syndrome? Searching for syndromes by factor analysis of symptoms, *JAMA.* **277**, 215-222.

5. Institute of, Medicine (2014) *Chronic Multisymptom Illness in Gulf War Veterans: Case Definitions Reexamined*, The National Academies Press, Washington, DC.

6. Gronseth, G. S. (2005) Gulf War Syndrome: A Toxic Exposure? A Systematic Review, *Neurol Clin.* **23**, 523-540.

7. Golomb, B. A. (2008) Acetylcholinesterase inhibitors and Gulf War illnesses, *Proc Natl Acad Sci.* **105**, 4295-4300.

8. Kerr Kathleen, J. (2015) Gulf War illness: an overview of events, most prevalent health outcomes, exposures, and clues as to pathogenesis in *Rev Environ Health* pp. 273-286

9. Cherry, N., Creed, F., Silman, A., Dunn, G., Baxter, D., Smedley, J., Taylor, S. & Macfarlane, G. (2001) Health and exposures of United Kingdom Gulf war veterans. Part II: The relation of health to exposure, *Occup Environ Med.* **58**, 299-306.

10. Nisenbaum, R., Barrett, D. H., Reyes, M. & Reeves, W. C. (2000) Deployment Stressors and a Chronic Multisymptom Illness among Gulf War Veterans, *J Nerv Ment Dis.* **188**, 259-266.

11. Wolfe, J., Proctor, S. P., Erickson, D. J. & Hu, H. (2002) Risk Factors for Multisymptom Illness in US Army Veterans of the Gulf War, *J Occup Environ Med.* **44**, 271-281.

12. Steele, L., Sastre, A., Gerkovich, M. M. & Cook, M. R. (2012) Complex Factors in the Etiology of Gulf War Illness: Wartime Exposures and Risk Factors in Veteran Subgroups, *Environ Health Perspect.* **120**, 112-118.

13. White, R. F., Steele, L., O'Callaghan, J. P., Sullivan, K., Binns, J. H., Golomb, B. A., Bloom, F. E., Bunker, J. A., Crawford, F., Graves, J. C., Hardie, A., Klimas, N., Knox, M., Meggs, W. J., Melling, J., Philbert, M. A. & Grashow, R. (2016) Recent

research on Gulf War illness and other health problems in veterans of the 1991 Gulf War: Effects of toxicant exposures during deployment, *Cortex.* **74**, 449-475.

14. Kang, H. K., Natelson, B. H., Mahan, C. M., Lee, K. Y. & Murphy, F. M. (2003) Post-traumatic stress disorder and chronic fatigue syndrome-like illness among Gulf War veterans: a population-based survey of 30,000 veterans, *Am J Epidemiol.* **157**, 141-148.

15. Eisen, S. A., Kang, H. K., Murphy, F. M., Blanchard, M. S., Reda, D. J., Henderson, W. G., Toomey, R., Jackson, L. W., Alpern, R., Parks, B. J., Klimas, N., Hall, C., Pak, H. S., Hunter, J., Karlinsky, J., Battistone, M. J., Lyons, M. J. & Investigators, G. W. S. P. (2005) Gulf war veterans' health: Medical evaluation of a U.S. cohort, *Ann Intern Med.* **142**, 881-890.

16. Nicolson, G. L. & Nicolson, N. L. (1998) Gulf War illnesses: Complex medical, scientific and political paradox, *Med Confl Surviv.* **14**, 156-165.

17. Crofford, L. J., Young, E. A., Engleberg, N. C., Korszun, A., Brucksch, C. B., McClure, L. A., Brown, M. B. & Demitrack, M. A. (2004) Basal circadian and pulsatile ACTH and cortisol secretion in patients with fibromyalgia and/or chronic fatigue syndrome, *Brain Behav Immun.* **18**, 314-325.

18. Demitrack, M. A., Dale, J. K., Straus, S. E., Laue, L., Listwak, S. J., Kruesi, M. J. P., Chrousos, G. P. & Gold, P. W. (1991) Evidence for Impaired Activation of the Hypothalamic-Pituitary-Adrenal Axis in Patients with Chronic Fatigue Syndrome, *J Clin Endocrinol Metab.* **73**, 1224-1234.

19. Fletcher, M. A., Maher, K. J. & Klimas, N. G. (2002) Natural killer cell function in chronic fatigue syndrome, *Clin Appl Immunol Rev.* **2**, 129-139.

20. Vojdani, A. & Thrasher, J. D. (2004) Cellular and humoral immune abnormalities in Gulf War veterans, *Environ Health Perspect.* **112**, 840-846.

21. Golier, J. A., Legge, J. & Yehuda, R. (2006) The ACTH Response to Dexamethasone in Persian Gulf War Veterans, *Ann N Y Acad Sci.* **1071**, 448-453.

22. Golier, J. A., Schmeidler, J., Legge, J. & Yehuda, R. (2006) Enhanced cortisol suppression to dexamethasone associated with Gulf War deployment, *Psychoneuroendocrinology.* **31**, 1181-1189.

23. Maher, K. J., Klimas, N. G. & Fletcher, M. A. (2005) Chronic fatigue syndrome is associated with diminished intracellular perforin, *Clin Exp Immunol.* **142**, 505-511.

24. Whistler, T., Fletcher, M. A., Lonergan, W., Zeng, X.-R., Lin, J.-M., LaPerriere, A., Vernon, S. D. & Klimas, N. G. (2009) Impaired immune function in Gulf War Illness, *BMC Med Genomics.* **2**, 12.

25. Ciccone, D. S., Weissman, L. & Natelson, B. H. (2008) Chronic Fatigue Syndrome in Male Gulf War Veterans and Civilians, *J Health Psychol.* **13**, 529-536.

26. Zhang, Q., Zhou, X.-D., Denny, T., Ottenweller, J. E., Lange, G., LaManca, J. J., Lavietes, M. H., Pollet, C., Gause, W. C. & Natelson, B. H. (1999) Changes in Immune Parameters Seen in Gulf War Veterans but Not in Civilians with Chronic Fatigue Syndrome, *Clin Diagn Lab Immunol.* **6**, 6-13.

27. Smylie, A. L., Broderick, G., Fernandes, H., Razdan, S., Barnes, Z., Collado, F., Sol, C., Fletcher, M. A. & Klimas, N. (2013) A comparison of sex-specific immune signatures in Gulf War illness and chronic fatigue syndrome, *BMC Immunology.* **14**, 29.

28. Broderick, G., Fletcher, M. A., Gallagher, M., Barnes, Z., Vernon, S. D. & Klimas, N. G. (2012) Exploring the Diagnostic Potential of Immune Biomarker Coexpression in Gulf War Illness in *Psychoneuroimmunology Methods Mol Biol (Methods and Protocols)* (Yan, Q., ed) pp. 145-164, Humana Press, Totowa, NJ.

29. Khaiboullina, S. F., DeMeirleir, K. L., Rawat, S., Berk, G. S., Gaynor-Berk, R. S., Mijatovic, T., Blatt, N., Rizvanov, A. A., Young, S. G. & Lombardi, V. C. (2015) Cytokine expression provides clues to the pathophysiology of Gulf War illness and myalgic encephalomyelitis, *Cytokine.* **72**, 1-8.

30. Janeway, C., Travers, P., Walport, M. & Shlomchik, M. (2001) *Immunobiology*, Fifth edn, New York and London: Garland Science.

31. Parkin, J. & Cohen, B. (2001) An overview of the immune system, *The Lancet.* **357**, 1777-1789.

32. Mack, C. L. (2007) Serum cytokines as biomarkers of disease and clues to pathogenesis, *Hepatology.* **46**, 6-8.

33. Dembic, Z. (2015) Chapter 1 - Introduction—Common Features About Cytokines in *The Cytokines of the Immune System* pp. 1-16, Academic Press, Amsterdam.

34. Monastero, R. N. & Pentyala, S. (2017) Cytokines as Biomarkers and Their Respective Clinical Cutoff Levels, *Int J Inflam.* **2017**, 1-12.

35. Rook, G. A. W. & Zumla, A. Gulf War syndrome: is it due to a systemic shift in cytokine balance towards a Th2 profile?, *The Lancet.* **349**, 1831-1833.

36. Skowera, A., Hotopf, M., Sawicka, E., Varela-Calvino, R., Unwin, C., Nikolaou, V., Hull, L., Ismail, K., David, A. S., Wessely, S. C. & Peakman, M. (2004) Cellular Immune Activation in Gulf War Veterans, *J Clin Immunol.* **24**, 66-73.

37. Brimacombe, M., Zhang, Q., Lange, G. & Natelson, B. H. (2002) Immunological Variables Mediate Cognitive Dysfunction in Gulf War Veterans but Not Civilians with Chronic Fatigue Syndrome, *Neuroimmunomodulation.* **10**, 93-100.

38. Peakman, M., Skowera, A. & Hotopf, M. (2006) Immunological dysfunction, vaccination and Gulf War illness, *Phil Trans R Soc B: Biol Sci.* **361**, 681-687.

39. Allen, J. S., Skowera, A., Rubin, G. J., Wessely, S. & Peakman, M. (2006) Long-Lasting T Cell Responses to Biological Warfare Vaccines in Human Vaccinees, *Clin Infect Dis.* **43**, 1-7.

40. Broderick, G., Kreitz, A., Fuite, J., Fletcher, M. A., Vernon, S. D. & Klimas, N. (2011) A pilot study of immune network remodeling under challenge in Gulf War Illness, *Brain Behav Immun.* **25**, 302-313.

41. Israeli, E. (2012) Gulf War Syndrome as a part of the autoimmune (autoinflammatory) syndrome induced by adjuvant (ASIA), *Lupus.* **21**, 190-194.

42. Moss, J. I. (2013) Gulf War illnesses are autoimmune illnesses caused by increased activity of the p38/MAPK pathway in CD4+ immune system cells, which was caused by nerve agent prophylaxis and adrenergic load, *Med Hypotheses.* **81**, 1002-1003.

43. Parkitny, L., Middleton, S., Baker, K. & Younger, J. (2015) Evidence for abnormal cytokine expression in Gulf War Illness: A preliminary analysis of daily immune monitoring data, *BMC Immunol.* **16**, 57.

44. Georgopoulos, A. P., James, L. M., Mahan, M. Y., Joseph, J., Georgopoulos, A. & Engdahl, B. E. (2015) Reduced Human Leukocyte Antigen (HLA) Protection in Gulf War Illness (GWI), *EBioMedicine.* **3**, 79-85.

45. Broderick, G., Ben-Hamo, R., Vashishtha, S., Efroni, S., Nathanson, L., Barnes, Z., Fletcher, M. A. & Klimas, N. (2013) Altered immune pathway activity under exercise challenge in Gulf War Illness: An exploratory analysis, *Brain Behav Immun.* **28**, 159-169.

46. Golier, J. A., Schmeidler, J., Legge, J. & Yehuda, R. (2007) Twenty-four Hour Plasma Cortisol and Adrenocorticotropic Hormone in Gulf War Veterans: Relationships to Posttraumatic Stress Disorder and Health Symptoms, *Biol Psychiatry.* **62**, 1175-1178.

47. Golier, J. A., Schmeidler, J. & Yehuda, R. (2009) Pituitary response to metyrapone in Gulf War veterans: Relationship to deployment, PTSD and unexplained health symptoms, *Psychoneuroendocrinology.* **34**, 1338-1345.

48. Johnson, J. D., O'Connor, K. A., Watkins, L. R. & Maier, S. F. (2004) The role of IL-1β in stress-induced sensitization of proinflammatory cytokine and corticosterone responses, *Neuroscience.* **127**, 569-577.

49. Morgan III, C. A., Rasmusson, A. M., Wang, S., Hoyt, G., Hauger, R. L. & Hazlett, G. (2002) Neuropeptide-Y, cortisol, and subjective distress in humans exposed to acute stress: replication and extension of previous report, *Biol Psychiatry.* **52**, 136-142.

50. Horner, R. D., Grambow, S. C., Coffman, C. J., Lindquist, J. H., Oddone, E. Z., Allen, K. D. & Kasarskis, E. J. (2008) Amyotrophic Lateral Sclerosis among 1991

Gulf War Veterans: Evidence for a Time-Limited Outbreak, *Neuroepidemiology.* **31**, 28-32.

51. Barth, S. K., Kang, H. K., Bullman, T. A. & Wallin, M. T. (2009) Neurological mortality among U.S. veterans of the Persian Gulf War: 13-year follow-up, *Am J Ind Med.* **52**, 663-670.

52. Wallin, M. T., Kurtzke, J. F., Culpepper, W. J., Coffman, P., Maloni, H., Haselkorn, J. K. & Mahan, C. M. (2014) Multiple Sclerosis in Gulf War Era Veterans. 2. Military Deployment and Risk of Multiple Sclerosis in the First Gulf War, *Neuroepidemiology.* **42**, 226-234.

53. Rayhan, R., Ravindran, M. & Baraniuk, J. (2013) Migraine in gulf war illness and chronic fatigue syndrome: prevalence, potential mechanisms, and evaluation, *Front Physiol.* **4**, 181.

54. Rayhan, R. U., Raksit, M. P., Timbol, C. R., Adewuyi, O., VanMeter, J. W. & Baraniuk, J. N. (2013) Prefrontal lactate predicts exercise-induced cognitive dysfunction in Gulf War Illness, *Am J Trans Res.* **5**, 212-223.

55. Weiner, M. W. (2005) Magnetic resonance and spectroscopy of the human brain in Gulf War illness in *Fort Detrick, MD: US Army Medical Research and Materiel Command*

56. Weiner, M. W., Meyerhoff, D. J., Neylan, T. C., Hlavin, J., Ramage, E. R., McCoy, D., Studholme, C., Cardenas, V., Marmar, C., Truran, D., Chu, P. W., Kornak, J., Furlong, C. E. & McCarthy, C. (2011) The Relationship Between Gulf War Illness, Brain N-acetylaspartate, and Post-Traumatic Stress Disorder, *Military Med.* **176**, 896-902.

57. Rayhan, R. U., Stevens, B. W., Timbol, C. R., Adewuyi, O., Walitt, B., VanMeter, J. W. & Baraniuk, J. N. (2013) Increased Brain White Matter Axial Diffusivity Associated with Fatigue, Pain and Hyperalgesia in Gulf War Illness, *PLOS ONE.* **8**, e58493.

58. Li, X., Spence, J. S., Buhner, D. M., Hart, J., Cullum, C. M., Biggs, M. M., Hester, A. L., Odegard, T. N., Carmack, P. S., Briggs, R. W. & Haley, R. W. (2011) Hippocampal Dysfunction in Gulf War Veterans: Investigation with ASL Perfusion MR Imaging and Physostigmine Challenge, *Radiology.* **261**, 218-225.

59. Chao, L. L., Abadjian, L., Hlavin, J., Meyerhoff, D. J. & Weiner, M. W. (2011) Effects of low-level sarin and cyclosarin exposure and Gulf War Illness on Brain Structure and Function: A study at 4T, *Neurotoxicology.* **32**, 814-822.

60. Haley, R. W., Spence, J. S., Carmack, P. S., Gunst, R. F., Schucany, W. R., Petty, F., Devous, M. D., Bonte, F. J. & Trivedi, M. H. (2009) Abnormal brain response to cholinergic challenge in chronic encephalopathy from the 1991 Gulf War, *Psychiatry Res.* **171**, 207-220.

61. James, L. M., Engdahl, B. E., Leuthold, A. C. & Georgopoulos, A. P. (2016) Brain Correlates of Human Leukocyte Antigen (HLA) Protection in Gulf War Illness (GWI), *EBioMedicine.* **13**, 72-79.

62. Koslik, H. J., Hamilton, G. & Golomb, B. A. (2014) Mitochondrial Dysfunction in Gulf War Illness Revealed by 31Phosphorus Magnetic Resonance Spectroscopy: A Case-Control Study, *PLOS ONE.* **9**, e92887.

63. Thompson, C. H., Kemp, G. J., Sanderson, A. L. & Radda, G. K. (1995) Skeletal muscle mitochondrial function studied by kinetic analysis of postexercise phosphocreatine resynthesis, *J Appl Physiol.* **78**, 2131-2139.

64. Chen, Y., Meyer, J. N., Hill, H. Z., Lange, G., Condon, M. R., Klein, J. C., Ndirangu, D. & Falvo, M. J. (2017) Role of mitochondrial DNA damage and dysfunction in veterans with Gulf War Illness, *PLOS ONE.* **12**, e0184832.

65. Čolović, M. B., Krstić, D. Z., Lazarević-Pašti, T. D., Bondžić, A. M. & Vasić, V. M. (2013) Acetylcholinesterase Inhibitors: Pharmacology and Toxicology, *Curr Neuropharmacol.* **11**, 315-335.

66. Golomb, B. A. & Anthony., C. R. (1999) A Review of the Scientific Literature as It Pertains to Gulf War Illnesses: Pyridostigmine Bromide. in Santa Monica, CA: RAND Corporation, .

67. Drake-Baumann, R. & Seil, F. J. (1999) Effects of exposure to low-dose pyridostigmine on neuromuscular junctions *in vitro* in *Muscle Nerve* pp. 696-703

68. Peden- Adams, M. M., Dudley, A. C., EuDaly, J. G., Allen, C. T., Gilkeson, G. S. & Keil, D. E. (2004) Pyridostigmine Bromide (PYR) Alters Immune Function in B6C3F1 Mice, *Immunopharmacol Immunotoxicol.* **26**, 1-15.

69. Bernatova, I., Babal P Fau - Grubbs, R. D., Grubbs Rd Fau - Morris, M. & Morris, M. (2006) Acetylcholinesterase inhibition affects cardiovascular structure in mice, *Physiol Res.* **55**, Suppl1:S89-97.

70. Adler, M., Deshpande, S. S., Foster, R. E., Maxwell, D. M. & Albuquerque, E. X. (1992) Effects of subacute pyridostigmine administration on mammalian skeletal muscle function, *J Appl Toxicol.* **12**, 25-33.

71. Kluwe, W. M., Page, J. G., Toft, J. D., Ridder, W. E. & Chung, H. (1990) Pharmacological and Toxicological Evaluation of Orally Administered Pyridostigmine in Dogs, *Toxicological Sci.* **14**, 40-53.

72. Lamproglou, I., Barbier, L., Diserbo, M., Fauvelle, F., Fauquette, W. & Amourette, C. (2009) Repeated stress in combination with pyridostigmine: Part I: Long-term behavioural consequences, *Behav Brain Res.* **197**, 301-310.

73. Barbier, L., Diserbo, M., Lamproglou, I., Amourette, C., Peinnequin, A. & Fauquette, W. (2009) Repeated stress in combination with pyridostigmine: Part II: Changes in cerebral gene expression, *Behav Brain Res.* **197**, 292-300.

74. Amourette, C., Lamproglou, I., Barbier, L., Fauquette, W., Zoppe, A., Viret, R. & Diserbo, M. (2009) Gulf War illness: Effects of repeated stress and pyridostigmine treatment on blood–brain barrier permeability and cholinesterase activity in rat brain, *Behav Brain Res.* **203**, 207-214.

75. Abdullah, L., Crynen, G., Reed, J., Bishop, A., Phillips, J., Ferguson, S., Mouzon, B., Mullan, M., Mathura, V., Mullan, M., Ait-Ghezala, G. & Crawford, F. (2011) Proteomic CNS Profile of Delayed Cognitive Impairment in Mice Exposed to Gulf War Agents, *NeuromolMed.* **13**, 275-288.

76. Abdullah, L., Evans, J. E., Montague, H., Reed, J. M., Moser, A., Crynen, G., Gonzalez, A., Zakirova, Z., Ross, I., Mullan, C., Mullan, M., Ait-Ghezala, G. & Crawford, F. (2013) Chronic elevation of phosphocholine containing lipids in mice exposed to Gulf War agents pyridostigmine bromide and permethrin, *Neurotoxicol Teratol.* **40**, 74-84.

77. Ojo, J. O., Abdullah, L., Evans, J., Reed, J. M., Montague, H., Mullan, M. J. & Crawford, F. C. (2014) Exposure to an organophosphate pesticide, individually or in combination with other Gulf War agents, impairs synaptic integrity and neuronal differentiation, and is accompanied by subtle microvascular injury in a mouse model of Gulf War agent exposure, *Neuropathology.* **34**, 109-127.

78. Parihar, V. K., Hattiangady, B., Shuai, B. & Shetty, A. K. (2013) Mood and Memory Deficits in a Model of Gulf War Illness Are Linked with Reduced Neurogenesis, Partial Neuron Loss, and Mild Inflammation in the Hippocampus, *Neuropsychopharmacology.* **38**, 2348-2362.

79. Torres-Altoro, M. I., Mathur, B. N., Drerup, J. M., Thomas, R., Lovinger, D. M., O'Callaghan, J. P. & Bibb, J. A. (2011) Organophosphates dysregulate dopamine signaling, glutamatergic neurotransmission, and induce neuronal injury markers in striatum, *J Neurochem.* **119**, 303-313.

80. Middlemore-Risher, M.-L., Adam, B.-L., Lambert, N. A. & Terry, A. V. (2011) Effects of Chlorpyrifos and Chlorpyrifos-Oxon on the Dynamics and Movement of Mitochondria in Rat Cortical Neurons, *J Pharmacol Exp Ther.* **339**, 341-349.

81. Speed, H. E., Blaiss, C. A., Kim, A., Haws, M. E., Melvin, N. R., Jennings, M., Eisch, A. J. & Powell, C. M. (2012) Delayed Reduction of Hippocampal Synaptic Transmission and Spines Following Exposure to Repeated Subclinical Doses of Organophosphorus Pesticide in Adult Mice, *Toxicoll Sci.* **125**, 196-208.

82. Phillips, K. F. & Deshpande, L. S. (2016) Repeated low-dose organophosphate DFP exposure leads to the development of depression and cognitive impairment in a rat model of Gulf War Illness, *Neurotoxicology.* **52**, 127-133.

83. O'Callaghan, J. P., Kelly, K. A., Locker, A. R., Miller, D. B. & Lasley, S. M. (2015) Corticosterone primes the neuroinflammatory response to DFP in mice: potential animal model of Gulf War Illness, *J Neurochem.* **133**, 708-721.

84. Koo, B.-B., Michalovicz, L. T., Calderazzo, S., Kelly, K. A., Sullivan, K., Killiany, R. J. & O'Callaghan, J. P. (2018) Corticosterone potentiates DFP-induced neuroinflammation and affects high-order diffusion imaging in a rat model of Gulf War Illness, *Brain Behav Immun.* **67**, 42-46.

85. Wright, H. L., Bucknall, R. C., Moots, R. J. & Edwards, S. W. (2012) Analysis of SF and plasma cytokines provides insights into the mechanisms of inflammatory arthritis and may predict response to therapy, *Rheumatology.* **51**, 451-459.

86. Wong, N., Nguyen, T., Brenu, E. W., Broadley, S., Staines, D. & Marshall-Gradisnik, S. (2015) A Comparison of Cytokine Profiles of Chronic Fatigue Syndrome/Myalgic Encephalomyelitis and Multiple Sclerosis Patients, *Int J Clin Med.* **06**, 769-783.

87. Montoya, J. G., Holmes, T. H., Anderson, J. N., Maecker, H. T., Rosenberg-Hasson, Y., Valencia, I. J., Chu, L., Younger, J. W., Tato, C. M. & Davis, M. M. (2017) Cytokine signature associated with disease severity in chronic fatigue syndrome patients, *Proc Natl Acad Sci.* **114**, E7150-E7158.

88. Oreja-Guevara, C., Ramos-Cejudo, J., Aroeira, L. S., Chamorro, B. & Diez-Tejedor, E. (2012) TH1/TH2 Cytokine profile in relapsing-remitting multiple sclerosis patients treated with Glatiramer acetate or Natalizumab, *BMC Neurol.* **12**, 95.

89. Kallaur, A. P., Oliveira, S. R., Simão, A. N. C., Alfieri, D. F., Flauzino, T., Lopes, J., de Carvalho Jennings Pereira, W. L., de Meleck Proença, C., Borelli, S. D., Kaimen-Maciel, D. R., Maes, M. & Reiche, E. M. V. (2017) Cytokine Profile in Patients with Progressive Multiple Sclerosis and Its Association with Disease Progression and Disability, *Mol Neurobiol.* **54**, 2950-2960.

90. Rodríguez-Perlvárez, M. L., García-Sánchez, V., Villar-Pastor, C. M., González, R., Iglesias-Flores, E., Muntane, J. & Gómez-Camacho, F. (2012) Role of serum cytokine profile in ulcerative colitis assessment, *Inflamm Bowel Dis.* **18**, 1864-1871.

91. Műzes, G., Molnár, B., Tulassay, Z. & Sipos, F. (2012) Changes of the cytokine profile in inflammatory bowel diseases, *World J Gastroenterol.* **18**, 5848-5861.

92. Zorzi, F., Monteleone, I., Sarra, M., Calabrese, E., Marafini, I., Cretella, M., Sedda, S., Biancone, L., Pallone, F. & Monteleone, G. (2013) Distinct Profiles of Effector Cytokines Mark the Different Phases of Crohn's Disease, *PLOS ONE.* **8**, e54562.

93. Kantola, T., Klintrup, K., Väyrynen, J. P., Vornanen, J., Bloigu, R., Karhu, T., Herzig, K. H., Näpänkangas, J., Mäkelä, J., Karttunen, T. J., Tuomisto, A. & Mäkinen, M. J. (2012) Stage-dependent alterations of the serum cytokine pattern in colorectal carcinoma, *Br J Cancer.* **107**, 1729-1736.

94. Matte, I., Lane, D., Laplante, C., Rancourt, C. & Piché, A. (2012) Profiling of cytokines in human epithelial ovarian cancer ascites, *Am J Cancer Res.* **2**, 566-580.

95. Roshani, R., McCarthy, F. & Hagemann, T. (2014) Inflammatory cytokines in human pancreatic cancer, *Cancer Lett.* **345**, 157-163.

96. Cutler, A. & Brombacher, F. (2005) Cytokine Therapy, *Ann N Y Acad Sci.* **1056**, 16-29.

97. Dustin, M. L. (2012) Signaling at neuro/immune synapses, *J Clin Invest.* **122**, 1149-1155.

98. Tracey, K. J. (2010) Understanding immunity requires more than immunology, *Nat Immunol.* **11**, 561-564.

99. Zhou, X., Fragala, M. S., McElhaney, J. E. & Kuchel, G. A. (2010) Conceptual and methodological issues relevant to cytokine and inflammatory marker measurements in clinical research, *Curr Opin Clin Nutr Metab Care.* **13**, 541-547.

100. Kitano, H. (2002) Computational systems biology, *Nature.* **420**, 206-210.

101. Kitano, H. (2004) Biological robustness, *Nat Rev Genet.* **5**, 826-837.

102. Li, J., Yuan, Z. & Zhang, Z. (2010) The Cellular Robustness by Genetic Redundancy in Budding Yeast, *PLOS Genet.* **6**, e1001187.

103. Gu, Z., Steinmetz, L. M., Gu, X., Scharfe, C., Davis, R. W. & Li, W.-H. (2003) Role of duplicate genes in genetic robustness against null mutations, *Nature.* **421**, 63-66.

104. Kelley, R. & Ideker, T. (2005) Systematic interpretation of genetic interactions using protein networks, *Nature Biotech.* **23**, 561-566.

105. Broderick, G. & Craddock, T. J. A. (2013) Systems biology of complex symptom profiles: Capturing interactivity across behaviour, brain and immune regulation, *Brain Behav Immun.* **29**, 1-8.

106. Barabasi, A.-L., Gulbahce, N. & Loscalzo, J. (2011) Network medicine: a network-based approach to human disease, *Nat Rev Genet.* **12**, 56-68.

107. de la Fuente, A. (2010) From 'differential expression' to 'differential networking' – identification of dysfunctional regulatory networks in diseases, *Trends Genet.* **26**, 326-333.

108. Margolin, A. A., Nemenman, I., Basso, K., Wiggins, C., Stolovitzky, G., Favera, R. D. & Califano, A. (2006) ARACNE: An Algorithm for the Reconstruction of Gene Regulatory Networks in a Mammalian Cellular Context, *BMC Bioinformatics.* **7**, S7.

109. Carro, M. S., Lim, W. K., Alvarez, M. J., Bollo, R. J., Zhao, X., Snyder, E. Y., Sulman, E. P., Anne, S. L., Doetsch, F., Colman, H., Lasorella, A., Aldape, K., Califano, A. & Iavarone, A. (2009) The transcriptional network for mesenchymal transformation of brain tumours, *Nature.* **463**, 318-325.

110. Sumazin, P., Yang, X., Chiu, H.-S., Chung, W.-J., Iyer, A., Llobet-Navas, D., Rajbhandari, P., Bansal, M., Guarnieri, P., Silva, J. & Califano, A. (2011) An Extensive MicroRNA-Mediated Network of RNA-RNA Interactions Regulates Established Oncogenic Pathways in Glioblastoma, *Cell.* **147**, 370-381.

111. Torkamani, A., Dean, B., Schork, N. J. & Thomas, E. A. (2010) Coexpression network analysis of neural tissue reveals perturbations in developmental processes in schizophrenia, *Genome Res.* **20**, 403-412.

112. Yu, J., Smith, V. A., Wang, P. P., Hartemink, A. J. & Jarvis, E. D. (2004) Advances to Bayesian network inference for generating causal networks from observational biological data, *Bioinformatics.* **20**, 3594-3603.

113. Haury, A.-C., Mordelet, F., Vera-Licona, P. & Vert, J.-P. (2012) TIGRESS: Trustful Inference of Gene REgulation using Stability Selection, *BMC Syst Biol.* **6**, 145.

114. Huynh-Thu, V. A., Irrthum, A., Wehenkel, L. & Geurts, P. (2010) Inferring Regulatory Networks from Expression Data Using Tree-Based Methods, *PLOS ONE.* **5**, e12776.

115. Guo, A.-Y., Sun, J., Jia, P. & Zhao, Z. (2010) A Novel microRNA and transcription factor mediated regulatory network in schizophrenia, *BMC Syst Biol.* **4**, 10.

116. Yeung, M. K. S., Tegner, J. & Collins, J. J. (2002) Reverse engineering gene networks using singular value decomposition and robust regression, *Proc Natl Acad Sci USA.* **99**, 6163-6168.

117. Schmidt, M. D., Vallabhajosyula, R. R., Jenkins, J. W., Hood, J. E., Soni, A. S., Wikswo, J. P. & Lipson, H. (2011) Automated refinement and inference of analytical models for metabolic networks., *Phys Biol* **8**, 055011.

118. Erdös, P. & Rényi, A. (1959) On random graphs, I, *Publ Math (Debrecen).* **6**, 290-297.

119. Watts, D. J. & Strogatz, S. H. (1998) Collective dynamics of 'small-world' networks, *Nature.* **393**, 440-442.

120. Barabási, A.-L. & Albert, R. (1999) Emergence of Scaling in Random Networks, *Science.* **286**, 509-512.

121. Fell, D. A. & Wagner, A. (2000) The small world of metabolism, *Nature Biotech.* **18**, 1121-1122.

122. Newman, M. (2003) The Structure and Function of Complex Networks, *SIAM Rev.* **45**, 167-256.

123. Ravasz, E., Somera, A. L., Mongru, D. A., Oltvai, Z. N. & Barabási, A. L. (2002) Hierarchical Organization of Modularity in Metabolic Networks, *Science.* **297**, 1551-1555.

124. Han, J.-D. J., Bertin, N., Hao, T., Goldberg, D. S., Berriz, G. F., Zhang, L. V., Dupuy, D., Walhout, A. J. M., Cusick, M. E., Roth, F. P. & Vidal, M. (2004) Evidence for dynamically organized modularity in the yeast protein–protein interaction network, *Nature.* **430**, 88-93.

125. Baldassano, S. N. & Bassett, D. S. (2016) Topological distortion and reorganized modular structure of gut microbial co-occurrence networks in inflammatory bowel disease, *Sci Rep.* **6**, 26087.

126. Palesi, F., Castellazzi, G., Casiraghi, L., Sinforiani, E., Vitali, P., Gandini Wheeler-Kingshott, C. A. M. & D'Angelo, E. (2016) Exploring Patterns of Alteration in Alzheimer's Disease Brain Networks: A Combined Structural and Functional Connectomics Analysis, *Front Neurosci.* **10**, 380.

127. Sang, L., Zhang, J., Wang, L., Zhang, J., Zhang, Y., Li, P., Wang, J. & Qiu, M. (2015) Alteration of Brain Functional Networks in Early-Stage Parkinson's Disease: A Resting-State fMRI Study, *PLOS ONE.* **10**, e0141815.

128. Albert, R., Jeong, H. & Barabási, A.-L. (2000) Error and attack tolerance of complex networks, *Nature.* **406**, 378-382.

129. Jeong, H., Mason, S. P., Barabási, A. L. & Oltvai, Z. N. (2001) Lethality and centrality in protein networks, *Nature.* **411**, 41-42.

130. Milo, R., Shen-Orr, S., Itzkovitz, S., Kashtan, N., Chklovskii, D. & Alon, U. (2002) Network Motifs: Simple Building Blocks of Complex Networks, *Science.* **298**, 824-827.

131. Prill, R. J., Iglesias, P. A. & Levchenko, A. (2005) Dynamic Properties of Network Motifs Contribute to Biological Network Organization, *PLOS Biol.* **3**, e343.

132. Alon, U., Surette, M. G., Barkai, N. & Leibler, S. (1999) Robustness in bacterial chemotaxis, *Nature.* **397**, 168-171.

133. Yu, H., Kim, P. M., Sprecher, E., Trifonov, V. & Gerstein, M. (2007) The Importance of Bottlenecks in Protein Networks: Correlation with Gene Essentiality and Expression Dynamics, *PLOS Comp Biol.* **3**, e59.

134. Vergelli, M., Mazzanti, B., Traggiai, E., Biagioli, T., Ballerini, C., Parigi, A., Konse, A., Pellicanò, G. & Massacesi, L. (2001) Short-term evolution of autoreactive T cell repertoire in multiple sclerosis, *J Neurosci Res.* **66**, 517-524.

135. Aschbacher, K., Adam, E. K., Crofford, L. J., Kemeny, M. E., Demitrack, M. A. & Ben-Zvi, A. (2012) Linking disease symptoms and subtypes with personalized systems-based phenotypes: A proof of concept study, *Brain Behav Immun.* **26**, 1047-1056.

Chapter 2: Inferring regulatory biology from time course data: Constraints Typical of *In vivo* studies

1. Barabasi, A.-L. & Oltvai, Z. N. (2004) Network Biology: Understanding the cell's functional organization, *Nat Rev Genet.* **5**, 101-113.

2. Barabasi, A.-L., Gulbahce, N. & Loscalzo, J. (2011) Network medicine: a network-based approach to human disease, *Nat Rev Genet.* **12**, 56-68.

3. Sauer, U., Heinemann, M. & Zamboni, N. (2007) Getting Closer to the Whole Picture, *Science.* **316**, 550-551.

4. Akutsu, T., Miyano, S. & Kuhara, S. (1999) Identification of genetic networks from a small number of gene expression patterns under the Boolean network model, *Pac Symp Biocomput*, 17-28.

5. Akutsu, T., Miyano, S. & Kuhara, S. (2000) Inferring qualitative relations in genetic networks and metabolic pathways, *Bioinformatics.* **16**, 727-734.

6. Liang, S., Fuhrman, S. & Somogyi, R. (1998) Reveal, a general reverse engineering algorithm for inference of genetic network architectures. in *Pac Symp Biocomput* pp. 18-29

7. Shmulevich, I., Dougherty, E. R., Kim, S. & Zhang, W. (2002) Probabilistic Boolean networks: a rule-based uncertainty model for gene regulatory networks, *Bioinformatics.* **18**, 261-274.

8. Martin, S., Zhang, Z., Martino, A. & Faulon, J.-L. (2007) Boolean dynamics of genetic regulatory networks inferred from microarray time series data, *Bioinformatics.* **23**, 866-874.

9. Kim, H., Lee, J. & Park, T. (2007) Boolean networks using the chi-square test for inferring large-scale gene regulatory networks, *BMC Bioinformatics.* **8**, 37.

10. Yu, J., Smith, V. A., Wang, P. P., Hartemink, A. J. & Jarvis, E. D. (2004) Advances to Bayesian network inference for generating causal networks from observational biological data, *Bioinformatics.* **20**, 3594-3603.

11. Zou, M. & Conzen, S. D. (2005) A new dynamic Bayesian network (DBN) approach for identifying gene regulatory networks from time course microarray data, *Bioinformatics.* **21**, 71-79.

12. Kim, S. Y., Imoto, S. & Miyano, S. (2003) Inferring gene networks from time series microarray data using dynamic Bayesian networks, *Brief Bioinform.* **4**, 228-235.

13. Vinh, N. X., Chetty, M., Coppel, R. & Wangikar, P. P. (2011) GlobalMIT: learning globally optimal dynamic bayesian network with the mutual information test criterion, *Bioinformatics.* **27**, 2765-2766.

14. Wilczyński, B. & Dojer, N. (2009) BNFinder: exact and efficient method for learning Bayesian networks, *Bioinformatics.* **25**, 286-287.

15. Dojer, N., Bednarz, P., Podsiadło, A. & Wilczyński, B. (2013) BNFinder2: Faster Bayesian network learning and Bayesian classification, *Bioinformatics.* **29**, 2068-2070.

16. Ernst, J., Vainas, O., Harbison, C. T., Simon, I. & Bar-Joseph, Z. (2007) Reconstructing dynamic regulatory maps, *Mol Syst Biol.* **3**, 74.

17. Schulz, M., Devanny, W., Gitter, A., Zhong, S., Ernst, J. & Bar-Joseph, Z. (2012) DREM 2.0: Improved reconstruction of dynamic regulatory networks from time-series expression data, *BMC Syst Biol.* **6**, 104.

18. Madar, A., Greenfield, A., Vanden-Eijnden, E. & Bonneau, R. (2010) DREAM3: Network Inference Using Dynamic Context Likelihood of Relatedness and the Inferelator, *PLoS ONE.* **5**, e9803.

19. Zoppoli, P., Morganella, S. & Ceccarelli, M. (2010) TimeDelay-ARACNE: Reverse engineering of gene networks from time-course data by an information theoretic approach, *BMC Bioinform.* **11**, 154.

20. Bansal, M. & di Bernardo, D. (2007) Inference of gene networks from temporal gene expression profiles, *IET Syst Biol.* **1**, 306-312.

21. Yeung, M. K. S., Tegner, J. & Collins, J. J. (2002) Reverse engineering gene networks using singular value decomposition and robust regression, *Proc Natl Acad Sci USA.* **99**, 6163-6168.

22. Gardner, T. S., di Bernardo, D., Lorenz, D. & Collins, J. J. (2003) Inferring Genetic Networks and Identifying Compound Mode of Action via Expression Profiling, *Science.* **301**, 102-105.

23. Tegner, J., Yeung, M. K. S., Hasty, J. & Collins, J. J. (2003) Reverse engineering gene networks: Integrating genetic perturbations with dynamical modeling, *Proc Natl Acad Sci.* **100**, 5944-5949.

24. Bansal, M., Gatta, G. D. & di Bernardo, D. (2006) Inference of gene regulatory networks and compound mode of action from time course gene expression profiles, *Bioinformatics.* **22**, 815-822.

25. Bonneau, R., Reiss, D., Shannon, P., Facciotti, M., Hood, L., Baliga, N. & Thorsson, V. (2006) The Inferelator: an algorithm for learning parsimonious regulatory networks from systems-biology data sets de novo, *Genome Biology.* **7**, R36.

26. Yip, K. Y., Alexander, R. P., Yan, K.-K. & Gerstein, M. (2010) Improved Reconstruction of In Silico Gene Regulatory Networks by Integrating Knockout and Perturbation Data, *PLoS ONE.* **5**, e8121.

27. Chowdhury, A., Chetty, M. & Vinh, N. (2013) Incorporating time-delays in S-System model for reverse engineering genetic networks, *BMC Bioinformatics.* **14**, 196.

28. Henderson, J. & Michailidis, G. (2014) Network Reconstruction Using Nonparametric Additive ODE Models, *PLoS ONE.* **9**, e94003.

29. Li, X., Rao, S., Jiang, W., Li, C., Xiao, Y., Guo, Z., Zhang, Q., Wang, L., Du, L., Li, J., Li, L., Zhang, T. & Wang, Q. K. (2006) Discovery of time-delayed gene regulatory networks based on temporal gene expression profiling, *BMC Bioinformatics.* **7**, 26.

30. Lozano, A. C., Abe, N., Liu, Y. & Rosset, S. (2009) Grouped graphical Granger modeling for gene expression regulatory networks discovery, *Bioinformatics.* **25**, 110-118.

31. ElBakry, O., Ahmad, M. O. & Swamy, M. N. S. (2013) Inference of Gene Regulatory Networks with Variable Time Delay from Time-Series Microarray Data, *IEEE/ACM Trans Comp Biol Bioinform* **10**, 671-687.

32. Greenfield, A., Madar, A., Ostrer, H. & Bonneau, R. (2010) DREAM4: Combining Genetic and Dynamic Information to Identify Biological Networks and Dynamical Models, *PLoS ONE.* **5**, e13397.

33. Greenfield, A., Hafemeister, C. & Bonneau, R. (2013) Robust data-driven incorporation of prior knowledge into the inference of dynamic regulatory networks, *Bioinformatics.* **29**, 1060-1067.

34. Li, Z., Li, P., Krishnan, A. & Liu, J. (2011) Large-scale dynamic gene regulatory network inference combining differential equation models with local dynamic Bayesian network analysis, *Bioinformatics.* **27**, 2686-2691.

35. Huynh-Thu, V. A. & Sanguinetti, G. (2015) Combining tree-based and dynamical systems for the inference of gene regulatory networks, *Bioinformatics*. **31**, 1614-1622

36. He, F., Balling, R. & Zeng, A.-P. (2009) Reverse engineering and verification of gene networks: Principles, assumptions, and limitations of present methods and future perspectives, *J Biotech.* **144**, 190-203.

37. Karlebach, G. & Shamir, R. (2008) Modelling and analysis of gene regulatory networks, *Nat Rev Mol Cell Biol.* **9**, 770-780.

38. Cho, K.-H., Choo, S.-M., Jung, S. H., Kim, J.-R., Choi, H.-S. & Kim, J. (2007) Reverse engineering of gene regulatory networks, *IET Syst Biol.* **1**, 149-163.

39. Markowetz, F. & Spang, R. (2007) Inferring cellular networks - a review, *BMC Bioinform.* **8**, S5.

40. Jong, H. d. (2002) Modeling and simulation of genetic regulatory systems: A literature review, *J Comp Biol.* **9**, 67-103.

41. Gardner, T. S. & Faith, J. J. (2005) Reverse-engineering transcription control networks, *Phys Life Rev.* **2**, 65-88.

42. Hecker, M., Lambeck, S., Toepfer, S., van Someren, E. & Guthke, R. (2009) Gene regulatory network inference: Data integration in dynamic models, A review, *Biosystems.* **96**, 86-103.

43. Chai, L. E., Loh, S. K., Low, S. T., Mohamad, M. S., Deris, S. & Zakaria, Z. (2014) A review on the computational approaches for gene regulatory network construction, *Comput Biol Med.* **48**, 55-65.

44. Villaverde, A. F. & Banga, J. R. (2013) Reverse engineering and identification in systems biology: strategies, perspectives and challenges, *J R Soc Interface.* **11,** 0505.

45. Kim, Y., Han, S., Choi, S. & Hwang, D. (2013) Inference of dynamic networks using time-course data, *Brief Bioinform*.**15**, 212-228.

46. Stolovitzky, G., Monroe, D. O. N. & Califano, A. (2007) Dialogue on Reverse-Engineering Assessment and Methods, *Ann N Y Acad Sci.* **1115**, 1-22.

47. Stolovitzky, G., Prill, R. J. & Califano, A. (2009) Lessons from the DREAM2 Challenges, *Ann N Y Acad Sci.* **1158**, 159-195.

48. Prill, R. J., Marbach, D., Saez-Rodriguez, J., Sorger, P. K., Alexopoulos, L. G., Xue, X., Clarke, N. D., Altan-Bonnet, G. & Stolovitzky, G. (2010) Towards a Rigorous Assessment of Systems Biology Models: The DREAM3 Challenges, *PLoS ONE.* **5**, e9202.

49. Marbach, D., Prill, R. J., Schaffter, T., Mattiussi, C., Floreano, D. & Stolovitzky, G. (2010) Revealing strengths and weaknesses of methods for gene network inference, *Proc Natl Acad Sci USA*. **107**, 6286-6291.

50. Marbach, D., Costello, J. C., Kuffner, R., Vega, N. M., Prill, R. J., Camacho, D. M., Allison, K. R., Kellis, M., Collins, J. J. & Stolovitzky, G. (2012) Wisdom of crowds for robust gene network inference, *Nat Meth.* **9**, 796-804.

51. Bansal, M., Belcastro, V., Ambesi-Impiombato, A. & di Bernardo, D. (2007) How to infer gene networks from expression profiles, *Mol Syst Biol.* **3**, 78.

52. Camacho, D., Vera Licona, P., Mendes, P. & Laubenbacher, R. (2007) Comparison of Reverse-Engineering Methods Using an in Silico Network, *Ann N Y Acad Sci.* **1115**, 73-89.

53. Penfold, C. A. & Wild, D. L. (2011) How to infer gene networks from expression profiles, revisited, *Interface Focus*. **1**, 857-870.

54. Hendrickx, D. M., Hendriks, M. M. W. B., Eilers, P. H. C., Smilde, A. K. & Hoefsloot, H. C. J. (2011) Reverse engineering of metabolic networks, a critical assessment, *Mol BioSyst.* **7**, 511-520.

55. Zhu J, C. Y., Leonardson AS, Wang K, Lamb JR, Emilsson V, Schadt EE (2010) Characterizing Dynamic Changes in the Human Blood Transcriptional Network, *PLoS Comput Biol.* **6(2)**, e1000671.

56. Hickman, G. J. & Hodgman, T. C. (2009) INFERENCE OF GENE REGULATORY NETWORKS USING BOOLEAN-NETWORK INFERENCE METHODS, *J Bioinform Comput Biol.* **07**, 1013-1029.

57. Li, P., Zhang, C., Perkins, E., Gong, P. & Deng, Y. (2007) Comparison of probabilistic Boolean network and dynamic Bayesian network approaches for inferring gene regulatory networks, *BMC Bioinformatics.* **8**, S13.

58. Steuer, R., Kurths, J., Daub, C. O., Weise, J. & Selbig, J. (2002) The mutual information: Detecting and evaluating dependencies between variables, *Bioinformatics.* **18**, S231-S240.

59. Zou, C. & Feng, J. (2009) Granger causality vs. dynamic Bayesian network inference: a comparative study, *BMC Bioinformatics.* **10**, 122.

60. Shojaie, A. & Michailidis, G. (2010) Discovering graphical Granger causality using the truncating lasso penalty, *Bioinformatics.* **26**, i517-i523.

61. Di Camillo, B., Toffolo, G. & Cobelli, C. (2009) A Gene Network Simulator to Assess Reverse Engineering Algorithms, *Annals New York Acad Sci.* **1158**, 125-142.

62. Cantone, I., Marucci, L., Iorio, F., Ricci, M. A., Belcastro, V., Bansal, M., Santini, S., di Bernardo, M., di Bernardo, D. & Cosma, M. P. (2009) A Yeast Synthetic Network for *In Vivo* Assessment of Reverse-Engineering and Modeling Approaches, *Cell.* **137**, 172-181.

63. Sambo, F., camillo, B. D. & Toffolo, G. (2008) CNET: an algorithm for reverse engineering of causalgene networks in *8th Workshop on Network Tools and Applications in Biology NETTAB 2008* pp. 134-136National Research Council, Milan, Italy.

64. di Bernardo, D., Thompson, M. J., Gardner, T. S., Chobot, S. E., Eastwood, E. L., Wojtovich, A. P., Elliott, S. J., Schaus, S. E. & Collins, J. J. (2005) Chemogenomic profiling on a genome-wide scale using reverse-engineered gene networks, *Nat Biotech.* **23**, 377-383.

65. Rawlings, J. O. (1988) Collinearity Diagnostics in *Applied Regression Analysis* (Barndorff-Nielsen, O., Bickel, PJ., Cleveland, WS., Dudley, RM., ed) pp. 273-281, Pacific Grove: Wadsworth and Brooks.

66. Draper, N. & Smith, H. (1998) Stepwise Regression in *Applied Regression Analysis* pp. 307-312, Wiley-Interscience, Hoboken, NJ.

67. Jackson, J. E. (1991) Singular Value Decomposition: Multidimensional Scaling I in *A User's Guide to Principal Components* pp. 189-232, John Wiley & Sons, Inc.

68. Wold, S., Sjöström, M. & Eriksson, L. (2001) PLS-regression: a basic tool of chemometrics, *Chemom Intell Lab Syst.* **58**, 109-130.

69. Wold, S., Trygg, J., Berglund, A. & Antti, H. (2001) Some recent developments in PLS modeling, *Chemom Intell Lab Syst.* **58**, 131-149.

70. Horn, J. L. (1965) A rationale and test for the number of factors in factor analysis, *Psychometrika.* **30**, 179-185.

71. Frontier, S. (1976) Étude de la décroissance des valeurs propres dans une analyse en composantes principales: comparaison avec le modèle de bâton brisé, *J Exp Marine Biol Ecol.* **25**, 67-75.

72. Bartlett, M. S. (1950) Tests of significance in factor analysis, *Br J Psych Stat Sec.* **3**, 77-85.

73. Jackson, J. E. (1991) PCA with more than Two Variables in *A User's Guide to Principal Components* (Shewhart, W. A., Wilks, S. S., ed) pp. 26-62, Wiley-Interscience, Hoboken, NJ.

74. Peres-Neto, P. R., Jackson, D. A. & Somers, K. M. (2005) How many principal components? Stopping rules for determining the number of non-trivial axes revisited., *Comp Stat Data An.* **49**, 974-997.

75. Margolin, A., Nemenman, I., Basso, K., Wiggins, C., Stolovitzky, G., Favera, R. & Califano, A. (2006) ARACNE: An Algorithm for the Reconstruction of Gene Regulatory Networks in a Mammalian Cellular Context, *BMC Bioinform.* **7**, S7.

76. Cover, T. M. & Thomas, J. A. (2006) *Elements of Information Theory*, John Wiley & Sons, New York.

77. Kaiser, M. (2011) A tutorial in connectome analysis: Topological and spatial features of brain networks, *NeuroImage.* **57**, 892-907.

78. Vinh, N. X., Chetty, M., Coppel, R. & Wangikar, P. P. (2012) Issues impacting genetic network reverse engineering algorithm validation using small networks, *Biochim Biophys Acta.* **1824**, 1434-1441.

79. Schaffter, T., Marbach, D. & Floreano, D. (2011) GeneNetWeaver: in silico benchmark generation and performance profiling of network inference methods, *Bioinformatics.* **27**, 2263-2270.

80. Gama-Castro, S., Salgado, H., Peralta-Gil, M., Santos-Zavaleta, A., Muñiz-Rascado, L., Solano-Lira, H., Jimenez-Jacinto, V., Weiss, V., García-Sotelo, J. S., López-Fuentes, A., Porrón-Sotelo, L., Alquicira-Hernández, S., Medina-Rivera, A., Martínez-Flores, I., Alquicira-Hernández, K., Martínez-Adame, R., Bonavides-Martínez, C., Miranda-Ríos, J., Huerta, A. M., Mendoza-Vargas, A., Collado-Torres, L., Taboada, B., Vega-Alvarado, L., Olvera, M., Olvera, L., Grande, R., Morett, E. & Collado-Vides, J. (2011) RegulonDB version 7.0: transcriptional regulation of Escherichia coli K-12 integrated within genetic sensory response units (Gensor Units), *Nucleic Acids Research.* **39**, D98-D105.

81. Ackers, G. K., Johnson, A. D. & Shea, M. A. (1982) Quantitative model for gene regulation by lambda phage repressor, *Proc Natl Acad Sci USA.* **79**, 1129-1133.

82. Whitfield, M. L., Sherlock, G., Saldanha, A. J., Murray, J. I., Ball, C. A., Alexander, K. E., Matese, J. C., Perou, C. M., Hurt, M. M., Brown, P. O. & Botstein, D. (2002) Identification of Genes Periodically Expressed in the Human Cell Cycle and Their Expression in Tumors, *Mol Biol Cell.* **13**, 1977-2000.

83. Wang, K., Saito, M., Bisikirska, B. C., Alvarez, M. J., Lim, W. K., Rajbhandari, P., Shen, Q., Nemenman, I., Basso, K., Margolin, A. A., Klein, U., Dalla-Favera, R. & Califano, A. (2009) Genome-wide identification of post-translational modulators of transcription factor activity in human B cells, *Nat Biotechnol.* **27**, 829-839.

84. Frankenstein, Z., Alon, U. & Cohen, I. (2006) The immune-body cytokine network defines a social architecture of cell interactions, *Biol Dir.* **1**, 32.

85. Margolin, A. A. & Califano, A. (2007) Theory and Limitations of Genetic Network Inference from Microarray Data, *Ann N Y Acad Sci.* **1115**, 51-72.

86. Margolin, A. A., Wang, K., Califano, A. & Nemenman, I. (2010) Multivariate dependence and genetic networks inference, *IET Syst Biol.* **4**, 428-440.

87. Guan, C., Ye, C., Yang, X. & Gao, J. (2010) A review of current large-scale mouse knockout efforts, *genesis.* **48**, 73-85.

88. Gollee, H., Mamma, A., Loram, I. & Gawthrop, P. (2012) Frequency-domain identification of the human controller, *Biol Cybern.* **106**, 359-372.

89. Kawada, T., Sato, T., Inagaki, M., Shishido, T., Tatewaki, T., Yanagiya, Y., Zheng, C., Sugimachi, M. & Sunagawa, K. (2000) Closed-Loop Identification of Carotid Sinus Baroreflex Transfer Characteristics Using Electrical Stimulation, *Jpn J Physiol.* **50**, 371-380.

90. Schmidt, M. D., Vallabhajosyula, R. R., Jenkins, J. W., Hood, J. E., Soni, A. S., Wikswo, J. P. & Lipson, H. (2011) Automated refinement and inference of analytical models for metabolic networks., *Phys Biol* **8**, 055011.

91. Dong, C.-Y., Yoon, T.-W., Bates, D. & Cho, K.-H. (2010) Identification of feedback loops embedded in cellular circuits by investigating non-causal impulse response components, *J Math Biol.* **60**, 285-312.

92. Dong, C.-Y., Shin, D., Joo, S., Nam, Y. & Cho, K.-H. (2012) Identification of feedback loops in neural networks based on multi-step Granger causality, *Bioinformatics.* **28**, 2146-2153.

Chapter 3: Leveraging Prior Knowledge to Recover Characteristic Immune Regulatory Motifs in Gulf War Illness.

1. Wolfe, J., Proctor Susan, P., Davis Jennifer, D., Borgos Marlana, S. & Friedman Matthew, J. (1998) Health symptoms reported by Persian Gulf War veterans two years after return, *Am J Ind Med.* **33**, 104-113.

2. Unwin, C., Blatchley, N., Coker, W., Ferry, S., Hotopf, M., Hull, L., Ismail, K., Palmer, I., David, A. & Wessely, S. (1999) Health of UK servicemen who served in Persian Gulf War, *The Lancet.* **353**, 169-178.

3. Bourdette, D. N., McCauley, L. A., Barkhuizen, A., Johnston, W., Wynn, M., Joos, S. K., Storzbach, D., Shuell, T. & Sticker, D. (2001) Symptom Factor Analysis, Clinical Findings, and Functional Status in a Population-Based Case Control Study of Gulf WarUnexplained Illness, *J Occup Environ Med.* **43**, 1026-40.

4. Kang, H. K., Natelson, B. H., Mahan, C. M., Lee, K. Y. & Murphy, F. M. (2003) Post-traumatic stress disorder and chronic fatigue syndrome-like illness among Gulf War veterans: a population-based survey of 30,000 veterans, *Am J Epidemiol.* **157**, 141-148.

5. Golier, J. A., Legge, J. & Yehuda, R. (2006) The ACTH Response to Dexamethasone in Persian Gulf War Veterans, *Ann N Y Acad Sci.* **1071**, 448-453.

6. Golier, J. A., Schmeidler, J., Legge, J. & Yehuda, R. (2007) Twenty-four Hour Plasma Cortisol and Adrenocorticotropic Hormone in Gulf War Veterans: Relationships to Posttraumatic Stress Disorder and Health Symptoms, *Biol Psychiatry.* **62**, 1175-1178.

7. Rice, M. A., Craddock, T. J. A., Folcik, V. A., del Rosario, R. M., Barnes, Z. M., Klimas, N. G., Fletcher, M. A., Zysman, J. & Broderick, G. (2014) Gulf War Illness: Is there lasting damage to the endocrine-immune circuitry?, *Sys Biomed.* **2**, 80-89.

8. Duclos, M. & Tabarin, A. (2016) Exercise and the Hypothalamo-Pituitary-Adrenal Axis in *Sports Endocrinology* (Lanfranco, F. & Strasburger, C., eds) pp. 12-26, Front Horm Res.

9. Nagelkirk, P. R., Cook, D. B., Peckerman, A., Kesil, W., Sakowski, T., Natelson, B. H. & LaManca, J. J. (2003) Aerobic capacity of Gulf War veterans with chronic fatigue syndrome, *Mil Med.* **168**, 750-55.

10. Cook, D. B., Nagelkirk, P. R., Peckerman, A., Poluri, A., Lamanca, J. J. & Natelson, B. H. (2003) Perceived Exertion in Fatiguing Illness: Gulf War Veterans with Chronic Fatigue Syndrome, *Med Sci Sports Exerc.* **35**, 569-574.

11. Rayhan, R. U., Stevens, B. W., Raksit, M. P., Ripple, J. A., Timbol, C. R., Adewuyi, O., VanMeter, J. W. & Baraniuk, J. N. (2013) Exercise Challenge in Gulf War Illness Reveals Two Subgroups with Altered Brain Structure and Function, *PLOS ONE.* **8**, e63903.

12. Chalder, T., G, B., Pawlikowska, T., Watts, L., Wessely, S., Wright, D. & Wallace, E. P. (1993) Development of a fatigue scale, *J Psychosom Res.* **37**, 147-53.

13. McManimen, S. L., Sunnquist, M. L. & Jason, L. A. (2016) Deconstructing post-exertional malaise: An exploratory factor analysis, *J health psychol*, 1359105316664139.

14. Snell, C. R., Stevens, S. R., Davenport, T. E. & Van Ness, J. M. (2013) Discriminative Validity of Metabolic and Workload Measurements for Identifying People With Chronic Fatigue Syndrome, *Phys Ther.* **93**, 1484-1492.

15. Broderick, G., Fletcher, M. A., Gallagher, M., Barnes, Z., Vernon, S. D. & Klimas, N. G. (2012) Exploring the Diagnostic Potential of Immune Biomarker Coexpression in Gulf War Illness in *Psychoneuroimmunology Methods Mol Biol (Methods and Protocols)* (Yan, Q., ed) pp. 145-164, Humana Press, Totowa, NJ.

16. Smylie, A. L., Broderick, G., Fernandes, H., Razdan, S., Barnes, Z., Collado, F., Sol, C., Fletcher, M. A. & Klimas, N. (2013) A comparison of sex-specific immune signatures in Gulf War illness and chronic fatigue syndrome, *BMC Immunology.* **14**, 29.

17. Broderick, G., Kreitz, A., Fuite, J., Fletcher, M. A., Vernon, S. D. & Klimas, N. (2011) A pilot study of immune network remodeling under challenge in Gulf War Illness, *Brain Behav Immun.* **25**, 302-313.

18. Whistler, T., Fletcher, M. A., Lonergan, W., Zeng, X.-R., Lin, J.-M., LaPerriere, A., Vernon, S. D. & Klimas, N. G. (2009) Impaired immune function in Gulf War Illness, *BMC Med Genomics.* **2**, 12.

19. Broderick, G., Ben-Hamo, R., Vashishtha, S., Efroni, S., Nathanson, L., Barnes, Z., Fletcher, M. A. & Klimas, N. (2013) Altered immune pathway activity under exercise challenge in Gulf War Illness: An exploratory analysis, *Brain Behav Immun.* **28**, 159-169.

20. Koslik, H. J., Hamilton, G. & Golomb, B. A. (2014) Mitochondrial Dysfunction in Gulf War Illness Revealed by 31Phosphorus Magnetic Resonance Spectroscopy: A Case-Control Study, *PLOS ONE.* **9**, e92887.

21. Lengert, N. & Drossel, B. (2015) In silico analysis of exercise intolerance in myalgic encephalomyelitis/chronic fatigue syndrome, *Biophys Chem.* **202**, 21-31.

22. Vashishtha, S., Broderick, G., Craddock, T. J. A., Fletcher, M. A. & Klimas, N. G. (2015) Inferring Broad Regulatory Biology from Time Course Data: Have We Reached an Upper Bound under Constraints Typical of *In Vivo* Studies?, *PLOS ONE.* **10**, e0127364.

23. Fritsch, P., Craddock, T. J. A., del Rosario, R. M., Rice, M. A., Smylie, A., Folcik, V. A., de Vries, G., Fletcher, M. A., Klimas, N. G. & Broderick, G. (2013) Succumbing to the laws of attraction, *Sys Biomed.* **1**, 179-194.

24. Folcik, V. A., An, G. C. & Orosz, C. G. (2007) The Basic Immune Simulator: An agent-based model to study the interactions between innate and adaptive immunity, *Theor Biol Med Model.* **4**, 39.

25. Folcik, V. A., Broderick, G., Mohan, S., Block, B., Ekbote, C., Doolittle, J., Khoury, M., Davis, L. & Marsh, C. B. (2011) Using an agent-based model to analyze the dynamic communication network of the immune response, *Theor Biol Med Model.* **8**, 1.

26. Craddock, T. J. A., Del Rosario, R. R., Rice, M., Zysman, J. P., Fletcher, M. A., Klimas, N. G. & Broderick, G. (2015) Achieving Remission in Gulf War Illness: A Simulation-Based Approach to Treatment Design, *PLoS ONE.* **10**, e0132774.

27. Fukuda, K., Nisenbaum, R., Stewart, G. Thompson, W. W., Robin, L., Washko, R. M., Noah, D. L., Barrett, D. H., Randall, B., Herwaldt, B. L., Mawle, A. C., Reeves, W. C., (1998) Chronic multisymptom illness affecting air force veterans of the gulf war, *JAMA.* **280**, 981-988.

28. Reeves, W. C., Lloyd, A., Vernon, S. D., Klimas, N., Jason, L. A., Bleijenberg, G., Evengard, B., White, P. D., Nisenbaum, R., Unger, E. R. & the International Chronic Fatigue Syndrome Study, G. (2003) Identification of ambiguities in the 1994 chronic fatigue syndrome research case definition and recommendations for resolution, *BMC Health Serv Res.* **3**, 25-25.

29. Collins, J. F., Donta, S. T., Engel, C. C., Baseman, J. B., Dever, L. L., Taylor, T., Boardman, K. D., Martin, S. E., Wiseman, A. L. & Feussner, J. R. (2002) The Antibiotic Treatment Trial of Gulf War Veterans' Illnesses: issues, design, screening, and baseline characteristics, *Control Clin Trials.* **23**, 333-353.

30. McArdle, W. D., Katch, F. L. & Katch, V. L. (2007) *Exercise Physiology: Nutrition, Energy, and Human Performance* Lippincott Williams & Wilkins, London.

31. Hurwitz, Barry E., Coryell, Virginia T., Parker, M., Martin, P., LaPerriere, A., Klimas, Nancy G., Sfakianakis, George N. & Bilsker, Martin S. (2009) Chronic fatigue syndrome: illness severity, sedentary lifestyle, blood volume and evidence of diminished cardiac function, *Clin Sci (Lond).* **118**, 125-135.

32. Broderick, G., Fuite, J., Kreitz, A., Vernon, S. D., Klimas, N. & Fletcher, M. A. (2010) A Formal Analysis of Cytokine Networks in Chronic Fatigue Syndrome, *Brain Behav Immun.* **24**, 1209-1217.

33. Tapinos, A. & Mendes, P. (2013) A Method for Comparing Multivariate Time Series with Different Dimensions, *PLOS ONE.* **8**, e54201.

34. Szklarczyk, D., Franceschini, A., Wyder, S., Forslund, K., Heller, D., Huerta-Cepas, J., Simonovic, M., Roth, A., Santos, A., Tsafou, K. P., Kuhn, M., Bork, P., Jensen, L. J. & von Mering, C. (2015) STRING v10: protein–protein interaction networks, integrated over the tree of life, *Nucleic Acids Res.* **43**, D447-D452.

35. Wold, S., Sjöström, M. & Eriksson, L. (2001) PLS-regression: a basic tool of chemometrics, *Chemom Intell Lab Syst.* **58**, 109-130.

36. Wold, S., Trygg, J., Berglund, A. & Antti, H. (2001) Some recent developments in PLS modeling, *Chemom Intell Lab Syst.* **58**, 131-149.

37. Horn, J. L. (1965) A rationale and test for the number of factors in factor analysis, *Psychometrika.* **30**, 179-185.

38. Bartlett, M. S. (1950) Tests of significance in factor analysis, *Br J Psych Stat Sec.* **3**, 77-85.

39. Jackson, J. E. (1991) PCA with more than Two Variables in *A User's Guide to Principal Components* (Shewhart, W. A., Wilks, S. S., ed) pp. 26-62, Wiley-Interscience, Hoboken, NJ.

40. Bunke, H. (2000). Graph matching: Theoretical foundations, algorithms, and applications. Paper presented at the *Proc Vision Interface*, Montreal.

41. Dickinson, P. J., Bunke, H., Dadej, A. & Kraetzl, M. (2004) Matching graphs with unique node labels, *Pattern Anal Applic.* **7**, 243-254.

42. Harper, G., Bravi, G. S., Pickett, S. D., Hussain, J. & Green, D. V. S. (2004) The Reduced Graph Descriptor in Virtual Screening and Data-Driven Clustering of High-Throughput Screening Data, *J Chem Inform Comput Sci.* **44**, 2145-2156.

43. Barabasi, A.-L. & Oltvai, Z. N. (2004) Network Biology: Understanding the cell's functional organization, *Nat Rev Genet.* **5**, 101-113.

44. Huber, W., Carey, V. J., Long, L., Falcon, S. & Gentleman, R. (2007) Graphs in molecular biology, *BMC Bioinformatics.* **8**, S8-S8.

45. Di Camillo, B., Toffolo, G. & Cobelli, C. (2009) A Gene Network Simulator to Assess Reverse Engineering Algorithms, *Annals New York Acad Sci.* **1158**, 125-142.

46. Rayhan, R. U., Raksit, M. P., Timbol, C. R., Adewuyi, O., VanMeter, J. W. & Baraniuk, J. N. (2013) Prefrontal lactate predicts exercise-induced cognitive dysfunction in Gulf War Illness, *Am J Trans Res.* **5**, 212-223.

47. Alon, U. (2007) Network motifs: theory and experimental approaches, *Nat Rev Genet.* **8**, 450-461.

48. Hart, Y. & Alon, U. (2013) The Utility of Paradoxical Components in Biological Circuits, *Mol Cell.* **49**, 213-221.

49. Goentoro, L., Shoval, O., Kirschner, M. & Alon, U. (2009) The incoherent feedforward loop can provide fold-change detection in gene regulation, *Mol cell.* **36**, 894-899.

50. Gaffen, S. L., Jain, R., Garg, A. V. & Cua, D. J. (2014) IL-23-IL-17 immune axis: Discovery, Mechanistic Understanding, and Clinical Testing, *Nat Rev Immunol.* **14**, 585-600.

51. Smets, E. M. A., Garssen, B., Bonke, B. & De Haes, J. C. J. M. (1995) The multidimensional Fatigue Inventory (MFI) psychometric qualities of an instrument to assess fatigue, *J Psychosom Res.* **39**, 315-325.

52. Ware, J. E., Jr. & Sherbourne, C. D. (1992) The MOS 36-item short-form health survey (SF-36). I. Conceptual framework and item selection, *Med Care.* **30**, 473-483.

53. Sasaki-Iwaoka, H., Ohori, M., Imasato, A., Taguchi, K., Minoura, K., Saito, T., Kushima, K., Imamura, E., Kubo, S., Furukawa, S. & Morokata, T. (2018) Generation and characterization of a potent fully human monoclonal antibody against the interleukin-23 receptor, *Eur J Pharmacol.* **828**, 89-96.

54. Yang, J., Sundrud, M. S., Skepner, J. & Yamagata, T. (2014) Targeting Th17 cells in autoimmune diseases, *Trends Pharmacol Sci.* **35**, 493-500.

55. Locker, A. R., Michalovicz, L. T., Kelly, K. A., Miller, J. V., Miller, D. B. & O'Callaghan, J. P. (2017) Corticosterone primes the neuroinflammatory response to Gulf War Illness- relevant organophosphates independently of acetylcholinesterase inhibition, *J Neurochem.* **142**, 444-455.

56. Tanaka, T., Narazaki, M. & Kishimoto, T. (2012) Therapeutic Targeting of the Interleukin-6 Receptor, *Annu Rev Pharmacol Toxicol.* **52**, 199-219.

57. Tanaka, Y. & Martin Mola, E. (2014) IL-6 targeting compared to TNF targeting in rheumatoid arthritis: studies of olokizumab, sarilumab and sirukumab, *Ann Rheum Dis.* **73**, 1595-1597.

58. Krupp, L. B., LaRocca, N. G., Muir-Nash, J. & Steinberg, A. D. (1989) The fatigue severity scale: Application to patients with multiple sclerosis and systemic lupus erythematosus, *Arch Neurol.* **46**, 1121-1123.

59. Craddock, T. J. A., Fritsch, P., Rice, M. A., Jr., del Rosario, R. M., Miller, D. B., Fletcher, M. A., Klimas, N. G. & Broderick, G. (2014) A Role for Homeostatic Drive

in the Perpetuation of Complex Chronic Illness: Gulf War Illness and Chronic Fatigue Syndrome, *PLOS ONE.* **9**, e84839.

Chapter 4: Potentiation of a persistent immune response to Gulf war related exposures by prior physiological stress is conserved across species: A network study

1. Fukuda, K., Nisenbaum, R., Stewart, G. & et al. (1998) Chronic multisymptom illness affecting air force veterans of the gulf war, *JAMA.* **280**, 981-988.

2. Steele, L. (2000) Prevalence and Patterns of Gulf War Illness in Kansas Veterans: Association of Symptoms with Characteristics of Person, Place, and Time of Military Service, *Am J Epidemiol.* **152**, 992-1002.

3. Dursa, E. K., Barth, S. K., Schneiderman, A. I. & Bossarte, R. M. (2016) Physical and Mental Health Status of Gulf War and Gulf Era Veterans: Results From a Large Population-Based Epidemiological Study, *J Occup Environ Med.* **58**, 41-46.

4. White, R. F., Steele, L., O'Callaghan, J. P., Sullivan, K., Binns, J. H., Golomb, B. A., Bloom, F. E., Bunker, J. A., Crawford, F., Graves, J. C., Hardie, A., Klimas, N., Knox, M., Meggs, W. J., Melling, J., Philbert, M. A. & Grashow, R. (2016) Recent research on Gulf War illness and other health problems in veterans of the 1991 Gulf War: Effects of toxicant exposures during deployment, *Cortex.* **74**, 449-475.

5. Dantzer, R., O'Connor, J. C., Freund, G. G., Johnson, R. W. & Kelley, K. W. (2008) From inflammation to sickness and depression: when the immune system subjugates the brain, *Nat Rev Neurosci.* **9**, 46-56.

6. O'Callaghan, J. P., Kelly, K. A., Locker, A. R., Miller, D. B. & Lasley, S. M. (2015) Corticosterone primes the neuroinflammatory response to DFP in mice: potential animal model of Gulf War Illness, *J Neurochem.* **133**, 708-721.

7. Locker, A. R., Michalovicz, L. T., Kelly, K. A., Miller, J. V., Miller, D. B. & O'Callaghan, J. P. (2017) Corticosterone primes the neuroinflammatory response to Gulf War Illness - relevant organophosphates independently of acetylcholinesterase inhibition, *J Neurochem.* **142**, 444-455.

8. Koo, B.-B., Michalovicz, L. T., Calderazzo, S., Kelly, K. A., Sullivan, K., Killiany, R. J. & O'Callaghan, J. P. (2018) Corticosterone potentiates DFP-induced neuroinflammation and affects high-order diffusion imaging in a rat model of Gulf War Illness, *Brain Behav Immun.* **67**, 42-46.

9. Miller, J. V., LeBouf, R. F., Kelly, K. A., Michalovicz, L. T., Ranpara, A., Locker, A. R., Miller, D. B. & O'Callaghan, J. P. (2018) The Neuroinflammatory Phenotype in a Mouse Model of Gulf War Illness is Unrelated to Brain Regional Levels of Acetylcholine as Measured by Quantitative HILIC-UPLC-MS/MS, *Toxicol Sci.* **165**, 302-313.

10. Xanthos, D. N. & Sandkühler, J. (2013) Neurogenic neuroinflammation: inflammatory CNS reactions in response to neuronal activity, *Nat Rev Neurosci.* **15**, 43-53.

11. Chiu, I. M., von Hehn, C. A. & Woolf, C. J. (2012) Neurogenic inflammation and the peripheral nervous system in host defense and immunopathology, *Nat Neurosci.* **15**, 1063-1067.

12. Banks, W. A. & Erickson, M. A. (2010) The blood–brain barrier and immune function and dysfunction, *Neurobiol Dis.* **37**, 26-32.

13. Procaccini, C., Pucino, V., De Rosa, V., Marone, G. & Matarese, G. (2014) Neuro-Endocrine Networks Controlling Immune System in Health and Disease, *Front Immunol.* **5**, 143.

14. Goehler, L. E., Gaykema, R. P. A., Hansen, M. K., Anderson, K., Maier, S. F. & Watkins, L. R. (2000) Vagal immune-to-brain communication: a visceral chemosensory pathway, *Auton Neurosci.* **85**, 49-59.

15. Romeo, H. E., Tio, D. L., Rahman, S. U., Chiappelli, F. & Taylor, A. N. (2001) The glossopharyngeal nerve as a novel pathway in immune-to-brain communication: relevance to neuroimmune surveillance of the oral cavity, *J Neuroimmunol.* **115**, 91-100.

16. Quan, N., Whiteside, M. & Herkenham, M. (1998) Time course and localization patterns of interleukin-1β messenger rna expression in brain and pituitary after peripheral administration of lipopolysaccharide, *Neurosci.* **83**, 281-293.

17. Biesmans, S., Meert, T. F., Bouwknecht, J. A., Acton, P. D., Davoodi, N., De Haes, P., Kuijlaars, J., Langlois, X., Matthews, L. J. R., Ver Donck, L., Hellings, N. & Nuydens, R. (2013) Systemic Immune Activation Leads to Neuroinflammation and Sickness Behavior in Mice, *Mediators Inflamm.* **2013**, 14.

18. Nguyen, K. T., Deak, T., Owens, S. M., Kohno, T., Fleshner, M., Watkins, L. R. & Maier, S. F. (1998) Exposure to Acute Stress Induces Brain Interleukin-1β Protein in the Rat, *J Neurosci.* **18**, 2239-2246.

19. Hathway, G. J., Vega-Avelaira, D., Moss, A., Ingram, R. & Fitzgerald, M. (2009) Brief, low frequency stimulation of rat peripheral C-fibres evokes prolonged microglial-induced central sensitization in adults but not in neonates, *PAIN.* **144**, 110-118.

20. Zhang, Q., Zhou, X.-D., Denny, T., Ottenweller, J. E., Lange, G., LaManca, J. J., Lavietes, M. H., Pollet, C., Gause, W. C. & Natelson, B. H. (1999) Changes in Immune Parameters Seen in Gulf War Veterans but Not in Civilians with Chronic Fatigue Syndrome, *Clin Diagn Lab Immunol.* **6**, 6-13.

21. Skowera, A., Hotopf, M., Sawicka, E., Varela-Calvino, R., Unwin, C., Nikolaou, V., Hull, L., Ismail, K., David, A. S., Wessely, S. C. & Peakman, M. (2004) Cellular Immune Activation in Gulf War Veterans, *J Clin Immunol.* **24**, 66-73.

22. Whistler, T., Fletcher, M. A., Lonergan, W., Zeng, X.-R., Lin, J.-M., LaPerriere, A., Vernon, S. D. & Klimas, N. G. (2009) Impaired immune function in Gulf War Illness, *BMC Med Genomics.* **2**, 12.

23. Parkitny, L., Middleton, S., Baker, K. & Younger, J. (2015) Evidence for abnormal cytokine expression in Gulf War Illness: A preliminary analysis of daily immune monitoring data, *BMC Immunol.* **16**, 57.

24. Broderick, G., Kreitz, A., Fuite, J., Fletcher, M. A., Vernon, S. D. & Klimas, N. (2011) A pilot study of immune network remodeling under challenge in Gulf War Illness, *Brain Behav Immun.* **25**, 302-313.

25. Broderick, G., Ben-Hamo, R., Vashishtha, S., Efroni, S., Nathanson, L., Barnes, Z., Fletcher, M. A. & Klimas, N. (2013) Altered immune pathway activity under exercise challenge in Gulf War Illness: An exploratory analysis, *Brain Behav Immun.* **28**, 159-169.

26. Illnesses, R. A. C. R. o. G. W. V. (2008) Gulf War Illness and the Health of Gulf War Veterans: Scientific Findings and Recommendations in, U.S. Government Printing Office, Washington, DC.

27. Illnesses, R. A. C. R. o. G. W. V. (2014) Gulf War Illness and the Health of Gulf War Veterans: Research Update and Recommendations, 2009-2013 in, U.S. Government Printing Office, Washington, DC.

28. Corbel, V., Stankiewicz, M., Pennetier, C., Fournier, D., Stojan, J., Girard, E., Dimitrov, M., Molgó, J., Hougard, J.-M. & Lapied, B. (2009) Evidence for inhibition of cholinesterases in insect and mammalian nervous systems by the insect repellent deet, *BMC Biol.* **7**, 47.

29. Kerr Kathleen, J. (2015) Gulf War illness: an overview of events, most prevalent health outcomes, exposures, and clues as to pathogenesis in *Rev Environ Health* pp. 273-286

30. Zakirova, Z., Tweed, M., Crynen, G., Reed, J., Abdullah, L., Nissanka, N., Mullan, M., Mullan, M. J., Mathura, V., Crawford, F. & Ait-Ghezala, G. (2015) Gulf War Agent Exposure Causes Impairment of Long-Term Memory Formation and Neuropathological Changes in a Mouse Model of Gulf War Illness, *PLOS ONE.* **10**, e0119579.

31. Abdullah, L., Evans, J. E., Bishop, A., Reed, J. M., Crynen, G., Phillips, J., Pelot, R., Mullan, M. A., Ferro, A., Mullan, C. M., Mullan, M. J., Ait-Ghezala, G. & Crawford, F. C. (2012) Lipidomic Profiling of Phosphocholine Containing Brain Lipids in Mice with Sensorimotor Deficits and Anxiety-Like Features After Exposure to Gulf War Agents, *NeuroMol Med.* **14**, 349-361.

32. Pierce, L. M., Kurata, W. E., Matsumoto, K. W., Clark, M. E. & Farmer, D. M. (2016) Long-term epigenetic alterations in a rat model of Gulf War Illness, *NeuroToxicol.* **55**, 20-32.

33. Steele, L., Sastre, A., Gerkovich, M. M. & Cook, M. R. (2012) Complex Factors in the Etiology of Gulf War Illness: Wartime Exposures and Risk Factors in Veteran Subgroups, *Environ Health Perspect.* **120**, 112-118.

34. Golomb, B. A. (2008) Acetylcholinesterase inhibitors and Gulf War illnesses, *Proc Natl Acad Sci.* **105**, 4295-4300.

35. Sullivan, K., Krengel, M., Bradford, W., Stone, C., Thompson, T. A., Heeren, T. & White, R. F. (2018) Neuropsychological functioning in military pesticide applicators from the Gulf War: Effects on information processing speed, attention and visual memory, *Neurotoxicol Teratol.* **65**, 1-13.

36. O'Callaghan, J. P., Brinton, R. E. & McEwen, B. S. (1991) Glucocorticoids Regulate the Synthesis of Glial Fibrillary Acidic Protein in Intact and Adrenalectomized Rats but Do Not Affect Its Expression Following Brain Injury, *J Neurochem.* **57**, 860-869.

37. Grippo, A. J. & Scotti, M. A. L. (2013) Stress and Neuroinflammation, *Mod Trends PharmacoPsychiatry.* **28**, 20-32.

38. Sorrells, S. F. & Sapolsky, R. M. (2007) An inflammatory review of glucocorticoid actions in the CNS, *Brain Behav Immun.* **21**, 259-272.

39. Sorrells, S. F., Caso, J. R., Munhoz, C. D. & Sapolsky, R. M. (2009) The Stressed CNS: When Glucocorticoids Aggravate Inflammation, *Neuron.* **64**, 33-39.

40. Goujon, E., Layé, S., Parnet, P. & Dantzer, R. (1997) Regulation of cytokine gene expression in the central nervous system by glucocorticoids: Mechanisms and functional consequences, *Psychoneuroendocrinol.* **22**, S75-S80.

41. Frank, M. G., Thompson, B. M., Watkins, L. R. & Maier, S. F. (2012) Glucocorticoids mediate stress-induced priming of microglial pro-inflammatory responses, *Brain Behav Immun.* **26**, 337-345.

42. Frank, M. G., Miguel, Z. D., Watkins, L. R. & Maier, S. F. (2010) Prior exposure to glucocorticoids sensitizes the neuroinflammatory and peripheral inflammatory responses to E. coli lipopolysaccharide, *Brain Behav Immun.* **24**, 19-30.

43. Gannon, M. N. & McEwen, B. S. (1990) Calmodulin Involvement in Stress- and Corticosterone-Induced Down-Regulation of Cyclic AMP-Generating Systems in Brain, *J Neurochem.* **55**, 276-284.

44. Kelly, K. A., Miller, D. B., Bowyer, J. F. & O'Callaghan, J. P. (2012) Chronic exposure to corticosterone enhances the neuroinflammatory and neurotoxic responses to methamphetamine, *J Neurochem.* **122**, 995-1009.

45. Kelly, K. A., Michalovicz, L. T., Miller, J. V., Castranova, V., Miller, D. B. & O'Callaghan, J. P. (2018) Prior exposure to corticosterone markedly enhances and prolongs the neuroinflammatory response to systemic challenge with LPS, *PLOS ONE.* **13**, e0190546.

46. de Pablos, R. M., Villarán, R. F., Argüelles, S., Herrera, A. J., Venero, J. L., Ayala, A., Cano, J. & Machado, A. (2006) Stress Increases Vulnerability to Inflammation in the Rat Prefrontal Cortex, *J Neurosci.* **26**, 5709-5719.

47. Johnson, J. D., O'Connor, K. A., Hansen, M. K., Watkins, L. R. & Maier, S. F. (2003) Effects of prior stress on LPS-induced cytokine and sickness responses, *Am J Physiol Regul Integr Comp Physiol.* **284**, R422-R432.

48. Munhoz, C. D., Lepsch, L. B., Kawamoto, E. M., Malta, M. B., Lima, L. d. S., Werneck Avellar, M. C., Sapolsky, R. M. & Scavone, C. (2006) Chronic Unpredictable Stress Exacerbates Lipopolysaccharide-Induced Activation of Nuclear Factor-κB in the Frontal Cortex and Hippocampus via Glucocorticoid Secretion, *J Neurosci.* **26**, 3813-3820.

49. Munhoz, C. D., Sorrells, S. F., Caso, J. R., Scavone, C. & Sapolsky, R. M. (2010) Glucocorticoids Exacerbate Lipopolysaccharide-Induced Signaling in the Frontal Cortex and Hippocampus in a Dose-Dependent Manner, *J Neurosci.* **30**, 13690-13698.

50. Liu, P., Aslan, S., Li, X., Buhner, D. M., Spence, J. S., Briggs, R. W., Haley, R. W. & Lu, H. (2011) Perfusion deficit to cholinergic challenge in veterans with Gulf War Illness, *NeuroToxicol.* **32**, 242-246.

51. Haley, R. W., Spence, J. S., Carmack, P. S., Gunst, R. F., Schucany, W. R., Petty, F., Devous, M. D., Bonte, F. J. & Trivedi, M. H. (2009) Abnormal brain response to cholinergic challenge in chronic encephalopathy from the 1991 Gulf War, *Psychiatry Res.* **171**, 207-220.

52. Chao, L. L., Abadjian, L., Hlavin, J., Meyerhoff, D. J. & Weiner, M. W. (2011) Effects of low-level sarin and cyclosarin exposure and Gulf War Illness on Brain Structure and Function: A study at 4T, *Neurotoxicology.* **32**, 814-822.

53. Rayhan, R. U., Stevens, B. W., Timbol, C. R., Adewuyi, O., Walitt, B., VanMeter, J. W. & Baraniuk, J. N. (2013) Increased Brain White Matter Axial Diffusivity Associated with Fatigue, Pain and Hyperalgesia in Gulf War Illness, *PLOS ONE.* **8**, e58493.

54. Jackson, S. J., Andrews, N., Ball, D., Bellantuono, I., Gray, J., Hachoumi, L., Holmes, A., Latcham, J., Petrie, A., Potter, P., Rice, A., Ritchie, A., Stewart, M., Strepka, C., Yeoman, M. & Chapman, K. (2017) Does age matter? The impact of rodent age on study outcomes, *Lab Anim.* **51**, 160-169.

55. Michalovicz, L. T., Locker, A. R., Kelly, K. A., Miller, J. V., Barnes, Z., Fletcher, M. A., Miller, D. B., Klimas, N. G., Morris, M., Lasley, S. M. & O'Callaghan, J. P. (2019) Corticosterone and pyridostigmine/DEET exposure attenuate peripheral cytokine expression: Supporting a dominant role for neuroinflammation in a mouse model of Gulf War Illness, *NeuroToxicology.* **70**, 26-32.

56. Reeves, W. C., Lloyd, A., Vernon, S. D., Klimas, N., Jason, L. A., Bleijenberg, G., Evengard, B., White, P. D., Nisenbaum, R., Unger, E. R. & the International Chronic Fatigue Syndrome Study, G. (2003) Identification of ambiguities in the 1994 chronic fatigue syndrome research case definition and recommendations for resolution, *BMC Health Serv Res.* **3**, 25-25.

57. Collins, J. F., Donta, S. T., Engel, C. C., Baseman, J. B., Dever, L. L., Taylor, T., Boardman, K. D., Martin, S. E., Wiseman, A. L. & Feussner, J. R. (2002) The Antibiotic Treatment Trial of Gulf War Veterans' Illnesses: issues, design, screening, and baseline characteristics, *Control Clin Trials.* **23**, 333-353.

58. Smets, E. M. A., Garssen, B., Bonke, B. & De Haes, J. C. J. M. (1995) The multidimensional Fatigue Inventory (MFI) psychometric qualities of an instrument to assess fatigue, *J Psychosom Res.* **39**, 315-325.

59. Ware, J. E., Jr. & Sherbourne, C. D. (1992) The MOS 36-item short-form health survey (SF-36). I. Conceptual framework and item selection, *Med Care.* **30**, 473-483.

60. Krupp, L. B., LaRocca, N. G., Muir-Nash, J. & Steinberg, A. D. (1989) The fatigue severity scale: Application to patients with multiple sclerosis and systemic lupus erythematosus, *Arch Neurol.* **46**, 1121-1123.

61. Bergner M, B. R., Carter WB, Gilson BS (1981) The Sickness Impact Profile: development and final revision of a health status measure, *Med Care.* **19**, 787-805.

62. Buysse, D. J., Reynolds, C. F., Monk, T. H., Berman, S. R. & Kupfer, D. J. (1989) The Pittsburgh sleep quality index: A new instrument for psychiatric practice and research, *Psychiatry Res.* **28**, 193-213.

63. Davidson, J. R. T. B., S. W.; Colket, J. T.; Tupler, L. A.; Roth, S.; David, D.; Hertzberg, M.; Mellman, T.; Beckham, J. C.; Smith, R. D.; Davison, R. M.; Katz, R.; Feldman, M. E. (1997) Assessment of a new self-rating scale for post-traumatic stress disorder, *Psychol Med.* **27**, 153-160.

64. Gronwall, D. M. A. (1977) Paced Auditory Serial-Addition Task: A Measure of Recovery from Concussion, *Percept Mot Skills.* **44**, 367-373.

65. McArdle, W. D., Katch, F. L. & Katch, V. L. (2007) *Exercise Physiology: Nutrition, Energy, and Human Performance* Lippincott Williams & Wilkins, London.

66. Hurwitz, Barry E., Coryell, Virginia T., Parker, M., Martin, P., LaPerriere, A., Klimas, Nancy G., Sfakianakis, George N. & Bilsker, Martin S. (2009) Chronic fatigue syndrome: illness severity, sedentary lifestyle, blood volume and evidence of diminished cardiac function, *Clin Sci (Lond).* **118**, 125-135.

67. Broderick, G., Fuite, J., Kreitz, A., Vernon, S. D., Klimas, N. & Fletcher, M. A. (2010) A Formal Analysis of Cytokine Networks in Chronic Fatigue Syndrome, *Brain Behav Immun.* **24**, 1209-1217.

68. Bunke, H. (2000). Graph matching: Theoretical foundations, algorithms, and applications. Paper presented at the *Proc Vision Interface*, Montreal.

69. Abdullah, L., Evans, J. E., Joshi, U., Crynen, G., Reed, J., Mouzon, B., Baumann, S., Montague, H., Zakirova, Z., Emmerich, T., Bachmeier, C., Klimas, N., Sullivan, K., Mullan, M., Ait-Ghezala, G. & Crawford, F. (2016) Translational potential of

long-term decreases in mitochondrial lipids in a mouse model of Gulf War Illness, *Toxicology.* **372**, 22-33.

70. Abdullah, L., Evans, J. E., Montague, H., Reed, J. M., Moser, A., Crynen, G., Gonzalez, A., Zakirova, Z., Ross, I., Mullan, C., Mullan, M., Ait-Ghezala, G. & Crawford, F. (2013) Chronic elevation of phosphocholine containing lipids in mice exposed to Gulf War agents pyridostigmine bromide and permethrin, *Neurotoxicol Teratol.* **40**, 74-84.

71. Brandt, C. & Pedersen, B. K. (2010) The Role of Exercise-Induced Myokines in Muscle Homeostasis and the Defense against Chronic Diseases, *J Biomed Biotechnol.* **2010**, 6.

72. Brydon, L., Edwards, S., Jia, H., Mohamed-Ali, V., Zachary, I., Martin, J. F. & Steptoe, A. (2005) Psychological stress activates interleukin-1β gene expression in human mononuclear cells, *Brain Behav Immun.* **19**, 540-546.

73. Gui, W.-S., Wei, X., Mai, C.-L., Murugan, M., Wu, L.-J., Xin, W.-J., Zhou, L.-J. & Liu, X.-G. (2016) Interleukin-1β overproduction is a common cause for neuropathic pain, memory deficit, and depression following peripheral nerve injury in rodents, *Mol Pain.* **12**, 1744806916646784.

74. Rethorst, C. D., Greer, T. L., Toups, M. S. P., Bernstein, I., Carmody, T. J. & Trivedi, M. H. (2015) IL-1β and BDNF are associated with improvement in hypersomnia but not insomnia following exercise in major depressive disorder, *Transl Psychiatry.* **5**, e611.

75. Pastva, A., Estell, K., Schoeb, T. R., Atkinson, T. P. & Schwiebert, L. M. (2004) Aerobic Exercise Attenuates Airway Inflammatory Responses in a Mouse Model of Atopic Asthma, *J Immunol.* **172**, 4520-4526.

76. Craddock, T. J. A., Del Rosario, R. R., Rice, M., Zysman, J. P., Fletcher, M. A., Klimas, N. G. & Broderick, G. (2015) Achieving Remission in Gulf War Illness: A Simulation-Based Approach to Treatment Design, *PLoS ONE.* **10**, e0132774.

Chapter 5 : Conclusions and Future Perspectives

1. Stolovitzky, G., Monroe, D. O. N. & Califano, A. (2007) Dialogue on Reverse-Engineering Assessment and Methods, *Ann N Y Acad Sci.* **1115**, 1-22.

2. Stolovitzky, G., Prill, R. J. & Califano, A. (2009) Lessons from the DREAM2 Challenges, *Ann N Y Acad Sci.* **1158**, 159-195.

3. Madar, A., Greenfield, A., Vanden-Eijnden, E. & Bonneau, R. (2010) DREAM3: Network Inference Using Dynamic Context Likelihood of Relatedness and the Inferelator, *PLoS ONE.* **5**, e9803.

4. Greenfield, A., Madar, A., Ostrer, H. & Bonneau, R. (2010) DREAM4: Combining Genetic and Dynamic Information to Identify Biological Networks and Dynamical Models, *PLoS ONE.* **5**, e13397.

5. Di Camillo, B., Toffolo, G. & Cobelli, C. (2009) A Gene Network Simulator to Assess Reverse Engineering Algorithms, *Annals New York Acad Sci.* **1158**, 125-142.

6. Bansal, M. & di Bernardo, D. (2007) Inference of gene networks from temporal gene expression profiles, *IET Syst Biol.* **1**, 306-312.

7. Zoppoli, P., Morganella, S. & Ceccarelli, M. (2010) TimeDelay-ARACNE: Reverse engineering of gene networks from time-course data by an information theoretic approach, *BMC Bioinform.* **11**, 154.

8. Cantone, I., Marucci, L., Iorio, F., Ricci, M. A., Belcastro, V., Bansal, M., Santini, S., di Bernardo, M., di Bernardo, D. & Cosma, M. P. (2009) A Yeast Synthetic Network for *In Vivo* Assessment of Reverse-Engineering and Modeling Approaches, *Cell.* **137**, 172-181.

9. Sambo, F., camillo, B. D. & Toffolo, G. (2008) CNET: an algorithm for reverse engineering of causalgene networks in *8th Workshop on Network Tools and Applications in Biology NETTAB 2008* pp. 134-136National Research Council, Milan, Italy.

10. Lozano, A. C., Abe, N., Liu, Y. & Rosset, S. (2009) Grouped graphical Granger modeling for gene expression regulatory networks discovery, *Bioinformatics.* **25**, 110-118.

11. Yip, K. Y., Alexander, R. P., Yan, K.-K. & Gerstein, M. (2010) Improved Reconstruction of In Silico Gene Regulatory Networks by Integrating Knockout and Perturbation Data, *PLoS ONE.* **5**, e8121.

12. Prill, R. J., Marbach, D., Saez-Rodriguez, J., Sorger, P. K., Alexopoulos, L. G., Xue, X., Clarke, N. D., Altan-Bonnet, G. & Stolovitzky, G. (2010) Towards a Rigorous Assessment of Systems Biology Models: The DREAM3 Challenges, *PLoS ONE.* **5**, e9202.

13. Marbach, D., Prill, R. J., Schaffter, T., Mattiussi, C., Floreano, D. & Stolovitzky, G. (2010) Revealing strengths and weaknesses of methods for gene network inference, *Proc Natl Acad Sci USA*. **107**, 6286-6291.

14. ElBakry, O., Ahmad, M. O. & Swamy, M. N. S. (2013) Inference of Gene Regulatory Networks with Variable Time Delay from Time-Series Microarray Data, *IEEE/ACM Trans Comp Biol Bioinform* **10**, 671-687.

15. Tapinos, A. & Mendes, P. (2013) A Method for Comparing Multivariate Time Series with Different Dimensions, *PLOS ONE.* **8**, e54201.

16. Folcik, V. A., An, G. C. & Orosz, C. G. (2007) The Basic Immune Simulator: An agent-based model to study the interactions between innate and adaptive immunity, *Theor Biol Med Model.* **4**, 39.

17. Folcik, V. A., Broderick, G., Mohan, S., Block, B., Ekbote, C., Doolittle, J., Khoury, M., Davis, L. & Marsh, C. B. (2011) Using an agent-based model to analyze the dynamic communication network of the immune response, *Theor Biol Med Model.* **8**, 1.

18. Fritsch, P., Craddock, T. J. A., del Rosario, R. M., Rice, M. A., Smylie, A., Folcik, V. A., de Vries, G., Fletcher, M. A., Klimas, N. G. & Broderick, G. (2013) Succumbing to the laws of attraction, *Sys Biomed.* **1**, 179-194.

19. Locker, A. R., Michalovicz, L. T., Kelly, K. A., Miller, J. V., Miller, D. B. & O'Callaghan, J. P. (2017) Corticosterone primes the neuroinflammatory response to Gulf War Illness- relevant organophosphates independently of acetylcholinesterase inhibition, *J Neurochem.* **142**, 444-455.

20. Broderick, G., Ben-Hamo, R., Vashishtha, S., Efroni, S., Nathanson, L., Barnes, Z., Fletcher, M. A. & Klimas, N. (2013) Altered immune pathway activity under exercise challenge in Gulf War Illness: An exploratory analysis, *Brain Behav Immun.* **28**, 159-169.

21. Tanaka, Y. & Martin Mola, E. (2014) IL-6 targeting compared to TNF targeting in rheumatoid arthritis: studies of olokizumab, sarilumab and sirukumab, *Ann Rheum Dis.* **73**, 1595-1597.

22. Smets, E. M. A., Garssen, B., Bonke, B. & De Haes, J. C. J. M. (1995) The multidimensional Fatigue Inventory (MFI) psychometric qualities of an instrument to assess fatigue, *J Psychosom Res.* **39**, 315-325.

23. Ware, J. E., Jr. & Sherbourne, C. D. (1992) The MOS 36-item short-form health survey (SF-36). I. Conceptual framework and item selection, *Med Care.* **30**, 473-483.

24. Krupp, L. B., LaRocca, N. G., Muir-Nash, J. & Steinberg, A. D. (1989) The fatigue severity scale: Application to patients with multiple sclerosis and systemic lupus erythematosus, *Arch Neurol.* **46**, 1121-1123.

25. Broderick, G., Kreitz, A., Fuite, J., Fletcher, M. A., Vernon, S. D. & Klimas, N. (2011) A pilot study of immune network remodeling under challenge in Gulf War Illness, *Brain Behav Immun.* **25**, 302-313.

26. Brandt, C. & Pedersen, B. K. (2010) The Role of Exercise-Induced Myokines in Muscle Homeostasis and the Defense against Chronic Diseases, *J Biomed Biotechnol.* **2010**, 6.

27. Whistler, T., Fletcher, M. A., Lonergan, W., Zeng, X. R., Lin, J. M., LaPerriere, A., Vernon, S. D., Klimas, N. G.(2009) Impaired immune function in Gulf War Illness, *BMC Med. Genomics.* **2**, 12.

Appendices

Appendices: Chapter 2

Appendix 2.1: Review of methods. Review of methods for the reverse engineering of directed networks from time course data published over the past 10 years with the inclusion of select older references describing seminal methods that remain popular.

Basic Model/Approach	Parameter estimation	Algorithm name	Features	Data used	References	URL
Logic based methods	Mutual iformation analysis	REVerse Engineering Algorithm (REVEAL)	infers RBNs from large volumes of expression data. Mutual information analysis to determine connections between the nodes. works best with only a low number of inputs (connections) per gene	N/A	Liang et al. 1998 Pacific Symposium on Biocomputing	N/A
	Coefficient of Determination	Probabilistic Boolean Network (PBN)	Incorporates probability in classical Boolean networks. Probabilistic Boolean networks can be inferred using Coefficient of Determination (COD)	N/A	Schmulevich et al. 2002 Bioinformatics	N/A
	K-means clustering + Support vector regression	N/A	Enumerate Boolean activation–inhibition networks to match discretized data. Algorithm generates several likely possibilities instead of a single network. Can be considered as a simple PBN	45,112 probes per array at 12 time points. 23 clusters were made using K-means which were further refined to 12 representing 903 networks	Martin et al. 2007 Bioinformatics	N/A
	Chi square test	Chi-square testing (CST) based Boolean network (BN)	Significantly improves the computation time: Approx. 70 times faster when error sizes of Best-fit extension problem are 0. False positive rate is less than original BN. Can be used to infer larger networks.	Simulated: 40 nodes*8 time points * 40 samples Real: Yeast cell cycle data: 20 genes* 18 time points Also applied to 800 genes related to Yeast cell cycle	Kim et al. 2007 BMC Bioinformatics	http://bibs.snu.ac.kr/supplement/2006/Boolean/

Conditional and/or joint probability	BDe (Bayesian Dirichlet equivalence)'OR' BIC (Bayesian inform. criterion)+ Influence score to predict the sign.	Bayesian ANalysis with Java Objects (BANJO)	Can infer directed acyclic networks from dynamic data. performance drops exponentially on using less than 300 data points. Bde scoring metric with heuristic search outperforms BIC. Novel Influence score helps in pruning network.	min- 20 genes*25 data points; max- 20 genes * 5000 data points 20 genes * 2000 observations-Smith et al.	Yu et al. 2004 Bioinformatics; Smith et al. 2006 PLoS Comp. Biol.	http://www.cs.duke.edu/~amink/software/banjo/
	information theoretic metric mutual information test (MIT)	GlobalMIT	Under some mild assumptions, global optimal Dynamic Bayesian networks can be reconstructed. Faster in runtime than another DBN based algorithm BNFINDER	20 genes * 2000 observations	Vinh et al. 2011.Bioinformatics	http://code.google.com/p/globalmit
	Bayesian–Dirichlet equivalence (BDe) & minimal description length (MDL) in BNFinder; Mutual Information Criteria (MIC) included in BNFinder2	BNFinder and BNFinder2	BNFinder2 is parallelized for faster learning of network. Able to choose network specificity based on statistical criteria Much Faster than BANJO and even BNFinder Directed acyclic graphs	20 variables * 2000 observations	Wilczynski and Dojer 2009. Bioinformatic; Dojer et al. 2013. Bioinformatics	https://launchpad.net/bnfinder; http://bioputer.mimuw.edu.pl/software/bnf/
	Input-Output Hidden Markov Model (IOHMM)/logistic regression classifier	Dynamic Regulatory Events Miner (DREM, DREM2.0)	Require dynamic expression data & static CHIP data. Identifies bifurcation events, places in the time series where a set of genes that were previously coexpressed diverges.	whole S.cerevisiae genome (~6200 genes) * 5 time points on Amino acid; strvation + 34 Transcription factor (TF) CHIP-CHIP data + 75 TF in Yeast growing media	Ernst et al. 2007 Mol.Sys bio. Schulz et al.2012 BMC systems Biol.	http://www.sb.cs.cmu.edu/drem

Information Theoretic	time dependent mutual information+data processing inequality (DPI)	Time-delay ARACNE	Capable of inferring directed networks of small size. Detect time-delayed dependencies between the expression profiles. Use of DPI to break up fully connected triplets	10 genes*10-50 time points *20 samples-simulated; 10-30 genes*50 time points * 20 samples-simulated; 5 profiles of 15 time points & 5 profiles of 21 time pts.- 5 node IRMA; 1 profile of 14 time points- 8 gene network	Zoppoli et al. 2010 BMC Bioinformatics	http://bioconductor.org/packages/release/bioc/html/TDARACNE.html
	Dynamic mutual information+ Background correction	Dynamic CLR (Context Likelihood of Relatedness)	Modification of a popular algorithm CLR to use with dynamic data. Developed as part of a pipeline to use with ODE model Inferelator. Compute mutual information using a smoothing B-spline approach. Background correction of dynamic MI values is the key step of algorithm	DREAM 2 50 node insilico network data. Time seires had 50 genes * 26 time points for each perturbation of 23 performed.	Madar et al. 2010 PLoS ONE	
Linear Ordinary Differential equations (ODE)	Singular Value Decomposition (SVD) / L1	N/A	Also uses L1 regression to select sparsest solution Ability to infer directed connections	Simulated networks from 10-1000 genes* 10-120 time points	Yeung et. al. 2002	N/A
	Multiple linear regression with multiple perturbation residual sum of square error (RSS) minimization criterion	Network inference by reverse engineering (NIR)	Assumes system at steady state and perturbations to be small so that system returns to steady state soon after the removal of perturbation. Can work on steady state as well as time series data	9 genes of E.coli SOS network* 9 perturbations	Gardner et al. Science 2003	http://dibernardo.tigem.it/softwares/network-inference-by-reverse-engineering-nir
	Regression/LASSO with CV to select shrinkage parameter	The Inferelator	Integration of gene knockout data with expression data Attractive ODE method for large network inference Method uses gene expression as a function of the levels of TFs. Model	72 TFs * 10 environmental factors as regulators*1934 genes of Halobacterium NRC-	Bonneau et al. 2006 Genome Biol.	http://err.bio.nyu.edu/inferelator/

			can predict time series and equilibirium expression levels.	1		
	Principal component analysis (PCA) for dimension reduction	Time Series Network Identification (TSNI)	Able to infer directed gene regulatory networks A gene of interest can be defined for perturbation More suitable for finding perturbation targets First model is converted to discrete form and then back to continuous.	10 genes* 5 time points - Simulated E.Coli SOS network with 5 time points - Real network 1000 genes*10 time points - Simulated	Bansal et al. 2006. Bioinformatics Della Gatta et al. 2008 Genome Research	http://dibernardo.tigem.it/softwares/time-series-network-identification-tsni
	forward step-wise regression method Bootstrapping /Akaike's Final Prediction error (FPE)	TSNI integral	Instead of converting to discrete form and back to continuous during taking derivative, model was integrated to deal with noise. Extended version of TSNI, Performs better than TSNI or in worst case similar	10 genes * 10,20,50,100 time points * 20 networks each- Simulated 20 genes*20,40,100 time points* 20 networks each- Simulated E.Coli SOS (9 genes)* 5 time pts. - Real	Bansal and Di Bernardo 2007. IET Syst. Biol.	http://dibernardo.tigem.it/softwares/time-series-network-identification-tsni-integral
	Newton's method to find local minima of objective function Runge-Kutta method for estimation of gradient and Hessian.	N/A	Two different models were used to infer networks from static and dynamicdata. Noise model- static data; Differential eq. model- Dynamic data and predictions were merged to made final prediction. Noise model has been found to infer more connection from deletion data.	DREAM 3 data: 5 datasets each for 10, 50 and 100 genes* 21 time pts	Yip et al. 2010 PLoS One	N/A
Nonlinear ordinary differential equations	Pearson correlation coeff. (PCC) to identify the most probable lag of the	Time-delayed S-system (TDSS) model	Capable of inferring time-delayed and instantaneous interactions time delay parameters can be fractional innovative model evaluation to narrow down the search space	Simulated data for 5 node and 20 node networks IRMA network- on: 5 genes * 15 time pts.; off: 5 genes * 21 time	Chowdhury et al. 2013 BMC Bioinform.	N/A

	interaction between any pair of genes. Trigonometric differential evolution (TDE) for optimization Multistage refinement algorithm (MRA) for pruning			pts. E.Coli SOS network: 8 genes * 50 time pts * 5 experiments		
	A novel coupling metric used to measure the effect of one component on another to rank potential edges.	Network Reconstruction via Dynamic Systems (NeRDS)	nonparametric, additive model used instead of linear approximation. Derivatives are estimated using smoothing-splines rather than finite differences. Large data requirements.	Data simulated from a model of Embden-Meyerhof glycolytic pathway in the Lactocaccus Lactis bacterium: 6 metabolites * 100 time pts * 6 exp. Simulated data for a model of mouse embryonic stem cells: 6 genes * 100 time pts * 6 exp. 10 and 100time series simulated using GeneNetweaver for DREAM 3 10-node and 100-node networks.	Henderson & Michalidis 2014 PLoSOne	N/A
Hybrid methods	Regression/LASSO with CV to select shrinkage parameter	The inferelator+ mixed CLR	Mixed-CLR is used for preprocessing step for inferelator 1.0	DREAM 3 100-gene network data	Madar et. al. 2010 PLoSOne	
	Same as above	T-test+mixed-CLR+The	2nd position in DREAM3 blind network inference challenge	Knockout: 100 observations steady	Greenfield et. al. 2010	

	inferelator		state	PLoSOne	
Bayesian formulation of linear regression /Zellner's g priors/Bayesian information criterion (BIC)	Bayesian Best Subset Regression (BBSR)+ Inferelator	Capable of using dynamic as well as static data. Knock-out data was found to be most informative. Performance of algorithm drops for high indegree genes & smaller networks. Second hybrid method ranked 1st in DREAM 4 100-gene challenge. T-test used for ranking interactions from only Knock-out data. BBSR is extension to inferelator that enables use of known regulatory edges to influence model selection.	Knockdown: 100 observations steady state time series: 100 genes* 966 observations	Greenfield et. al. 2013 Bioinformatics	http://bonneaulab.bio.nyu.edu/software.html
Decision trees based method called "jump trees" for identifying the promoter state trajectory that maximises log-likelihood. Also to identify regulators of target genes.	Jump 3	stochastic differential eq used to model dynamics of each node. Can reconstruct large networks. Performs better for inferring larger networks but lags behind model based methods such as TSNI and INFERELATOR on smaller networks.	DREAM 4: 10 node* 105 observations DREAM 4: 100 node *210 observations IFN-gamma activated regulatory interactions: 1000 genes * 25 time pts. 2 types of data was used: Toy data for traning & Experimental data	Huynh-Thu & Sanguinetti Bioinformatics 2015	http://homepages.inf.ed.ac.uk/vhuynht/misc/jump3.zip
growth-shrink algorithm for smaller network. Incremental association Markov blanket (IAMB) for large networks.	Differential Equation-based Local Dynamic Bayesian Network (DELDBN)	improves the scalability to large networks. Can also be used to infer smaller networks. Do not require enormous data for inference of causal networks. Shown to perform better than ODE methods alone as well as Bayesian methods alone on Yeast synthetic data.	5 genes* 10-15 time points * 5 time series switch on data IRMA network. 1099genes * 48 time points HeLa cell time series data	Li et al. 2011 Bioinformatics	R Scripts are freely available in supp. information

Other (Machine learning/Data mining)	Correlation+Decision tree	Time delay gene regulatory network (TdGRN)	No prior model defined. Needs training dataset to model variable time delays between genes Use decision tree to discover time delayed regulation of every gene	20 genes* 19 time pts for training (cdc15 from yeast cell cycle). 20 genes * 18 , 17 time pts for inference (alpha-factor & cdc-28). Human Hela cells data: 20 genes* 47 time pts for cross validation 20 genes *26, 19 time pts for testing	Li et al. 2006 BMC Bioinformatics	N/A
	Granger causality+Grouped LASSO	grouped graphical Granger modeling (GGGM) method	No prior model define. Needs training dataset to model variable time delays between genes Make use of the group structure of time variables in a time series	1134 genes* 3 experiments (12, 27, 48 time pts) Human Hela cell data	Lozano et al. 2009 Bioinformatics	N/A
	Pair-wise correlation+LASSO	Delay-Detection LASSO (DD-LASSO)	Able to model variable time delays between any two genes. Pair-wise correlation is used to evaluate the correct time delays b/w different genes. LASSO is used to differentiate b/w direct and indirect relationships. Training dataset not needed	Simulated data: Genes- 50 & 100; Time points: 10 & 20; Samples: 4, 10 & 50. Real data: 9 genes * 47 time pts from Hela Cell cycle data. 11 genes * 18 time pts. From Yeast cell cycle data	AlBakry et. al. 2013 IEEE/ACM Trans. Comp. Biol. Bioinform.	N/A
	Multi variate auto regression(MVAR)+ Coeff. of determination	Extension of GENIE	Extension of popular GENIE algorithm for time course data. Random forest based algorithm. Introduces adjusted coefficient of determination. Performs better or equivalent to other established methods	10,30,50,100 genes * 10,30,50 time points * 50 datasets each-simulated 9 genes* 17 time points - Real E.Coli cell cycle data	D.A.K. Maduranga et al. 2013 PRIB	N/A

Appendix 2.2a. Summary performance statistics on single time course: Median (a) and Mean (b) performance of all selected methods in recovering 20 different 10-node simulated networks, each from a single time course sampled at 10, 25 and 50 time points (Figure 2.1)

Methods	Time_points	10		25		50	
	Noise level (%)	0	20	0	20	0	20
Bartlett's method	Median PPV (MAD)	0.14 (0.02)	0.15 (0.02)	0.15 (0.005)	0.15 (0.01)	0.15 (0.01)	0.14 (0.02)
	Median Recall (MAD)	0.85 (0.07)	0.85 (0.06)	0.85 (0.07)	0.93 (0.07)	0.79 (0.05)	0.67 (0.09)
	Median F score (MAD)	0.24 (0.03)	0.26 (0.03)	0.26 (0.01)	0.26 (0.02)	0.24 (0.02)	0.23 (0.03)
Broken stick	Median PPV (MAD)	0.14 (0.01)	0.16 (0.03)	0.15 (0.01)	0.15 (0.01)	0.15 (0.02)	0.15 (0.02)
	Median Recall (MAD)	0.83 (0.05)	0.65 (0.09)	0.73 (0.06)	0.85 (0.08)	0.79 (0.08)	0.79 (0.07)
	Median F score (MAD)	0.23 (0.02)	0.26 (0.04)	0.25 (0.02)	0.25 (0.02)	0.25 (0.03)	0.24 (0.03)
TSNI integral	Median PPV (MAD)	0.17 (0.02)	0.17 (0.02)	0.17 (0.03)	0.16 (0.03)	0.18 (0.04)	0.16 (0.02)
	Median Recall (MAD)	0.61 (0.13)	0.5 (0.09)	0.65 (0.12)	0.55 (0.12)	0.59 (0.12)	0.59 (0.09)
	Median F score (MAD)	0.26 (0.04)	0.25 (0.04)	0.27 (0.04)	0.25 (0.05)	0.27 (0.06)	0.26 (0.03)
Stepwise	Median PPV (MAD)	0.18 (0.04)	0.15 (0.03)	0.16 (0.02)	0.21 (0.06)	0.16 (0.02)	0.2 (0.09)
	Median Recall (MAD)	0.31 (0.11)	0.27 (0.07)	0.57 (0.07)	0.17 (0.09)	0.64 (0.13)	0.15 (0.09)
	Median F score (MAD)	0.22 (0.06)	0.19 (0.04)	0.24 (0.03)	0.18 (0.08)	0.26 (0.03)	0.19 (0.09)
TD-ARACNE	Median PPV (MAD)	0.17 (0.05)	0.22 (0.05)	0.23 (0.12)	0.23 (0.08)	0.2 (0.07)	0.19 (0.07)
	Median Recall (MAD)	0.25 (0.07)	0.24 (0.08)	0.28 (0.09)	0.23 (0.09)	0.2 (0.08)	0.21 (0.05)
	Median F score (MAD)	0.2 (0.03)	0.24 (0.05)	0.24 (0.07)	0.22 (0.07)	0.19 (0.06)	0.21 (0.05)

Appendix 2.2b: Summary performance statistics on single time course: Mean performance of all selected methods in recovering 20 different 10-node simulated networks, each from a single time course sampled at 10, 25 and 50 time points (Figure 2.1)

Methods	Time_points	10		25		50	
	Noise level (%)	0	20	0	20	0	20
Bartlett's method	Mean PPV (SE)	0.15 (0.004)	0.15 (0.006)	0.15 (0.004)	0.15 (0.004)	0.15 (0.005)	0.14 (0.005)
	Mean Recall (SE)	0.85 (0.02)	0.85 (0.02)	0.86 (0.02)	0.93 (0.02)	0.81 (0.02)	0.69 (0.02)
	Mean F score (SE)	0.25 (0.007)	0.26 (0.008)	0.26 (0.005)	0.26 (0.006)	0.25 (0.007)	0.24 (0.008)
Broken stick	Mean PPV (SE)	0.15 (0.005)	0.16 (0.01)	0.15 (0.005)	0.15 (0.004)	0.15 (0.006)	0.15 (0.005)
	Mean Recall (SE)	0.82 (0.02)	0.65 (0.03)	0.76 (0.02)	0.82 (0.02)	0.8 (0.02)	0.81 (0.02)
	Mean F score (SE)	0.25 (0.007)	0.25 (0.01)	0.25 (0.008)	0.25 (0.007)	0.25 (0.009)	0.25 (0.008)
TSNI integral	Mean PPV (SE)	0.16 (0.01)	0.14 (0.01)	0.16 (0.01)	0.16 (0.01)	0.16 (0.01)	0.15 (0.01)
	Mean Recall (SE)	0.61 (0.04)	0.41 (0.04)	0.65 (0.03)	0.53 (0.03)	0.56 (0.03)	0.6 (0.04)
	Mean F score (SE)	0.25 (0.01)	0.21 (0.02)	0.25 (0.01)	0.24 (0.02)	0.25 (0.02)	0.24 (0.01)
Stepwise	Mean PPV (SE)	0.17 (0.02)	0.17 (0.015)	0.16 (0.009)	0.2 (0.03)	0.16 (0.008)	0.22 (0.04)
	Mean Recall (SE)	0.32 (0.03)	0.29 (0.03)	0.56 (0.03)	0.16 (0.02)	0.63 (0.04)	0.15 (0.02)
	Mean F score (SE)	0.22 (0.02)	0.21 (0.02)	0.25 (0.01)	0.19 (0.02)	0.25 (0.01)	0.19 (0.02)
TD-ARACNE	Mean PPV (SE)	0.17 (0.02)	0.19 (0.02)	0.25 (0.03)	0.23 (0.03)	0.21 (0.03)	0.22 (0.07)
	Mean Recall (SE)	0.23 (0.025)	0.22 (0.03)	0.26 (0.03)	0.25 (0.03)	0.19 (0.02)	0.22 (0.05)
	Mean F score (SE)	0.2 (0.02)	0.22 (0.02)	0.26 (0.02)	0.24 (0.02)	0.2 (0.02)	0.23 (0.05)

Appendix 2.3 Median performance of all selected methods across different expression profiles for random networks of increasing node degree: Each network was used to generate 20 simulated time course experiments, sampled at 50 time points, where 20% Gaussian noise was added to mimic experimental noise.

Network size		5 Nodes	10 Nodes	15 Nodes	20 Nodes	30 Nodes	50 Nodes
Edge density (%)		40	21	11	8	5	3
Bartlett's method	**Median PPV (MAD)**	0.35 (0.03)	0.21 (0.02)	0.1 (0.002)	0.08 (0.0009)	<0.1 (0.002)	<0.1 (0.0004)
	Median recall (MAD)	0.87 (0.13)	0.76 (0.08)	0.91 (0.04)	0.9 (0.03)	0.78 (0.02)	0.93 (0.014)
	Median F score (MAD)	0.5 (0.04)	0.33 (0.02)	0.18 (0.004)	0.15 (0.001)	<0.1 (0.004)	<0.1 (0.0009)
Broken stick	**Median PPV (MAD)**	0.32 (0.03)	0.19 (0.01)	0.12 (0.01)	<0.1 (0.006)	<0.1 (0.004)	<0.1 (0.003)
	Median Recall (MAD)	0.88 (0.13)	0.84 (0.05)	0.52 (0.04)	0.74 (0.05)	0.82 (0.05)	0.4 (0.04)
	Median F score (MAD)	0.47 (0.04)	0.31 (0.02)	0.19 (0.02)	0.16 (0.01)	<0.1 (0.007)	<0.1 (0.006)
TSNI integral	**Median PPV (MAD)**	0.4 (0.05)	0.25 (0.025)	0.13 (0.02)	<0.1 (0.01)	<0.1 (0.006)	<0.1 (0.004)
	Median Recall (MAD)	0.75 (0.13)	0.53 (0.05)	0.35 (0.04)	0.26 (0.05)	0.33 (0.06)	0.2 (0.03)
	Median F score (MAD)	0.52 (0.07)	0.34 (0.03)	0.19 (0.03)	0.1 (0.02)	<0.1 (0.01)	<0.1 (0.007)
Stepwise	**Median PPV (MAD)**	0.5 (0.17)	0.23 (0.05)	0.19 (0.03)	<0.1 (0.02)	<0.1 (0.01)	<0.1 (0.008)
	Median Recall (MAD)	0.25 (0.06)	0.16 (0.05)	0.13 (0)	0.14 (0.03)	<0.1 (0.02)	<0.1 (0.03)
	Median F score (MAD)	0.33 (0.05)	0.19 (0.05)	0.16 (0.02)	0.11 (0.02)	<0.1 (0.009)	<0.1 (0.01)
TD-ARACNE	**Median PPV (MAD)**	0.5 (0.17)	0.25 (0.11)	0.14 (0.06)	0.12 (0.06)	<0.1 (0.04)	<0.1 (0.01)
	Median Recall (MAD)	0.25 (0.13)	0.16 (0.08)	0.17 (0.04)	<0.1 (0.03)	<0.1 (0.02)	<0.1 (0.01)
	Median F score (MAD)	0.3 (0.1)	0.19 (0.1)	0.16 (0.06)	0.08 (0.03)	<0.1 (0.02)	<0.1 (0.009)

Appendix 2.4: Comparing the performance of methods on NetSim and DREAM3 data. Median PPV, recall and F score obtained by applying broken stick, Bartlett's and TSNI integral methods on comparable networks of DREAM 3 challenge (E.coli2 with 15 interactions) and NetSim (median value of14 interactions). A set of 20 different networks consisting of 12–17 interactions were simulated by NetSim whereas, 4 time series provided in DREAM 3 challenge were used for E.Coli2 network. Values in parentheses show the performance when self-regulation is not considered.

	Broken stick		Bartlett's method		TSNI Integral	
	NetSim data	Dream3 data	NetSim data	Dream3 data	NetSim data	Dream3 data
Median PPV	0.15(0.16)	0.15(0.16)	0.15(0.15)	0.15(0.21)	0.15(0.16)	0.15(0.17)
Median recall	0.84(0.84)	0.8(0.8)	0.5(0.5)	0.4(0.4)	0.93(0.92)	0.9(0.9)
Median F score	0.25(0.26)	0.25(0.27)	0.23(0.23)	0.22(0.27)	0.26(0.27)	0.26(0.28)

Appendices: Chapter 3

Appendix 3.1: Summary statistics of Cytokines. Average cytokine levels with standard error () at each time point across both groups were calculated by replacing missing values with the minimum values across both subject groups. Mean values were calculated across both populations by leaving outliers out of sample size, resulting into n=12 GWI and n=11 HC

Cytokines	T0		T0+3		T1		T1+10	
	GWI	Healthy	GWI	Healthy	GWI	Healthy	GWI	Heathy
hIL-1a	9.49 (2.46)	6.22 (1.40)	7.25 (1.69)	12.02 (3.65)	12.14 (3.25)	12.50 (3.34)	9.79 (2.54)	13.04 (2.97)
hIL-1b	22.54 (4.36)	21.76(2.26)	21.36 (3.19)	22.82 (4.46)	23.09 (3.89)	19.97 (4.16)	19.73 (2.85)	24.11 (4.23)
hIL-2	8.20 (1.75)	8.04 (2.04)	8.49 (1.46)	12.00 (2.26)	12.88 (1.73)	9.16 (1.54)	10.43 (2.28)	11.74 (2.70)
hIL-4	2.09 (0.77)	1.49 (0.49)	2.57 (0.80)	1.00 (0.26)	2.45 (0.62)	1.77 (0.57)	2.29 (0.84)	2.71 (0.75)
hIL-5	1.59 (0.44)	2.08 (0.46)	1.40 (0.39)	2.15 (0.44)	2.09 (0.48)	2.27 (0.52)	2.11 (0.41)	1.75 (0.44)
hIL-6	2.25 (0.84)	1.04 (0.34)	1.49 (0.24)	1.41 (0.44)	1.63 (0.62)	2.51 (1.01)	1.60 (0.61)	2.45 (0.71)
hIL-8	0.82 (0.21)	0.86 (0.16)	0.71 (0.17)	1.13 (0.27)	0.81 (0.16)	1.18 (0.29)	0.71 (0.14)	0.88 (0.23)
hIL-10	6.45 (1.03)	8.48 (1.80)	6.04 (1.25)	8.38 (1.65)	6.95 (1.43)	5.43 (1.16)	5.85 (1.17)	4.91 (0.93)
hIL-12	5.80 (0.77)	6.08 (0.72)	5.92 (0.94)	4.48 (0.93)	4.35 (0.65)	5.09 (0.47)	5.22 (0.64)	5.17 (0.59)
hIL-13	3.24 (0.55)	2.23 (0.57)	3.08 (0.65)	4.08 (1.10)	2.28 (0.68)	3.69 (1.01)	2.74 (0.73)	3.17 (0.72)
hIL-15	8.09 (2.61)	9.12 (2.28)	8.29 (2.37)	5.92 (1.70)	7.10 (2.14)	7.82 (2.90)	8.61 (1.73)	7.64 (2.19)
hIL-17	5.07 (1.14)	2.98 (0.60)	4.77 (1.13)	4.26 (0.57)	4.46 (0.87)	4.60 (0.99)	5.77 (0.98)	4.39 (1.07)
hIL-23	267.65 (5.46)	282.15 (10.84)	265.67 (4.21)	275.23 (7.47)	272.45 (5.52)	271.90 (8.02)	269.99 (5.98)	270.83 (6.95)
hIFNy	0.98 (0.11)	0.88 (0.12)	0.81 (0.10)	0.67 (0.12)	0.93 (0.10)	0.82 (0.09)	0.77 (0.08)	0.78 (0.11)
hTNFa	8.87 (1.65)	8.77 (1.67)	7.21 (1.65)	8.77 (1.85)	9.08 (1.65)	9.13 (1.46)	7.62 (1.77)	7.76 (1.14)
hTNFb	2.37 (0.55)	2.34 (0.52)	3.51 (0.75)	2.54 (0.54)	2.45 (0.45)	2.00 (0.38)	2.70 (0.61)	2.55 (0.48)

Cytokines	T1+20		T1+30		T1+60		T1+4hrs	
	GWI	Healthy	GWI	Healthy	GWI	Healthy	GWI	Healthy
hIL-1a	8.60 (2.43)	11.32 (3.35)	11.31 (2.88)	12.19 (4.08)	11.88 (3.13)	9.16 (3.22)	11.51 (2.60)	9.68 (2.54)
hIL-1b	21.99 (3.70)	27.28 (3.56)	20.44 (4.13)	21.64 (3.89)	18.51 (3.54)	22.67 (4.08)	22.07 (4.35)	22.77 (4.27)
hIL-2	7.63 (1.40)	9.89 (1.58)	10.69 (1.60)	11.03 (3.13)	9.30 (1.56)	13.30 (3.40)	10.51 (2.17)	12.60 (1.67)
hIL-4	2.10 (0.51)	1.89 (0.53)	2.29 (0.66)	2.18 (0.77)	3.21 (0.75)	2.31 (0.52)	1.81 (0.48)	2.50 (0.69)
hIL-5	1.97 (0.41)	2.53 (0.49)	1.84 (0.36)	1.79 (0.35)	2.56 (0.48)	3.18 (0.60)	1.95 (0.37)	1.80 (0.46)
hIL-6	2.62 (0.81)	3.00 (0.96)	1.96 (0.74)	1.48 (0.26)	1.67 (0.83)	2.55 (0.87)	2.56 (0.50)	2.26 (0.60)

hIL-8	0.60 (0.15)	1.12 (0.24)	0.80 (0.19)	0.73 (0.21)	0.63 (0.12)	0.83 (0.20)	1.19 (0.28)	0.68 (0.21)
hIL-10	9.37 (1.91)	5.91 (1.33)	8.21 (1.47)	6.58 (0.88)	7.19 (1.23)	8.20 (2.03)	7.88 (1.74)	6.77 (1.61)
hIL-12	5.64 (0.44)	4.53 (0.54)	4.79 (0.73)	4.66 (0.85)	5.28 (1.07)	5.68 (0.90)	4.38 (0.41)	4.61 (0.75)
hIL-13	3.42 (0.87)	1.70 (0.61)	3.57 (1.11)	3.97 (0.90)	3.18 (0.84)	2.74 (0.72)	3.03 (0.89)	3.92 (1.24)
hIL-15	9.94 (2.18)	6.74 (1.73)	7.87 (1.65)	12.25 (3.52)	10.29 (2.46)	4.24 (1.70)	8.13 (2.26)	7.86 (1.67)
hIL-17	2.52 (0.56)	5.89 (1.16)	4.59 (0.96)	3.54 (0.67)	4.62 (1.15)	3.52 (0.85)	4.32 (0.57)	5.30 (1.13)
hIL-23	265.90 (4.11)	268.29 (6.13)	271.33 (5.48)	271.38 (6.57)	277.35 (9.85)	281.82 (8.37)	267.29 (4.50)	277.65 (9.35)
hIFNy	0.83 (0.09)	0.72 (0.09)	0.83 (0.10)	0.79 (0.10)	0.77 (0.12)	0.76 (0.12)	0.73 (0.09)	0.83 (0.12)
hTNFa	6.83 (1.58)	9.57 (1.77)	9.76 (2.15)	9.88 (1.65)	6.90 (1.18)	7.18 (1.38)	9.64 (1.87)	11.06 (2.69)
hTNFb	3.05 (0.51)	2.64 (0.66)	2.76 (0.56)	2.21 (0.59)	2.05 (0.32)	3.23 (0.72)	2.30 (0.54)	2.28 (0.60)

Appendix 3.2: Overview of cytokine expression. Fold change in cytokine expression at each time point over average levels in the control group for (A) individual healthy control subjects (HC) and (B) individual GWI subjects

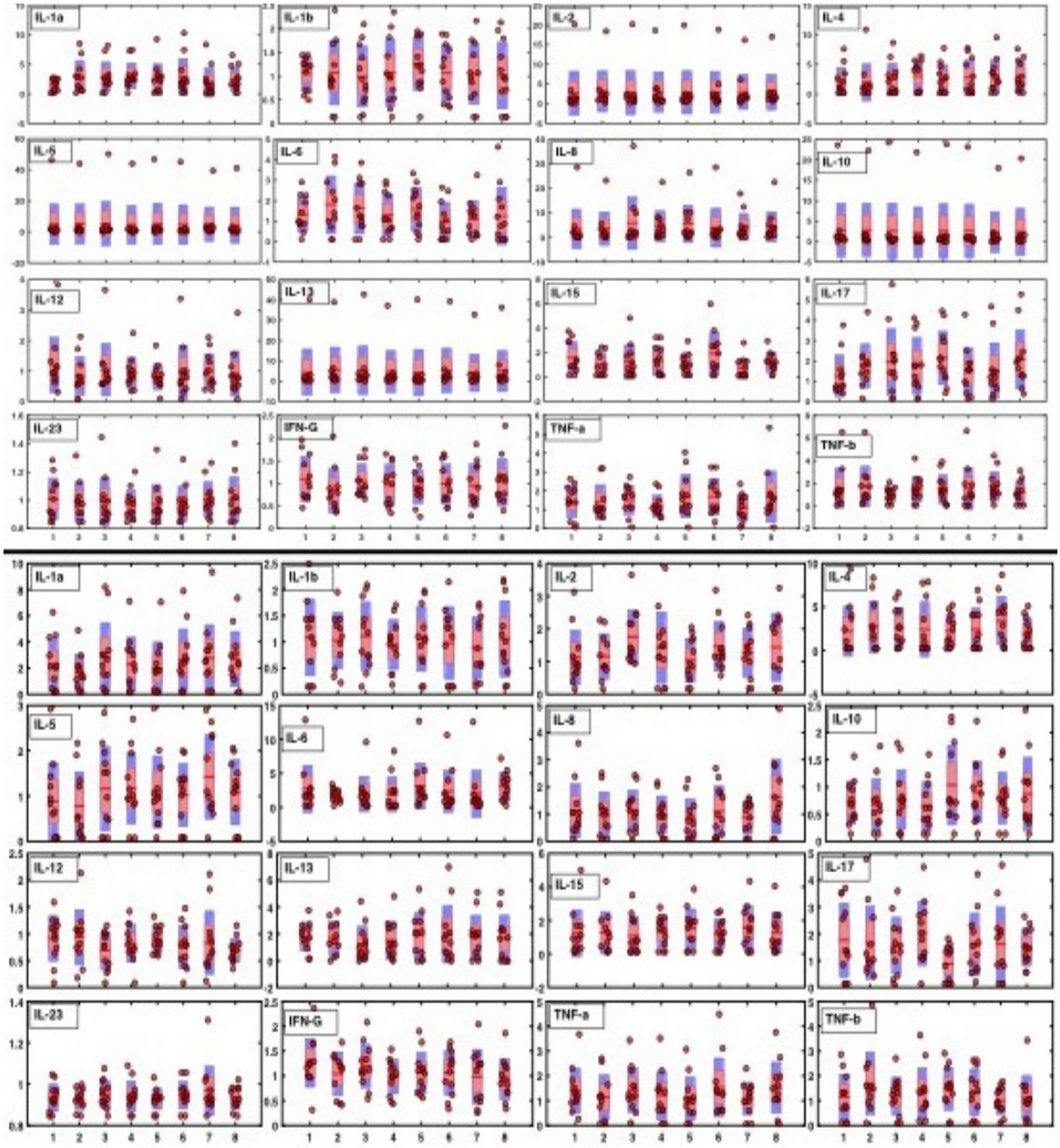

Appendix 3.3: ***The SMETS algorithm***

Differences in the dynamic evolution of every cytokine across subject groups were characterized by using an algorithm specifically developed for the comparison of multiple time series with arbitrary dimensions named as SMETS *(***S**emi **M**etric **E**nsemble **T**ime **S**eries*)* [1]. More precisely, we randomly sub-sampled without replacement groups of n=10 of 11 (HC) time series and compared these with similarly sub-sampled groups of n=10 of 12 (GWI) time series for each of the 16 cytokines. This process was repeated 100 times to yield a 100 x 100 array of SMETS distances separating HC and GWI subsamples each consisting of 10 trajectories.

SMETS is a semi-metric that satisfies all the conditions to be a metric such as non-negativity, symmetry, identity and reflexivity except triangle-inequality. The *SMETS* distance between two groups of multiple time series and can be expressed as:

$$SMETS = \sqrt{\left(\left\|d\right\|_n + EP\right)^2 + P^2}$$

(1), SMETS values in equation (1) are calculated in the following two steps:

Step 1: Partial matching between two groups of multiple time series is performed as follows:

I. First, the Euclidean distances between each of the component time series were calculated.

II. The smallest distance between two component time series (one from each model) was calculated as p-norm of d (eq.2).

$$\|d\|_n = \sqrt[n]{\sum_{i=1}^{n} d_m^n} \quad (2)$$

III. The two most similar component time series were removed from further calculations.

IV. Steps I to III were repeated until all time series from the model with the smallest cardinality have been matched.

Step 2: Penalizing unmatched series

Unmatched component time series were penalized not only on the basis of being unmatched but also with the consideration of information content in that unmatched component. Therefore, unmatched component time series with little information content would add much less to the overall distance between two groups of multiple time series. Information stored in the component time series is measured in terms of Shannon entropy (H).

$$H_{j=-\sum_{i=1}^{q}\rho(t_{j,i})} log2\rho(t_{j,i}) \quad (3),$$

where, $t_{j,i}$ is the *i-th* data point of the component time series t_j; q is the length of the component time series, and p($t_{j,i}$) is the frequency of the value $t_{j,i}$ in the time series. The relative information content RE_j of each unmatched component time series j is then:

$$RE_j = \frac{\min\left(d_j\right)'\left(H_j\right)}{\sum_{i=1}^{m} H_i} \quad (4),$$

where d_j is the smallest distance between the *j-th* unmatched component time series and any component time series from the smallest model; m is the dimension of the larger time series. Therefore the overall entropy penalty *EP* that accounts for the distance of the unmatched components is:

$$EP = \sum_{j=1}^{m-n} RE_j \quad (5),$$

Another weaker penalty *P* is calculated as the ratio of difference and sum of dimensions and 2-norm was added to entropy penalty (*EP*) to comply with the identity condition of semi-metric.

$$P = \frac{m-n}{m+n} \quad (6)$$

These penalties (*EP* and *P*) along with the distance calculated in equation (2) denote the

SMETS value calculated in equation (1). For detailed description of SMETS algorithm, we refer reader to [1].

Appendix 3.4: Source and target nodes with their respective score in every edge of the reference network obtained from STRING database

#node1	node2	coexpression	Experimentally determined interaction	database annotated	Automated textmining	combined score
IL13	IL4	0	0.576	0.8	0.974	0.997
IL4	IL2	0	0	0.8	0.979	0.995
IL5	IL4	0	0	0.8	0.979	0.995
TNF	IFNG	0	0.576	0	0.987	0.994
IL1B	IL1A	0.266	0	0.9	0.917	0.993
IL17A	IL6	0	0	0.9	0.941	0.993
IL5	IL2	0	0	0.8	0.959	0.991
IL8	IL6	0.169	0	0	0.98	0.983
IL10	IL4	0	0	0	0.979	0.979
IL10	IL6	0	0	0	0.979	0.979
IFNG	IL2	0	0	0.9	0.795	0.978
IL1B	IL6	0.158	0	0	0.973	0.976
TNF	IL1B	0.247	0	0	0.96	0.968
IL10	IL2	0	0	0	0.963	0.963
IL8	IL1B	0.091	0	0	0.961	0.963
IL1A	IL6	0.226	0	0	0.954	0.962
IL6	IL2	0	0	0	0.962	0.962
IL6	IL4	0	0	0	0.961	0.961
IL13	IL5	0	0	0.8	0.817	0.961
IL10	IL8	0	0	0	0.961	0.961
TNF	IL8	0	0	0	0.953	0.953
IL10	TNF	0	0	0	0.949	0.949
IL12A	IL4	0	0	0.9	0.484	0.946
IL12A	IFNG	0	0	0.9	0.47	0.944
TNF	IL2	0	0	0	0.943	0.943
IL10	IL17A	0	0	0	0.942	0.942
IL8	IL4	0	0	0	0.939	0.939
IL8	IL2	0	0	0	0.937	0.937
IL15	IL2	0	0	0.8	0.7	0.937
IL1B	IL23A	0	0	0.9	0.345	0.931
IL1B	IL4	0	0	0	0.928	0.928
IL17A	IL1B	0	0	0	0.928	0.928
IL1B	IL2	0	0	0	0.928	0.928
IL17A	IL23A	0	0	0	0.927	0.927
IFNG	IL23A	0	0	0.9	0.294	0.926
IL17A	IL8	0	0	0	0.925	0.925
IL13	IL6	0	0	0	0.924	0.924

IL13	IL2	0	0	0.8	0.623	0.921
IL6	IL23A	0	0	0.9	0.202	0.916
IL12A	IL1B	0	0	0.9	0.18	0.914
IL12A	IL6	0	0	0.8	0.545	0.905

* scores for choromosomal neighborhood, gene fusion, phylogenetic cooccurence and homology were zero for all edges.

Appendix 3.5: Literature based aggregated cytokine network. Cytokine network extracted from the immune signaling network in Fritsch et al. 2014 combined with cytokine network extracted from the STRING database. Arrow shape (→) represents activation whereas T-shape (----|) represents inhibition. Edges with solid lines represent edges common to both networks in terms of direction.

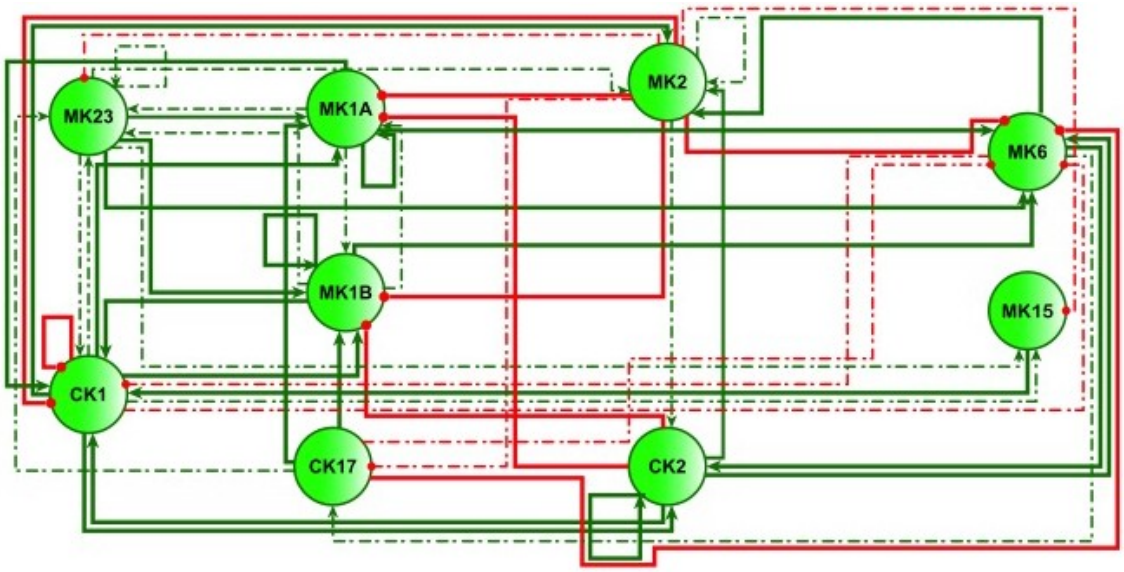

Appendix 3.6: Graph Theoretical Metrics

Node degree centrality. The node degree of a node *i* is the number of edges linked to *i*. A directed network has two kinds of node degree parameters i.e. *Outdegree* and *Indegree*. The number of edges directed outwards from a node is counted as *outdegree* whereas number of edges directed towards a node is counted as *Indegree*.

Node betweenness centrality. Node betweenness centrality for each node of inferred networks was calculated using Brandes algorithm [2]. Betweenness centrality of a node *n* reflects the amount of control that this node employs over the interactions of other nodes in the network [3] and can be computed as follows:

$$C_b(n) = \sum_{s \neq n \neq t} (\sigma_{st}(n)/\sigma_{st}) \quad (7),$$

where *s* and *t* are nodes in the network different from *n*, σ_{st} denotes the number of shortest paths from *s* to *t*, and $\sigma_{st}(n)$ is the number of shortest paths from *s* to *t* that *n* lies on. Weighted and unweighted *betweenness* were calculated for each node of every network. Note that, weighted and unweighted *betweenness* centrality scores were normalized for every node as $C_b(n)/(N-1).(N-2)$.

Closeness centrality. Closeness centrality of a node is the inverse sum of the shortest path length from a node to all other nodes of the network and represents the importance of a node in context of information processing. It is a measure of how fast information spreads from a given node to other reachable nodes in the network [4] and can be calculated as follows:

$$c(i) = \left(\frac{A_i}{N-1}\right)^2 \frac{1}{C_i} \quad (8),$$

where A_i is the number of reachable nodes from node *i, N* is the number of nodes in the network and C_i is the sum of path lengths from node i to all reachable nodes. In directed

networks, closeness is represented as *'Incloseness'* and *'Outcloseness'*. Unlike *Outcloseness*, *incloseness* is a measure of path lengths from all other nodes to a node *i.* Weighted and unweighted *in* and *out* closeness centrality scores were calculated for each network.

Hubs and authorities. The '*hubs*' and *'authorities'* centrality scores are two linked centrality measures that are recursive. Klienberg's **HITS** algorithm (Klienberg, 1999 [5]) was used to iteratively calculate weighted and unweighted scores. The *hubs* score of a node is the sum of the *authorities* scores of all its successors. Similarly, the *authorities* score is the sum of the *hubs* scores of all its predecessors. Both scores are normalized such that the sum of all hubs scores as well as sum of all authorities scores is 1. As a result nodes that receive high Hub scores typically have broadly distributed outgoing traffic whereas nodes with high Authority scores typically show broad incoming traffic.

Appendix 3.7A: Mean multivariate intra and inter SMETS values with std. errors obtained using leave-one-out subsampling

	n=55		n=55		n=110		n=121	
Cytokine	**SMETS HC Vs HC**		**SMETS GWI Vs GWI**		**Pooled intra (HC+GWI)SMETS**		**Inter SMETS (HC Vs GWI)**	
	Mean	**Std. error**	**Mean**	**Std. error**	**Mean**	**Std. error**	**Mean**	**Std. error**
IL-1a	11.23	0.71	10.57	0.62	10.90	0.47	12.07	0.31
IL-1b	2.52	0.09	2.38	0.10	2.45	0.07	2.81	0.04
IL-2	3.57	0.32	3.01	0.17	***3.29***	***0.18***	***5.04***	***0.08***
IL-4	9.65	0.40	8.86	0.40	9.25	0.28	12.01	0.13
IL-5	2.98	0.15	3.47	0.14	***3.23***	***0.10***	***4.63***	***0.04***
IL-6	13.14	0.62	11.94	0.68	12.54	0.46	15.84	0.22
IL-8	4.28	0.23	3.84	0.18	***4.06***	***0.15***	***6.03***	***0.07***
IL-10	2.05	0.10	2.38	0.12	2.21	0.08	2.94	0.04
IL-12	1.51	0.08	1.50	0.07	1.51	0.05	1.93	0.02
IL-13	4.97	0.30	5.05	0.33	***5.01***	***0.22***	***7.06***	***0.12***
IL-15	5.10	0.30	4.97	0.25	5.03	0.19	6.26	0.14
IL-17	4.68	0.23	4.05	0.16	***4.37***	***0.14***	***6.63***	***0.05***
IL-23	0.36	0.02	0.27	0.01	0.31	0.01	0.37	0.00
IFNy	1.93	0.09	1.83	0.08	1.88	0.06	2.44	0.02
TNFa	3.93	0.23	3.71	0.18	3.82	0.15	4.20	0.09
TNFb	3.74	0.26	2.98	0.20	3.36	0.17	4.08	0.11

Appendix 3.7B: Median multivariate intra and inter SMETS values with median absolute deviation from median obtained using leave-one-out subsampling

Cytokine	SMETS HC Vs HC		SMETS GWI Vs GWI		Pooled intra (HC+GWI)SMETS		Inter SMETS (HC Vs GWI)	
	Median	MAD	Median	MAD	Median	MAD	Median	MAD
IL-1a	12.69	3.74	12.44	2.84	12.57	2.91	12.74	3.20
IL-1b	2.55	0.54	2.48	0.63	2.49	0.55	2.80	0.29
IL-2	2.34	0.94	2.83	0.87	***2.59***	***0.94***	***4.59***	***0.27***
IL-4	10.80	2.10	9.06	2.16	9.60	2.44	12.24	0.97
IL-5	2.96	0.93	3.56	0.79	***3.34***	***0.82***	***4.59***	***0.31***
IL-6	12.97	3.31	13.30	3.64	13.17	3.69	15.50	1.85
IL-8	4.74	1.45	4.05	1.12	***4.28***	***1.13***	***6.05***	***0.53***
IL-10	2.06	0.66	2.44	0.81	***2.23***	***0.72***	***3.07***	***0.34***
IL-12	1.38	0.55	1.59	0.42	1.47	0.47	1.91	0.20
IL-13	4.06	1.52	4.23	1.46	***4.19***	***1.51***	***7.03***	***1.00***
IL-15	4.64	1.38	5.34	1.57	5.18	1.50	5.86	1.22
IL-17	4.50	1.70	4.16	0.82	***4.28***	***1.13***	***6.83***	***0.30***
IL-23	0.39	0.07	0.26	0.07	0.32	0.10	0.36	0.03
IFNy	2.07	0.52	1.77	0.49	1.88	0.48	2.40	0.18
TNFa	3.59	1.34	3.94	0.93	3.81	1.24	3.99	0.87
TNFb	3.13	1.75	2.74	1.21	3.04	1.61	3.46	0.64

Appendix 3.7C: Statistical significance of differences in between and within-group SMETS values obtained using leave-one-out sub-sampling

Cyto-kines	Multiple time series comparison							
	Inter healthy-GWI SMETS Vs Intra Healthy+GWI SMETS		Inter healthy-GWI SMETS Vs Intra healthy SMETS		Inter healthy-GWI SMETS Vs Intra GWI SMETS		Intra GWI SMETS Vs Intra healthy SMETS values	
	Wilcoxon ranksum	Two tailed t test	Wilcoxon ranksum	Two tailed t test	Wilcoxon ranksum	Two tailed t test	Wilcoxon ranksum	t test
IL-1a	0.13	***0.02***	0.61	0.10	***0.02***	***0.01***	0.25	0.48
IL-1b	***0.00***	***0.00***	***0.00***	***0.00***	***0.00***	***0.00***	0.36	0.29
IL-2	***0.00***	***0.00***	***0.00***	***0.00***	***0.00***	***0.00***	0.98	0.12
IL-4	***0.00***	***0.00***	***0.00***	***0.00***	***0.00***	***0.00***	0.14	0.17
IL-5	***0.00***	***0.00***	***0.00***	***0.00***	***0.00***	***0.00***	***0.02***	***0.01***
IL-6	***0.00***	***0.00***	***0.00***	***0.00***	***0.00***	***0.00***	0.21	0.19
IL-8	***0.00***	***0.00***	***0.00***	***0.00***	***0.00***	***0.00***	0.13	0.13
IL-10	***0.00***	***0.00***	***0.00***	***0.00***	***0.00***	***0.00***	***0.02***	***0.04***
IL-12	***0.00***	***0.00***	***0.00***	***0.00***	***0.00***	***0.00***	0.96	0.93
IL-13	***0.00***	***0.00***	***0.00***	***0.00***	***0.00***	***0.00***	0.88	0.86
IL-15	***0.00***	***0.00***	***0.00***	***0.00***	***0.00***	***0.00***	0.91	0.75
IL-17	***0.00***	***0.00***	***0.00***	***0.00***	***0.00***	***0.00***	***0.04***	***0.03***
IL-23	***0.00***	***0.00***	0.81	0.35	***0.00***	***0.00***	***0.00***	***0.00***
IFNy	***0.00***	***0.00***	***0.00***	***0.00***	***0.00***	***0.00***	0.34	0.41
TNFa	0.04	***0.01***	0.12	0.09	0.05	***0.00***	0.44	0.46
TNFb	***0.00***	***0.00***	0.06	0.08	***0.00***	***0.00***	***0.03***	***0.02***

Appendix 3.8: Comparison of weighted node centrality measures. Weighted betweenness, incloseness, outcloseness, hub and authority centrality scores of healthy consensus networks (Black boxes) were compared with their counterparts in GWI consensus networks (red boxes). Lines inside the boxplots show the median values and red (+) signs show outliers.

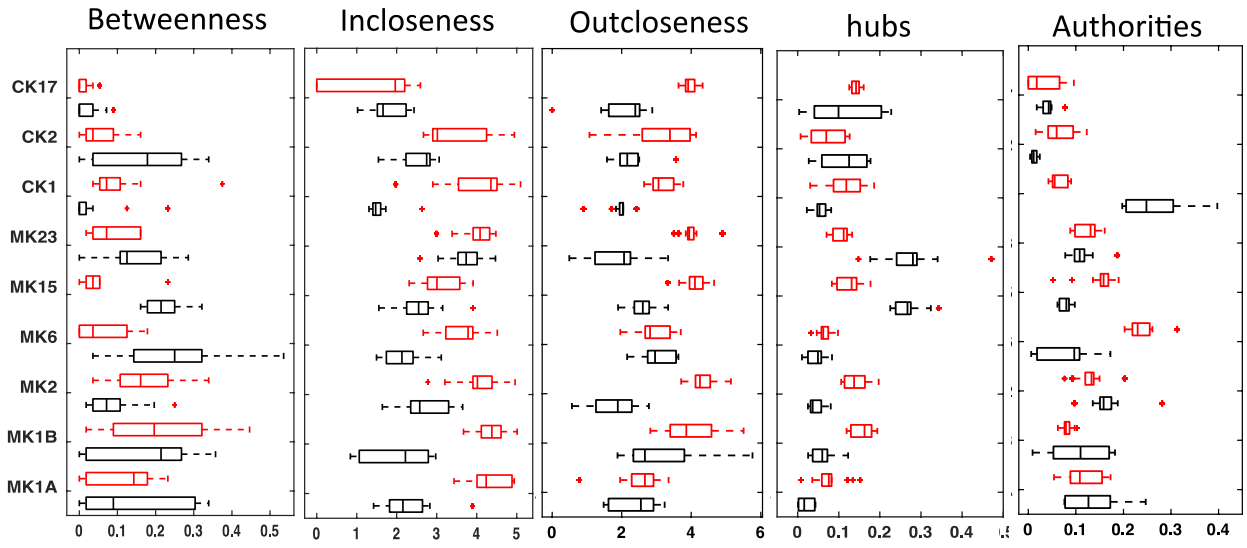

Appendix 3.9A: Weighted and unweighted median betweenness centrality with p values obtained from their comparisons through Mann Whitney Wilcoxon ranksum test

Node names	Median Betw. Cent.					
	Weighted			Unweighted		
	Healthy	GWI	P values	Healthy	GWI	P values
MK1A	0.09	0.14	***0.02***	0.09	0.12	0.19
MK1B	0.21	0.20	0.22	0.14	0.09	0.27
MK2	0.07	0.16	***0.00***	0.06	0.10	***0.00***
MK6	0.25	0.04	***0.00***	0.17	0.07	***0.00***
MK15	0.21	0.04	***0.00***	0.12	0.05	***0.00***
MK23	0.13	0.07	***0.00***	0.19	0.03	***0.00***
CK1	0.00	0.07	***0.00***	0.08	0.05	0.70
CK2	0.18	0.04	***0.00***	0.19	0.03	***0.00***
CK17	0.00	0.00	***0.01***	0.03	0.03	0.12

Appendix 3.9B: Weighted and unweighted closeness (in and out) centrality with p-values obtained from the comparison of median closeness centralities through Mann Whitney Wilcoxon ranksum test

Node names	Median incloseness Cent.					
	Weighted			Unweighted		
	Healthy	GWI	P values	Healthy	GWI	P values
MK1A	2.15	***4.24***	***0.00***	0.067	0.077	***0.00***
MK1B	2.22	***4.38***	***0.00***	0.067	0.083	***0.00***
MK2	***2.57***	4.02	***0.00***	0.083	0.083	0.10
MK6	2.13	3.78	***0.00***	0.067	0.100	***0.00***
MK15	2.55	3.00	***0.00***	0.056	0.077	***0.00***
MK23	***3.74***	4.08	***0.00***	0.077	0.083	0.33
CK1	1.47	***4.35***	***0.00***	0.067	0.077	***0.00***
CK2	***2.75***	3.02	***0.00***	0.063	0.067	***0.00***
CK17	1.66	1.96	***0.04***	0.057	0.053	0.00

Node names	Median outcloseness Cent.					
	Weighted			Unweighted		
	Healthy	GWI	P values	Healthy	GWI	P values
MK1A	2.55	2.67	***0.02***	0.063	0.067	0.63
MK1B	***2.67***	3.86	***0.00***	0.071	0.088	***0.00***
MK2	1.89	***4.25***	***0.00***	0.050	0.091	***0.00***
MK6	***2.96***	2.81	***0.00***	0.077	0.067	***0.00***
MK15	***2.61***	***4.11***	***0.00***	0.091	0.077	***0.00***
MK23	2.07	***3.94***	***0.00***	0.067	0.077	***0.00***
CK1	2.04	3.06	***0.00***	0.063	0.070	***0.00***
CK2	2.16	3.38	***0.00***	0.077	0.070	***0.00***
CK17	2.39	***3.91***	***0.00***	0.067	0.083	***0.00***

Appendix 3.9C: Median indegree and outdegree centralities in healthy and GWI subjects with the p values obtained from their comparison using Mann Whitney Wilcoxon ranksum test

Node names	Median degree centrality					
	indegree			outdegree		
	Healthy	GWI	P values	Healthy	GWI	P values
MK1A	3	5	***0.00***	2	3	***0.00***
MK1B	2	4	***0.00***	4	5	***0.00***
MK2	6	5	***0.00***	***2***	***6***	***0.00***
MK6	***3***	***7***	***0.00***	3	3	***0.00***
MK15	3	4	***0.00***	6	6	***0.01***
MK23	5	4.5	***0.00***	4	4	***0.00***
CK1	2	3	***0.00***	2	3	***0.00***
CK2	3	3	0.52	3	3	***0.00***
CK17	3	1	***0.00***	3	4	***0.00***

Appendix 3.9D: Weighted and unweighted hub and authority scores with p-values obtained from the comparison of median closeness centralities through Mann Whitney Wilcoxon ranksum test

Node names	Median hub ranks					
	Weighted			Unweighted		
	HC	GWI	P values	HC	GWI	P values
MK1A	0.02	0.08	***0.00***	0.05	0.06	***0.01***
MK1B	0.06	0.16	***0.00***	0.12	0.14	0.20
MK2	0.04	0.14	***0.00***	0.11	0.15	***0.00***
MK6	0.05	0.06	***0.00***	0.12	0.08	***0.00***
MK15	0.27	0.13	***0.00***	0.21	0.15	***0.00***
MK23	0.28	0.11	***0.00***	0.12	0.12	0.17
CK1	0.05	0.12	***0.00***	0.08	0.09	***0.00***
CK2	0.13	0.07	***0.00***	0.09	0.09	0.13
CK17	0.10	0.14	***0.01***	0.10	0.13	***0.00***

Node names	Median authority ranks					
	Weighted			Unweighted		
	HC	GWI	P values	HC	GWI	P values
MK1A	0.13	0.11	***0.00***	0.13	0.13	0.26
MK1B	0.11	0.08	0.03	0.08	0.11	***0.00***
MK2	0.16	0.13	***0.00***	0.19	0.14	***0.00***
MK6	0.10	0.23	***0.00***	0.09	0.18	***0.00***
MK15	0.08	0.16	***0.00***	0.13	0.13	0.27
MK23	0.11	0.13	***0.00***	0.18	0.13	***0.00***
CK1	0.25	0.06	***0.00***	0.10	0.09	0.04
CK2	0.01	0.06	***0.00***	0.06	0.07	0.90
CK17	0.04	0.02	***0.00***	0.07	0.02	***0.00***

Appendix 3.10: Agreement of empirical and literature-based reference networks. Edge density, PPV, recall and F1 score in the overall group consensus, subject sub-sample consensus, and single-subject networks repeatedly subsampled without replacement. Significance based on Wilcoxon rank sum test.

	HC	GWI	P value (1)
A) 1000 individual networks (100 repeat subsamples of n=10)			
Inferred Networks			
Median edge abundance	66(3)	69(4)	***0.00***
Median edge density (MAD)	0.81(0.04)	0.85 (0.05)	***0.00***
Reference network recovery			
Median PPV (MAD)	0.61(0.02)	0.60(0.006)	***0.00***
Median Recall (MAD)	0.82(0.04)	0.84(0.04)	***0.00***
Median F score (MAD)	0.71(0.009)	0.70(0.01)	0.16
B) 100 within subsample consensus networks (intersection of 10 networks within each of 100 subsamples)			
Inferred Networks			
Median edge abundance	29(1)	35(1)	***0.00***
Median edge density (MAD)	0.36(0.01)	0.43(0.01)	***0.00***
Reference network recovery			
Median PPV (MAD)	0.65(0.01)	0.54(0.01)	***0.00***
Median Recall (MAD)	0.37(0.02)	0.39(0.02)	***0.00***
Median F score (MAD)	0.47(0.03)	0.45(0.02)	***0.00***
C) Conserved across all subsample consensus networks (intersection of 100 subsample consensus networks)			
Inferred Network			
Edge abundance	19	24	NA
Edge density	0.23	0.30	NA
Reference network recovery			
PPV	0.74	0.46	NA
Recall	0.29	0.22	NA
F1 score	0.41	0.30	NA

Appendix 3.11: Expanded inferred association of MK23 with CK17. Deconstruction of overall net inhibition of CK17 by MK 23 inferred from the data (dashed lines) into the cumulative indirect component control actions documented in the literature (solid lines) (green edges promote; red edges inhibit). The apparent inconsistency with reported stimulation of the Th17 axis by IL-23 consists of indirect effects involving mediation unmeasured immune elements (grey nodes), specifically cortisol and dendritic cell (DC) abundance.

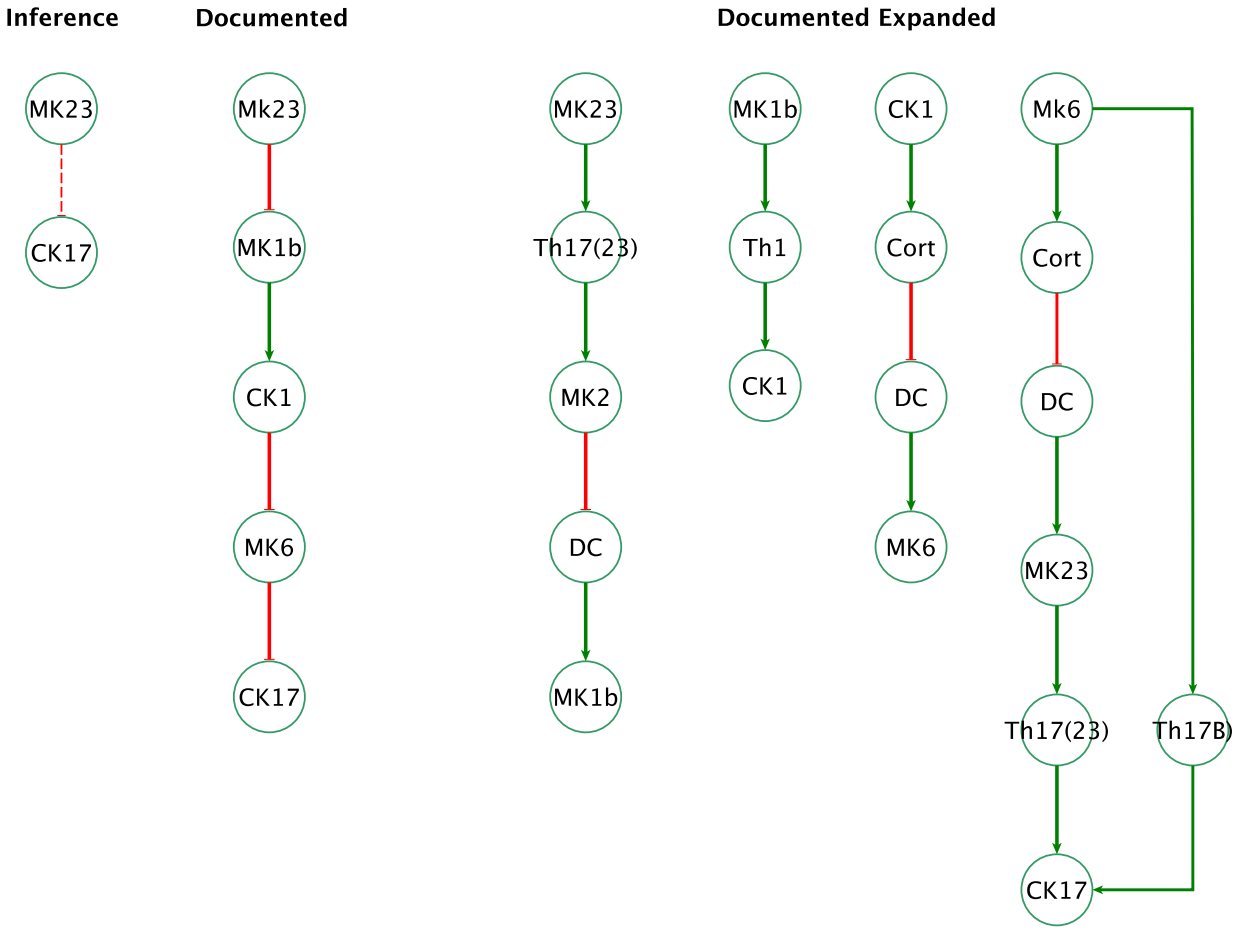

Appendix 3.12: Mean (standard error) GED on blocking all the outgoing edges from a group of two aggregate cytokines in 11 leave one out subsamples with false discovery rate (FDR) values obtained from their comparison through the Benjamini Hochberg test.

Original Mean GED= 0.2569 Std. err= 0.0021

	MK1A	MK1B	MK2	***MK6***	***MK15***	***MK23***	***CK1***	CK2	***CK17***
MK1A	0.2511(0.0020)	0.2498(0.0021)	0.2476(0.0020)	***0.2365(0.0020)***	0.2465(0.0020)	0.2432(0.0020)	0.2425(0.0020)	0.2502(0.0020)	0.2473(0.0020)
MK1B	0	0.2557(0.0022)	0.2522(0.0022)	0.2414(0.0021)	0.2511(0.0022)	0.2480(0.0023)	0.2473(0.0022)	0.2548(0.0022)	0.2520(0.0022)
MK2	0	0	0.2535(0.0021)	***0.2390(0.0022)***	0.2489(0.0022)	0.2457(0.0022)	0.2450(0.0021)	0.2526(0.0021)	0.2497(0.0022)
MK6	0	0	0	0.2427(0.0022)	***0.2379(0.0022)***	***0.2345(0.0022)***	***0.2338(0.0022)***	0.2418(0.0022)	***0.2388(0.0022)***
MK15	0	0	0	0	0.2524(0.0021)	0.2446(0.0022)	0.2439(0.0021)	0.2515(0.0021)	0.2486(0.0021)
MK23	0	0	0	0	0	0.2493(0.0022)	0.2406(0.0022)	0.2484(0.0022)	0.2454(0.0022)
CK1	0	0	0	0	0	0	0.2486(0.0021)	0.2477(0.0021)	0.2447(0.0021)
CK2	0	0	0	0	0	0	0	0.2561(0.0021)	0.2524(0.0021)
CK17	0	0	0	0	0	0	0	0	0.2532(0.0021)

	MK1A	MK1B	MK2	MK6	MK15	***MK23***	***CK1***	CK2	CK17
MK1A	0.0594	0.0246	0.0031	***0.0000***	***0.0009***	***0.0000***	***0.0000***	0.0291	0.0022
MK1B	1	0.6967	0.1502	***0.0000***	0.0778	0.0072	0.0033	0.5116	0.1294
MK2	1	1	0.2670	***0.0000***	0.0132	***0.0007***	***0.0003***	0.1697	0.0250
MK6	1	1	1	***0.0000***	***0.0000***	***0.0000***	***0.0000***	***0.0000***	***0.0000***
MK15	1	1	1	1	0.1513	***0.0002***	***0.0001***	0.0937	0.0102
MK23	1	1	1	1	1	0.0175	***0.0000***	0.0088	***0.0005***
CK1	1	1	1	1	1	1	0.0089	0.0041	***0.0002***
CK2	1	1	1	1	1	1	1	0.7741	0.1502
CK17	1	1	1	1	1	1	1	1	0.2356

References

1. Tapinos, A. & Mendes, P. (2013) A Method for Comparing Multivariate Time Series with Different Dimensions, *PLOS ONE.* **8**, e54201.

2. Brandes, U. (2001) A faster algorithm for betweenness centrality, *J Math Sociol.* **25**, 163-177.

3. Yoon, J., Blumer, A. & Lee, K. (2006) An algorithm for modularity analysis of directed and weighted biological networks based on edge-betweenness centrality, *Bioinformatics.* **22**, 3106-3108.

4. Newman, M. (2003) The Structure and Function of Complex Networks, *SIAM Rev.* **45**, 167-256.

5. Kleinberg, J. M. (1998) Authoritative sources in a hyperlinked environment in *Proceedings of the ninth annual ACM-SIAM symposium on Discrete algorithms* pp. 668-677San Francisco, California, USA.

Appendices: Chapter 4

Appendix 4.1: Demographics details of healthy and GWI subjects. GWI subjects are also classified as high trauma on the basis of DTS score

	HC	All GWI	high trauma GWI
Number of subjects	27	27	17
Race			
Caucasian	6	9	6
Hispanic	12	12	6
African American	0	1	1
Asian	5	4	3
Not recorded	4	1	1
Age	43(0.29)	42(0.24)	42(0.36)
Body Mass index (BMI)	27.7 (0.2)	28.6(0.1)	29.6(0.2)
Peak VO2 max (mL/kg/min)	28.4(1.21)	23.9(1.01)*	24(1)*
% Predicted peak VO2 max (%)	76(2.9)	65.2(2.6)*	65.06(2.64)*
Time to VO2 max (min)	8.26(0.55)	6.37(0.46)*	6.18(0.49)*

* Significantly different from HC in two-tailed t-test

Appendix 4.2: Davidson Trauma Scales of different categories in 27 GWI subjects. DTS scores for 6 subjects were not known

	High Trauma GWI	Low trauma GWI
No. of subjects	17	4
Davidson Trauma Scale (DTS)		
Total DTS	92(5)	27(7)
Intrusion score	27(1)	7(2)
Avoidance	36(3)	9(3)
Hyperarousal	29(1)	11(3)

Appendix 4.3: P values obtained from Mann Whitney ranksum test. Cytokine profiles for each exposure was compared to median cytokine levels in response to Saline

Cytokine	Saline/LPS	Saline/ CORT LPS	Saline/DFP LPS	Saline/CORT DFP LPS
21-day comparison				
IL-1a	0.15	***0.01***	0.22	***0.00***
IL-1b	0.84	***0.03***	0.42	***0.02***
IL-2	0.55	0.22	1.00	0.36
IL-4	0.42	0.42	0.42	***0.00***
IL-5	0.84	0.06	0.31	***0.03***
IL-6	***0.01***	***0.01***	***0.01***	***0.00***
IL-10	0.45	0.06	0.72	0.08
IL-12	0.55	0.31	0.84	0.33
IFNg	1.00	***0.02***	0.84	0.13
TNFa	***0.02***	***0.01***	***0.02***	***0.00***
KC	***0.01***	***0.01***	***0.01***	***0.00***
MIP2	0.94	***0.01***	0.51	***0.01***
90 day comparison				
IL-1a	0.15	***0.04***	0.14	***0.01***
IL-1b	1.00	***0.04***	**0.07**	***0.01***
IL-2	0.31	0.07	0.14	***0.03***
IL-4	0.84	0.57	0.57	0.15
IL-5	0.10	0.07	0.57	***0.01***
IL-6	***0.01***	***0.04***	**0.07**	***0.01***
IL-10	***0.02***	***0.04***	0.57	***0.01***
IL-12	0.55	0.39	0.39	0.55
IFNg	1.00	***0.04***	1.00	***0.01***
TNFa	***0.01***	***0.04***	0.39	***0.01***
KC	***0.02***	***0.04***	**0.07**	***0.01***
MIP2	0.06	***0.04***	0.39	***0.01***

Appendix 4.4: Node centrality measures for the nodes of consensus networks in response to LPS exposure on 21 and 90 days after periodic CORT exposures with (CDL) or without (CL) DFP exposure on day 15

		Betweenness centrality				Degree centrality			
S.No.	Node	CL_ 21d	CL_ 90d	CDL_ 21d	CDL_ 90d	CL_ 21d	CL_ 90d	CDL_ 21d	CDL_ 90d
1	IL-1a	0	0	1	0	0	1	3	4
2	IL-1b	***5***	***5***	1.533 3	2.05	***4***	3	3	7
3	IL-2	0	0	0	1	0	0	0	4
4	IL-4	0	0	0	0	0	0	0	2
5	IL-5	0	0	1.233 3	0	3	0	4	3
6	IL-6	***5.5***	0	***5.6***	0.866 7	3	4	***6***	5
7	IL-10	0	0	0	0.95	1	4	0	6
8	IL-12p70	0	0	0	0	0	0	0	0
9	IFNg	0	0	0	***11.4***	0	0	2	***9***
10	TNF-a	2.5	***3***	1.233 3	***4.383*** ***3***	***4***	***5***	4	8
11	IL-8 (KC)	1	0	0.5	***4.4***	2	4	3	8
12	IL-8 (MIP-2)	0	***3***	***2.9***	0.95	3	***5***	5	6
		Eigenvector centrality				Closeness centrality			
1	IL-1a	0.08	0.01	0.06	0.06	0.00	0.02	0.03	0.05
2	IL-1b	***0.12***	0.06	0.06	***0.11***	***0.04***	0.03	0.04	0.06
3	IL-2	0.08	0.08	0.08	0.05	0.00	0.00	0.00	0.05
4	IL-4	0.08	0.08	0.08	0.03	0.00	0.00	0.00	0.04
5	IL-5	0.11	0.08	0.09	0.05	0.03	0.00	0.04	0.05
6	IL-6	0.06	0.10	***0.12***	0.08	0.03	0.03	***0.05***	0.06
7	IL-10	0.02	0.10	0.08	0.10	0.02	0.03	0.00	0.06
8	IL-12p70	0.08	0.08	0.08	0.08	0.00	0.00	0.00	0.00
9	IFNg	0.08	0.08	0.06	***0.12***	0.00	0.00	0.03	***0.08***
10	TNF-a	***0.12***	***0.11***	0.09	***0.11***	0.03	***0.04***	0.04	***0.07***
11	IL-8 (KC)	0.05	0.10	0.07	***0.11***	0.03	0.03	0.04	***0.07***
12	IL-8 (MIP-2)	0.11	***0.11***	***0.11***	0.10	0.03	***0.04***	***0.05***	0.06

Appendix 4.5: Comparison of node centrality measures in response to exposure to LPS challenge after a repeated priming with CORT with and without prior exposure to DFP. Wilcoxon ranksum test was used to compare the median node centrality measures.

Nodes	Median Betweeness centrality											
	CL 21d	MAD	CDL 21d	MAD	P val CL/CDL 21d	CL 90d	MAD	CDL 90d	MAD	P val CL/CDL 90d	P val CL 21/90d	P val CDL 21/90 d
IL-1a	0.00	0.00	0.50	0.50	***0.00***	0.00	0.00	0.00	0.00	***0.01***	***0.01***	***0.00***
IL-1b	**3.00**	2.00	0.46	0.46	***0.00***	**3.00**	3.00	0.90	0.50	0.14	0.92	***0.01***
IL-2	0.00	0.00	0.00	0.00		0.00	0.00	1.00	0.70	***0.00***		***0.00***
IL-4	0.00	0.00	0.00	0.00	***0.02***	0.00	0.00	0.00	0.00	0.47		0.07
IL-5	0.00	0.00	0.21	0.21	***0.00***	0.00	0.00	0.00	0.00	0.61	0.70	***0.05***
IL-6	**5.50**	2.50	**2.08**	1.08	***0.01***	0.00	0.00	0.25	0.25	0.07	***0.00***	***0.00***
IL-10	0.00	0.00	0.00	0.00	***0.04***	0.00	0.00	0.67	0.28	***0.00***	***0.00***	***0.00***
IL-12p70	0.00	0.00	0.00	0.00	0.38	0.00	0.00	0.00	0.00			0.38
IFNg	0.00	0.00	0.00	0.00	0.30	0.00	0.00	**6.40**	3.60	***0.00***	0.11	***0.00***
TNFa	**2.50**	1.83	**1.80**	1.28	0.27	0.20	0.20	2.15	1.25	0.08	0.19	0.89
IL8(KC)	1.00	1.00	0.75	0.50	0.77	0.00	0.00	**4.40**	1.67	***0.00***	0.06	***0.00***
IL8 (MIP-2)	0.00	0.00	**1.88**	0.68	***0.00***	**3.20**	3.00	0.72	0.23	0.30	0.08	***0.00***
Nodes	Median eigenvector centrality											
IL-1a	0.08	0.00	0.08	0.01	0.56	0.03	0.02	0.07	0.01	***0.01***	***0.00***	0.07
IL-1b	**0.11**	0.01	0.08	0.01	***0.00***	0.08	0.01	**0.10**	0.00	***0.00***	***0.00***	***0.00***
IL-2	0.08	0.00	0.08	0.00	0.38	0.08	0.00	0.06	0.01	0.05	***0.01***	***0.00***
IL-4	0.08	0.00	0.08	0.00	***0.02***	0.08	0.00	0.03	0.01	***0.00***		***0.00***
IL-5	0.09	0.01	0.08	0.01	0.18	0.08	0.00	0.08	0.02	0.70	0.10	0.06
IL-6	0.09	0.01	**0.11**	0.01	***0.00***	**0.09**	0.01	0.08	0.00	***0.00***	0.37	***0.00***
IL-10	0.03	0.02	0.08	0.00	***0.00***	**0.09**	0.01	**0.10**	0.00	0.87	***0.00***	***0.00***
IL-12p70	0.08	0.00	0.08	0.00	0.85	0.08	0.00	0.08	0.00	0.16	0.08	0.22
IFNg	0.08	0.00	0.06	0.01	***0.04***	0.08	0.00	**0.11**	0.01	***0.00***	0.42	***0.00***

TNFa	**0.12**	0.01	**0.10**	0.01	***0.00***	**0.09**	0.01	**0.10**	0.01	0.08	***0.02***	0.07
IL8(KC)	0.07	0.01	0.08	0.01	***0.00***	**0.09**	0.01	**0.10**	0.01	0.11	***0.00***	***0.00***
IL8 (MIP-2)	0.10	0.01	**0.10**	0.01	0.73	**0.10**	0.01	**0.10**	0.00	0.50	1.00	0.34

Median closeness centrality

Nodes	CL 21d	MAD	CDL 21 d	MAD	P val CL/CDL 21d	CL 90d	MAD	CDL 90d	MAD	P val CL/CDL 90d	P val CL 21/90d	P val CDL 21/90 d
IL-1a	0.00	0.00	0.04	0.01	***0.00***	0.04	0.01	0.05	0.00	***0.03***	***0.00***	***0.01***
IL-1b	**0.04**	0.00	0.04	0.01	0.36	0.06	0.00	0.06	0.01	***0.00***	***0.01***	***0.00***
IL-2	0.00	0.00	0.00	0.00	0.38	0.00	0.00	0.05	0.00	***0.00***	***0.01***	***0.00***
IL-4	0.00	0.00	0.03	0.03	***0.00***	0.00	0.00	0.04	0.00	***0.00***		0.06
IL-5	0.03	0.00	0.04	0.00	***0.00***	0.02	0.02	0.05	0.02	***0.00***	0.07	***0.00***
IL-6	**0.04**	0.00	**0.06**	0.01	***0.00***	0.05	0.01	0.06	0.00	0.06	***0.02***	0.49
IL-10	0.02	0.00	0.00	0.00	***0.00***	0.05	0.01	0.06	0.00	***0.00***	***0.00***	***0.00***
IL-12p70	0.00	0.00	0.00	0.00	0.76	0.00	0.00	0.00	0.00	0.71	0.67	0.26
IFNg	0.00	0.00	0.04	0.01	***0.00***	0.03	0.03	0.08	0.00	***0.00***	0.11	***0.00***
TNFa	**0.04**	0.01	**0.05**	0.01	***0.02***	0.05	0.01	0.07	0.01	***0.00***	***0.00***	***0.00***
IL-8(KC)	0.03	0.00	**0.05**	0.01	***0.00***	0.05	0.01	0.08	0.01	***0.00***	***0.00***	***0.00***
IL-8 (MIP-2)	0.03	0.00	**0.05**	0.01	***0.00***	0.06	0.00	0.06	0.00	***0.00***	***0.00***	***0.00***

Median degree centrality

Nodes	CL 21d	MAD	CDL 21 d	MAD	P val CL/CDL 21d	CL 90d	MAD	CDL 90d	MAD	P val CL/CDL 90d	P val CL 21/90d	P val CDL 21/90 d
IL-1a	0	0	4	1	***0.00***	3	1	5	1	***0.03***	***0.00***	0.07
IL-1b	4	1	4	1	0.33	7	0	7	1	***0.01***	0.07	***0.00***
IL-2	0	0	0	0	0.38	0	0	4	1	***0.00***	***0.01***	***0.00***
IL-4	0	0	1	1	***0.00***	0	0	2	0	***0.00***		0.25
IL-5	3	1	4.5	0.5	***0.02***	1	1	3	3	***0.03***	0.06	0.82
IL-6	5	1	7	1	***0.00***	6	1	6	1	0.72	***0.00***	0.09
IL-10	1	0	0	0	***0.00***	6	1	7	1	***0.03***	***0.00***	***0.00***
IL-12p70	0	0	0	0	0.86	0	0	0	0	0.71	0.67	0.26

IFNg	0	0	3	1	***0.00***	3	3	9	0	***0.00***	0.05	***0.00***
TNFa	4	1	6	2	0.15	6	1	8	1	***0.00***	***0.00***	***0.00***
IL-8(KC)	2	1	5	1	***0.00***	6	1	9	1	***0.00***	***0.00***	***0.00***
IL-8 (MIP-2)	3	0	6	1	***0.00***	7	0	7	1	0.51	***0.00***	***0.00***

Appendix 4.6A: Mean fold change levels and standard error for all cytokines in all GWI subjects and in only high trauma subjects

	HC T0	std. err	GWI T0	std. err.	HC T1	std.err	GWI T1	std. err.	HC T2	std. err.	GWI T2	std. err.
All subjects												
IL-1a	2.85	0.66	1.73	0.35	3.71	0.84	5.41	2.48	3.12	0.69	3.02	0.96
IL-1b	1.91	0.47	1.35	0.47	2.09	0.45	2.52	0.72	1.55	0.29	1.63	0.46
IL-2	2.86	1.11	6.73	2.22	3.97	1.55	7.68	2.68	2.10	0.47	6.60	2.23
IL-4	3.71	2.40	2.77	1.83	7.39	5.77	1.86	0.54	4.71	3.71	1.05	0.19
IL-5	2.73	1.02	5.27	2.54	3.79	1.44	7.44	3.27	2.51	0.85	4.51	1.90
IL-6	1.82	0.39	3.67	1.47	2.21	0.43	5.63	2.27	1.70	0.27	4.26	1.56
IL-10	1.65	0.39	1.29	0.29	2.18	0.47	1.55	0.49	1.67	0.36	1.31	0.30
IL-12p70	2.94	1.67	2.44	0.71	4.51	2.63	4.74	3.33	1.86	0.56	6.26	4.37
IFNg	4.17	1.62	15.19	6.72	7.46	3.15	20.01	7.09	4.47	1.72	19.24	6.88
TNFa	2.54	0.69	2.90	1.01	3.23	0.90	4.23	1.62	2.53	0.70	4.01	1.72
IL-8 (KC/MIP-2)	1.99	0.51	7.62	2.28	2.58	0.69	7.94	2.13	2.54	0.67	8.58	2.51
High Trauma subjects												
IL-1a	2.45	0.60	2.28	0.49	3.63	0.92	8.72	4.87	3.14	0.90	4.90	1.75
IL-1b	1.59	0.31	2.58	1.20	1.81	0.41	5.63	1.78	2.01	0.37	3.25	1.15
IL-2	3.00	1.47	5.53	1.74	3.49	1.99	8.78	3.47	1.95	0.47	6.93	2.54
IL-4	5.60	4.69	1.48	0.23	12.15	11.32	3.28	0.99	8.12	7.27	1.59	0.34
IL-5	3.50	1.69	4.32	1.62	4.70	2.40	11.99	5.32	2.85	1.41	6.94	3.11
IL-6	1.69	0.52	6.87	3.57	2.14	0.65	12.50	5.62	1.81	0.36	9.22	3.81
IL-10	1.64	0.43	1.47	0.41	2.44	0.62	2.22	0.90	1.67	0.34	1.85	0.53
IL-12p70	3.22	2.23	2.02	0.71	5.00	3.50	1.47	0.42	1.77	0.73	2.09	0.85
IFNg	3.91	1.74	25.54	11.87	7.34	4.59	33.89	12.13	5.01	2.54	33.34	11.77
TNFa	2.02	0.57	4.37	1.71	2.58	0.84	6.53	2.77	2.80	1.00	6.30	2.97
IL-8 (KC/MIP-2)	1.94	0.59	12.27	4.04	2.50	0.80	13.55	3.61	2.83	1.00	14.56	4.37

Appendix 4.6B P values obtained from the comparison of HC and GWI fold change levels through Wilcoxon ranksum test

Cytokines	P values T0	P values T1	P values T2
All subjects			
IL-1a	0.31	0.62	0.58
IL-1b	0.11	0.71	0.30
IL-2	0.50	0.45	0.71
IL-4	0.46	0.94	0.96
IL-5	0.23	0.48	0.62
IL-6	0.16	0.39	0.42
IL-10	0.21	0.10	0.15
IL-12p70	0.51	0.10	0.46
IFNg	0.08	***0.05***	0.11
TNFa	0.87	0.70	0.48
IL-8 (KC/MIP-2)	***0.03***	***0.05***	**0.06**
High Trauma subjects			
IL-1a	0.81	0.82	0.51
IL-1b	0.86	0.22	0.74
IL-2	0.34	0.21	0.35
IL-4	0.16	***0.03***	0.36
IL-5	***0.05***	***0.05***	0.09
IL-6	***0.00***	***0.05***	***0.03***
IL-10	0.65	0.49	0.63
IL-12p70	0.40	0.20	0.61
IFNg	***0.01***	***0.00***	0.07
TNFa	0.13	***0.04***	0.31
IL-8 (KC/MIP-2)	***0.01***	***0.00***	***0.03***

Appendix 4.7: P values for group, time and combined effects obtained from two-way analysis of variance (ANOVA) in all GWI subjects and high trauma subjects.

Cytokine	Group	time	interaction
All subjects			
IL-1a	0.87	0.17	0.50
IL-1b	0.96	0.27	0.61
IL-2	***0.01***	0.72	0.98
IL-4	0.18	0.84	0.75
IL-5	0.10	0.55	0.92
IL-6	***0.02***	0.63	0.83
IL-10	0.16	0.52	0.92
IL-12p70	0.52	0.75	0.60
IFNg	***0.00***	0.73	0.93
TNFa	0.33	0.70	0.89
IL-8 (KC/MIP-2)	***0.00***	0.90	0.98
High trauma subjects			
IL-1a	0.218	0.227	0.485
IL-1b	***0.018***	0.274	0.319
IL-2	***0.017***	0.632	0.783
IL-4	0.175	0.766	0.921
IL-5	0.091	0.285	0.544
IL-6	***0.004***	0.626	0.713
IL-10	0.878	0.373	0.930
IL-12p70	0.315	0.766	0.558
IFNg	***0.001***	0.781	0.924
TNFa	***0.037***	0.709	0.909
IL-8 (KC/MIP2)	***0.000***	0.859	0.971